

**THE FABRICATION AND STUDY OF METAL CHELATING STATIONARY
PHASES FOR THE HIGH PERFORMANCE SEPARATION OF METAL IONS**

by

Matthew James Shaw

A thesis submitted to the University of Plymouth
in partial fulfilment for the degree of

DOCTOR OF PHILOSOPHY

Department of Environmental Sciences
Faculty of Science

March 2000

UNIVERSITY OF PLYMOUTH	
Item No.	900 4263319
Date	18 MAY 2000 S
Class No.	T 543.0893 SHA
Contl. No.	X 904068132
LIBRARY SERVICES	

900426331 9



REFERENCE ONLY

LIBRARY STORE

ABSTRACT

THE FABRICATION AND STUDY OF METAL CHELATING STATIONARY PHASES FOR THE HIGH PERFORMANCE SEPARATION OF METAL IONS

By Matthew J. Shaw

The preparation and characterisation of chelating sorbents suitable for the high efficiency separation of trace metals in complex samples, using a single column and isocratic elution, is described.

Hydrophobic, neutral polystyrene divinylbenzene resins were either impregnated with chelating dyes or dynamically modified with heterocyclic organic acids, using physical adsorption and chemisorption processes respectively. A hydrophilic silica substrate was covalently bonded with a chelating aminomethylphosphonic acid group, to assess the chelating potential of this molecule.

These substrates were characterised in terms of metal retention capability (selectivity coefficients and capacity factors), separation performance, column efficiency and suitability for analytical applications. Chelating molecules with different ligand groups were found to have unique selectivity patterns dependant upon the conditional stability constants of the chelate.

Other factors, including mobile phase constituents – complexing agents, ionic strength and pH, column length and column capacity were additionally investigated to examine their effect upon the separation profiles achieved.

The promising metal separation abilities illustrated by a number of these chelating columns were exploited for the determination of trace toxic metals in complex sample matrices using High Performance Chelation Ion Chromatography (HPCIC). This included the determination of beryllium in a certified stream sediment, uranium in seawater and a certified stream sediment, and cadmium, lead and copper in a certified rice flour. The results for each analysis fell within the certified limits, and reproducibility was good. The optimisation of post column detection systems using chromogenic ligands additionally gave good detection limits for the metals in each separation system.

LIST OF CONTENTS

Copyright statement	i
Title Page	ii
Abstract	iii
List of Contents	iv
List of Tables	x
List of Figures	xii
Acknowledgements	xxiii
Author's Declaration	xxiv

CHAPTER 1. Introduction

1.1	Trace metal analysis	1
1.2	Principles of the liquid chromatographic process	3
1.3	Ion chromatography	6
	1.3.1 Simple ion – exchange	7
	1.3.2 Chelating ion exchange	12
	1.3.2.1 Principles of chelation	14
1.4	Chelating substrates	24
1.5	Ion chromatographic analysis of metal ions – a review	26
	1.5.1 Polystyrene Resins	28
	1.5.2 Silica Substrates	31
	1.5.3 Chelation Ion Chromatography (CIC)	32
	1.5.4 High Performance Chelation Ion Chromatography (HPCIC)	33
1.6	Detection of metal ions	37
1.7	Aims and objectives of this work	40

CHAPTER 2. A Comparison of Chelating Dyes Impregnated onto Polystyrene resins for Trace Metal Separations

2.1	Introduction	43
	2.1.1 Dye immobilised low efficiency supports	43
	2.1.2 High performance dye impregnated supports	47
	2.1.3 Dyes added to the mobile phase for high efficiency separations	49
	2.1.4 Aims of this study	51
2.2	Experimental	54
	2.2.1 Instrumentation	54
	2.2.2 Reagents	54
	2.2.3 Dye types studied	56
	2.2.4 Procedures	57
	2.2.4.1 Column Preparation	57
	2.2.4.2 Column Capacity Measurement	57
	2.2.4.3 Capacity Factor Determination	58
2.3	Results and Discussion	61
	2.3.1 Aurin Tricarboxylic Acid (ATA) Column	61
	2.3.2 Pyrocatechol Violet (PCV) Column	69
	2.3.3 <i>O</i> -Cresolphthalein Complexone (CPC) Column	73
	2.3.4 Calmagite (CAL) Column	78
	2.3.5 4-(2-pyridylazo)resorcinol (PAR) Column	82
	2.3.6 2-(3-sulphobenzoyl)pyridine 2-pyridylhydrazone (SPP) Column	88
	2.3.7 Effect of System Parameters on Metal Ion Separations	94
	2.3.7.1 Column Length	94
	2.3.7.2 Column Capacity	98
	2.3.7.3 Mobile phase ionic strength	104
	2.3.7.4 Complexing eluent effects	107
	2.3.7.5 Bare resin characteristics	108
2.4	Summary	109

CHAPTER 3. Chelating Exchange Separation Properties of Aminophosphonate Functionalised Silica.

3.1	Introduction	113
3.2	Experimental	118
	3.2.1 Instrumentation	118
	3.2.2 Reagents	118
	3.2.3 Sorbent Preparation	118
	3.2.3.1. Silica Bound Aminophosphonic acid (APAS)	119
	3.2.3.2 Silica Bound Phenylphosphonic Acid (PPAS)	119
3.3	Results and Discussion	120
	3.3.1 Chelating Mechanism of Aminophosphonate Functional Groups	120
	3.3.2 APAS Column Selectivity	122
	3.3.3 Phenylphosphonic Acid Column Selectivity	140
3.4	Summary	144

CHAPTER 4. The Determination of Trace Beryllium in a Stream Sediment.

4.1	Introduction	145
4.2	Experimental	148
	4.2.1 Instrumentation	148
	4.2.2. Reagents	148
	4.2.3 Sample pre-treatment	148
4.3	Results and Discussion	149
	4.3.1 Choice of Chelating Column	149
	4.3.2 Retention Characteristics and Selectivity of Be(II) and Selected Trivalent Metal Ions on APAS.	150
	4.3.3 Method Development	155
	4.3.3.1 Effect of Sample Ionic Strength on Metal Retention Characteristics	155
	4.3.3.2 Separation Conditions	155
	4.3.3.3 Detection Conditions	159
	4.3.4 Analytical Performance Characteristics	167
4.4	Summary	170

CHAPTER 5. Separation of Metal Ions using Neutral Substrates Dynamically Modified with Low Molecular Weight Chelating Molecules

5.1	Introduction	171
5.2	Experimental	173
	5.2.1 Instrumentation	173
	5.2.2 Reagents	174
	5.2.3 4-Chlorodipicolinic acid synthesis	174
	5.2.4 Preparation of the mobile phase	174
5.3	Results and Discussion	175
	5.3.1 Measurement of the dynamic loading of each carboxylic acid	175
	5.3.2 Effect of ionic strength on dynamic loading	177
	5.3.3 Effect of particle size on dynamic loading	177
	5.3.4 Reproducibility of dynamically modified substrates	178
	5.3.5 Chelating exchange properties of the dynamically coated carboxylic acids	179
	5.3.5.1 Picolinic Acid	180
	5.3.5.2 Quinaldic acid	182
	5.3.5.3 Dipicolinic acid	188
	5.3.5.4 4-Chlorodipicolinic acid	194
	5.3.5.4.1 Preliminary 100mm PS-DVB column investigations	195
	5.3.5.4.2 250mm PS-DVB column investigations	203
	5.3.6 L -Tryptophan	209
	5.3.7 2-hydroxyhexadecanoic acid	210
5.4	Summary	211

CHAPTER 6. Determination of Trace Metals in Environmental Samples using Dynamically Modified Substrates.

Part 1. Determination of Uranium in a Stream Sediment and Complex Aqueous Matrices.

6.1	Introduction	213
6.2	Experimental	216
	6.2.1 Instrumentation	216
	6.2.2 Reagents	216
	6.2.3 Sample Pre-treatment	217
6.3	Results and Discussion	219
	6.3.1 Retention Characteristics of Uranium on the Dynamically Modified Substrate	219
	6.3.2 Method Development – Separation Conditions	221
	6.3.3 Method Development – Detection Conditions	224
	6.3.4 Analytical Characteristics for the Determination of Uranium	229
6.4	Summary	236

Part 2. The Determination of Pb(II), Cd(II) and Cu(II) in Rice Flour

6.5	Introduction	237
6.6	Experimental	242
	6.6.1 Instrumentation	242
	6.6.2 Reagents	242
	6.6.3 Sample Pre-treatment	242
6.7	Results and Discussion	244
	6.7.1 Choice of Digestion Procedure	244
	6.7.2 Method Development – Detection Conditions	245
	6.7.3 Method Development – Separation conditions	247
	6.7.4 Analytical Characteristics of the Analysis	257
6.8	Summary	258

CHAPTER 7. Conclusions and Suggestions for Further Work

7.1	Conclusions	260
7.2	Further Work	265

REFERENCES	269
-------------------	------------

LIST OF TABLES

CHAPTER 1.

Table 1.1	Metal ions as hard or soft acids	15
Table 1.2	Ligands as hard or soft bases	16
Table 1.3	Stepwise formation constants of selected nitrogen complexes	20

CHAPTER 2.

Table 2.1	Chelating dyes studied, and resins used	56
Table 2.2	Log stability constants of metal complexes with ATA	61
Table 2.3	Log stability constants of metal complexes with CPC	74
Table 2.4	Log stability constants of selected metal ions with CAL	78
Table 2.5	Log stability constants of metal ions with PAR	82
Table 2.6	Efficiency of analyte peak, Pb(II), with column length	95
Table 2.7	Change in the Selectivity factors with column capacity	98
Table 2.8	Effect of Acetate Concentration on Metal Retention	107
Table 2.9	Retention of selected transition metals on Dionex resins	108
Table 2.10	Dye immobilised resin characteristics	109
Table 2.11	Metal selectivity on each dye column	110

CHAPTER 3.

Table 3.1	Log stability constants of selected metal complexes with iminodiacetate	114
Table 3.2	Log stability constants of selected metals with aminoethylphosphonic acid	116
Table 3.3	Column efficiency (N) on the APAS substrate at 0.5 and 1M KNO₃ (pH 2.3)	134

CHAPTER 4.

Table 4.1	Log stability Constants of Selected Metals with Methylphosphonic Acid	153
Table 4.2	Analytical Characteristics of Be(II) Determination	167

CHAPTER 5.

Table 5.1	k' values for the three heterocyclic carboxylic acids on neutral polystyrene with varying ionic strength	176
Table 5.2	Effect of substrate particle size on k' values for heterocyclic carboxylic acids	177
Table 5.3	The reproducibility of selected metal ion retention times on a quinaldic acid coated polystyrene column repeatedly stripped and re-coated over a 5 day period.	178

CHAPTER 6.

Table 6.1	Effect of particle size on the dynamic loading of dipicolinic acid and corresponding retention for U(VI) on the modified substrate	223
Table 6.2	The analytical characteristics of the sediment analysis.	233
Table 6.3	Sample matrices that have been analysed to quantify concentrations of Pb(II) and Cd(II)	241
Table 6.4	Log stability constants of selected metals with ammonia and boric acid	245
Table 6.5	The absorbance of selected transition metal ions (1mg l⁻¹) with PAR post column reagents (tenfold dilution) buffered with either ammonia or borate	246
Table 6.6	Analytical Characteristics achieved with the 300mm Column length with an eluent of 1M KNO₃ 6mM HNO₃ and 0.25mM chlorodipicolinic acid.	253
Table 6.7	Results achieved with the certified soft water sample, TMDA 54.2	254

Table 6.8	Analytical Characteristics achieved with the 100mm Column with an eluent of 1M KNO ₃ 30mM HNO ₃ and 0.25mM chlorodipicolinic acid.	257
------------------	--	-----

Table 6.9	The Results obtained for the certified rice flour analysis	258
------------------	--	-----

LIST OF FIGURES

CHAPTER 1.

Figure 1.1	A chromatographic separation illustrating the parameters used to obtain calculations.	6
Figure 1.2	The synthesis and structure of: (1) polystyrene divinylbenzene (PS-DVB) (C) from styrene (A) and divinyl benzene (B); (2) a typical reaction scheme for introducing sulfonic acid groups onto PS-DVB; and (3) mechanism for synthesising a silica sorbent.	9
Figure 1.3	Representation of equilibria existing between a solute cation M^{2+} , en, and an added ligand H_2L , at the surface of an ion exchanger	12
Figure 1.4	Simple ion-exchange (1) and chelating ion-exchange (2) mechanisms	14
Figure 1.5	Example of a 1. Six membered chelate ring (salicylic acid) and 2. five membered ring (pyrocatechol).	19
Figure 1.6	Steric configuration of the anion of a divalent metal-EDTA complex	19
Figure 1.7	The different species of EDTA in solution as a function of pH	22
Figure 1.8	Conditional stability constants, $\log K_{M'Y'}$, of selected metal EDTA complexes as a function of pH	23
Figure 1.9	Chelating groups immobilised onto PS-DVB for the preconcentration of trace metals. 1: Benzimidylazolyazo, 2: α -nitroso- β -naphthol, 3: Bicine and 4: 2-mercaptobenzothiazole.	27
Figure 1.10	Chromatogram illustrating the effect of 'kinetic broadening' on analyte peak shapes	36

Figure 1.11	A selection of chromogenic reagents used to detect metal ions. 1: Arsenazo III, 2: Methylthymol Blue, 3: Xylenol Orange, 4: Pyrocatechol Violet and 5: 4-(2-pyridylazo)resorcinol	41
--------------------	---	----

CHAPTER 2.

Figure 2.1	Structures of dye molecules used for the preconcentration and separation of metal ions: 1. Calmagite; 2. 1-(2-pyridylazo)-2-naphthol; 3. 4-(2-thiazolylazo)resorcinol.	52
Figure 2.2	Structures of dye molecules used for the preconcentration and separation of metal ions: 1. Chrome Azurol S; 2. <i>O</i> -Cresolphthalein Complexone; 3. Acid orange 8 (acid orange 7 has no methyl group) and 4. Dithizone.	53
Figure 2.3	A schematic diagram of the chromatographic system	55
Figure 2.4	Absorbance spectra of selected metals (1 mg l^{-1}) with the PAR post-column reagent.	59
Figure 2.5	Absorbance spectra of selected metals (1 mg l^{-1}) with PCV post-column reagent.	60
Figure 2.6	The dependence of capacity factors for transition and trivalent metal ions on eluent pH, with the ATA loaded column. Eluent: 1 M KNO_3 , 50 mM acetic acid .	64
Figure 2.7	The dependence of capacity factors for alkaline earth metals on eluent pH, with the ATA loaded column. Eluent: 1 M KNO_3 , 50 mM acetic acid .	65
Figure 2.8	Separation of $\text{Ba(II)}\ 10\text{ mg l}^{-1}$, $\text{Sr(II)}\ 10\text{ mg l}^{-1}$, $\text{Ca(II)}\ 5\text{ mg l}^{-1}$ and $\text{Mg(II)}\ 10\text{ mg l}^{-1}$, on the $100\text{ mm} \cdot 4.6\text{ mm}$ ATA column. Eluent 1 M KNO_3 50 mM acetic acid at pH 10.5. Detection: PAR/ Zn-EDTA at 490nm.	66
Figure 2.9	Separation of $\text{Zn(II)}\ 10\text{ mg l}^{-1}$, $\text{Cd(II)}\ 20\text{ mg l}^{-1}$ and $\text{Pb(II)}\ 40\text{ mg l}^{-1}$, on the $100\text{ mm} \cdot 4.6\text{ mm}$ ATA column. Eluent 1 M KNO_3 50 mM acetic acid at pH 3.7. Detection: PAR at 490nm	67
Figure 2.10	Separation of $\text{Al(III)}\ 2\text{ mg l}^{-1}$, $\text{Ga(III)}\ 10\text{ mg l}^{-1}$ and $\text{In(III)}\ 10\text{ mg l}^{-1}$, on the $100\text{ mm} \cdot 4.6\text{ mm}$ ATA column. Eluent 1 M KNO_3 50 mM acetic acid at pH 2.0. Detection: PCV at 580nm	68
Figure 2.11	The dependence of capacity factors for selected metals on eluent	71

	pH, with the PCV loaded column. Eluent: 1M KNO ₃ 50mM acetic acid	
Figure 2.12	Separation of Sr(II) 1mg l ⁻¹ , Ca(II) 1mg l ⁻¹ and Mg(II) 1mg l ⁻¹ , on the 100 · 4.6mm PCV column. Eluent: 1M KNO ₃ 50mM acetic acid at pH 10.2. Detection: PAR/ Zn-EDTA at 490nm.	72
Figure 2.13	The dependence of capacity factors for selected metals on eluent pH, with the CPC loaded column. Eluent: 1M KNO ₃ 50mM acetic acid.	75
Figure 2.14	Separation of Ba(II) 10mg l ⁻¹ , Sr(II) 10mg l ⁻¹ , Ca(II) 10mg l ⁻¹ and Mg(II) 20mg l ⁻¹ , on the 100 · 4.6mm CPC column. Eluent: 1M KNO ₃ 50mM acetic acid at pH 10.3. Detection: PAR/ Zn-EDTA at 490nm.	76
Figure 2.15	Separation of Cd(II) 10mg l ⁻¹ , Zn(II) 20mg l ⁻¹ and Pb(II) 20mg l ⁻¹ , on the 100 · 4.6mm CPC column. Eluent: 1M KNO ₃ 50mM acetic acid at pH 3.9. Detection: PAR at 490nm.	77
Figure 2.16	Separation of Ba(II) 10mg l ⁻¹ , Sr(II) 10mg l ⁻¹ , Ca(II) 10mg l ⁻¹ and Mg(II) 20mg l ⁻¹ , on the 100 · 4.6mm CAL column. Eluent: 1M KNO ₃ 50mM acetic acid at pH 10.1. Detection: PAR/ Zn-EDTA at 490nm.	80
Figure 2.17	The dependence of capacity factors for selected metals on eluent pH, with the CAL loaded column. Eluent: 1M KNO ₃ 50mM acetic acid	81
Figure 2.18	Separation of Mn(II) 0.5mg l ⁻¹ , Cd(II) 10mg l ⁻¹ and Pb(II) 5mg l ⁻¹ , on the 100 · 4.6mm PAR column. Eluent: 1M KNO ₃ 50mM acetic acid at pH 2.2. Detection: PAR at 490nm.	84
Figure 2.19	Separation of Mg(II) 1mg l ⁻¹ , Sr(II) 5mg l ⁻¹ and Ca(II) 10mg l ⁻¹ , on the 100 · 4.6mm PAR column. Eluent: 1M KNO ₃ 50mM acetic acid at pH 9. Detection PAR/ Zn-EDTA at 490nm	85
Figure 2.20	Separation of Al(III) 0.2mg l ⁻¹ , Ga(III) 10mg l ⁻¹ and In(III) 80mg l ⁻¹ , on the 100 · 4.6mm PAR column. Eluent: 1M KNO ₃ 50mM acetic acid at pH 1.4. Detection: PCV at 580nm.	86
Figure 2.21	The dependence of capacity factors for selected metal ions on eluent pH, with the PAR loaded column. Eluent: 1M KNO ₃ 50mM acetic acid.	87
Figure 2.22	Separation of Pb(II) 5mg l ⁻¹ , Cd(II) 10mg l ⁻¹ and Zn(II) 20mg l ⁻¹ ,	90

	on the 100 · 4.6mm impregnated SPP column. Eluent: 1M KNO ₃ 50mM acetic acid at pH 3.2. Detection: PAR at 490nm.	
Figure 2.23	Separation of Mn(II) 2mg l ⁻¹ , Pb(II) 20mg l ⁻¹ and Cd(II) 60mg l ⁻¹ , on the 100 · 4.6mm impregnated SPP column. Eluent: 1M KNO ₃ 50mM acetic acid at pH 3.5. Detection: PAR at 490nm	91
Figure 2.24	The dependence of capacity factors on the eluent pH, with the dynamically loaded SPP column. Eluent: 1M KNO ₃ 50mM acetic acid and 0.1mM SPP.	92
Figure 2.25	Separation of Pb(II) 5mg l ⁻¹ , Cd(II) 20mg l ⁻¹ and Zn(II) 40mg l ⁻¹ , on the 100 · 4.6mm dynamically loaded SPP column. Eluent: 1M KNO ₃ 50mM acetic acid, 0.1mM SPP at pH 2.3. Detection: PAR at 490nm	93
Figure 2.26	Zn(II) peak efficiency on CPC columns: retention time 2.6 minutes, achieved at pH 3.9 on 100mm column, and pH 3.3 with 200mm column length. Eluent: 1M KNO ₃ 50mM acetic acid. Detection: PAR at 490nm	96
Figure 2.27	Separation of Mn(II) 2mg l ⁻¹ , Cd(II) 40mg l ⁻¹ , Zn(II) 10mg l ⁻¹ and Pb(II) 30mg l ⁻¹ , on a 200 · 4.6mm CPC loaded column. Eluent: 1M KNO ₃ 50mM acetic acid at pH 4.2. Detection: PAR at 490nm.	97
Figure 2.28	Effect of column capacity on metal ion separations. Columns: 100 · 4.6mm impregnated with CPC. Capacity: A: 0.01mM Cu(II) /g resin, B: 0.005mM Cu(II) /g resin. 1: Cd(II) 10mg l ⁻¹ , 2: Zn(II) 20mg l ⁻¹ and 3: Pb(II) 20mg l ⁻¹ . Eluent: 1M KNO ₃ 50mM acetic acid at pH 3.9. Detection: PAR at 490nm.	99
Figure 2.29	The dependence of capacity factors on pH, as a function of column capacity. Columns: 100 · 4.6mm impregnated with CPC. Capacity: 1: 0.01mM Cu(II) /g resin, 2: 0.005mM Cu(II) /g resin. Eluent: 1M KNO ₃ 50mM acetic acid.	101
Figure 2.30	The dependence of capacity factors on eluent pH, as a function of column capacity. Columns: 100 · 4.6mm impregnated with CAL. Capacity: 1: 0.02mM Cu(II) /g resin, 2: 0.0004mM Cu(II) /g resin. Eluent: 1M KNO ₃ 50mM acetic acid	102
Figure 2.31	Affect of sample pH on Cd(II) peak with low capacity CPC column, 0.005mM Cu(II) /g resin. Eluent: 1M KNO ₃ 50mM	103

acetic acid at pH 4.5.

- Figure 2.32** Effect of mobile phase ionic strength (KNO_3) on retention of Pb(II) and Cu(II) with the 100 · 4.6mm ATA column. Eluent contained 50mM acetic acid, adjusted to pH 3.1 or 3.5. 105
- Figure 2.33** Effect of mobile phase ionic strength (KNO_3) on the retention of selected transition metal ions with the 100 · 4.6mm ATA column. Eluent contained 50mM acetic acid, adjusted to pH 3.5 or 4.5. 106

CHAPTER 3.

- Figure 3.1** Possible Structures of Complexes Formed at the Surface of APAS 121
- Figure 3.2** Separation of Ni(II) 1mg l^{-1} , Zn(II) 10mg l^{-1} , Cu(II) 2mg l^{-1} , Pb(II) 25mg l^{-1} and Mn(II) 5mg l^{-1} , on the 150 · 4.6mm APAS column. Eluent: 0.5M KNO_3 at pH 1.5. Detection: PAR at 490nm 124
- Figure 3.3** The dependence of capacity factors for transition metals on eluent pH, with the APAS column. Eluent: 1M KNO_3 adjusted to the appropriate pH with HNO_3 . 125
- Figure 3.4** The dependence of capacity factors for alkaline earth metals on eluent pH, with the APAS column. Eluent: 1M KNO_3 adjusted to the appropriate pH with HNO_3 126
- Figure 3.5** Dependence of aminophosphonate functionality on eluent pH. Based on the acid dissociation constants for β -propylaminophosphonic acid (homogeneous analogue of APAS) 127
- Figure 3.6** Speciation diagram of Cu(II) with aminoethanephosphonic acid 129
- Figure 3.7** Speciation diagram of Zn(II) with aminoethanephosphonic acid 130
- Figure 3.8** Speciation diagram of Mn(II) with aminoethanephosphonic acid 131

Figure 3.9	Separation of Ni(II) 1mg l ⁻¹ , Zn(II) 2mg l ⁻¹ , Cu(II) 1mg l ⁻¹ , Cd(II) 1mg l ⁻¹ and Mn(II) 1mg l ⁻¹ on the 250mm · 4.6mm APAS column. Eluent: 1M KNO ₃ 100mM HNO ₃ (pH 1). Detection: PAR at 490nm	135
Figure 3.10	Separation of Ba(II) 1.5mg l ⁻¹ , Ni(II) 1mg l ⁻¹ , Co(II) 2mg l ⁻¹ , Zn(II) 1mg l ⁻¹ , Pb(II) 5mg l ⁻¹ , Cd(II) 2.5mg l ⁻¹ , Mn(II) 1.5mg l ⁻¹ and Cu(II) 5mg l ⁻¹ , on the 250 · 4.6mm APAS column. Eluent: 1M KNO ₃ 5mM HNO ₃ (pH 2.3). Detection: PAR / Zn-EDTA at 490nm.	136
Figure 3.11	Separation of Ba(II) 1mg l ⁻¹ , Sr(II) 1mg l ⁻¹ , Ca(II) 1mg l ⁻¹ and Mg(II) 1mg l ⁻¹ on the 250 · 4.6mm APAS column. Eluent: 1M KNO ₃ at pH 5. Detection: PAR / Zn-EDTA at 490nm.	137
Figure 3.12	The dependence of capacity factors for transition metals on eluent pH, with the APAS column. Eluent: 0.5M KNO ₃ adjusted to the appropriate pH with HNO ₃	138
Figure 3.13	Separation of Ba(II) 1.5mg l ⁻¹ , Ni(II) 1mg l ⁻¹ , Co(II) 2mg l ⁻¹ , Zn(II) 1mg l ⁻¹ , Pb(II) 5mg l ⁻¹ , Cd(II) 2.5mg l ⁻¹ , Mn(II) 1.5mg l ⁻¹ and Cu(II) 5mg l ⁻¹ , on the 250 · 4.6mm APAS column. Eluent: 0.5M KNO ₃ 5mM HNO ₃ (pH 2.3). Detection: PAR / Zn-EDTA at 490nm.	139
Figure 3.14	The dependence of capacity factors on eluent pH for selected alkali metals on the PPAS column. Eluent: Milli-Q water adjusted to the appropriate pH with HNO ₃ .	142
Figure 3.15	Separation of Li(I) 1mg l ⁻¹ , Na(I) 5mg l ⁻¹ and K(I) 30mg l ⁻¹ on the 150 · 4.6mm PPAS column. Eluent: 0.4mM HNO ₃ (pH 3.4). Detection: Conductometric.	143

CHAPTER 4.

Figure 4.1	Chromatogram of Be(II) 20mg l ⁻¹ on the 100 · 4.6mm ATA Column. Eluent: 1M KNO ₃ 1mM HNO ₃ (pH 3). Detection: CAS at 560nm	151
Figure 4.2	Dependence of Capacity Factors on Eluent pH for Be(II),	152

	La(III), Lu(III) and Al(III), with the APAS Column. Eluent: 1M KNO ₃ adjusted to the required pH with HNO ₃	
Figure 4.3	Effect of Eluent pH on the Be(II) (10mg l ⁻¹) Peak Shape with the 50 · 4.6mm APAS Column. Eluent: 1M KNO ₃ adjusted to the required pH with HNO ₃ (1: 750mM, 2: 500mM, 3: 100mM, 4: 25mM, 5: 10mM and 6: 5mM HNO ₃). Detection: CAS at 560nm.	156
Figure 4.4	The Effect of Sample Ionic Strength: 1: Milli-Q, 2: 2M KNO ₃ , on the Separation of a Group of Metals, Ni(II) 0.5mg l ⁻¹ , Zn(II) 0.5mg l ⁻¹ , Cd(II) 2mg l ⁻¹ and Mn(II) 0.5mg l ⁻¹ with the 250 · 4.6mm APAS Column. Eluent: 1M KNO ₃ 5mM HNO ₃ . Detection: PAR at 490nm.	157
Figure 4.5	Structure of the Ascorbate : Iron(III) Complex	159
Figure 4.6	Absorbance Spectra for Be(II) with the CAS Post Column Reagent.	160
Figure 4.7	Speciation Diagram of Be(II) with EDTA	162
Figure 4.8	Effect of EDTA Concentration in Post Column Reagent (CAS) on Signal for 1mg l ⁻¹ Be(II) at 560nm.	163
Figure 4.9	Separation of Be(II) 5mg l ⁻¹ , from Al(III) 500mg l ⁻¹ , Fe(III) 300mg l ⁻¹ , Mn(II) 25mg l ⁻¹ , Zn(II) 4mg l ⁻¹ and Cu(II) 1mg l ⁻¹ on the 50 · 4.6mm APAS Column. Eluent: 1M KNO ₃ 0.5M HNO ₃ and 0.08M Ascorbic Acid. Detection: CAS at 560nm.	165
Figure 4.10	Speciation Diagram of Be(II) with the Fluoride ion	166
Figure 4.11	Sample 4 Standard Addition Curve.	168
Figure 4.12	Separation of Be(II) from Matrix Metals in a Certified Reference Material (GBW07311)	169

CHAPTER 5.

Figure 5.1	The separation of Pb(II) 4 mg l ⁻¹ , Cd(II) 10 mg l ⁻¹ , Co(II) 1 mg l ⁻¹ and Ni(II) mg l ⁻¹ on a 100 · 4.6mm PLRP-S 8µm PS-DVB Column. Eluent: 1M KNO ₃ , 1mM Quinaldic acid at pH 1.5. Detection: PAR at 490nm.	184
Figure 5.2	The separation of Mn(II) 0.5 mg l ⁻¹ , Pb(II) 5mg l ⁻¹ , Zn(II) 15 mg l ⁻¹	185

	I^- and Co(II) 5 mg l^{-1} on a $100 \cdot 4.6\text{mm}$ PLRP-S $8\mu\text{m}$ PS-DVB Column. Eluent: 1M KNO_3 , 0.1mM quinaldic acid at $\text{pH } 2.6$. Detection: PAR at 490nm .	
Figure 5.3	The separation of Pb(II) 2 mg l^{-1} , Cd(II) 10 mg l^{-1} , Co(II) 1 mg l^{-1} and Ni(II) 20 mg l^{-1} on a $100 \cdot 4.6\text{mm}$ C_{18} silica column. Eluent: 1M KNO_3 , 1mM Quinaldic acid at $\text{pH } 2$. Detection: PAR at 490nm .	186
Figure 5.4	The dependence of capacity factors for transition and heavy metal ions on eluent pH . Eluent: 1M KNO_3 0.1mM Quinaldic acid.	187
Figure 5.5	The separation of Mn(II) 2 mg l^{-1} , Pb(II) 70 mg l^{-1} and Cd(II) 80 mg l^{-1} , on a $100 \cdot 4.6\text{mm}$ PLRP-S $8\mu\text{m}$ PS-DVB Column. Eluent: 1M KNO_3 , 1mM dipicolinic acid at $\text{pH } 1.5$. Detection: PAR at 490nm .	190
Figure 5.6	The separation of Pb(II) 5 mg l^{-1} , Cu(II) 1 mg l^{-1} , Fe(III) 1 mg l^{-1} and U(VI) 40 mg l^{-1} , on a $100 \cdot 4.6\text{mm}$ PLRP-S $8\mu\text{m}$ PS-DVB Column. Eluent: 1M KNO_3 , 1mM dipicolinic acid at $\text{pH } 1.5$. Detection: PAR at 490nm .	191
Figure 5.7	The dependence of capacity factors for transition and heavy metal ions on eluent pH . Eluent: 1M KNO_3 1mM dipicolinic acid.	192
Figure 5.8	The dependence of capacity factors for transition and heavy metals on eluent pH . Eluent: 1M KNO_3 0.1mM dipicolinic acid.	193
Figure 5.9	The dependence of capacity factors for transition and heavy metals on the concentration of chlorodipicolinic acid in the eluent. Eluent: chlorodipicolinic acid in 1M KNO_3 at $\text{pH } 1.2$.	197
Figure 5.10	The separation of Mn(II) 0.5 mg l^{-1} , Co(II) 0.5 mg l^{-1} , Ni(II) 0.5 mg l^{-1} , Pb(II) 10 mg l^{-1} and Cd(II) 20 mg l^{-1} , on a $100 \cdot 4.6\text{mm}$ PRP-1 $7\mu\text{m}$ PS-DVB Column. Eluent: 1M KNO_3 , 1mM chlorodipicolinic acid at $\text{pH } 1.2$. Detection: PAR at 490nm .	198
Figure 5.11	The separation of Mn(II) 0.5 mg l^{-1} , Co(II) 1 mg l^{-1} , Ni(II) 0.5 mg l^{-1} , Zn(II) 2 mg l^{-1} , Cu(II) 1 mg l^{-1} , Pb(II) 10 mg l^{-1} and Cd(II) 20 mg l^{-1} , on a $100 \cdot 4.6\text{mm}$ PRP-1 $7\mu\text{m}$ PS-DVB Column. Eluent: 1M KNO_3 , 0.5mM chlorodipicolinic acid at $\text{pH } 1.2$.	199

Figure 5.12	The dependence of capacity factors for transition and heavy metals on eluent pH. Eluent: 1M KNO ₃ 1mM dipicolinic acid.	200
Figure 5.13	The dependence of capacity factors for (1) chlorodipicolinic acid and (2) dipicolinic acid on eluent pH. Eluent: 1M KNO ₃ .	202
Figure 5.14	The dependence of capacity factors for transition and heavy metal ions on eluent pH. Eluent: 1M KNO ₃ , 0.5mM Chlorodipicolinic acid	204
Figure 5.15	The separation of Mn(II) 0.5 mg l ⁻¹ , Co(II) 0.5 mg l ⁻¹ , Ni(II) 0.5 mg l ⁻¹ , Zn(II) 2 mg l ⁻¹ , Cu(II) 2 mg l ⁻¹ , Pb(II) 10 mg l ⁻¹ and Cd(II) 20 mg l ⁻¹ on a 250 · 4.6mm PRP-1 7µm PS-DVB Column. Eluent: 1M KNO ₃ , 0.5mM Chlorodipicolinic acid and 10mM HNO ₃ (pH 2). Detection: PAR at 490nm.	205
Figure 5.16	The dependence of capacity factors for selected metals on eluent pH. Eluent: 1M KNO ₃ , 0.25mM chlorodipicolinic acid	206
Figure 5.17	The separation of Mn(II) 0.5 mg l ⁻¹ , Co(II) 0.5 mg l ⁻¹ , Ni(II) 0.5 mg l ⁻¹ , Zn(II) 2 mg l ⁻¹ , Cu(II) 2 mg l ⁻¹ , Pb(II) 10 mg l ⁻¹ and Cd(II) 20 mg l ⁻¹ on a 250 · 4.6mm PRP-1 7µm PS-DVB Column. Eluent: 1M KNO ₃ , 0.25mM Chlorodipicolinic acid and 6mM HNO ₃ (pH 2.2). Detection: PAR at 490nm	207
Figure 5.18	The separation of Mn(II) 0.5 mg l ⁻¹ , Co(II) 0.5 mg l ⁻¹ , Ni(II) 0.5 mg l ⁻¹ , Zn(II) 2 mg l ⁻¹ , Cu(II) 1 mg l ⁻¹ , Pb(II) 10 mg l ⁻¹ and Cd(II) 20 mg l ⁻¹ on a 300 · 4.6mm PRP-1 7µm PS-DVB Column. Eluent: 1M KNO ₃ , 0.25mM Chlorodipicolinic acid and 6.25mM HNO ₃ (pH 2.2). Detection: PAR at 490nm.	208

CHAPTER 6.

Figure 6.1	Absorbance spectra of U(VI) with the Arsenazo III post column reagent.	218
Figure 6.2	The dependence of capacity factors for U(VI) and Fe(III) on eluent pH. Eluent: 1M KNO ₃ with various concentrations of dipicolinic acid adjusted to the appropriate pH with HNO ₃	220
Figure 6.3	The separation of U(VI) 20mg l ⁻¹ from Fe(III) 2mg l ⁻¹ on a 100 · 4.6mm PRP-1 7µm PS-DVB column. Eluent: 1M KNO ₃ , 0.1M	222

	HNO ₃ (pH 1) and 0.1mM dipicolinic acid. Detection: PAR at 490nm.	
Figure 6.4	The leaching of dipicolinic from the 100 · 4.6mm PRP-1 7µm PS-DVB column, shown with the repeat injection of U(VI). Eluent: 1M KNO ₃ 0.5M HNO ₃ .	225
Figure 6.5	Effect of sample loop volume (100µl – 1ml) on the U(VI) peak, using a 100 · 4.6mm PRP-1 7µm PS-DVB column. Eluent: 1M KNO ₃ 0.5M HNO ₃ and 0.1mM dipicolinic acid. Detection: Arsenazo III at 654nm	227
Figure 6.6	Speciation diagram of the uranyl ion UO ₂ ²⁺ with the fluoride ion.	228
Figure 6.7	The separation of 50µg l ⁻¹ U(VI) from matrix metals in a spiked mineral water, on the 100 · 4.6mm PRP-1 7µm PS-DVB column. Eluent: 1M KNO ₃ 0.5M HNO ₃ and 0.1mM dipicolinic acid. Detection: Arsenazo III at 654nm.	231
Figure 6.8	The separation of 50µg l ⁻¹ U(VI) from matrix metals in a spiked seawater on the 100 · 4.6mm PRP-1 7µm PS-DVB column. Eluent: 1M KNO ₃ 0.5M HNO ₃ and 0.1mM dipicolinic acid. Detection: Arsenazo III at 654nm.	232
Figure 6.9	The standard addition calibration curve for sample 3.	234
Figure 6.10	The separation of U(VI) from matrix metals in the certified sediment sample GBW07311, on a 100 · 4.6mm PRP-1 7µm PS-DVB column. Eluent: 1M KNO ₃ 0.5M HNO ₃ and 0.1mM dipicolinic acid. Detection: Arsenazo III at 654nm.	235
Figure 6.11	Absorbance spectra of selected transition metals (1mg l ⁻¹) with the PAR – borate post column reagent.	243
Figure 6.12	The effect of 500mg l ⁻¹ Ca(II) and Mg(II) on the dynamically modified substrate. Column: 300 · 4.6mm PRP-1 7µm PS-DVB. Eluent: 1M KNO ₃ 6mM HNO ₃ and 0.25mM chlorodipicolinic acid (pH 2.2). Detection: PAR at 520nm.	249
Figure 6.13	The effect of 500mg l ⁻¹ Ca(II) and Mg(II) on the dynamically modified substrate. Column: 300 · 4.6mm PRP-1 7µm PS-DVB. Eluent: 1M KNO ₃ 30mM HNO ₃ and 0.25mM chlorodipicolinic acid (pH 1.5). Detection: PAR at 520nm.	250
Figure 6.14	The separation of Cd(II) 100µg l ⁻¹ , Pb(II) 500µg l ⁻¹ and Cu(II) 200µg l ⁻¹ on the 100 · 4.6mm PLRP-S 5µm PS-DVB column.	252

Eluent: 1M KNO₃ 30mM HNO₃ and 0.25mM chlorodipicolinic acid (pH 1.5). Detection: PAR at 520nm.

- Figure 6.15** Chromatogram of the transition metal ions in the certified soft water sample TMDA 54.2 on the 300 · 4.6mm PRP-1 7µm PS-DVB column. Eluent: 1M KNO₃ 6mM HNO₃ and 0.25mM chlorodipicolinic acid. Detection: PAR at 520nm. 255
- Figure 6.16** Determination of Cd(II) 1-4µg l⁻¹ on the 100 · 4.6mm PLRP-S 5µm PS-DVB column. Eluent: 1M KNO₃ 30mM HNO₃ and 0.25mM chlorodipicolinic acid. Detection: PAR at 520nm. 256
- Figure 6.17** The separation of Cd(II), Pb(II) and Cu(II) from matrix interferences in the certified rice flour GBW08502 on the 100 · 4.6mm PLRP-S 5µm PS-DVB column. Eluent: 1M KNO₃ 30mM HNO₃ and 0.25mM chlorodipicolinic acid. Detection: PAR at 520nm 259

ACKNOWLEDGEMENTS

First and foremost, I would like to thank my supervisor, Dr. Phil Jones, for his continuous support, encouragement and friendship throughout the last three years. A big thanks also to Dr. Pavel Nesterenko, for helpful advice during his visits to Plymouth and for being a good snooker opponent.

For financial support of this work I would like to acknowledge the University of Plymouth. I would like to thank the staff at the University for their help during the three years including Andy 'the tetris king' Arnold, Dr. Roger Evans and Derek Henon.

A big up thanks also to my mates at the University, especially 'dodgy' Dave Whitworth, Lesley 'farmer' Johns, Andy 'beech' Bowie and Toby 'cheeky boy' Mathews. Good times on the travelling and festivals front. I would also like to give thanks to my ex-lab partner Simon 'nukem' Hardy, especially for his invaluable assistance in fixing my computer innumerable times. Thanks also to James Cowan, a fellow sci-fi fan, for his friendship and making me realise it wasn't just my work that could go awry on occasions. Additional thanks to Paul Sutton for the squash thrashings, and Stewart Niven for supporting Stockport.

I would also like to express sincere thanks to my parents and sister Liz for their support throughout this period.

Finally, I would like to thank my best mate Cathy 'heidi' Ridgway, for her friendship, encouragement and ability to chill me out when required.

Cheers.

AUTHORS DECLARATION

At no time during the registration for the degree of Doctor of Philosophy has the author been registered for any other University award.

This study was financed with the aid of a studentship from the University of Plymouth.

A programme of advanced study was undertaken, which included instruction in high performance liquid chromatography theory and instrument operation and metal chelation theory.

Relevant scientific seminars and conferences were regularly attended at which work was often presented, and several papers prepared for publication.

Publications

1. Aminophosphonate – functionalized silica: A versatile chromatographic stationary phase for High Performance Chelation Ion Chromatography. P.N. Nesterenko, M.J. Shaw, S.J. Hill and P. Jones, *Microchem. J.*, 62 (1999) 58-69.
2. Chelation ion chromatography of metal ions using high performance substrates dynamically modified with heterocyclic carboxylic acids. M.J. Shaw, S.J. Hill and P. Jones, *Anal. Chim. Acta*, 401 (1999) 65-71.
3. High-performance chelation ion chromatography of transition metal ions on polystyrene-divinylbenzene resin dynamically modified with 4-chlorodipicolinic acid. M.J. Shaw, S.J. Hill, P. Jones and P.N. Nesterenko, *Anal. Comm.*, 36 (1999) 399-401.
4. Determination of Beryllium in a Stream Sediment by High Performance Chelation Ion Chromatography. M.J. Shaw, S.J. Hill, P. Jones and P.N. Nesterenko, *J. Chromatogr. A*, (2000) in the press.
5. Determination of Uranium in Environmental Matrices by Chelation Ion Chromatography using a High Performance Substrate Dynamically Modified with 2,6-Pyridinedicarboxylic Acid. M.J. Shaw, S.J. Hill, P. Jones and P.N. Nesterenko, *Chromatographia*, (2000) in the press.

Presentations and Conferences Attended

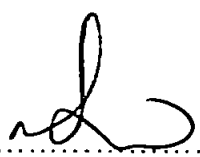
Research and Development Topics in Analytical Chemistry, University of Northumbria, UK, 1997. Poster presentation.

International Ion Chromatography Symposium, San Francisco, USA, 1997. Poster presentation.

IONEX '98, Wrexham, UK, 1998. Poster presentation.

Pittcon '99, Orlando, USA, 1999. Attendance.

Departmental Research Lectures, University of Plymouth, UK, 1997, 1998 and 1999. Oral presentations.

Signed..... 

Date..... 20/4/00

Chapter 1. Introduction

1.1 Trace metal analysis

The term 'trace' elements refers to those which are present at concentrations between 1-100mg l⁻¹ (0.01%) [1], now routinely determined due to gradual developments in sample handling techniques and advances in instrumentation. 'Ultra-trace' refers to concentrations of <1mg l⁻¹, whilst 'minor' denotes a concentration between 0.01-1%. Above this, concentrations are referred to as major.

Concerning trace metals, it is imperative to monitor their fate in the environment due to the potential toxicity many resulting metal compounds have, after release from various anthropogenic sources including industrial effluents from process streams. Increasing concentrations above natural levels can have a devastating impact upon the surrounding ecosystem, and can lead to accumulation through the food chain to potentially lethal levels. Many serious pollution incidents have resulted in the implementation of legislation, through which the levels permissible for discharge into the environment are continuously regulated and enforced.

The determination of trace metals is important for other reasons than to control release into the environment. It has, for example, increased our understanding of the distribution of trace metals through the oceanic water column, and metabolism within biological systems.

Many metals can exist as either toxic or non-toxic moieties dependent upon their speciation in various environments.

These species can often be converted into different forms by such actions as weathering, uptake and elimination from biota, fixation in sediments or re-mobilisation. Speciation is important as different inorganic species can possess markedly different biological and toxicological properties, demonstrated by Cr(III), essential to human nutrition, whilst Cr(VI) compounds are highly toxic to aquatic plants and animal life.

It can also be very important to quantify total element concentrations in samples, some metals including Cd(II) and Pb(II) being potentially toxic in any form.

Many analytical techniques have been improved to detect total metal concentrations at natural and elevated levels. Atomic spectrometry, voltammetry and inductively coupled plasma mass spectrometry (ICP-MS) have all been developed to determine trace concentrations of metals in aqueous media.

A significant advantage of modern liquid chromatographic (LC) techniques, including ion chromatography, is the ability to separate individual element species, in addition to separating metal ion groups themselves. Hyphenation of LC with analytical instrumentation including ICP-mass spectrometers has become a powerful tool for the determination of metals in various samples, combining the separation power of chromatography with detection sensitivity.

Indeed, liquid chromatography alone has become a valuable alternative to the aforementioned techniques. Improvements in instrumentation, stationary phases and detection systems have dramatically increased the viability of LC as a tool for metal ion determinations. Significant advantages of selecting LC for this task include system simplicity, speed of analysis, low running costs and a potential for on-line monitoring. In essence, modern day chromatography exemplifies the successful marriage of analyte separation and essentially instantaneous measurement of separated components, all within a cost effective package.

This introduction will provide an overview of the background and developments of liquid chromatography for the determination of trace metals in sample matrices.

1.2 Principles of the liquid chromatographic process

The purpose of chromatography is to separate analytes into discrete bands [2]. The IUPAC definition of chromatography states it as 'a method used primarily for the separation of the components of a sample, in which the components are distributed between two phases, one of which is stationary while the other moves'.

Hence, liquid chromatography consists of a **stationary phase**, usually a column packed with a solid or gel in a finely divided spherical form, and the **mobile phase**, a liquid continuously pumped through the column which fills the space between the packing particles – the interstitial or void volume. When a third component, denoted the **solute**, is added to the system, it will distribute between the phases, eventually establishing an equilibrium which is described by the **partition or distribution coefficient, K_D** :

$$K_D = C_S / C_M$$

C_S and C_M are the concentrations of the solute in the stationary phase and mobile phase respectively. A solute with a larger K_D value will spend more time in the stationary phase than one with a smaller value. Indeed, this retention of the solute, or analyte of interest, controlled by K_D , is expressed as the retention time and represents the time taken after sample injection into the chromatographic system for the maximum concentration of analyte to be eluted.

Another important parameter that is widely used to describe the migration rate of a solute through a column is the **capacity factor**, denoted k' . This can be expressed as shown in the following equation:

$$k' = t_R - t_0 / t_0$$

t_R is the retention time of the analyte peak, t_0 representing the retention time of an unretained peak, also described as the **dead-time** of the system. k' is a simple and experimentally more accessible term than K_D , as it involves the determination of two

readily measurable quantities, and provides information about the relative speed of separation.

To describe the relative separation of two analyte species, the **selectivity factor**, α is needed, expressed as:

$$\alpha = k'_2 / k'_1$$

k'_2 is the capacity factor of the more strongly retained analyte. It should be noted that small k' values imply that the analytes elute close to the void volume, which would result in a poor chromatographic separation. However, large k' values indicate that an analyte is strongly held up on the column, which can result in peak broadening and a consequent loss of sensitivity. Thus, column selectivity is a very important parameter in a chromatographic system, with k' values for solutes ideally being not too small or large to maintain a reasonable analysis time. This can be achieved by altering the mobile phase and/or the stationary phase constituents.

As solute components traverse a chromatographic column, the width of the band travelling through the stationary phase increases, a process known as 'band broadening'. The degree to which two components are separated is governed, amongst other factors, by the amount of band broadening which has occurred. An optimum chromatographic system is one in which band broadening is minimised, and this can be achieved by increasing the column efficiency.

Column efficiency can be represented by the number of **theoretical plates**, N , which can be calculated from the retention time of the peak, and the width at full or half peak height ($W_{1/2}$). Half peak height is more commonly used as this gives an accurate width at half the peak height, whereas tangent lines are extrapolated to the baseline to determine the peak width at full height. Therefore, N can be written as:

$$N = 16(t_R / W)^2 \text{ or } N = 5.54(t_R / W_{1/2})^2$$

However, these equations do not take into consideration the dead – time of the system. To account for this, the number of effective plates, N_{eff} , provides a more accurate

representation of column efficiency. N_{eff} is actually lower than N , since the dead – time of the system is excluded from the calculation. Efficiency increases with an increasing number of effective plates, with a more efficient column having more separating power.

N or N_{eff} are related to the **plate height, H** , by the equation:

$$H = L / N$$

L is the length of the column packing. This parameter can provide a direct comparison about the quality of two columns, as it accounts for unit column length.

The actual difference between the retention times of two analyte peaks can be given by their **resolution, R** . This is the term most commonly applied to describe the quality of a chromatographic separation, and is the ratio of the distance between the analyte peak maxima to the mean width W of the analyte peak.

It can be expressed as:

$$R = 2(t_{R2} - t_{R1}) / W_1 + W_2$$

Theoretically, an eluting peak will assume a Gaussian distribution in which the concentration of the solute is related to the time elapsed from the point of injection. Unfortunately, this is not the case, as a disadvantage of chromatography is the broadening of the solute zone during its passage through a column. The longer the solute remains in the system, the greater the degree of dispersion. Therefore, highly efficient columns are required to produce sharper peaks in comparison with less efficient columns over the same retention time.

The parameters R , N , α and k' can all be connected by the equation:

$$R = \sqrt{N/4} (\alpha - 1/\alpha) (k'/1+k')$$

Figure 1.1 gives a diagrammatical representation of the key parameters associated with chromatographic separations.

All of the parameters outlined here can provide a basic evaluation of the liquid chromatographic system. Further details on the fundamentals and applications of these

liquid chromatographic methods can be found in various books including Katz *et al* [3], Lough *et al* [4] and Hanai [5].

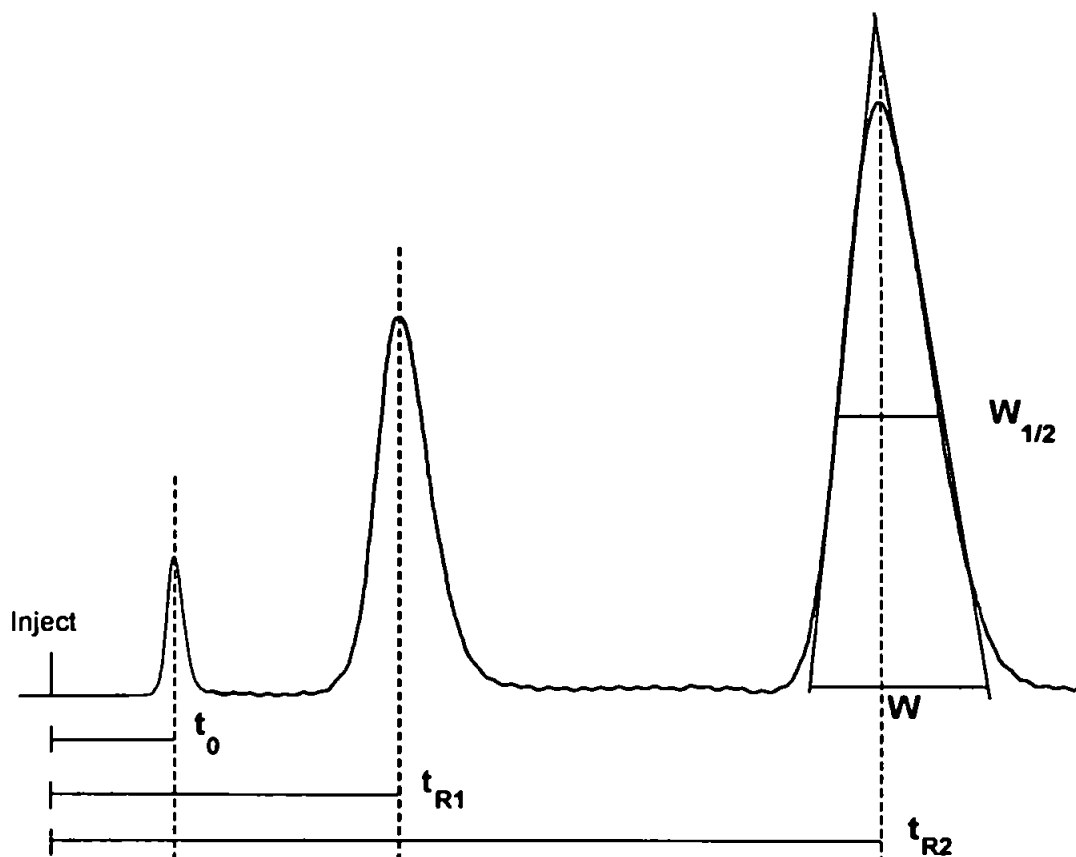


Figure 1.1 A chromatographic separation illustrating the parameters used to obtain calculations.

Any methods which are used for the separation and analysis of ionic species now fall under the general heading entitled 'ion chromatography', which encompasses the studies undertaken in this thesis.

1.3 Ion chromatography

Ion chromatography (IC) is an analytical technique for the separation and determination of ionic solutes [6]. The term was first used in 1975, by Small *et al* [7], when they described a novel ion – exchange chromatographic method utilising high efficiency latex

agglomerated pellicular anion – exchange columns for the separation and conductimetric detection of anionic species.

This technique has since developed rapidly, providing a reliable and accurate method for the simultaneous determination of many simple inorganic cations and anions. IC was originally ‘coined’ to describe the use of ion – exchange materials in the separation process, but has now evolved to include any chromatographic technique which allows the determination of ions, principally ion – exchange, ion exclusion and ion – pair chromatography. However, of these three mechanisms, ion – exchange is the most widely used, and can be further subdivided into two distinct categories: simple ion – exchange and chelating ion – exchange, the latter suitable for metal ion separations only. This distinction was made in a review paper by Jones and Nesterenko [8].

1.3.1 Simple ion – exchange

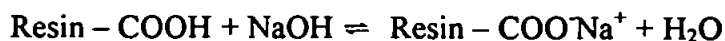
The basic premise of ion – exchange involves competitive ionic attraction for the ionic sites on the stationary phase, as the solutes travel through a column. A more precise definition of ion – exchange was given by Harjula and Lehto [9], who stated: ‘ion – exchange is the equivalent exchange of ions between two or more ionised species located in different phases, at least one of which is an ion – exchanger, without the formation of new types of chemical bonds’. They state that ‘an ion – exchanger is a phase containing an osmotically inactive insoluble carrier of the electrical charge (matrix)’. This means that the carrier, the ionic functional groups, which are attached to the support framework by covalent bonding, cannot migrate into the mobile phase.

The ionic functional groups are referred to as the **fixed ions**, with the ions of opposite charge referred to as the **counter ions**, which are held in place by electrostatic forces. The insoluble support matrix is usually a styrene / divinylbenzene co – polymer, as this framework is stable over a wide pH range 0 – 14. Divinylbenzene is necessary to maintain

the stability of the resin, by cross – linking the styrene chains. When extremes of pH are not required for good chromatography, silica based exchangers can be employed. Silica based materials can exhibit a higher chromatographic efficiency as it is possible to pack the particles at high pressure (5000psi), which produces a uniform and stable chromatographic bed. A significant drawback of polymeric resins is that they are often subject to pressure limitations (<2000psi). Figure 1.2 illustrates the basic framework of the polymeric co – polymer and silica substrates.

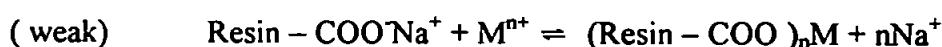
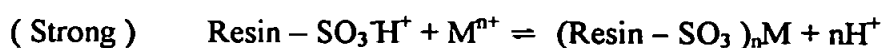
During the ion – exchange process, counter – ions are replaced by ions of the same charge from the external solution. The ion – exchanger is classified as a cation – exchange material when the fixed ion carries a negative charge, and as an anion – exchange material when the fixed ion carries a positive charge. Both cation and anion – exchangers can be denoted as either strong or weak, depending upon the nature of the bonded functional groups.

A strong cation – exchanger is sulfonate, $-\text{SO}_3\text{M}^{n+}$, which retains the negative charge on the fixed ion over a wide pH range from 1-14. Weak cation – exchangers include carboxylate $-\text{COO}^- \text{M}^{n+}$, phosphonate $-\text{PO}_3\text{H}^- \text{M}^{n+}$ and phenolate $-\text{OM}^{n+}$. These functional groups are ionised over a much narrower pH range, typically 5-14, and require a sufficiently high pH for use, as exemplified by the use of a sodium hydroxide eluent with a carboxylic acid exchanger:



Quaternary amine functional groups $-\text{N}(\text{CH}_3)_3^+\text{OH}^-$ form very strong anion - exchangers, whilst less substituted amines form weak anion – exchangers.

Cation exchange is used to separate free metal ions M^{n+} , this metal exchanging with either the free acid (H^+) or salt, for example Na^+ or NH_4^+ , which are present as the counter ions:



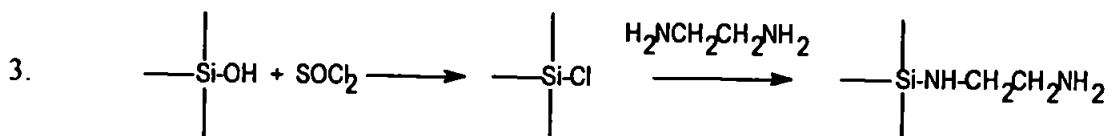
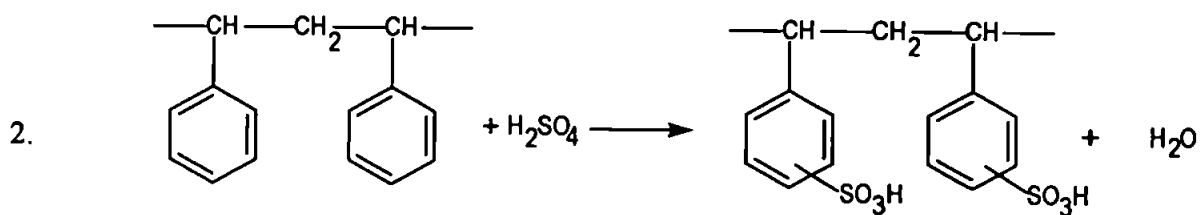
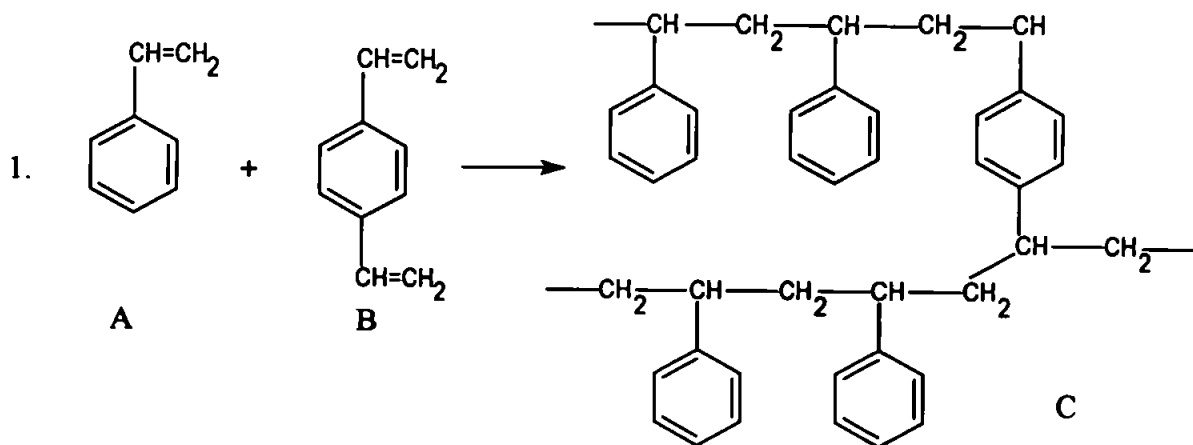
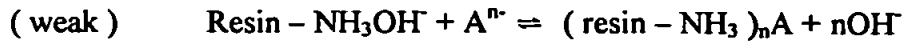
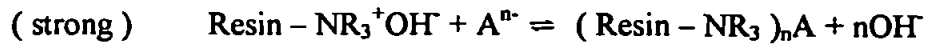


Figure 1.2 The synthesis and structure of: (1) polystyrene divinylbenzene (PS-DVB) (C) from styrene (A) and divinyl benzene (B); (2) a typical reaction scheme for introducing sulfonic acid groups onto PS-DVB; and (3) a mechanism for synthesising a silica sorbent.

With anion exchange reactions, the counter ion charge is simply reversed:



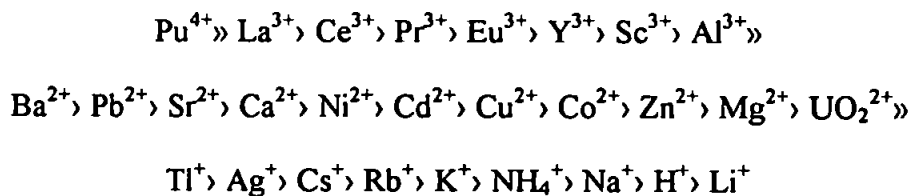
It should be noted that during the elution, the solution concentration of counter ions is much greater than the concentration of M^{n+} or A^{n-} ions in the mobile phase. Furthermore, the ion exchanger has a vast number of exchange sites relative to the number of solute ions being retained, and there is little change in the overall concentrations of counter ions in both the solution and on the fixed ion sites with this shift in equilibrium.

The equilibrium constants for the exchanging of a counter ion with a solute ion is known as the selectivity coefficient, and provides a means for determining the relative affinities of an ion-exchanger for different ions. It can be expressed as:

$$K_{M,C} = [\text{M}_r^{x+}]^y [\text{C}_e^{y+}]^x / [\text{M}_e^{x+}]^y [\text{C}_r^{y+}]^x$$

Thereby, a solute cation M^+ displaces a counter ion C^+ (the competing ion). 'y' moles of M^{x+} are exchanged with 'x' moles of C^{y+} , the subscript 'r' denoting the resin (stationary phase) and 'e' the eluent (mobile phase).

The selectivity coefficients for the uptake of cations by a strong cation exchange resin are generally in the following order [6]:



This selectivity is dependent upon several controlling factors. One is the electroselectivity, where an increase in the charge on the solute ion increases its affinity for an ion exchanger through increased coulombic interactions. This trend is reflected in the series $\text{Pu}^{4+} \gg \text{La}^{3+} \gg \text{Ba}^{2+} \gg \text{Tl}^+$. The size of the solvated solute ion also has a significant impact, with ions of smaller solvated size showing greater affinity than larger ions. This is illustrated in the sequences $\text{Ba}^{2+} \gg \text{Sr}^{2+} \gg \text{Ca}^{2+} \gg \text{Mg}^{2+}$ and $\text{Cs}^+ \gg \text{Rb}^+ \gg \text{K}^+ \gg \text{Na}^+ \gg \text{Li}^+$. This is exactly the reverse of the sequence of ionic radii for the hydrated ions, with the most strongly hydrated ion, Li^+ ,

being the most weakly held. This parameter is related to swelling of the resin, since a smaller ion is more easily accommodated in the resin pores. For example, Mg^{2+} has a much larger charge density compared with Ba^{2+} which has a much greater atomic weight. Therefore, Ba^{2+} is less hydrated in aqueous solution and has a smaller radius than the hydrated Mg^{2+} , which is more weakly retained. Other factors which can affect the ion exchange selectivity include the functional group on the ion exchanger, the ion exchange capacity and the use of complexing agents in the eluent.

A limitation of IC is that high capacity ion exchangers require an eluent containing a high concentration of competing ions in order to elute the solutes within a reasonable time scale. However, this increased concentration of background electrolyte can swamp the analyte signal when using conductivity detection, which lead to the development of suppressed conductivity systems to overcome this problem. UV-Vis based detection systems are not prone to this complication, however. Low capacity ion exchangers can utilise non – suppressed conductivity detection, but these resins are prone to ‘swamping’ of the fixed ion sites by high ionic strength samples, which can affect the separation efficiency and detection sensitivity.

Adding a complexing agent to an eluent, which already contains a competing ion can add a further dimension to the selectivity. For example, for metal ions a complex can be formed between the ligand species and the metal ion, reducing the effective charge of M^{n+} , thereby the solute is less successful in competing for the cation exchange sites, decreasing analysis time. Typical complexing agents include tartaric acid, citric acid and 2-hydroxyisobutyric acid (HIBA). Weaker liquids can sometimes be used including acetic acid and lactic acid. An example of this approach is shown in figure 1.3 with an eluent containing both a ligand (e.g. tartrate) and a competing cation: ethylenediammonium (enH_2^{2+}). The retention of the solute cation M^{2+} , is influenced by the competitive effect for the sulfonic acid groups exerted by enH_2^{2+} (pushing effect A) and also by the complexation of M^{2+} by the

deprotonated ligand L^{2-} (pulling effect B). This 'pushing' and 'pulling' affects the elution of the solute.

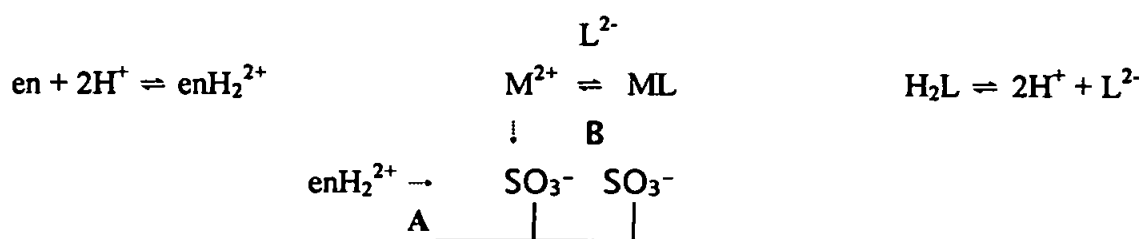


Figure 1.3. Representation of equilibria existing between a solute cation M^{2+} , en, and an added ligand H_2L , at the surface of an ion exchanger.

The eluent pH controls the protonation of enH_2^{2+} and the deprotonation of the ligand, which in turn controls the degree of complex formation and retention of the solute. For this system to be effective, the degree of complexation should be only partial, otherwise the metal ions are complexed too strongly and would elute rapidly with little or no separation. A review detailing the use of complexing agents for ion chromatographic separations is given by Timerbaev and Bohn [10] and a book chapter by Karcher and Krull [11].

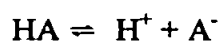
Further details concerning the theory and application of ion chromatography are given in books by Small [2], Haddad and Jackson [6], and Weiss [12].

1.3.2 Chelating ion exchange

Chelation ion – exchange involves the formation of a co-ordinate bond between a cation and a ligand immobilised on a stationary phase support, during the exchange process. This sorption is dependent upon the conditional stability constants between the metal ion and complexing agent, and potentially offers a far more selective separation process than simple ion - exchange. Chelating groups have little or no affinity for monovalent salt ions, which form very weak co-ordinate bonds, but this affinity increases for divalent and trivalent metals. A diagram depicting the sorption mechanisms of simple ion-exchange and

chelation ion-exchange is given in Figure 1.4. Different chelating functional groups can exhibit unique metal selectivities as a function of the conditional stability constants of the metal chelate, providing this technique with an advantage in analysing complex matrices. In addition, pH is a dominant factor in the separation of metal ions by chelation ion – exchange, as the hydrogen ion concentration determines the values of the conditional stability constants of the metal complexes on the substrate surface. This is because most chelating ligands are conjugate bases of weak acid groups, and consequently have a strong affinity for H⁺ ions.

A conjugate base is the species formed when an acid loses a proton, becoming a proton acceptor:



HA is the conjugate acid, A⁻ the conjugate base, the reaction controlled by the acid dissociation constant K_a. A weak acid is one which reacts incompletely with water to give both the parent acid and its conjugate base. The weaker the acid group, the stronger the conjugate base and corresponding ligand for metal ions. For example, 1,2-dihydroxybenzene (pyrocatechol) which contains two OH groups is a weaker acid than 1,2-benzenedicarboxylic acid (phthalic acid) containing two COOH groups, and therefore forms a stronger conjugate base. Therefore, metal selectivities can be tailored by modifying a substrate with a particular chelating functionality and altering the mobile phase pH. Unfortunately, chelation ion- exchange kinetics can be slower than for simple ion – exchange, resulting in broader peaks with increasing analysis time. This effect can be somewhat remedied by modifying high efficiency substrates with a smaller particle size, which has resulted in the technique being termed ‘High Performance Chelation Ion Chromatography’ (HPCIC). This term distinguishes high performance chelating substrates, from low efficiency columns employed for general sample clean – up and batch preconcentration. A comprehensive study of this HPCIC approach to metal ion separation is given in a review by Jones and Nesterenko [8].

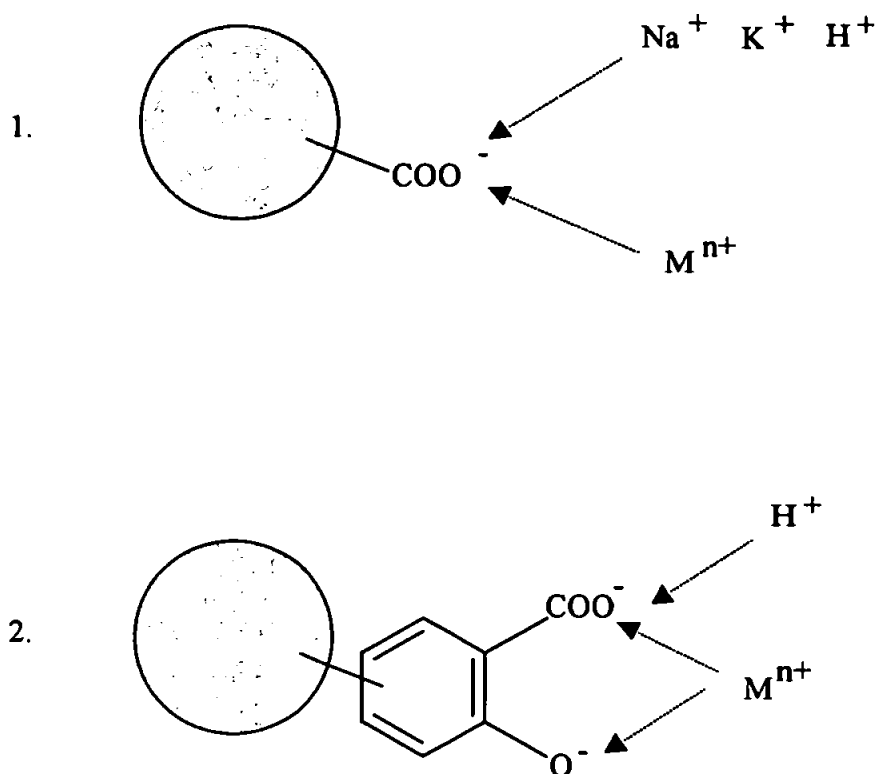


Figure 1.4 Simple ion-exchange (1) and chelating ion-exchange (2) mechanisms

1.3.2.1 Principles of chelation

The branch of science which involves the formation and dissociation of metal complexes is known as co-ordination chemistry. The association of a metal ion with an anion or polar molecule, known as the ligand forms the complex. A simple description of the nature of the metal – ligand bond treats the metal as an electron pair acceptor and the ligand as an electron pair donor. This is the Lewis concept of acids and bases: the metal being a Lewis acid and the ligand a Lewis base [13]. These acids and bases can be hard, soft or show intermediate behaviour.

A metal ion is a hard acid if it is small, carries a high positive charge, has a small ionic radius and is not easily polarised. Conversely, a soft metal ion has a low positive charge, is large and contains easily excited outer electrons.

A ligand is a soft base if it is highly polarised and easily excited, has low electronegativity and is easily distorted, with high energy empty molecular orbitals. A hard base demonstrates the opposite characteristics.

Tables 1.1 and 1.2 display metal ions and ligands as hard, soft or intermediate acids and bases respectively. It can be seen that the order for bases follows the general trend of $S < N < O$, with ligands containing oxygen being the hardest. For the cations, the trivalent Al^{3+} ion with a radius of 0.51 \AA is a hard acid, whereas Ag^+ , a monovalent ion of radius 1.26 \AA , is a soft acid.

As a general rule, hard acids form stronger bonds with hard bases (having a large degree of ionic character in the bond), with soft acids preferring to co-ordinate with soft bases (having mainly covalent character in the bond). However, there are exceptions. Hard bases, for example carboxylic acids, can bind more strongly to soft cations than hard cations of the same ionic charge [14]. This is because the ionic radius of a cation can be important in complexing with hard ligands. With the alkaline earth metals, the stability of complexes formed usually decreases with an increasing cation size for small ligands (hard base), whilst increasing for larger ligands (softer bases). Soft ligands, nevertheless, will always complex more strongly to soft cations.

Table 1.1 Metal ions as hard or soft acids [14]

<i>Hard</i>	$H^+ Li^+ Na^+ K^+ Rb^+ Cs^+ Be^{2+} Mg^{2+} Ca^{2+} Sr^{2+} Ba^{2+} Ra^{2+} Mn^{2+} UO_2^{2+} VO^{2+}$ $Al^{3+} Sc^{3+} Ti^{3+} Cr^{3+} Fe^{3+} Co^{3+} Ga^{3+} In^{3+} MoO_3^{3+} Y^{3+} La^{3+} -Lu^{3+} Zr^{4+} Hf^{4+} Th^{4+} U^{4+}$
<i>Intermediate</i>	$Cr^{2+} Fe^{2+} Ru^{2+} Os^{2+} Co^{2+} Ni^{2+} Cu^{2+} Zn^{2+} Sn^{2+} Pb^{2+} Rh^{3+} Ir^{3+} Sb^{3+} Bi^{3+}$
<i>Soft</i>	$Cu^+ Ag^+ Au^+ Hg^+ Tl^+ Pt^{2+} Pd^{2+} Cd^{2+} Tl^{3+} Pt^{4+} Te^{4+}$

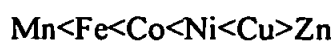
Table 1.2 Ligands as hard or soft bases [14]

Hard H₂O ROH R₂O HO[•] RO[•] RCO₂⁻ NO₃⁻ ClO₄⁻ F⁻ Cl⁻ CO₃²⁻ SO₄²⁻ PO₄²⁻

Intermediate NH₃ RNH₂ Aniline Pyridine N₂H₄ N₃⁻ NO₂⁻ ClO₃⁻ Br⁻ SO₃²⁻

Soft R₂S RSH R₃P (RO)₃P RS⁻ SCN⁻ I⁻ CN⁻ S₂O₃²⁻

Other concepts can be applied to explain trends in the stability of complexes within certain groups. For example, the stability of divalent metal complexes of the first row transition elements almost always follow the Irving – Williams series:



In this particular series, the ionic radius decreases and the ionisation potential increases up to copper, thereby complex stability increases progressively in the series, reaching a maximum with this metal. This rule holds true irrespective of the nature of the co-ordinated ligand or the number of ligands involved. Only steric hindrance can have an effect on this cation order. For the transition metals, this trend can also be explained by the concept of crystal field theory. This is based on the stabilisation energies of the *d* orbitals for each metal. Up to Cu(II), the ligation enthalpy increases due to an increased number of *d* orbital electrons which correspondingly increases the stabilisation energy of the complex. Zn(II) has no *d* orbital and thus no stabilisation energy, hence the drop from Cu > Zn.

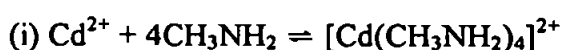
The number of ligating atoms bound by a metal ion is expressed as the **co-ordination number**. The most common number is six, followed by 4, but numbers as high as ten and twelve can be found with the largest metal ions. The smallest co-ordination number is two, of which there are only two geometric possibilities, linear or bent. This number is limited mainly to complexes of Cu(I), Ag(I), Au(I) and Hg(II) [15].

Ligands can also be expressed as the number of electron pairs available for donation to a metal ion. Simple ligands which are only able to donate a single electron pair are termed

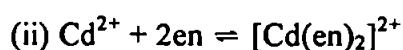
monodentate. These include H₂O, OH⁻, NH₃ and CN⁻. Ligands capable of donating more than a single pair are grouped together as polydentate ligands. For example, a bidentate ligand is ethylenediamine (en), NH₂CH₂CH₂NH₂, which contains two nitrogen donor atoms.

Polydentate ligands are known as chelating agents because they bind to metals in such a way that a ring structure is formed. This ring formation is termed **chelation**, the cyclic complexes known as **chelates**, from the Greek meaning 'crab's claw'.

Chelates are far more stable than analogous complexes of the same metal containing no ring structure, and this is termed the **chelate effect** [16]. This can be illustrated by comparing the complexing of Cd(II) by methylamine and ethylenediamine (en) [17]:



$$\Delta H = -57.3\text{KJ mol}^{-1} \quad \Delta S = -67.3\text{JK mol}^{-1} \quad \Delta G = -37.2\text{KJ mol}^{-1} \quad \beta_n = 10^{6.5}$$



$$\Delta H = -56.5\text{KJ mol}^{-1} \quad \Delta S = +14.1\text{JK mol}^{-1} \quad \Delta G = -60.7\text{KJ mol}^{-1} \quad \beta_n = 10^{10.6}$$

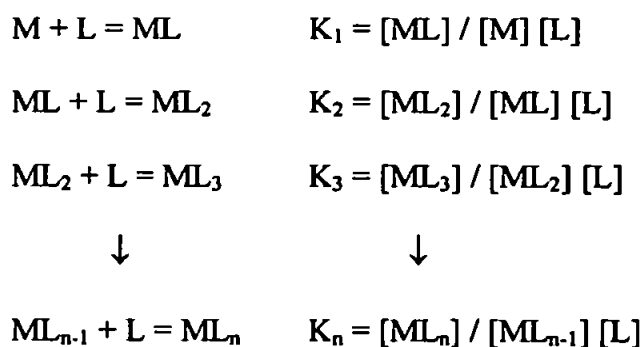
Although the enthalpy (ΔH) values for both reactions are almost identical, the overall formation constant β_n for the reaction with en is nearly 10⁴ times more stable than the methylamine complex. From the values of ΔG where $\Delta G = \Delta H - T\Delta S$, it can be seen that the second reaction, (ii), has a more favourable entropy (ΔS) change.

This can be explained by the loss of water molecules from the aquo ion $[\text{Cd}(\text{H}_2\text{O})_6]^{2+}$. In aqueous solution, the Cd(II) ion is co-ordinated by six water molecules, and in reactions (i) and (ii) four of these are liberated when the metal binds with the nitrogen ligands. In (i) four methylamine molecules replace four water molecules, resulting in a net change of zero in the number of free molecules. However, with the addition of two ens, four water molecules are still replaced, which results in a net increase of 2 moles of individual molecules. This causes a greater degree of disorder, and therefore ΔS is more positive (more favourable). Thus, the chelate effect is essentially an entropy effect [15].

The strongest complexing agents are polydentate, particularly those that form five, followed by six membered rings, due to favourable thermodynamics. An example of a five and six membered chelate is given in Figure 1.5. Suitable chelating agents of this type are organic molecules containing both oxygen and nitrogen as donor atoms, which explains why ethylenediamine tetraacetic acid (EDTA) shown in Figure 1.6, a hexadentate ligand (four oxygen and two nitrogen donor atoms), forms very stable complexes having five 5 membered rings [14].

If the number of members forming the ring is either too small (≤ 4) or too large (≥ 7), the probability of ring closure is reduced. For example, a ring with >6 members approaches that of a complex of two unidentate ligands having the same donor atoms, which decreases the chelate stability.

A quantitative indication of complex formation is given by evaluating the stability constants, which characterise the equilibria corresponding to the successive addition of ligands. Thus, for a metal ion 'M' and a monodentate ligand 'L', the equilibria can be expressed as:



For monodentate ligands, 'n' represents the maximum co-ordination number of the metal ion M for the ligand L.

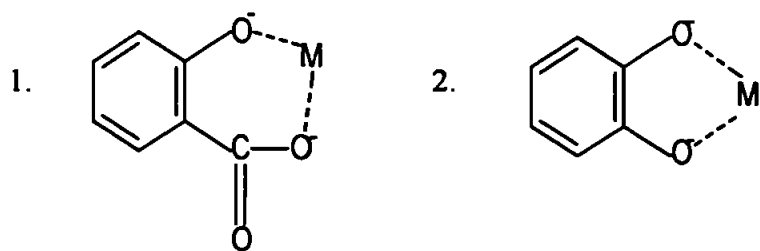


Figure 1.5 Example of a 1. Six membered chelate ring (salicylic acid) and 2. five membered ring (pyrocatechol).

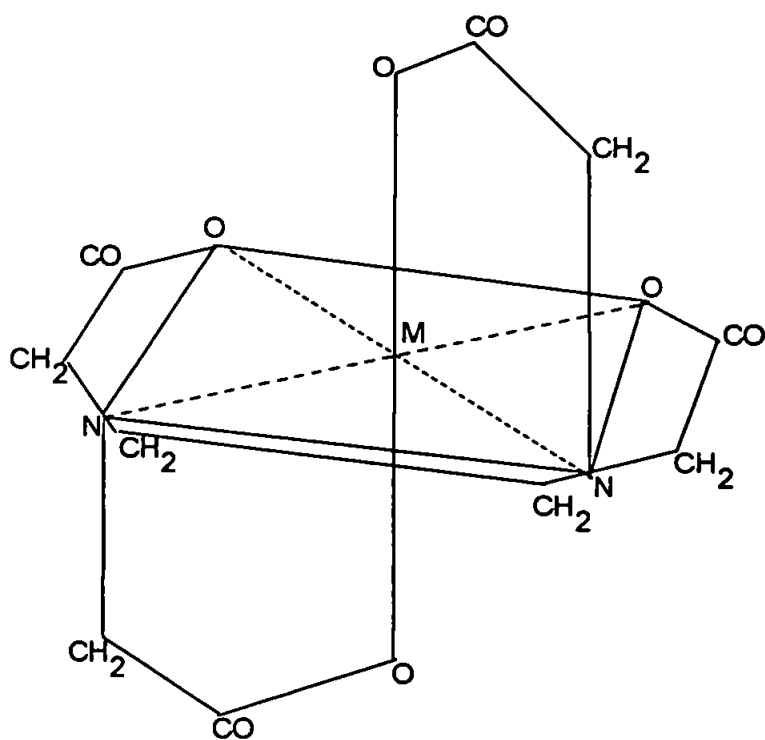
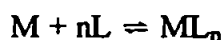


Figure 1.6 Steric configuration of the anion of a divalent metal-EDTA complex

The constants K_n are termed the **stepwise formation constants**. An alternative formulation is to consider the overall formation reaction:



This can be characterised by the **overall formation constant**, β_n :

$$\beta_n = [ML_n] / [M] [L]^n = K_1 K_2 K_3 \dots K_n \quad \text{i.e. } \beta_2 = K_1 K_2$$

β_n can also be referred to as the stability constant K_{stab} .

Either expression is useful, K_n providing information concerning the concentrations of various species, β_n conveying the concentration of the combined species present. In general, there is a slow decrease in K values, expressed as $\log K$, with these complex systems, as shown in Table 1.3.

Table 1.3 Stepwise formation constants of selected nitrogen complexes [18]

ligand	Log K_n	Co^{2+}	Ni^{2+}	Cu^{2+}	Zn^{2+}
NH_3	K_1	2.1	2.8	4.2	2.4
	K_2	1.6	2.2	3.5	2.4
	K_3	1.1	1.7	2.9	2.5
	K_4	0.8	1.2	2.1	2.2
	K_5	0.2	0.8	-0.5	
	K_6	-0.6	0.03		
en	K_1	6.0	7.5	10.6	5.7
	K_2	4.8	6.3	9.1	4.7
	K_3	3.1	4.3	-1.0	1.7

This can also be illustrated with the $\text{Cd}^{2+} - \text{NH}_3$ system:





The values quoted for stepwise and overall formation constants are based on various assumptions, most notably that the metal and ligand are 100% ionised and exist as a solitary species in solution (ML). Other conditions are also assumed to remain constant, namely ionic strength and temperature. In reality, this is often not the case, with many ligands and metal ions existing as different species, for example $\text{M}(\text{OH})_x$, MHL , MH_2L and $\text{M}(\text{OH})\text{L}$, dependant upon solution conditions. The most important parameter is the pH of the solution. An adjustment in pH can dramatically alter the concentration of the reacting metal or ligand species in solution. As the overall formation constant does not change, to take into account that the metal and ligand will be in other forms, we can define an operational stability constant as the **conditional stability constant, K'** :

$$K'_{\text{M'L}} = [\text{ML}] / [\text{M}'] [\text{L}']$$

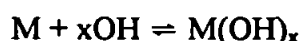
M' is the concentration of all the metal in solution that has not reacted with the ligand, and not just the concentration of free metal ions present. Correspondingly, L' represents the concentration of all species of the complexing agent not bound to the metal. K' is therefore not governed solely by thermodynamics, as experimental conditions play an important role, the solution pH determining the K' values of the metal chelates. Herein lies the key to chelating ion – exchange: the ability to control the conditional stability of complexes through pH adjustment.

This concept can be explained with M^{n+} - EDTA (Y) complexes:



EDTA can exist as one of five species in solution dependant upon the pH, as it is the conjugate base of a weak acid (H_4Y). This is shown in Figure 1.7. These species are H_4Y (zwitterion), H_3Y^- , H_2Y^{2-} , HY^{3-} and Y^{4-} , which is the fully deprotonated ion. Dependent

upon the pH, the most dominant species will change. Figure 1.8, shows the conditional constants of various metal – EDTA complexes as a function of pH. At low pH (<3), the increasing concentration of the non-complexing species H_4Y , causes a decrease in complexed metal ions, and therefore K'_{MY} , whilst above pH 10 many metals form stable hydroxy species which prevents complexation with the EDTA ligands, and reduces the concentration of free metal ions in solution:



In comparison, the overall formation constant would have assumed that EDTA, in solution, would be in its fully ionised form Y^{4-} , complexing with 'free' metal ions, which is not the case over a wide pH range.

In summary, there are various parameters which are an important part of the chelation ion – exchange mechanism. These include the choice of chelating group, which will determine the formation constants of metal ions, the pH which can alter the conditional stability constant as well as the kinetics of complex formation and dissociation, and high efficiency substrates required to separate analytes within a reasonable time frame. The ionic strength also plays a key role, ensuring that chelation is the dominant exchange mechanism for metal ions

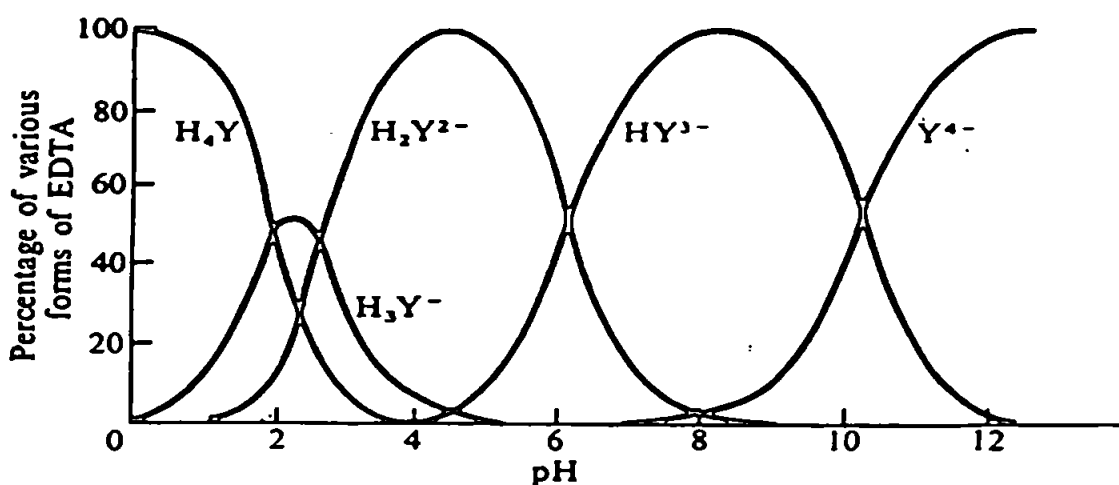


Figure 1.7 The different species of EDTA in solution as a function of pH [19]

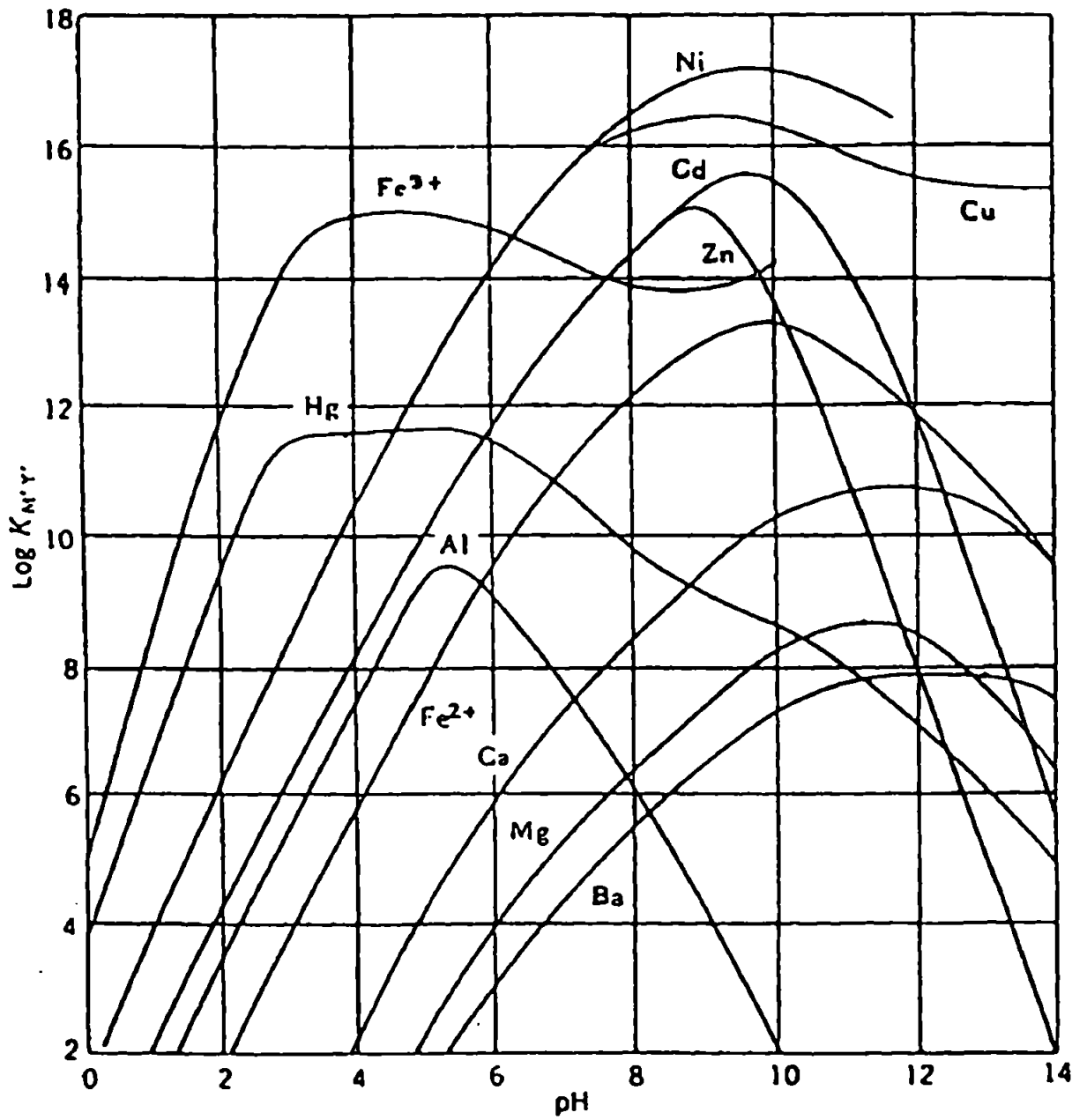


Figure 1.8 Conditional stability constants, $\log K_{M'Y'}$, of selected metal EDTA complexes as a function of pH [14].

1.4 Chelating substrates

Chelating ion – exchange substrates, functionalised with various ligands, have found extensive use in the separation and concentration of metal ions from many sample matrices. An important feature of these exchangers is the greater selectivity which they can offer in comparison with conventional ion – exchangers. For example, transition metals cannot be easily pre – concentrated on cation – exchange columns, due to interference from alkali and alkaline earth metals for the ion – exchange sites.

There are predominantly two types of substrate that have been used as chelating ion – exchangers. The first of these are low crosslinked polymer gels, suitable for low to medium pressure systems. There are a multitude of these commercially available low efficiency substrates, primarily used for the batch extraction of selected metals and matrix removal purposes. Examples include Chelex – 100 (Bio-Rad) with iminodiacetate (IDA) functionality, and Duolite ES-467 (Duolite) with aminophosphonate groups, both employed for the pre – concentration of transition, heavy and rare – earth metals.

A problem encountered with these low crosslinked polymers is swelling and contracting of the resin, associated with changes in its ionic form as a function of buffer pH. This swelling can cause high back pressure problems with such techniques as flow injection analysis, due to the resin collapsing under pressure which will restrict the eluent flow. For example, Chelex-100 increases in relative volume by 0.66 when changing from H^+ to Na^+ as the counter ion. This effect can be overcome by using the second type of substrate: macroporous supports with increased rigidity.

For example, the Dionex Metpac CC-1, which also contains IDA groups, does not suffer from swelling effects because of a more highly crosslinked PS-DVB substrate onto which the functional group is immobilised.

The functional groups can be attached to the sorbent backbone by two distinct methods. The first is to covalently bind the chelating group to a substrate, the second being to

permanently adsorb or impregnate a chelating agent into a substrate surface. The latter approach can provide such benefits as a reduction in preparation time, due in part to negating the often lengthy organic synthesis required with many bonded phases. This is additionally useful in that a novel chelating phase prepared in this manner can provide quick results regarding its scope and potential for separating metal ions.

There are some comprehensive reviews comparing and listing the chelating sorbents suitable for metal ion analysis. Two very detailed studies have been undertaken by Myasoedova and Savvin [20], and Sahni and Reedijk [21]. These list the many chelating groups studied, and give examples of metal ions separated in various matrices. Biernat *et al* [22], investigated chelating agents immobilised onto silica substrates for metal ion separations, whilst Kantipuly *et al* [23], principally reviewed inorganic and organic polymers, modified with chelating groups for the same purpose. More recent reviews, detailing developments in the field together with applications for metal ion analysis are given by Nickson *et al* [24], and Garg *et al* [25].

Further developments to produce ever more efficient chelating sorbents for specific metals and / or sample types is an ongoing process. This is because many commercial chelating ion – exchangers have certain drawbacks, limiting their use. Although Chelex – 100 is one of the most widely used polymers for separating and concentrating rare earth and heavy metals, especially in sea water, swelling effects during use can prevent its adaptation to on-line monitoring systems. Another problem is the similar affinity for certain chelating groups for both analytes of interest and matrix interferences including the alkaline earth metals.

Ahuja *et al* [26], investigated hydroxamic acid functionalised divinylbenzene styrene copolymers to overcome this problem. It was found that the resin selectivity for transition and highly charged ions including U(VI) was higher than for the alkaline earths.

Wang *et al* [27], incorporated a novel IDA – ethylcellulose membrane as an effective technique for the on – line preconcentration of various transition metals. The use of a

membrane instead of a conventional column resulted in advantages including easy operation and a high sample throughput.

Other novel resins recently developed as chelating ion – exchangers include a styrene divinylbenzene copolymer functionalised with α -nitroso- β -naphthol for the selective separation of Fe(III) and Cu(II) [28]; amberlite XAD-4 functionalised with bicine ligands for the selective retention of selected lanthanides, U(VI) and Th(IV) [29]; a PS-DVB polymer containing benzimidazolylazo groups, highly selective for Hg(II), Ag(I) and Pd(II) with no affinity for alkali and alkaline earth metals [30]; chitosan, a naturally occurring polymer, immobilised with EDTA ligands for the selective elution of transition and heavy metal ions [31]; and a commercial resin, Bio-Beads SM-7 (acrylic ester polymer, Bio-Rad) loaded with 2-mercaptobenzothiazole for the separation of inorganic and alkylmercury species [32]. A selection of these chelating agents are given in Figure 1.9.

These examples illustrate the diverse supports and chelating groups being investigated as possible solutions for trace metal analysis in complex sample types. It should be noted that nearly all of these substrates use low efficiency substrates and so are not suitable for analytical separations. The development of high efficiency chelating sorbents formed the basis of this work as described later.

1.5 Ion chromatographic analysis of metal ions – a review

The rapid development of IC since its inception, has meant that today it has become a mature technique with dedicated instrumentation, available for the trace analysis of many ionic species. A historical account detailing this ‘evolution’ of innovation in IC is described in a review by its founder, Small [33].

Current research is primarily aimed at applying the technique to determine ions in various complex matrices, and developing detection systems to increase sensitivity and selectivity.

With regards to inorganic analysis, there is particular emphasis on developing methodology for the transition metals and heavier elements. A series of reviews, encapsulating the development of chromatographic methods for the determination and

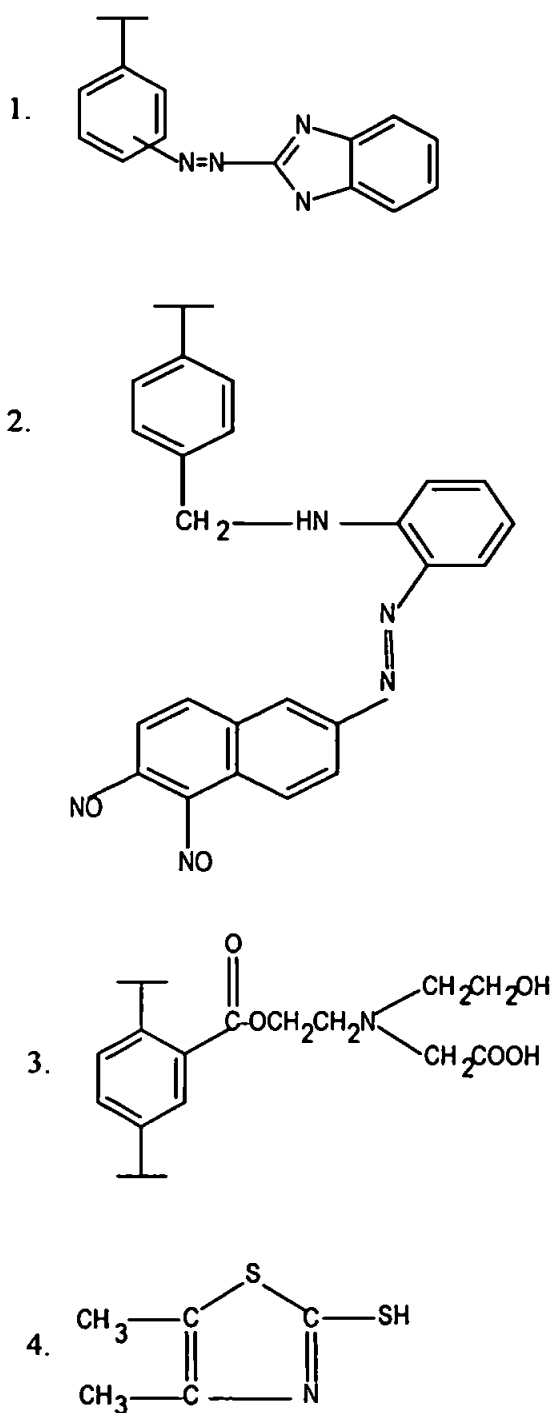


Figure 1.9 Chelating groups immobilised onto PS-DVB for the preconcentration of trace metals. 1: Benzimidazolylazo, 2: α -nitroso- β -naphthol, 3: Bicine and 4: 2-mercaptobenzothiazole.

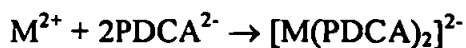
speciation of metal ions in various matrices are given collectively by Marina *et al* [34], Frankenburger *et al* [35], Robards *et al* [36], Buldini *et al* [37], and Sarzanini [38,39].

A review detailing developments in sample preparation and separation of inorganic ions by IC is given by Haddad *et al* [40]. Pohl *et al* [41], have reviewed the parameters which can control ion – exchange selectivity for inorganic ions, the most important factor being the composition of the stationary phase. The most commonly used substrates are based on either polystyrene or silica, examples given in the following sections

1.5.1 Polystyrene Resins

The Dionex corporation markets various ion – exchange columns for the separation of metal ions. These include the IonPac CS3 and CS5 columns, which are PS – DVB resins with sulfonic acid groups, the CS5 column additionally containing alkyl quaternary amine groups, which results in a mixed mode mechanism of cation and anion exchange. The CS3 column is marketed as suitable for the separation of alkali and alkaline earth metals, the CS5 column more appropriate for the transition metals and heavier elements including the lanthanides. Other commercial columns include ethylene vinylbenzene – DVB polymers grafted with carboxylic groups (IonPac CS14) and both carboxylic and phosphonic acid groups (Ionpac CS12). Morris and Fritz have investigated the ion – exchange of metal ions on carboxylic acid functionalised polymers [42]. These and other manufacturers columns have been applied to a wide range of sample types, though usually in conjunction with a sample preparation step to reduce the ionic strength.

Basta and Tabatabai [43] developed a method for the isocratic separation and determination of Cu(II), Ni(II) and Zn(II) in soils using a CS5 column with 4-(2-pyridylazo) resorcinol (PAR) detection. The eluent was buffered to pH 4.8 and 2,6-pyridinedicarboxylic acid, or dipicolinic acid (PDCA) added as a complexing agent to optimise separation efficiency, forming anionic complexes with the metals:

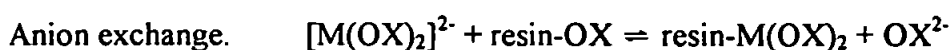
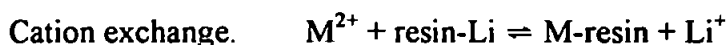


Sample preparation was achieved using acid digestion.

Ruth and Shaw [44] developed a similar system to determine transition metal contamination in silicon wafers. This was achieved using a CS5 column with isocratic elution of the metal anionic dipicolinic complexes, buffered with LiOH and NaCl. Detection was achieved using PAR. A study of the ion – exchange mechanisms that occur when complexing transition metal ions with dipicolinic acid, to separate them as anionic complexes on the mixed – mode CS5 column is given by Janvion *et al* [45].

Buldini *et al* [46], incorporated this IC system to determine various transition metals in vegetable oils, the organic matrix removed using saponification and oxidative UV photolysis. Cardellicchio *et al* [47], used this system to analyse transition metals in sewage waters, eight metals being separated within twenty minutes. Other recent applications of IC have included the determination of transition metals in mineral waters [48] and lead battery electrolyte [49]. In the electrolyte, Mg(II) and Ca(II) were also analysed using a CS10 column with suppressed conductivity detection.

A limitation of separating metal ions as anionic complexes with dipicolinic acid, typically added to the eluent at a concentration of 6mM, is the stability of these species which can affect the sensitivity of a post column reaction (PCR) detection system. This point is further addressed in section 1.6. An alternative to adding dipicolinic acid to the eluent is to switch to oxalic acid as a complexing agent. Metal – oxalate complexes are less stable than the corresponding dipicolinic acid complexes, and metals can therefore be separated as both cationic and anionic species, when a displacing ion is present – usually an alkali metal:



Cd(II) forms weak oxalate complexes ($\log K_1 = 2.9$) and so is separated dominantly by cation – exchange, whilst Pb(II) ($\log K_1 = 3.3$), Co(II) ($\log K_1 = 3.5$), Zn(II) ($\log K_1 = 3.7$) and Ni(II) ($\log K_1 = 4.1$) form relatively stable complexes, and so are separated using anion exchange.

An oxalic acid, LiOH eluent, together with a CS5 column, was used to determine Cu(II) and Zn(II) in blood plasma, with PAR detection [50]. However, as metal – oxalate complexes are weaker than their corresponding dipicolinic acid complexes, column selectivity is reduced, with Cd(II) and Mn(II) co-eluting on a typical ion – exchange column. Al-Shawi and Dahl [51] solved this problem by developing a gradient elution system, varying the concentration of oxalic acid and Cl⁻ as the displacing ion (NaCl) in the mobile phase. This was optimised to determine Cd(II) and six other heavy metals in nitrate / phosphate fertiliser solution, with PAR detection.

Unfortunately, use of either complexing agent in an eluent is not suitable for the analysis of Pb(II), and to some degree Cd(II) also, as detection limits are too high for practical purposes. Riviello *et al* [52,53], have recently developed a novel strategy based on incorporating a gradient system with an oxalic acid / NaCl eluent, and a CS5 column, together with another post column reagent, 2-(5-bromo-2-pyridylazo)-5-diethylaminophenol (5-Br-PADAP). A comparison between the system with this new reagent and PAR detection, found that detection sensitivity was improved for Cd(II), Cu(II), Zn(II) and Mn(II) [52]. For the other metals though, Ni(II), Co(II), Fe(II), Fe(III) and Pb(II), detection sensitivity was reduced, dramatically so for Pb(II) and Ni(II). However, Cu(II), Cd(II), Ni(II), Zn(II), Co(II) and Mn(II), in that elution order, were determined in various biochemical samples using this method [53].

Bruzzoniti *et al* [54], developed an alternative approach, whereby Pb(II), Cd(II), Ni(II) and Cu(II) could be separated as EDTA complexes on an anion – exchange column, with a carbonate eluent and conductivity detection. Unfortunately, even with a gradient elution program, Pb(II) and Cd(II) co-elute.

1.5.2 Silica Substrates

An alternative to polymer based substrates are silica ion – exchangers, which can provide increased resolution due to a reduced particle size and high pressure column packing regime, though within a narrower pH range, typically 2 – 6.

Nesterenko *et al* synthesised zwitterion-exchange stationary phases by immobilising amino acids onto silica to separate alkali and alkaline earth metals [55].

It has recently been discovered by Haddad *et al* [56,57], that an un – modified silica gel column (Develosil 30-5), is capable of acting as a cation exchanger, due to Al^{3+} present as an impurity, which enhances the acidity of the silanol group (pK_a 7.1). It was shown to effectively separate alkali, alkaline earth and transition metal ions using an oxalate eluent.

Silica based ion – exchangers have also been used to determine the alkali and alkaline earth metals in soil solution [58], transition metals in pharmaceutical solutions [59], Fe(II), Fe(III) and Mn(II) in environmental samples [60], and Pb(II), Zn(II), Cu(II) and Mn(II) in waters and compost [61]. In all cases, detection was achieved using post column reaction with PAR, except for the soil analysis, in which conductivity detection was employed.

In addition to the separation of alkali, alkaline earth and transition metal ions, there is a significant interest in developing methods to analyse samples for heavier elements.

Al – Shawi and Dahl [62] determined lanthanide concentrations in nitrophosphate solution using a silica based strong cation exchanger, together with a gradient elution of α - hydroxyisobutyric acid buffered with LiOH. Detection was achieved using PAR or 2,7-*bis*(2-arsenophenylazo)-1,8-dihydroxynaphthalene-3,6-disulfonic acid or Arsenazo III.

Finally, Bruzzoniti *et al* [63,64], separated and determined certain lanthanides in YbF_3 using the Dionex CS5 column together with a gradient elution of oxalic acid, and PAR detection.

The separation of other heavy elements including uranium and thorium are discussed in more detail in Chapter 6.

To summarise this review, a major disadvantage of current ion – exchange materials is the inability to cope with complex sample types. This problem can be overcome using matrix elimination, with a selective preconcentration step on a chelating resin for example, but then analyte losses and time constraints may come into effect. This approach to metal ion separation is termed ‘Chelation Ion Chromatography’ and is reviewed in the following section. Additionally, commercial strong and weak ion – exchange systems are presently not suitable for trace Pb(II) analysis, and in some cases Cd(II) analysis also, due to sensitivity reductions occurring with complexation in the eluent.

As is apparent from this review, however, novel methodologies are under continuous investigation to develop systems that can overcome these present flaws, both to increase column selectivity and analyte sensitivity.

1.5.3 Chelation Ion Chromatography (CIC)

As already mentioned, this technique essentially involves the ion-exchange separation of metal ions, which have been isolated from matrix interferences and preconcentrated using a low efficiency chelating column. The method, first published in 1990 by Siriraks *et al* [65], involves a complicated and lengthy three column system connected by several valves, to analyse metals in complex samples. The approach utilises an on – line preconcentrating column with IDA groups to concentrate metal ions whilst removing alkali and alkaline earth metal ions with a selective elution program. This column is interfaced with a cation concentrator column to collect the retained metals, before separation on an analytical ion – exchange column as dipicolinic acid complexes.

This method has been used to separate and determine selected transition metals in seawater [66,67], coral skeletons [68], and drinking water [69]. The lanthanides have also been determined in agricultural samples [70,71].

Changing from IDA groups to use γ -aminobutyrohydroxamate resins, the lanthanides have been determined in seawater [72], and selected transition metals in oyster tissue [73]. An advantage of using this chelating agent, as mentioned previously, is that the alkaline earth metals are very weakly retained in comparison with iminodiacetate, making their elimination from the sample matrix easier.

Motellier and Pitsch [74] incorporated an on – line preconcentration step using an iminodiacetate (IDA) chelating column to determine transition metal ions in mineral waters, whilst Laikhtman *et al* [75], used this chelating column for on – line matrix elimination, to determine Mg(II) and Ca(II) in high ionic strength media (30% NaCl brines) with suppressed conductivity detection.

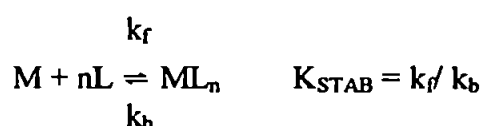
1.5.4 High Performance Chelation Ion Chromatography (HPCIC)

An alternative to separating metal ions using ion-exchange columns has been to utilise high efficiency supports containing chelating groups for this purpose. The technique has been termed High Performance Chelation Ion Chromatography (HPCIC), and can be differentiated markedly from CIC in that one column can act as both a combined preconcentration and separation step. This is because chelating agents are immobilised onto high efficiency substrates, increasing the separation power, and not low efficiency sorbents which are generally suitable for preconcentration and batch extraction purposes only. Using this approach, metal ions are separated as a function of the conditional stability constants between the metal and complexing ligand, which can be influenced by eluent pH. Chelating molecules with different types of donor atoms can also change the individual

selectivity coefficients towards metal ions, which can then be exploited to separate analytes of interest.

A significant advantage of this technique, in comparison to IC, is the ability to separate metal ions in samples of high ionic strength. These samples contain a high concentration of salt ions which can swamp ion-exchange sites, leading to a reduction in column capacity. These interfering matrix ions can frequently be removed by incorporating sample pre-treatment steps including solvent extraction or chelating pre-concentration columns (the CIC approach), which retain only the ions of interest. Unfortunately, these procedures can lengthen the analysis time, give poor recoveries of analyte ions, or add contaminants to the sample through increased use of reagents. Many sample matrices, whether biological, environmental, industrial or geological, contain a high concentration of salts, necessitating a requirement for simple effective techniques to analyse them, hence the ongoing development of HPCIC.

A disadvantage of HPCIC is a more pronounced broadening of analyte bands as the solute ions traverse the chelating column, resulting in asymmetric peak tailing. This is due to the reaction kinetics:



The reaction velocity to reach ML is in constant flux as ML continuously dissociates to give an equilibrium between ML and its constituents M and L. If K_{STAB} is large, then the velocity of the forward reaction (k_f) is much higher than the backward reaction (k_b).

Thereby, a chelating substrate will complex a metal ion quickly, but release it slowly, resulting in peak tailing. Therefore, those solutes with small conditional constants, that is, short retention times will have reasonably quick dissociation kinetics, whereas those solutes with larger conditional constants, that is, longer retention times will have slower dissociating kinetics. The consequence of this is that this slower dissociation will add to the already natural broadening process in chromatography and could produce very broad

peaks with a relatively small increase in retention time. An example is given in Figure 1.10, showing solute ions 1 and 2 that are complexed and dissociated quickly. This results in sharp peak shapes enabling them to be separated with good efficiency. This is in contrast to peak 3, which is dissociating more slowly and produces a peak much broader with more tailing than would be expected from the increase in retention time. This is a significant problem with chelating ion-exchange, reducing detection limits and separation efficiency, and is termed 'kinetic broadening'.

This effect can be somewhat overcome by increasing column capacity and reducing the particle size. Increasing the capacity enables the pH to be lowered to sharpen solute peaks, by decreasing the conditional stability constants of the metal – ligand complexes. As the pH is reduced, k_b nears the velocity of k_f , giving closely eluting sharp resolved peaks in a shorter analysis time. Decreasing the particle size reduces the rate of diffusion of solute ions into particle pores, therefore they are eluted from the column as a more compact band with less broadening.

There are three mechanisms available to prepare a chelating sorbent. The first is to impregnate a chelating dye into the pores of substrates. This approach is reviewed and detailed in Chapter 2. The second, relatively novel procedure is to dynamically modify a substrate with a chelating molecule. In this instance the chelating ligand is continuously present in the eluent. Over time, an equilibrium is established between a sorbed layer of ligand on the substrate surface, and the concentration of ligand in the mobile phase. By optimising eluent and stationary phase conditions, the column can act as a high efficiency chelating sorbent for metal separations. Dynamically modified substrates are reviewed in Chapter 5. The last approach is to covalently bond chelating groups to high efficiency sorbents, demonstrated by the following examples.

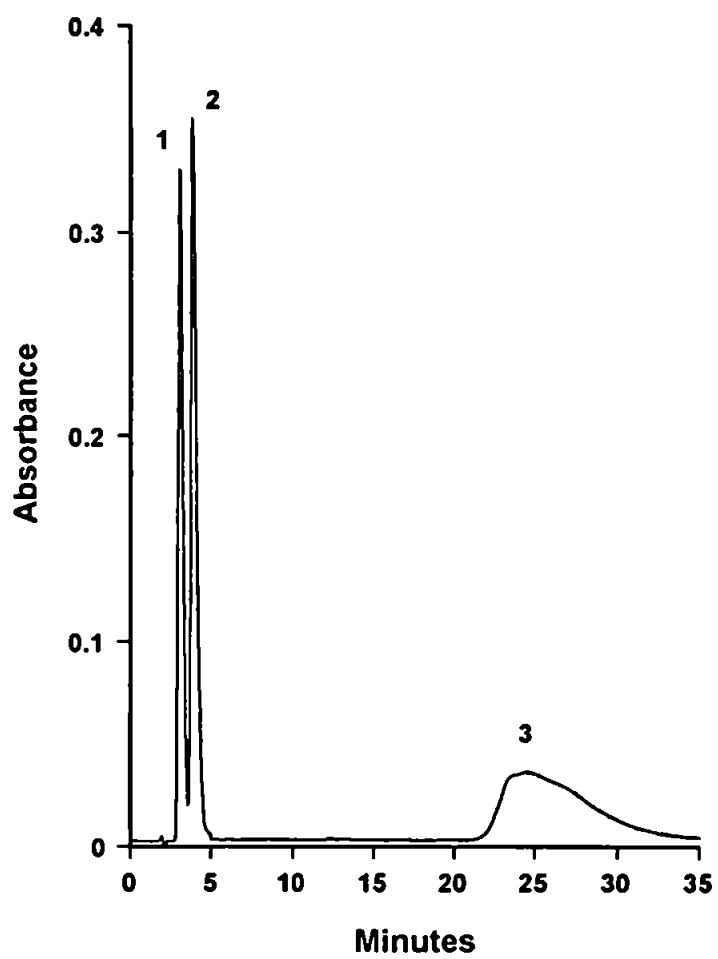


Figure 1.10 Chromatogram illustrating the effect of 'kinetic broadening' on analyte peak shapes.

Jones and Nesterenko have developed methods using silica modified with IDA moiety for the analysis of transition metals in various complex samples including brines, with PAR detection [76,77]. This column has also been used to isocratically separate the lanthanides and yttrium [78,79]. Using a high ionic strength eluent to suppress ion – exchange interactions, it was found that the chromatographic efficiency remained high over a 70 minute elution period for these metals, dispelling the notion that chelating substrates cannot give good separation efficiencies over a lengthy analysis time. Sutton *et al* [80], used HPCIC to determine trace Bi(II) in Pb(II), using a hypercrosslinked polystyrene column (MN200, Purolite), which displayed metal complexing properties. The trace Bi(II) was eluted as a chloride complex with detection at 370nm.

Faltynski and Jezorek [81], investigated several azo coupled silica bound stationary phases for the separation of metal ions, using tartrate or sulfate based eluents. Bonn *et al* [82], covalently bound IDA to silica for the separation of transition metals. Using a tartrate eluent at pH 2.5, Co(II), Zn(II) and Cd(II) were separated in a sea – water matrix.

Aminocarboxylic functionalised silica based ion – exchangers have been developed by Nesterenko *et al* [83,84], for the simultaneous separation of alkali and alkaline earth metals, using a perchloric acid eluent.

O'Connell *et al* [85], used a porous graphitic carbon column (Hypercarb, Hypersil) to separate and determine Pb(II) in environmental samples using a nitric acid eluent with PAR detection.

Inoue *et al* [86], separated rare-earth elements using a nitrilotriacetic acid (NTA) functionalised methylacrylate gel with a gradient program of nitric acid.

1.6 Detection of metal ions

The progress of inorganic liquid chromatography has been very dependant upon the development of detection systems to analyse these ions at trace levels. For the majority of

inorganic cations, such as the alkaline earths, transition metals and heavier elements, post column reaction systems (PCR) utilising a colour forming reagent with spectrophotometric detection is the preferred technique.

PCR detection involves the introduction of a suitable reagent into the column effluent which reacts with the eluting solutes changing the spectral characteristics prior to their passage to the detector. This reagent can be delivered to the effluent using either a pump with a mixing chamber (usually a T – piece and reaction coil) as used throughout these studies (see Figure 2.3), or a membrane reactor, whereby the reagent diffuses through a semi – permeable fibre using external pressure, to mix with the effluent.

PCR reagents for metal ion analysis are usually chelating agents with a strong chromophore. The chromophore is a covalently unsaturated group responsible for electronic absorption, typically conjugated C=C and C=O groups [87]. Energy absorbed in the UV-Vis region produces changes in the electronic energy of the molecule, resulting from transitions of electrons to a higher energy orbital. The chromophoric absorbance can be affected by the attachment of saturated groups, denoted auxochromes, for example :ÖH, :NH₂ and ::Cl:. This approach provides various advantages:

- (a) many metal chelates exhibit intensely strong absorbance in the visible region of the spectrum, which can minimise interference from background absorbance due to the eluent characteristics;
- (b) detection selectivity can be varied by the selection of chelating agent or use of masking agents;
- (c) many metal – chelate reactions are fast and require minimal mixing, which reduces the dead volume of the system and correspondingly reduces peak broadening.

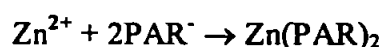
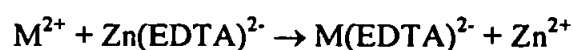
In addition, the reagent should be stable in the effluent to minimise baseline drift and detector noise.

The most common broad – based reagent for the analysis of transition and heavy metals metals is PAR. The application of this spectrophotometric reagent for these metals is

illustrated in articles by Gomez *et al* [88], and more recently Engstrom *et al* [89]. The application of this reagent as a PCR in IC systems can also be found in articles reviewed in section 1.5.

Co *et al* [90] investigated the selectivity of this reagent towards transition metals when adding aminocarboxylate ligands to the PCR solution. Using this approach, the PAR postcolumn reagent could be altered to behave more selectively for certain metals. For example, nitriloacetic acid (NTA) could suppress the PAR response to all metals except Cu(II) and Co(II), resulting from the slow rate of conversion of metal ions from $M(NTA)_2^{4-}$ to $M(PAR)_2$. This example also illustrates the considerations of adding complexing agents to the eluent. Although these ligands can improve the selectivity of IC columns (e.g. PDCA for the Dionex CS5 column), the PCR reagent must be capable of displacing the eluent ligand from the metal ion, otherwise this may result in a drastic reduction in sensitivity. This point is addressed in a paper by Vasconcelos and Gomes [91]. A review of alternative heterocyclic azo reagents suitable for the spectrophotometric determination of metal ions is given by Oswaldowski and Jarosz [92].

For the detection of alkaline earth metals, Zinc – EDTA is added to the PAR reagent. These metals do not form strongly absorbing complexes with PAR, but will displace Zn^{2+} from EDTA which co-ordinates with the azo reagent:



The kinetics and equilibria of this displacement reaction is given by Lucy and Dinh [93].

Other reagents for transition metals include triphenylmethane based dyes with iminodiacetate functionality, which includes methylthymol blue and xylenol orange [94]. Xylenol orange has also been applied as a post column reagent for the determination of the lanthanides [95].

The most frequently used broad – based reagent for the heavier elements including U(VI) [96] and the lanthanides [97,98] is Arsenazo III. For Iron species, the triphenylmethane

molecule pyrocatechol violet gives intensely coloured complexes with few interfering ions [99]. Recently, dibromo-*p*-methyl-methylsulfonazo (DBM-MSA) has been included as a highly sensitive and selective chromogenic reagent for Pb(II), with only Ca(II) and Ba(II) interfering [100]. 2-(5-nitro-2-pyridylazo)-5-(*N*-propyl-*N*-sulfopropylamino)phenol or nitro-PAPS has been investigated as a spectrophotometric reagent for Pb(II), Cd(II) and Mn(II) [101]. Thus, dependent upon the chelating group, individual ions can be determined in the presence of matrix interferences which do not react, or groups of metal ions can be detected simultaneously.

An extensive study of reagents suitable for the spectrophotometric determination of metal ions can be found in books by Sandell [102], Holzbecher [103] and Snell [104]. A selection of these chromogenic reagents are given in Figure 1.11.

It should be noted that in addition to these colorimetric reagents, certain metals can also be detected using electrochemical, fluorescence and luminescence methods, whether as free ions or as complexes. Details on all of these systems can be found in a book article by Cassidy and Karcher [105], and a review by Buchberger and Haddad [106].

1.7 Aims and objectives of this work

Previous work to develop the HPCIC technique has concentrated mainly on impregnating various PS-DVB resins with chelating dyes for the preconcentration and separation of trace metals using a single column [107-109].

To date, this approach has not 'evolved' beyond an empirical level, dye loaded substrates investigated principally for the purpose of determining trace metals in complex samples not easily analysed by ion chromatography, for example sea water.

Therefore, initial investigations will characterise different chelating dyes to determine the effect of ligating atoms on metal ion retention as a function of pH. This could provide a useful framework whereby specific donor atom groups could be applied to separate metals

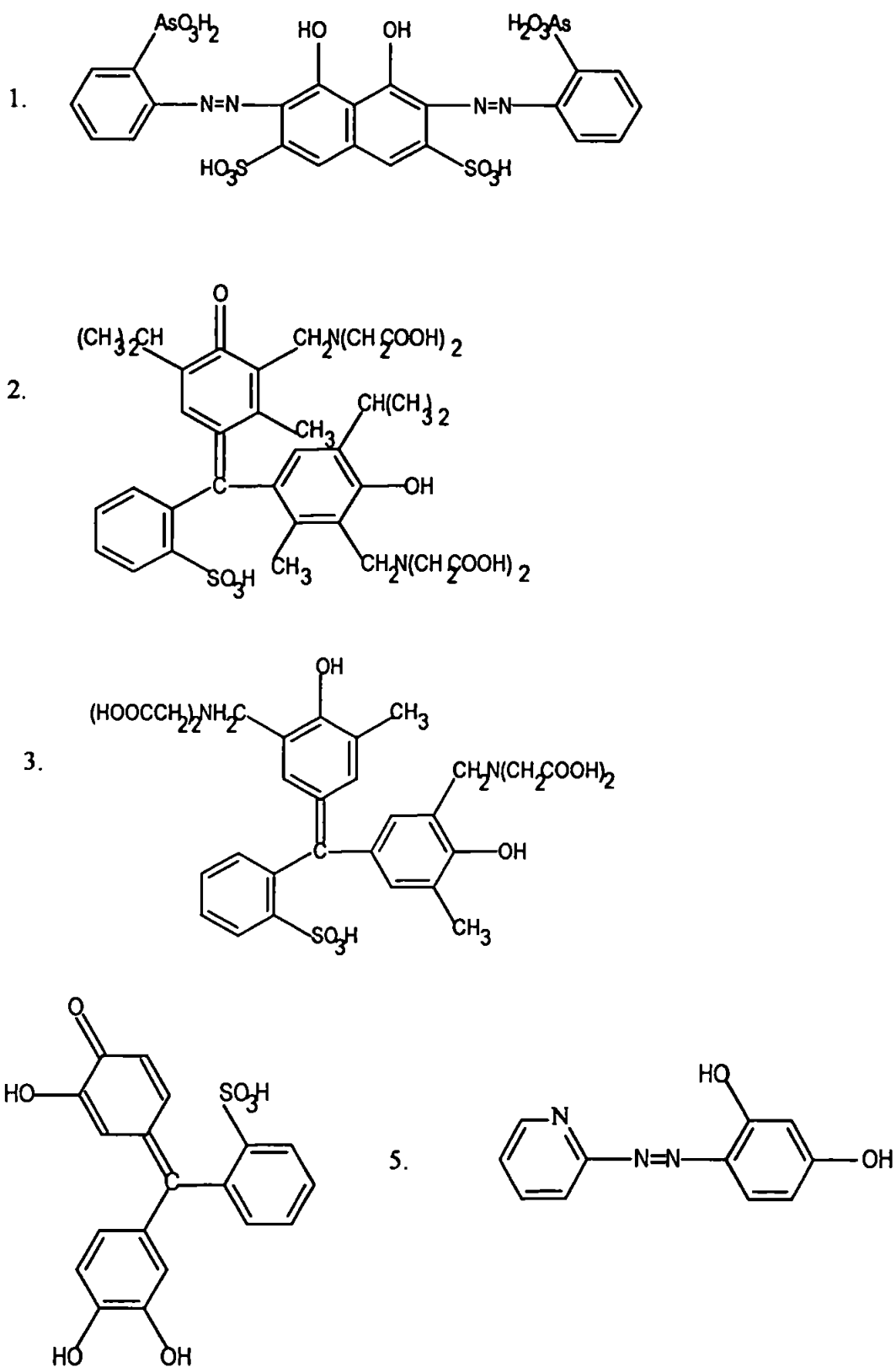


Figure 1.11 A selection of chromogenic reagents used to detect metal ions. 1: Arsenazo III, 2: Methylthymol Blue, 3: Xylenol Orange, 4: Pyrocatechol Violet and 5: 4-(2-pyridylazo)resorcinol.

of interest. In addition, the effect of other system parameters including column length, column capacity and mobile phase ionic strength upon the separation properties of chelating substrates will be investigated.

A novel, high efficiency silica substrate, functionalised with aminophosphonate groups, will also be characterised for metal ion separations. This chelating surface has the potential to bind metal ions through a nitrogen and two oxygen donor atoms (N,O,O chelation), and will be compared with the promising results achieved with iminodiacetate, another N,O,O chelating ligand.

Dynamic modification of neutral substrates with small chelating molecules is another type of chelating surface that will be investigated. Various organic acids will be studied, together with system parameters including ligand concentration in the eluent, mobile phase pH and stationary phase characteristics, to determine their affect on metal ion retention.

Another objective of this work will be to apply the most promising chelating columns for the determination of environmentally harmful metals in complex samples, that cannot be easily analysed by IC. This could be due to a high ionic strength, or significant concentration of interfering matrix metals, for example the alkaline earths, Fe(III) and Al(III), present in many environmental matrices. Post-column detection systems will also be improved as necessary to lower the detection limits for the analytes of interest.

Chapter 2. A Comparison of Chelating Dyes Impregnated onto Polystyrene resins for Trace Metal Separations

2.1 Introduction

The modification of substrates with chelating dyes, can provide a quick, simple and convenient technique for evaluating the metal retaining abilities of a ligand.

Aromatic dyes can be easily adsorbed onto polymeric resins by a combination of both physical impregnation within pore structures, and π - π interactions between the aromatic groups on the PS-DVB and corresponding dye.

Many of these chelating dye sorbents have been applied for both the preconcentration and separation of metal ions, dependant upon resin characteristics.

2.1.1 Dye immobilised low efficiency supports

Chelating dyestuffs, permanently immobilised onto large particle size substrates, have found widespread applications in the batch extraction and selective separation of traces of metal ions from aqueous solutions. Two reviews detailing the developments of these 'ligand – loaded' complexing substrates, are given by Marina *et al* [110,111]. A further selection of dye loaded chelating substrates, together with more recent applications, is given here.

Xylenol orange (XO) (Figure 1.11), a sulfonephthalein based dye with two IDA groups, able to chelate metals through a nitrogen and possible two oxygen atoms (N,O,O chelation), has been applied by various authors for the selective separation of metal ions.

Brajter and Olbrych-Sleszynska [112], loaded XO onto a strong base anion exchange resin, Amberlyst A-26, for the selective separation of trivalent and divalent groups of metal ions.

The resin was applied to the analysis of In(III) in a Ga-In alloy. The dye is loaded onto the resin by exchange of the Cl⁻ counter ion with the sulphonate group on the dye, and π - π interactions arising from the aromatic nature of the resin and reagent.

Ebdon *et al* [113,114], extended this approach by loading XO onto Dowex 1-X8 anion exchange resin, and packing this material into a 100mm titanium column. This column was applied to preconcentrate Al(III), Ba(II), Ca(II), Mg(II), Sr(II) and Zn(II) from concentrated brine solutions, before determination using backflushing into an analytical cation exchange column by means of switching valves. This system illustrated the potential for on-line monitoring of chlor-alkali process streams.

A similar sulfonephthalein dye, methylthymol blue (MTB) (Figure 1.11), which also contains two IDA groups, was impregnated onto silica gel by Kocjan and Garbacka [115]. This chelating substrate was packed into a 65mm polypropylene column, and used to separate heavy metals from the alkali and alkaline earth metals at pH <5. The column was also very stable, even after many repetitive washings with mineral acids (0.1M), required to displace heavy metals including Pb(II) and Cd(II).

Pyrocatechol violet (PCV) (Figure 1.11), another sulfonephthalein type dye, has also been used for the separation of metal ions. This molecule differs from both XO and MTB in that it is an oxygen chelating ligand (O,O), binding metals through its two hydroxyl groups, resulting in two possible chelating sites. This molecule is also a weaker acid than either XO or MTB, containing only oxygen donor atoms. This results in a stronger conjugate base and consequently very strong complex formation with metal ions. However, because oxygen chelating ligands are very weak acids, a high pH is required to dissociate the OH groups. Consequently, many oxygen ligating molecules are actually weaker, in terms of the magnitude of the conditional constants, than corresponding nitrogen containing molecules in acidic solutions. The acidity constant K_a and corresponding pK_a values can be used to estimate the chelating strength of a ligand. Increasing pK_a values will result in weaker acids, with correspondingly stronger conjugate bases, enhancing the chelating strength.

Brajter *et al* [116], immobilised PCV onto Amberlite XAD-2, a neutral PS-DVB resin, for the selective preconcentration of Pb(II) in tap water. Singh *et al* [117-120], have extensively studied the properties of this dye for the preconcentration of trace metals. Using Amberlite XAD-2, this modified resin was used to preconcentrate Zn(II) and Cd(II) [117], changing to an anionic resin, Amberlyst A-26, for the preconcentration of Pb(II) and Cd(II) [118], both in river water, prior to their determination by AAS. The anion exchanger, Dowex-2, modified with either PCV or XO, was used to compare the properties of each chelating agent for the preconcentration of Cu(II) and Cd(II) [119]. Similar loadings of each dye were calculated, but PCV offered a wider practical pH range for the collection of Cu(II), with the XO resin having a greater sorbing capacity for both metals. A recent development has been to couple this ligand to Amberlite XAD-2, using an azo - N=N- spacer [120]. Using this approach, which created a more stable substrate, Zn(II), Ni(II) and Pb(II) were preconcentrated and extracted from well-water, prior to determination using AAS.

Another oxygen ligating sulfonephthalein molecule, similar to PCV, is Chrome – Azurol S (CAS). This dye also has two possible complexing sites, able to bind metals through two hydroxyl and carboxyl groups. The carboxyl groups make this molecule more weakly chelating than PCV, as carboxylic acids are stronger acids than phenol groups and consequently have weaker conjugate bases. Molodovan and Vladescu [121], immobilised this reagent onto Dowex 2x4 anion exchange resin, for the selective extraction of Al(III) from other metals, applied to the determination of this metal in a Zn(II) sample using ICP-AES.

In addition to the use of these large triphenylmethane based metallochromic molecules, extensive studies have been undertaken using smaller azo based reagents, which bind metals using azo nitrogen and hydroxyl oxygen donor atoms. One such dye which has been immobilised onto substrates is PAR. Brajter and Dabek-Zlotorzynska [122], immobilised this dye onto Amberlite XAD-2, for the selective extraction of Ag(I) in copper ores, with

AAS detection, whilst Pilipenko *et al* [123], modified a macroporous cation exchanger, KU-23, for the preconcentration of various heavy metals in high purity salts and tap water. More recently, Su and Huang [124], impregnated PAR onto C₁₈ silica gel for the selective extraction of Cd(II) from seawater, whilst Chakrapani *et al* [125], used PAR to preconcentrate various heavy metals in ground water. Both methods determined analytes using AAS.

Morozko and Ivanov [126,127], have undertaken detailed investigations on transition metal retention properties and loading characteristics of PAR and 1-(2-pyridylazo)-2-naphthol (PAN), immobilised onto cellulose and silica sorbents. Cornejo-Ponce *et al* [128], immobilised PAN onto silica gel for the preconcentration of rare-earth metals, whilst Ferreira *et al* [129], selectively separated and preconcentrated Ni(II) from saline matrices, using Amberlite XAD-2 loaded with PAN, with ICP-AES detection.

Lee *et al* [130,131], synthesised a 4-(2-thiazolylazo)resorcinol (TAR) sorbent by coupling it to a styrene divinylbenzene polymer, for the preconcentration and separation of U(VI) from transition, alkali and alkaline earth metals.

Ferreira *et al* [132], adsorbed 1-(2-thiazolylazo)-2-naphthol (TAN) onto Amberlite XAD-2, for the selective preconcentration of Zn(II) and Cu(II) ions in natural water samples, with ICP-AES detection. Zaporozhets *et al* [133], used this azo molecule, loaded onto silica gel for the same purpose.

Other azo dye reagents, used for metal ion separations, include Acid Orange 7 (Orange II) [134] and Acid Orange 8 [135], impregnated onto silica gel for the preconcentration of heavy metal ions, and Calmagite (CAL), loaded onto Amberlite XAD-2, for Cu(II) determination in natural waters using AAS [136].

Shah and Devi [137], synthesised a Dithizone loaded polymer for the separation of Cu(II), Ni(II) and Zn(II) from complex matrices.

These few examples illustrate recent ongoing developments to modify substrates with various chelating dyestuffs, the purpose being to optimise systems for preconcentrating and

separating various metal ions from complex matrices, which remains a challenge for most analytical techniques. By altering the chelating functionality, structure of the dye and elution parameters, a method can be obtained which is specific for groups or individual ions, dependant upon analysis requirements, emphasising the suitability of chelating sorbents for metal ion separations.

In addition to investigating different dyes for metal extraction purposes, novel approaches to loading these reagents onto various sorbents are under investigation. Morosanova *et al* [138], investigated immobilising complex forming reagents including PAN, PAR and XO, using a sol-gel doping procedure, whereby the reagents are introduced during silica glass preparation, forming chelating 'Xerogels'. These sorbents were investigated for metal sorption properties, and applied to the determination of various heavy metals in environmental samples including waste waters.

Huddersman *et al* [139], developed a novel diazotisation method to synthesise and encapsulate azo dyes within aluminosilicate mineral (Zeolite) cavities, which could be applied with development, as solid metal ion indicators for process streams.

The dye loaded substrates outlined above are primarily used to preconcentrate analytes of interest. Using large particle sized substrates reduces system efficiency, and prevents the individual separation of metal ions. To perform analytical separations, whereby individual analytes can be separated and determined using a single column, small particle size, high efficiency sorbents are required. The following section gives examples of this type of fabricated high efficiency chelating column.

2.1.2 High performance dye impregnated supports

Various metallochromic dyes have been immobilised onto high efficiency substrates, to separate and determine trace metals in various complex matrices using the HPCIC approach.

Jones and Schwedt [140], developed this technique by permanently coating a 150mm 10 μ m neutral polystyrene resin with CAS. The analytical separation of divalent and trivalent metal ions was strongly influenced by pH, but little affected by ionic strength, which paved the way for further development in this field.

Challenger *et al* [141], continued these studies, using HPCIC for the determination of trace metals in high ionic strength media. An initial comparison, illustrating the metal separation ability of CAS and XO, loaded onto 8 μ m neutral PS-DVB, is given in [142], which resulted in the single column separation and determination of the alkaline earth metals and selected transition metals in concentrated brines and seawater [143]. Jones *et al* [144], used another sulfonephthalein molecule, *O*-Cresolphthalein Complexone (CPC), also known as Phthalein Purple, for the determination of Sr(II) in milk powder, with Zn-EDTA/PAR PCR detection. Using an eluent containing 1M KNO₃ to suppress ion-exchange interactions, the chelating ability of the CPC column reversed the selectivity for the alkaline earth metals, allowing trace Sr(II) to elute before Ca(II).

Using a XO chelating column and a pH step gradient program, transition metals have been preconcentrated and determined in seawater, with PAR detection [145], and the alkaline earth metals determined in oil-well brines using a MTB column with isocratic elution and Zn-EDTA/PAR detection [146].

A comparison between the metal selective properties of these various dye impregnated high efficiency resins has been undertaken by Paull and Jones [147]. Findings indicate that triphenylmethane based dyes with IDA functionality, for example XO and MTB, provided the most stable coatings and column capacities. This paper also detailed the determination of Al(III) in seawater using a CAS loaded column.

A comparison between different substrates loaded with chelating dyes for the separation of metal ions was undertaken by Sutton *et al* [148]. Four different macroreticular polystyrene resins were impregnated with PAR: a strong base anion exchange resin, Amberlite IRA 904; a weak base anionic macronet resin, Purolite MN100; and two neutral resins,

Amberlite XAD-2 and Purolite MN200, a macronet resin. Amberlite IRA 904 gave the poorest performance in terms of chelating strength, with the macronets illustrating the highest capacity, possibly due to the high surface areas of these resins. A cellulose column, impregnated with Procion Violet P-3R (Zeneca), was also prepared, but this had a low capacity, rendering metal separations unfeasible. However, Cu(II) was strongly retained on this column, which should allow its isolation and removal from various complex samples.

2.1.3 Dyes added to the mobile phase for high efficiency separations

An alternative approach to 'pre-coating' substrates with dyes, has been to include the ligand within the mobile phase, resulting in a dynamic coating on the stationary phase. Eventually an equilibrium establishes between the amount of dye adsorbed onto the substrate, and that in the eluent. Dependant upon the ligand concentration in the mobile phase, and pH, this system is capable of high efficiency separation of metal ions. The technique offers certain advantages over pre-coated columns. A significant drawback of current pre-coated substrates is the relatively poor efficiency in comparison with covalently bonded high performance chelating columns. Using high efficiency small particle size substrates, ≤ 5 metal ions can generally be separated isocratically. This is related to the 'kinetic broadening' principle with more slowly eluting peaks exhibiting asymmetric tailing, as mentioned in Chapter 1. Inclusion of the dye within the mobile phase can increase the capacity, allowing the pH to be reduced to improve the efficiency, in terms of a decrease in kinetic broadening effects. Dynamic loading additionally provides a more stable coating, in comparison with certain pre-coated columns which can degrade when using highly acidic or alkaline eluents over a long length of time. In addition, the concentration of ligand in the eluent can alter the column selectivity for certain metal ions,

and certain metal-ligand complexes can form coloured species amenable to direct detection, negating the requirement for PCR systems.

A possible disadvantage of dynamically loaded columns is the effect of complex sample constituents on system stability. For instance, it is unclear whether a sample injection containing a large concentration of matrix metals would upset the ligand equilibrium, and temporarily leach a proportion of the dye from the column, thereby upsetting the baseline which could interfere with the sensitive detection of analyte ions. Nevertheless, a number of studies have been undertaken using dynamic coating procedures.

In an early paper by Dinunzio *et al* [149], trace concentrations of Zn(II), Fe(II), Ni(II) and Cu(II) were separated as PAR complexes on a C₁₈ silica column. The complexes were determined directly at 525nm, the mobile phase containing 0.1mM PAR buffered with acetate (0.01M).

This introduction of a colour forming reagent within the mobile phase to determine metal ions has been extensively studied by Toei [150-154]. The alkaline earth metals were separated using gradient elution with a carboxylic acid cation exchanger and 1mM CPC present in the eluent, with detection at 575nm [150]. This system was developed, changing to an IDA cation exchanger (Tosoh), together with 0.1mM CPC, present in the mobile phase, to determine Ca(II) and Mg(II) in seawater [151] and clinical samples [152]. Arsenazo III, at a concentration of 1mM in the mobile phase, together with a sulfonic acid cation exchanger, was also studied as a system for separating and directly detecting the alkaline earth metals [153]. Ni(II) and Zn(II) were also separated and detected directly at 575nm, as their XO complexes (0.1mM XO in the mobile phase) using an anion exchange column [154].

Walker [155], used a mobile phase containing 0.1mM thymol blue, together with a neutral PS-DVB substrate, to separate various transition and alkaline earth metal ions, with direct detection of the coloured metal complexes at 428nm.

The determination of Ca(II) and Mg(II) in water samples was undertaken by Paull *et al* [156,157], using a mobile phase containing 0.4mM CPC and a graphitic carbon column. As the separation of these metals was achieved at pH 10.5, the coloured complexes could be determined directly at 572nm, without the need of a post column pump. Earlier work with this dye, undertaken by Toei, still required a post column pump to deliver an ammonia solution to raise the pH and form the coloured metal ligand complexes.

Additional work by Paull *et al* [158-160], has involved using a high ionic strength eluent (0.5M KNO₃) to suppress ion-exchange interactions, ensuring that interactions between the metal ions and chelating dye present in the mobile and stationary phases becomes the dominant retention mechanism. Using this system, a 0.2mM MTB containing mobile phase has been used to separate selected transition and rare earth metal ions, with detection as their coloured complexes at 600nm, using both a PS-DVB column [158] and an ODS silica column [159]. A mobile phase containing 0.2mM CPC, with direct metal complex detection at 575nm, together with a PS-DVB column, was used to separate the alkaline earth metal ions, with the determination of Sr(II) in an Antarctic brine sample [160].

A recent review paper comparing the relative merits of HPCIC using either pre-coated or dynamically coated dye loaded columns, for the separation of metal ions is given by Paull and Haddad [161].

An illustration of various dye molecule structures mentioned in this section, are given in Figures 2.1 and 2.2.

2.1.4 Aims of this study

As shown in the preceding sections, a range of pre-coated and dynamically coated dye loaded columns have been utilised for the high performance separation of metal ions. The performance characteristics of each chelating ligand have not yet been fully classified, however. It is of special interest to investigate the effect of dye structure and ligating atoms

(oxygen and nitrogen combinations), on the capacity, selectivity and separation efficiency for selected groups of metal ions demonstrating soft through to hard base character.

This evaluation of ligand-metal complex behaviour can provide a source of reference for producing high performance chelating columns, dye impregnated, dynamically loaded or covalently bonded, for analytical separations of metal ions in various sample types for specific applications. Other factors will also be investigated, namely the effect of column length, capacity and mobile phase characteristics on metal ion retention using chelating columns.

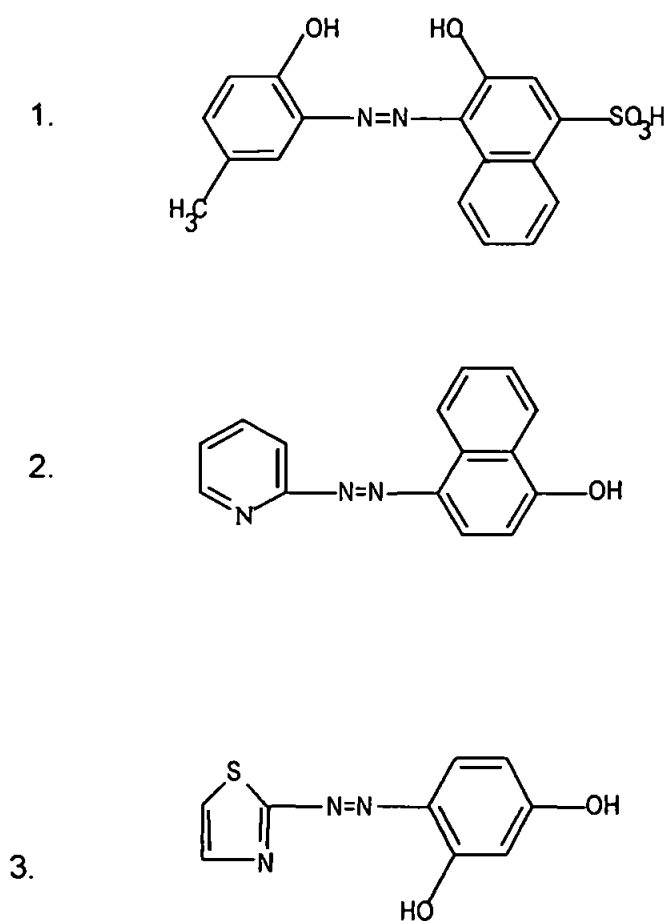


Figure 2.1. Structures of dye molecules used for the preconcentration and separation of metal ions: 1. Calmagite; 2. 1-(2-pyridylazo)-2-naphthol; 3. 4-(2-thiazolylazo)resorcinol.

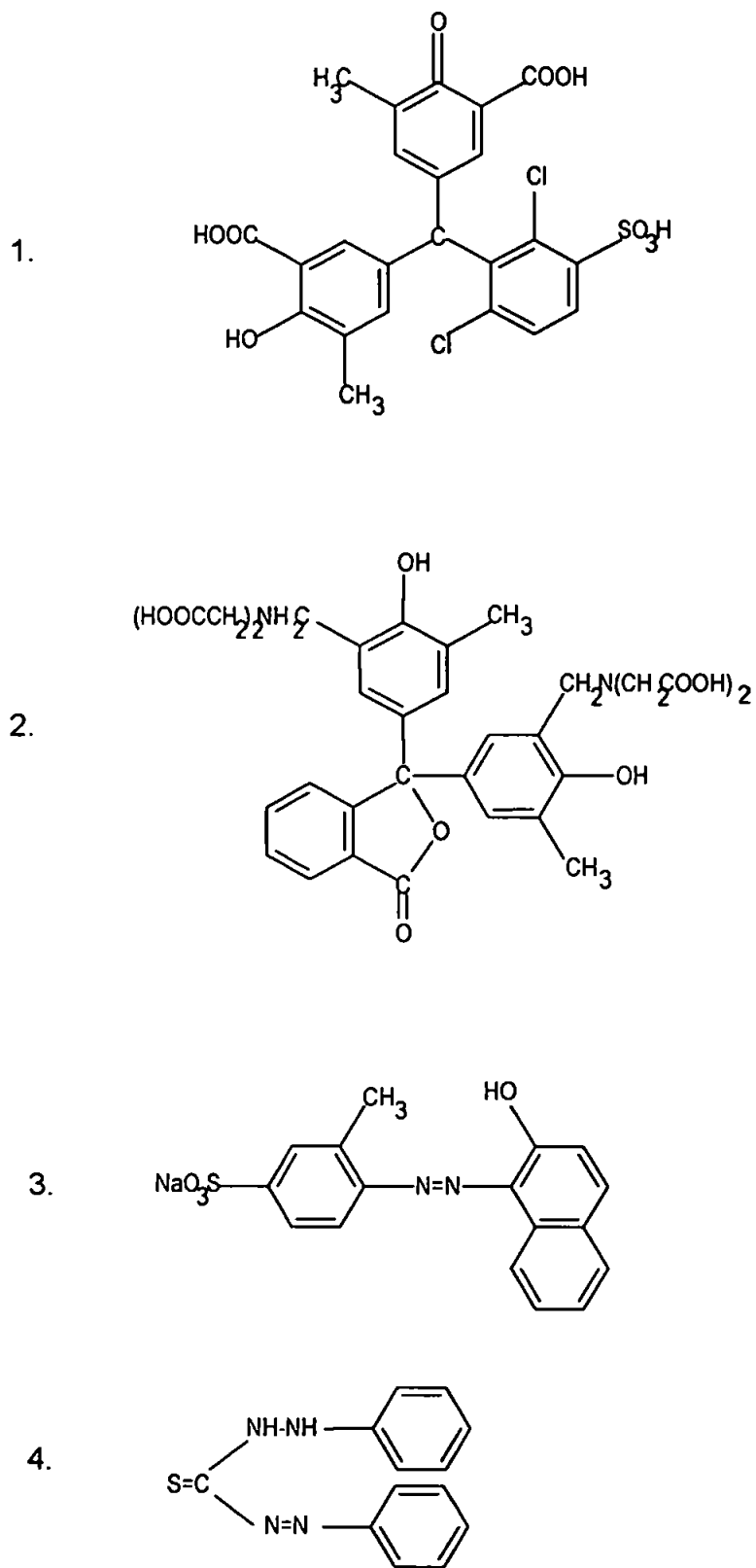


Figure 2.2 Structures of dye molecules used for the preconcentration and separation of metal ions: 1. Chrome Azurol S; 2. *O*-Cresolphthalein Complexone; 3. Acid orange 8 (acid orange 7 has no methyl group) and 4. Dithizone.

2.2 Experimental

2.2.1 Instrumentation

The basic instrumentation used throughout the studies presented in this thesis is shown schematically in Figure 2.3.

The ion chromatographic system consisted of a Dionex GP40 gradient pump (Dionex, Sunnyvale, CA, USA), a Rheodyne 9010 polyether ether ketone (PEEK) liquid six port injection valve (Rheodyne, Cotati, CA, USA), fitted with a 100 μ l PEEK sample loop. The analytical column was a PEEK (100 mm \times 4.6 mm I.D.) casing, slurry packed with PS-DVB resins as given in Table 2.1, using 30% methanol under a constant pressure of 2000psi on a Shandon packing machine (Shandon Southern Products Ltd, Cheshire, UK). The post-column detection system included a Constametric III HPLC pump (LDC, Riviera beach, FL, USA) delivering the postcolumn reagent (PCR), a zero dead volume PTFE tee and a 1.4 m \times 0.3 mm I.D. PTFE reaction coil. Detection was achieved using a spectral array detector (Dionex, Sunnyvale, CA, USA). Chromatograms were recorded using either a Dionex AI450 integration system, or Dionex Peaknet software.

2.2.2 Reagents

For the majority of studies, the mobile phase consisted of 1M KNO₃, present to suppress ion-exchange interactions, and a weak complexing agent, acetic acid, at 50 – 100mM concentration, present to keep metals in solution at higher pH values. The mobile phase was adjusted to the appropriate pH (Model 3010, Jenway, Essex, UK) using dilute solutions of NH₃ and HNO₃, and made up to the correct volume with distilled deionised water (MilliQ, Millipore, Milford, MA, USA). The eluent was degassed using argon.

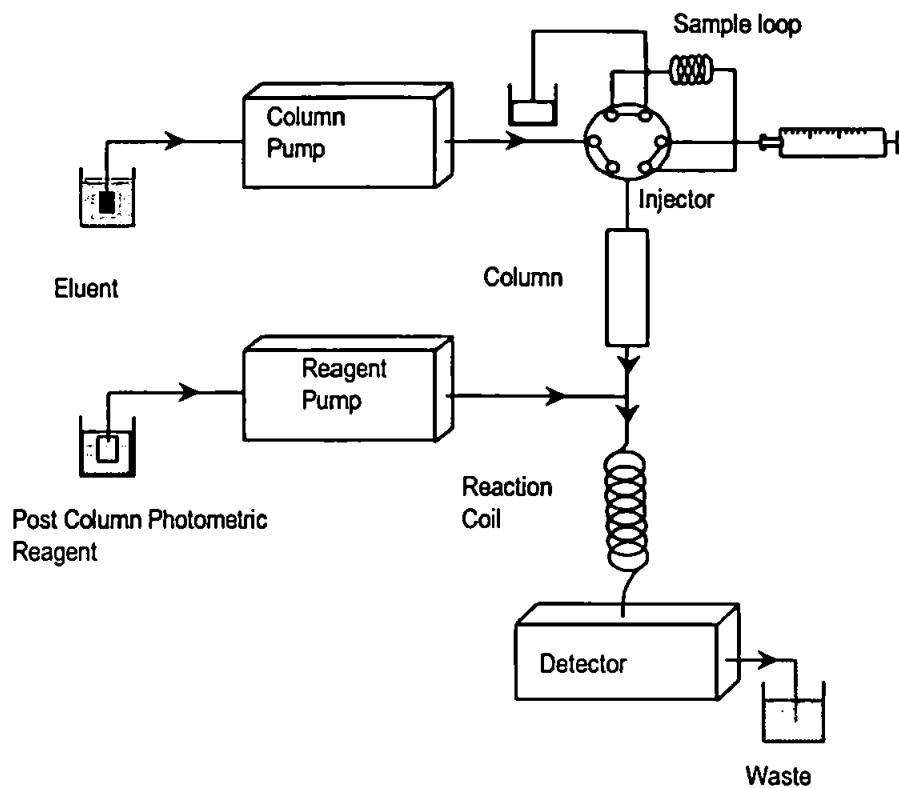


Figure 2.3. A schematic diagram of the chromatographic system.

The post column metallochromic reagents used were:

1. 0.12mM PAR, buffered to pH 10.2 with 2.6M NH_4OH and 0.85M NH_4NO_3 for the transition and heavy metal ions. (30ml stock 4mM PAR, 192ml 35% NH_3 and 54ml 69% HNO_3 , made up to 1 litre with Milli-Q water);
2. 0.12mM PAR, 0.2mM Zn-EDTA and 2M 35% NH_3 for the alkaline earth metals;
3. 0.004% PCV, buffered to pH 6.9 using 2M hexamine and dil. NH_3 , for the trivalent metal ions.

Absorbance spectra for selected metals with these post column solutions are given as Figures 2.4 and 2.5.

Detection of the transition and alkaline earth metals was achieved with PAR at 490nm, the trivalent ions monitored at 580nm using PCV. Both the eluent and PCR were delivered at 1ml min⁻¹. All reagents were of AnalaR grade (BDH, Poole, Dorset, UK), with the exception of PAR and Zn-EDTA (Fluka, Glossop, Derbyshire, UK) and PCV (BDH). Metal standards were prepared from Spectrosol 1000mg l⁻¹ stock solutions (BDH), using Milli-Q water, and stored in poly(propylene) bottles (BDH).

2.2.3 Dye types studied

Six dyes, demonstrating a range of chelating functionalities, were procured from various companies, as shown in Table 2.1.

Table 2.1 Chelating dyes studied, and resins used.

Dye	PS-DVB Resin	
	Particle size μm	Pore size \AA
Aurin tricarboxylic acid ¹	8.8 ⁴	120
Pyrocatechol violet ²	7 ⁵	100
Calmagite ¹	9 ⁴	120
<i>o</i> -cresolphthalein complexone ¹	8.8 ⁴	120
4-(2-pyridylazo)resorcinol ²	8 ⁶	120
2-(3-sulphobenzoyl)pyridine-2-pyridyl hydrazone ³	9 ⁴	120

1. Sigma Chemicals, Poole, UK.
2. Aldrich, Gillingham, UK.
3. Fluka.
4. Dionex.
5. Hamilton, Reno, NV, USA.
6. Polymer Labs, Shropshire, UK.

2.2.4 Procedures

2.2.4.1 Column Preparation.

For each resin, 1g was sonicated in 30ml methanol:Milli-Q water (10:20), and slurry packed into the 100-4.6mm PEEK column using the Shandon Packer at 2000psi, with a 30% methanol solvent. The column, end fittings and frits were sonicated in 10% methanol for 1 hour prior to packing.

Impregnation was achieved by recycling a dye solution through the column overnight at 1 ml min^{-1} . The dye solutions were made up to 100ml using 1:10 v/v methanol:Milli-Q water, at a concentration of 0.2%, and adjusted to pH 5, with the exception of PAR and SPP, which were adjusted to pH 7. Below this pH, these dyes are insoluble. The other dyes were loaded at pH 5, due to previous investigations [147], which found this value optimal for obtaining a stable coating.

The loaded columns were conditioned by pumping through HNO_3 (0.1M), NH_3 (0.1M) and Milli-Q water, until the loosely associated dye had been cleared from the column. The dye washings were collected for analysis by UV-VIS spectrophotometry (Model 8453, Hewlett Packard, OR, USA). The absorbances of the dye solutions were determined prior to and after the dyeing process, the difference being proportional to the concentration of dye coated onto the resin.

2.2.4.2 Column Capacity Measurement.

The capacity of each column was calculated from the mid-point of the S-shaped breakthrough curves, using a known quantity of Cu(II), buffered to a pH, which ensured complete retention. A typical Cu(II) solution, at 50 mg l^{-1} , in 1M KNO_3 , was buffered with

1M ammonium acetate, to pH 6.5. Detection was achieved with PAR at 490nm. Both solutions were delivered at 1 ml min^{-1} . The column was pre-equilibrated to pH 6.5, before the Cu(II) solution was pumped through the system.

The breakthrough time, from the injector onwards, was adjusted to subtract the system dead-time, and used to calculate the concentration of Cu(II) held on the resin. This value, together with the concentration of dye immobilised onto the resin support, provides an indicative value of the percentage available sites for chelation.

2.2.4.3 Capacity Factor Determination

The capacity factors for each dye loaded resin were obtained from the repeat injections of metal ions at various pH values, after column equilibration with the mobile phase.

Three metals were chosen to represent the range of chelating strengths. In(III) is a relatively hard acid, which generally forms very strong chelates, with Zn(II) and Mg(II) forming medium to relatively weak complexes respectively. Other metal ions have been included in the k' plots if sufficient retention was found over the pH range studied.

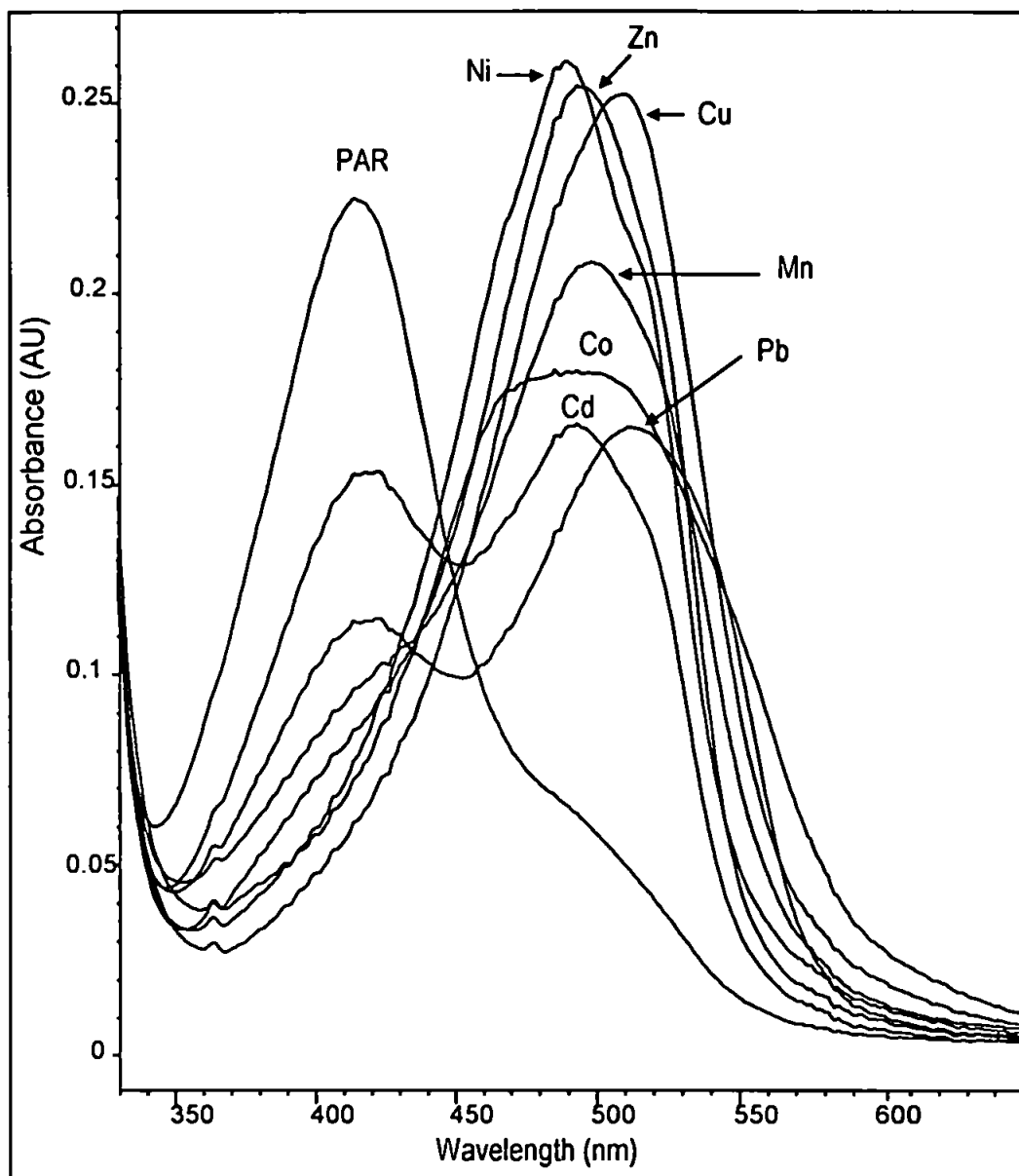


Figure 2.4. Absorbance spectra of selected metals (1 mg l^{-1}) with the PAR post-column reagent.

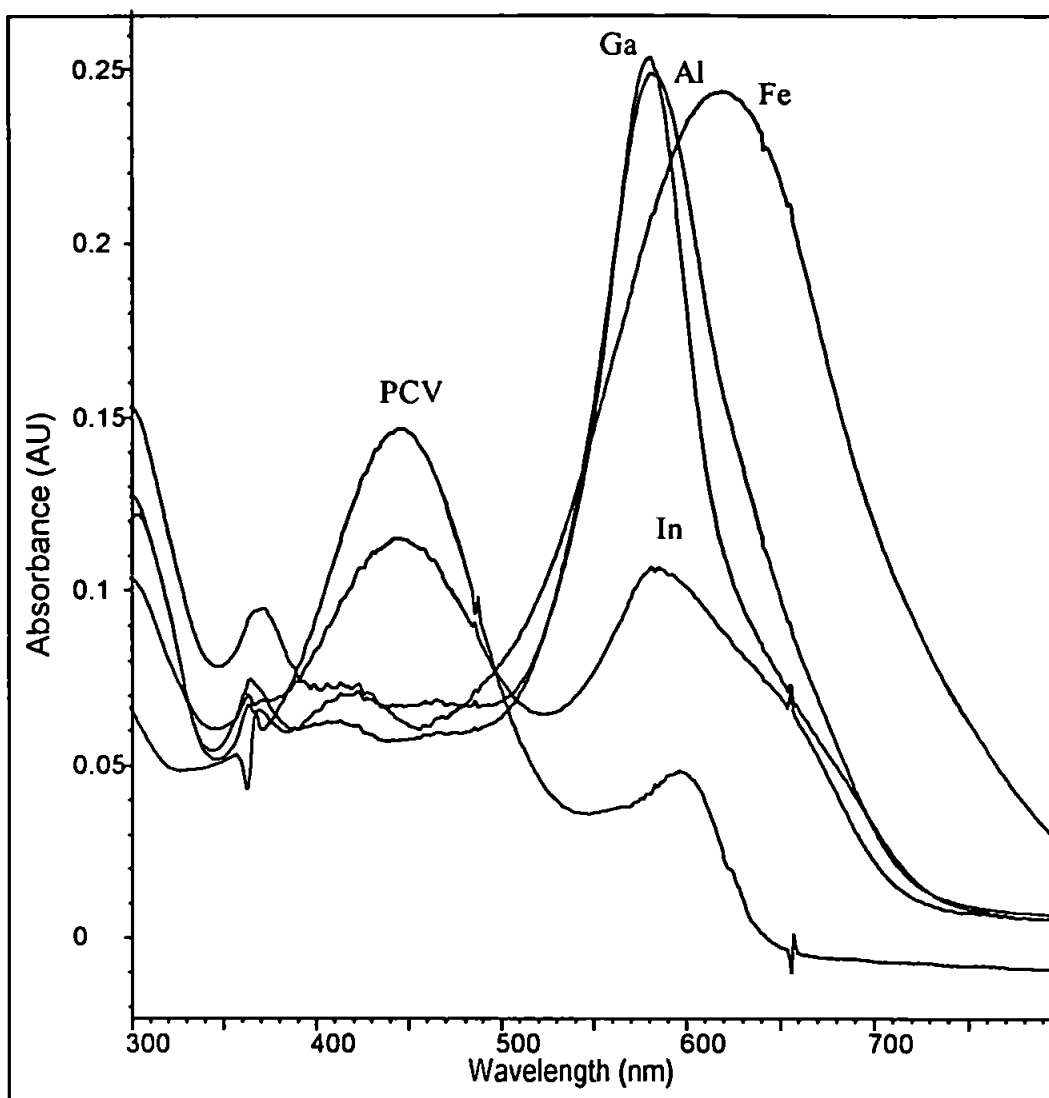
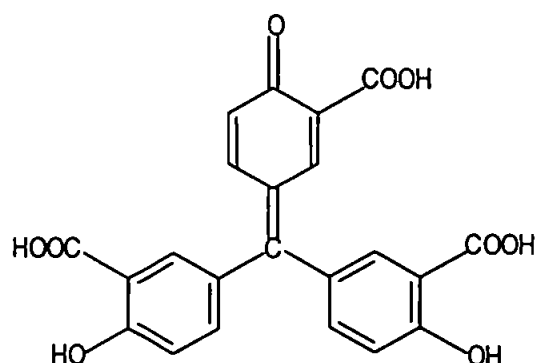


Figure 2.5. Absorbance spectra of selected metals (1 mg l^{-1}) with PCV post-column reagent.

2.3 Results and Discussion

2.3.1 Aurin Tricarboxylic Acid (ATA) Column



H₅L fw. 422.3

ATA is an oxygen (O,O) chelating molecule, able to bind metal ions at three separate sites, which contain carboxyl groups adjacent to hydroxyl groups. It has a large, triphenylmethane based structure, and has been used as a metallochromic indicator for Al(III) and Be(II) [103]. The log stability constants of selected metal complexes with this ligand are given in Table 2.2, which demonstrates the relatively low stabilities between the dissociated ligand and metals of various valences.

Table 2.2 Log stability constants of metal complexes with ATA [162] (0.1M Ionic strength)

M ⁿ⁺	logK ₁
Be ²⁺	5.38
Cu ²⁺	4.1
Fe ³⁺	4.68
Th ⁴⁺	5.04
UO ₂ ²⁺	4.77

After column equilibration, 107mg /g resin of this dye had impregnated within the pores, equivalent to 0.253mM /g resin. This immobilised dye was able to bind with 0.01mM Cu(II) /g resin, indicating only 3.8% available sites for chelation. The percentage of dye loaded, which is actively chelating is apparently low. This could be due to steric effects within the column 'hiding' the chelating group from metal ions, which would depend upon the resin pore size and structure of the dye. Previous investigations, however [147], have concluded that impregnated resins with values <5% chelating activity, are still capable of retaining and giving good separations of metal ions.

The analytical separation potential of the ATA column was investigated with the injection of various divalent and trivalent metal ions over a wide pH range. Due to the reaction kinetics of complex formation and dissociation, peak asymmetry increased with increasing eluent pH. The k' vs. pH plot for selected trivalent and transition metal ions are given in Figure 2.6, a similar plot for the alkaline earth metals given in Figure 2.7. As expected, the slopes illustrate that this ligand chelates strongly with In(III), less so with Zn(II) and only weakly with Mg(II). Indeed, the alkaline earths only start becoming retained noticeably above pH 6, which could be applied to the separation of these metals from the transition and heavier elements, strongly retained at this pH. Unlike the other alkaline earth metals, Mg(II) reflects a far stronger retention on this chelating substrate at higher pH values, becoming more strongly retained than Ca(II) in the process. The reasons for this are uncertain, as it was initially thought to be partly due to the differing concentrations of hydroxide species present at high pH, hydroxide formation weakening the ligands ability to complex the remaining free metal ions. Mg(II), however, forms hydroxide species at a lower pH than Ca(II), which doesn't support this explanation. An alternative explanation might relate to the size of the metal ions, and subsequent ability to 'fit' with the ligand groups. This ligand-metal character has been demonstrated previously [107], when Mg(II) became more strongly retained than the other alkaline earth metals on another oxygen

chelating CAS impregnated resin, at 1M ionic strength. This behaviour could therefore be a characteristic of oxygen chelating ligands.

Apart from this Mg(II) shift, the retention order followed a more predictable pattern for the investigated metal ions which did not alter with pH, and was found to be:

Mn(II)<Co(II)<Zn(II)<Ni(II)<Cd(II)<Pb(II)<Cu(II)<La(III)<Lu(III)<Ga(III)<In(III), for the trivalent and transition metal ions, with the alkaline earths Ba(II)<Sr(II)<Ca(II)<Mg(II) retained more weakly. The separation of the alkaline earth metals at pH 10.5 is given in Figure 2.8. For the transition metal ions, only 3 could be separated isocratically on the 100mm column, before slow reaction kinetics made peak shapes too broad. An unusual retention order was noted for the transition and heavy metal ions studied, in that Cd(II) was more strongly retained than Zn(II). This has not been found with any of the previously published work on high performance dye coated columns. In addition, there was also a large gap between Cd(II) and Pb(II), illustrating the differences in the conditional stability constants between these two heavy metals. A separation of Zn(II), Cd(II) and Pb(II) at pH 3.7 is shown in Figure 2.9. This column was also capable of separating various trivalent metals, for instance Al(III), Ga(III) and In(III) at pH 2, shown in Figure 2.10.

This separation was achieved at a higher pH than expected for these 'hard' acid metals, and is due to the weaker complex formation of oxygen ligands in acidic eluents. That is, the ligand requires a higher pH to dissociate its donor atom groups. This can be advantageous in that heavier elements can be separated without necessitating the use of very acidic eluents which would be required to elute the metals within a reasonable time on nitrogen containing chelating sorbents.

It is also interesting to note that the In(III) peak is not as susceptible to the kinetic broadening effect as the earlier eluting Ga(III). This is because In(III) is a more kinetically labile metal and dissociates from the ligand at a faster rate than Ga(III).

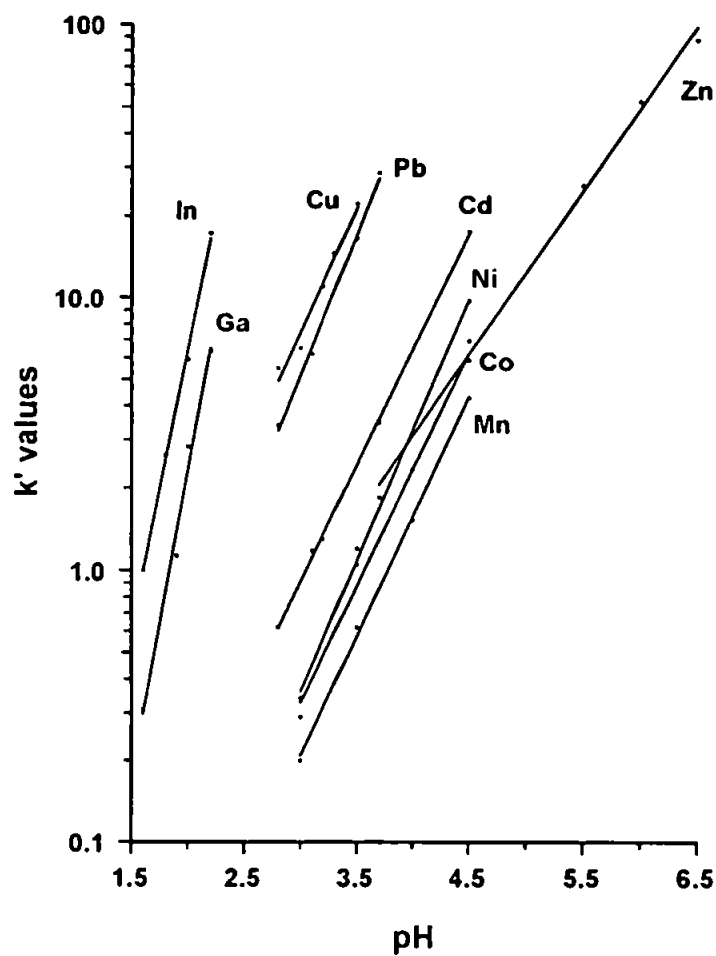


Figure 2.6. The dependence of capacity factors for transition and trivalent metal ions on eluent pH, with the ATA loaded column. Eluent: 1M KNO₃, 50mM acetic acid.

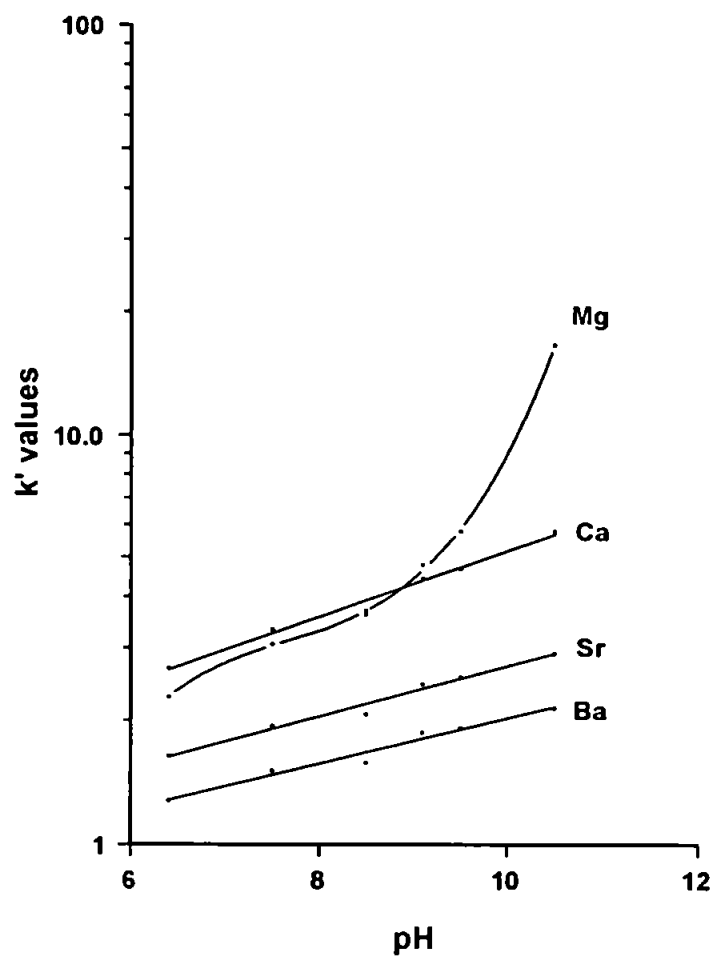


Figure 2.7. The dependence of capacity factors for alkaline earth metals on eluent pH, with the ATA loaded column. Eluent: 1M KNO₃, 50mM acetic acid.

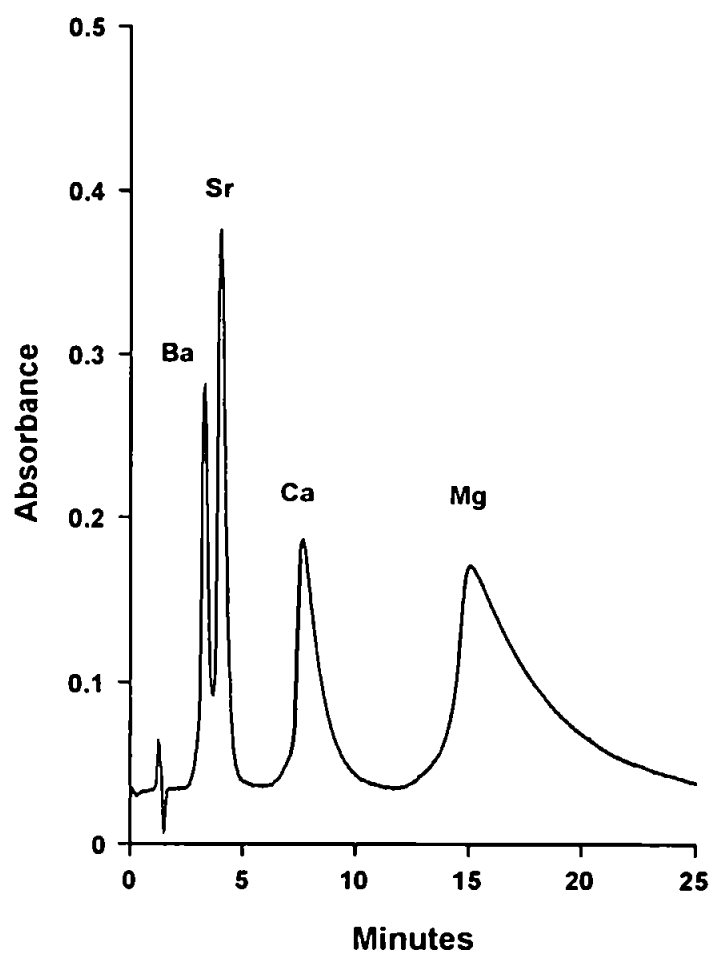


Figure 2.8. Separation of Ba(II) 10mg l⁻¹, Sr(II) 10mg l⁻¹, Ca(II) 5mg l⁻¹ and Mg(II) 10mg l⁻¹, on the 100mm · 4.6mm ATA column. Eluent 1M KNO₃ 50mM acetic acid at pH 10.5. Detection: PAR/ Zn-EDTA at 490nm.

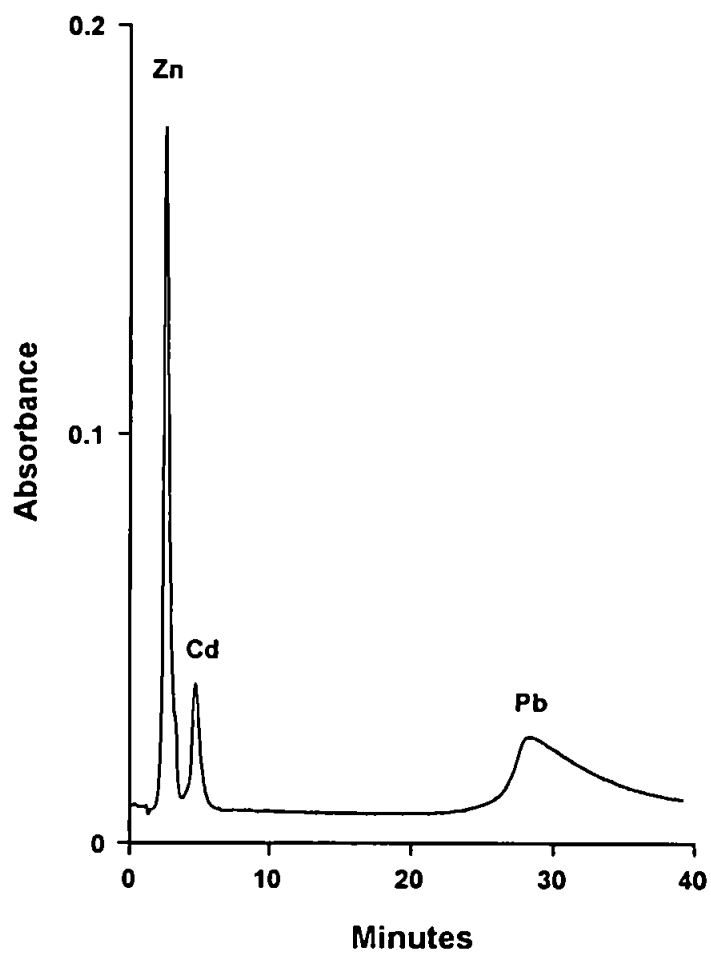


Figure 2.9. Separation of Zn(II) 10mg l⁻¹, Cd(II) 20mg l⁻¹ and Pb(II) 40mg l⁻¹, on the 100mm · 4.6mm ATA column. Eluent 1M KNO₃ 50mM acetic acid at pH 3.7. Detection: PAR at 490nm.

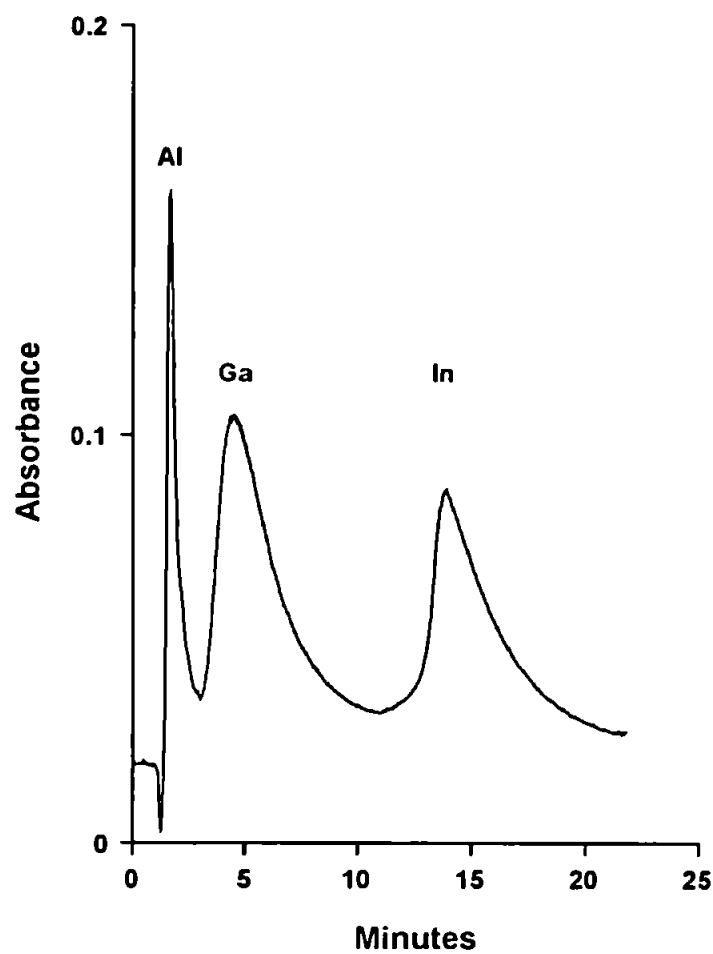
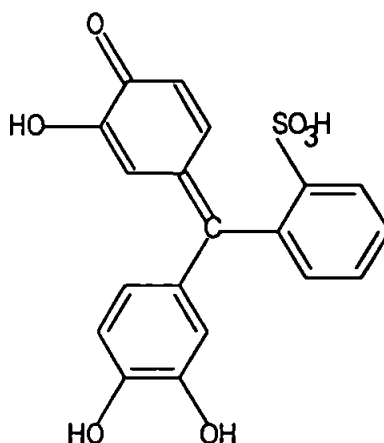


Figure 2.10. Separation of Al(III) 2mg l^{-1} , Ga(III) 10mg l^{-1} and In(III) 10mg l^{-1} , on the $100\text{mm} \cdot 4.6\text{mm}$ ATA column. Eluent 1M KNO_3 50mM acetic acid at pH 2.0. Detection: PCV at 580nm .

2.3.2 Pyrocatechol Violet (PCV) Column



H₃L fw. 386.4 pK₃ = 11.7

PCV, like ATA is also a triphenylmethane based oxygen (O,O) chelator, but with two chelating sites containing hydroxyl groups only. As previously mentioned in Chapter 1, hydroxyl groups can form stronger complexes with metal ions than carboxyl groups. Thereby the hydroxyl groups on PCV could make this molecule a stronger chelating agent than ATA. However, a higher pH is required to dissociate the hydroxyl groups, meaning that PCV could actually exhibit a weaker nature in acidic media. In addition, the sulphonate group signifies that this molecule has an increased solubility in acidic media.

As already mentioned, the larger the pK_a value, the weaker the acid, resulting in a stronger base. PCV is a weak acid, with a pK_a value in its dissociated form of 11.7 [162]. Unfortunately, this could not be compared with ATA, as no values were found in the literature for this molecule. Stability constant data for metal ion complexes with PCV was also sparse, but logK₁ values of 12.28 for Zn(II) and 25.12 for Al(III) have been quoted [163]. Compared with the values given for ATA in Table 2.2, this is indicative that PCV is a stronger chelating agent. It has been utilised as a metallochromic indicator for many metal ions including Fe(III), Ga(III), In(III) and certain transition metals [102].

A much reduced loading of this dye was achieved on the resin, 46.4 mg /g resin, equating to 0.12mM /g resin, in comparison with ATA (0.253mM/g), which could be associated

with the resins reduced particle and pore size, or the increased dye solubility, resulting in additional leaching during column equilibration. The impregnated coating had a capacity of 0.006mg Cu(II) /g resin, which actually gave an increased percentage of available sites for chelation, 4.6%, which again could be attributed to resin characteristics in combination with steric effects on the dye. A comparison of the dye loaded column characteristics in tabular form, is given in the summary at the end of this chapter.

The retention of transition and lanthanide ions over the pH range 2.5 – 4.5 was poor, with the exception of Cu(II), which became strongly retained, k' 2.9 at pH 2.5, increasing to k' 43.3 at pH 3. Pb(II) was also retained more strongly than the other transition metal ions, with a k' value of 5.9 at pH 4. The alkaline earth metals remained on the solvent front until around pH 9, 3 pH units different to results recorded on the ATA column, which could be attributed to either the weaker nature of the PCV ligating atoms in the acid region, or a factor of the low column capacity. The trivalent ions Ga(III) and In(III) were strongly retained at low pH (< 2), though eluting closely together, with Al(III) being very weakly retained. The elution order for selected metals on this column was Ba(II) $<$ Sr(II) $<$ Ca(II) $<$ Mg(II), Mn(II) $<$ Cd(II) $<$ Co(II) $<$ Ni(II) $<$ Zn(II) $<$ Pb(II) $<$ Cu(II) for the transition metal ions, and Al(III) $<$ Ga(III) $<$ In(III) for the trivalent metal ions. A significant difference between the ATA column and this PCV loaded substrate, was the selectivity differences for the transition metal ions. Both molecules are oxygen chelators, but Cd(II) is retained very weakly on the PCV column. The elution order for the alkaline earth and trivalent metal ions are identical. The k' vs. pH plot for selected metals on this column is given in Figure 2.11.

Unfortunately, possibly due to a low capacity in conjunction with weakly chelating donor atoms in acidic eluents, high efficiency separations of transition and trivalent metal ions were unfeasible. In addition, peak shapes on this column were poor, which could be attributed to the capacity. A separation of Sr(II), Ca(II) and Mg(II) at pH 10.2 was achieved (Figure 2.12), but peak shapes were poor.

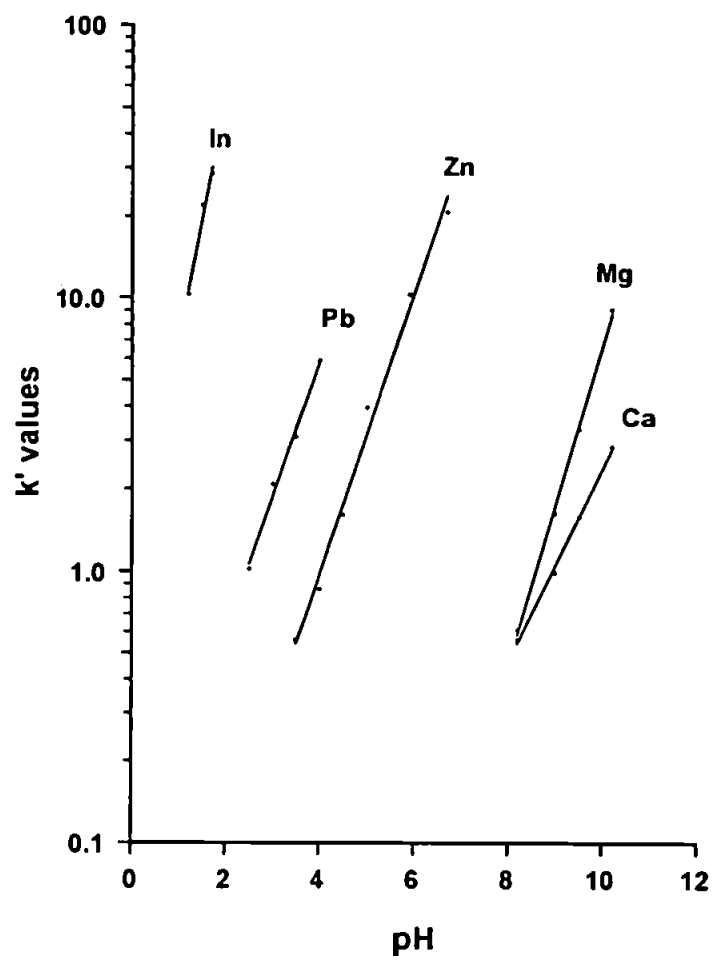


Figure 2.11. The dependence of capacity factors for selected metals on eluent pH, with the PCV loaded column. Eluent: 1M KNO₃ 50mM acetic acid.

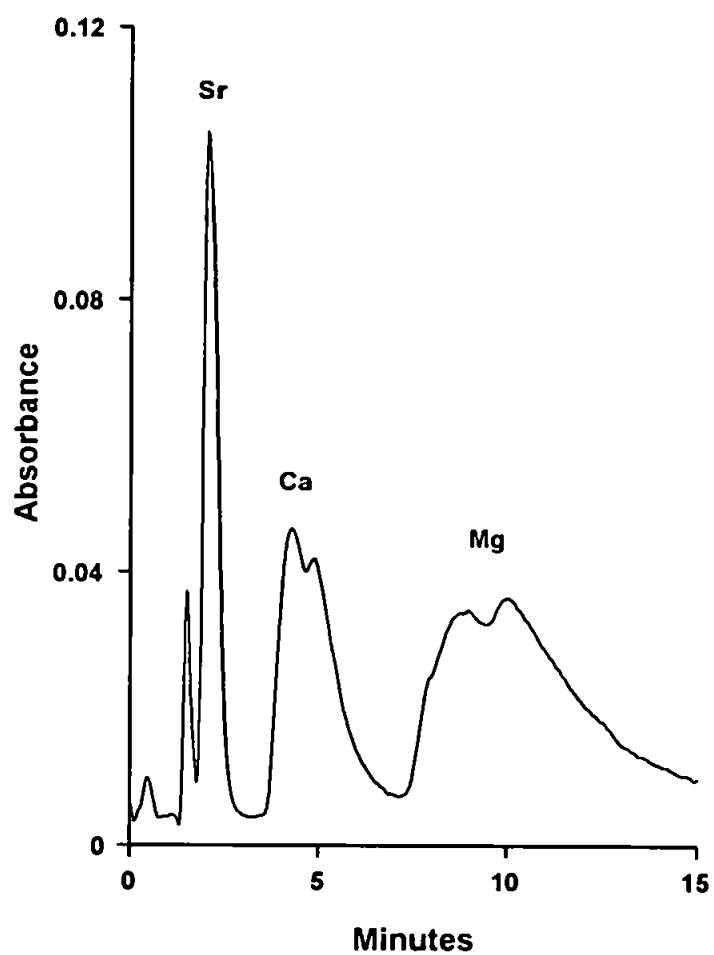
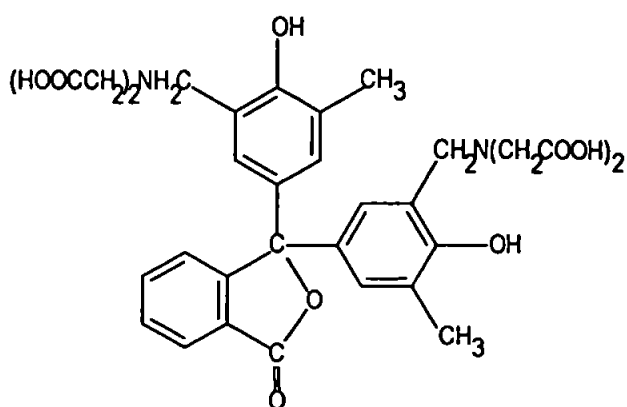


Figure 2.12. Separation of Sr(II) 1 mg l^{-1} , Ca(II) 1 mg l^{-1} and Mg(II) 1 mg l^{-1} , on the 100 · 4.6mm PCV column. Eluent: 1M KNO_3 50mM acetic acid at pH 10.2. Detection: PAR/ Zn-EDTA at 490nm.

2.3.3 *O*-Cresolphthalein Complexone (CPC) Column



H₆L fw. 672.7 pK_a = 12.0

CPC, like ATA and PCV, has a triphenylmethane based structure but this time with two iminodiacetate (IDA) groups, able to chelate metals with nitrogen and oxygen donor atoms (N,O,O). Adjacent hydroxyl groups might also play a minor role in chelation. CPC has been applied as an indicator for the alkaline earth metals [103], and previous impregnation of this molecule onto a high efficiency PS-DVB resin was used to determine trace Sr(II) in milk powder, which contains high concentrations of Ca(II) [144].

CPC is a slightly weaker acid than PCV, with an acid dissociation constant of 12 [162]. In addition, the presence of nitrogen donor atoms, which dissociate at a lower pH than oxygen ligands, enables N,O groups to be consequently more strongly chelating in acidic eluents. The stability constants for this ligand and selected metal ions are given in Table 2.3 [162], and a comparison with Zn(II) illustrates that CPC does indeed form stronger complexes than PCV.

62.7 mg /g resin (0.09mM dye) of this large molecule was coated onto the resin, which was able to bind with 0.005mM Cu(II), giving the largest percentage activity of the six dyes investigated, equal to 5%. As with the PCV molecule, even though only a small amount of dye was immobilised, its arrangement within the resin pores was optimised to allow chelation to occur.

Table 2.3 log stability constants of metal complexes with CPC [162] 0.1M Ionic strength

M^{n+}	$\log K_1$
Ba^{2+}	6.2
Ca^{2+}	7.8
Mg^{2+}	8.9
Zn^{2+}	15.1

The k' vs. pH plots for selected metal ions is given in Figure 2.13. The retention order for metals on this chelating resin was Ba(II)<Sr(II)<Ca(II)<Mg(II) for the alkaline earth metals, Mn(II),Ni(II),Cd(II)<Co(II)<Zn(II)<Pb(II)<Cu(II) for the transition metal ions, and Al(III)<Ga(III)<In(III) for the trivalent metals. A separation of the alkaline earth metals at pH 10.3 is shown in Figure 2.14. This illustrates the greater resolution between Ca(II) and the weakly retained Ba(II) and Sr(II) peaks. The degree of separation between Ca(II) and Mg(II) was even greater than that between Ca(II) and Sr(II), signifying that the conditional stability constants of the alkaline earth metal chelates with this immobilised ligand are more varied than for the oxygen chelators investigated.

The conditional stability constants for the transition metal ions were quite similar, with the exception of Cu(II), which was completely retained at low pH < 1.5. Only 3 transition metals could be separated isocratically on a 100mm column, before reaction kinetics became too prominent in broadening peak shapes. A separation of Cd(II), Zn(II) and Pb(II) at pH 3.9 is shown in Figure 2.15, and illustrates the small difference in selectivity coefficients on the IDA group for these metals in comparison with the ATA column. Regarding the trivalent metal ions, In(III) was very strongly retained on this column. At pH 2.5, this metal has a retention time nearing 65 minutes, yet unexpectedly Ga(III) remains virtually unretained with Al(III). To increase the pH required to separate Ga(III) and

Al(III), In(III) would near complete retention on this column, and so a separation of these metals was unsuccessful.

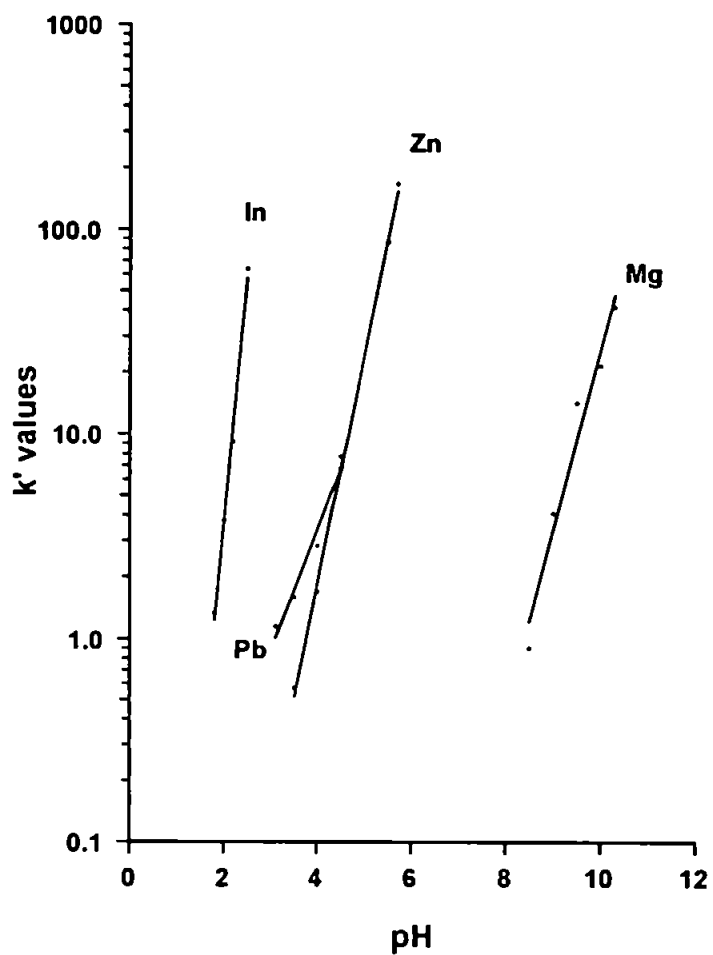


Figure 2.13. The dependence of capacity factors for selected metals on eluent pH, with the CPC loaded column. Eluent: 1M KNO_3 50mM acetic acid.

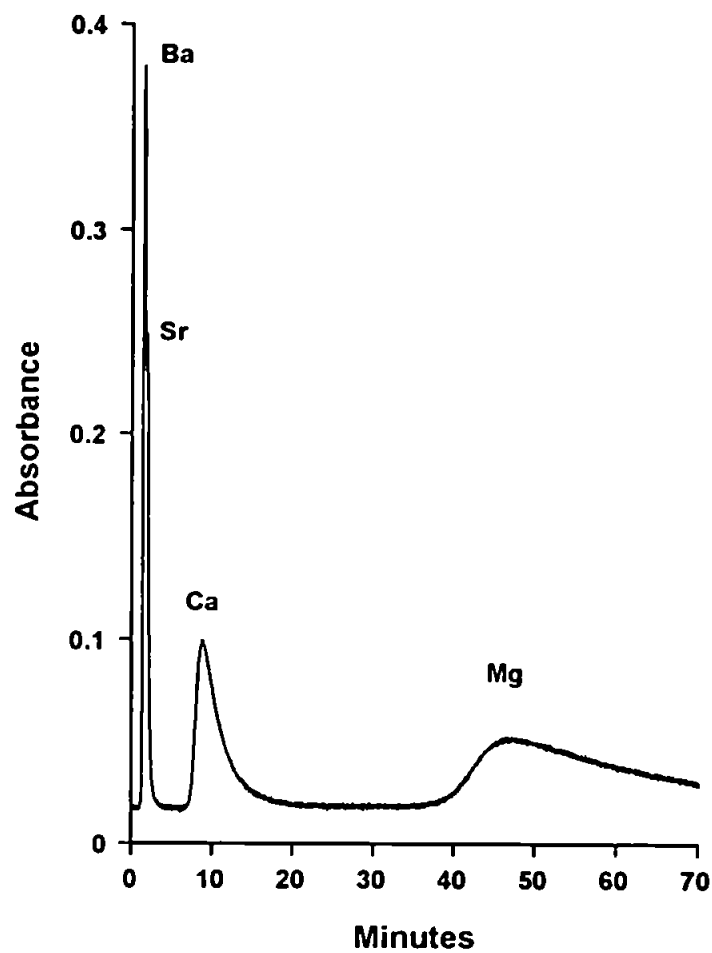


Figure 2.14. Separation of Ba(II) 10mg l⁻¹, Sr(II) 10mg l⁻¹, Ca(II) 10mg l⁻¹ and Mg(II) 20mg l⁻¹, on the 100 · 4.6mm CPC column. Eluent: 1M KNO₃ 50mM acetic acid at pH 10.3. Detection: PAR/ Zn-EDTA at 490nm.

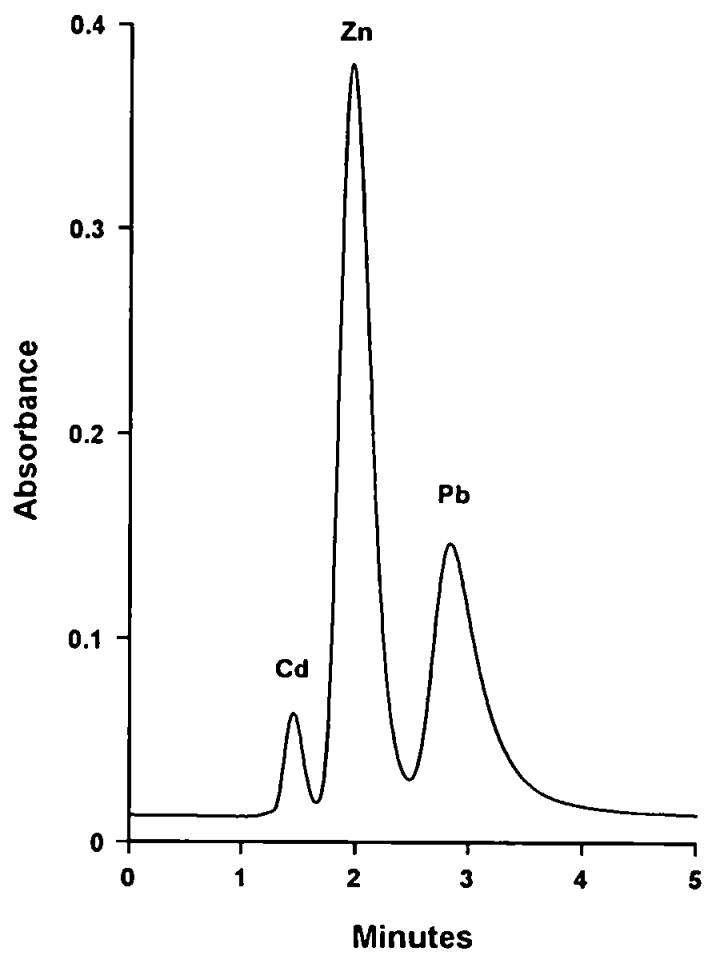
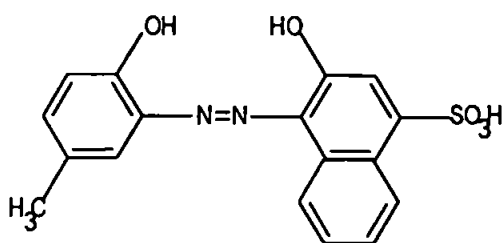


Figure 2.15. Separation of Cd(II) 10mg l^{-1} , Zn(II) 20mg l^{-1} and Pb(II) 20mg l^{-1} , on the $100 \times 4.6\text{mm}$ CPC column. Eluent: 1M KNO_3 50mM acetic acid at pH 3.9. Detection: PAR at 490nm .

2.3.4 Calmagite (CAL) Column



H₂L fw. 358.4 p*k*₂ = 12.5

Calmagite is one of two azo type dyes immobilised onto a stationary phase support. It chelates metals using nitrogen and oxygen donor atoms (N,O,O), through its -N=N- azo linkage and two hydroxyl groups. This molecule also contains a sulphonate group to increase its solubility in acidic solutions. It has been used for the absorptiometric determination of Mg(II) [102].

With an acid dissociation constant of 12.5 [163], CAL is essentially a stronger chelating agent than the three dyes examined thus far: ATA, PCV and CPC. This can be seen with the large log stability constant values for divalent metal ions given in Table 2.4.

Table 2.4 Log stability constants of selected metal ions with CAL [163] (0.1M Ionic Strength)

M ⁿ⁺	logK ₁
Cu ²⁺	21.7
Ni ²⁺	21.63
Zn ²⁺	12.37
Cd ²⁺	12.59
Co ²⁺	21.03
Pb ²⁺	21.9
UO ₂ ²⁺	16.87

Cu(II) was very strongly retained on this column, >80 minutes at pH 3, with other transition metals only being weakly retained at pH 5. Above this value, Pb(II), Zn(II) and Co(II) were more strongly retained, and the elution order on this column was Mn(II)<Cd(II)<Co(II)<Pb(II)<Zn(II)<Cu(II). It is interesting to note that Cd(II) is only weakly retained in comparison with Pb(II), with Zn(II) more strongly retained than Pb(II) at higher pH values (Zn(II) k' 25.8, Pb(II) k' 5.6 at pH 6). This selectivity has not been demonstrated on previously investigated dye loaded columns.

A high loading of this dye was achieved, 184 mg /g resin (0.51mM dye), which was able to bind with 0.02mM Cu(II). This resulted in only 3.7% activity, which is low considering the amount impregnated. The reduced size of this molecule in comparison with triphenylmethane dyes might contribute to the increased loading, but its positioning within the pore structures might inhibit chelation of metal ions through the azo nitrogen and hydroxyl groupings. The low dye activity also prevented a high efficiency isocratic separation of the transition metal ions over the pH range studied, pH 4 – 6.5.

The alkaline earth metals were eluted in the order shown with the other dyes, as were the trivalent metal ions. A separation of Ca(II) and Mg(II) from Ba(II) and Sr(II) was achieved at pH 10.1 (Figure 2.16), illustrating the large difference in the conditional stability constants between Mg(II) and the other alkaline earth metals. The trivalent ions appeared to be more weakly retained on this column than with the ATA, PCV and CPC columns, shown with the slope of In(III) which was not as steep as those for Zn(II) and Mg(II) in the k' plot given in Figure 2.17.

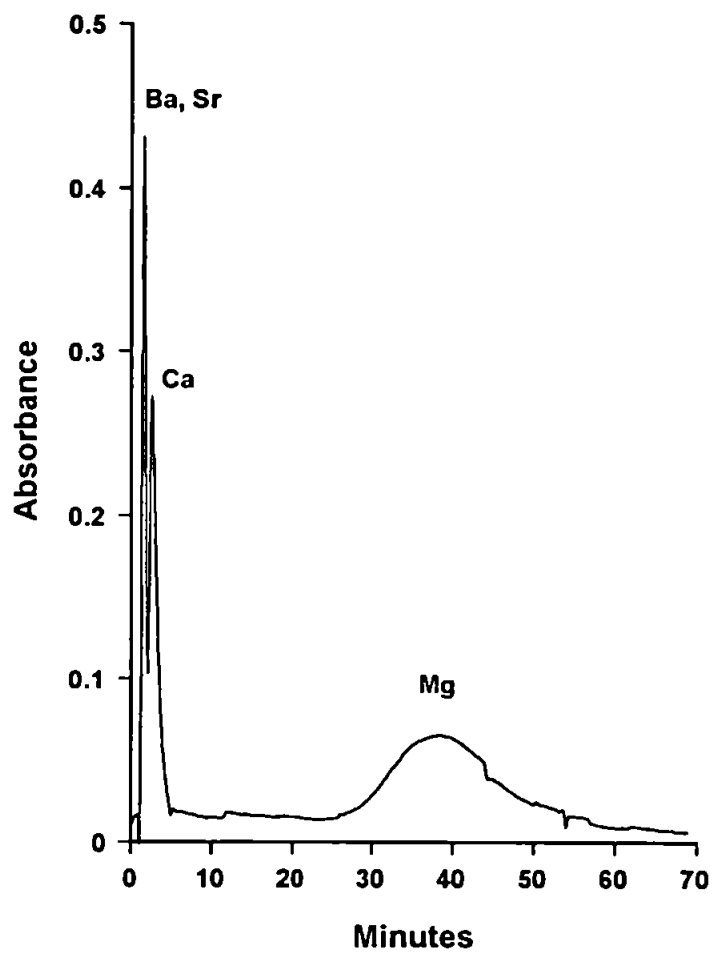


Figure 2.16. Separation of Ba(II) 10mg l⁻¹, Sr(II) 10mg l⁻¹, Ca(II) 10mg l⁻¹ and Mg(II) 20mg l⁻¹, on the 100 · 4.6mm CAL column. Eluent: 1M KNO₃ 50mM acetic acid at pH 10.1. Detection: PAR/ Zn-EDTA at 490nm.

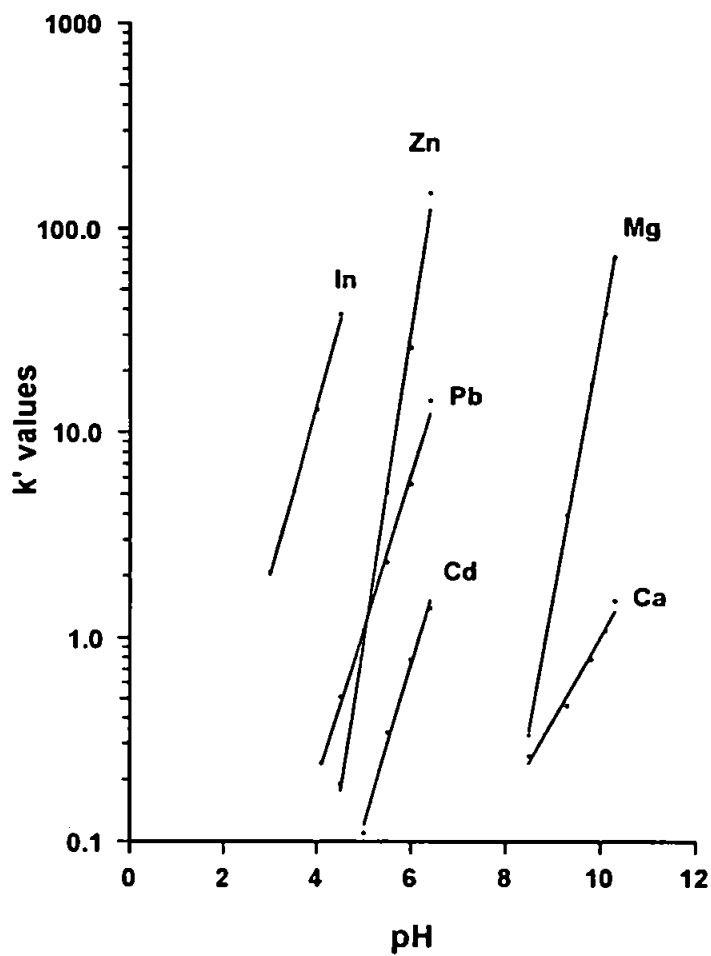
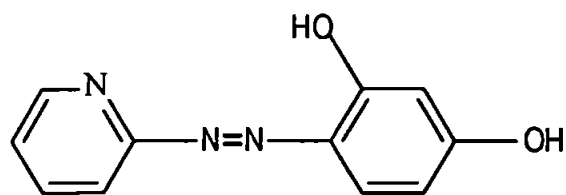


Figure 2.17. The dependence of capacity factors for selected metals on eluent pH, with the CAL loaded column. Eluent: 1M KNO_3 50mM acetic acid.

2.3.5 4-(2-pyridylazo)resorcinol (PAR) Column



H_2L fw. 215.2 $pk_2 = 12.5$

The second azo dye studied, PAR, exhibits a different type of chelation to CAL, chelating metal ions through an azo nitrogen, pyridyl nitrogen and hydroxyl oxygen (N,N,O). The presence of a second ligating nitrogen atom could make this molecule more strongly complexing than CAL, or indeed ATA, PCV and CPC in acidic eluents.

As already emphasised in the introductory chapter, PAR is a universal spectrophotometric reagent for many metal ions. It has the same acid dissociation constant as CAL, and as a comparison the stability constants between this ligand and selected metals are given in Table 2.5.

Table 2.5 Log stability constants of metal ions with PAR [162]. 0.1M Ionic strength.

M^{n+}	$\log K_1$	M^{n+}	$\log K_1$
Mn^{2+}	9.7	Pb^{2+}	11.2
Co^{2+}	10	La^{3+}	9.2
Ni^{2+}	13.2	In^{3+}	9.3
Zn^{2+}	11.9	Al^{3+}	11.5
Cu^{2+}	11.7	UO_2^{2+}	12.5

The highest loading was achieved with this dye, 168 mg /g resin (0.78mM dye), which correspondingly gave the highest capacity of 0.036mM Cu(II) /g resin. However, as with the other azo molecule, CAL, only a relatively low dye activity of 4.6% was calculated. It was, however, apparent from the retention of metal ions, that this column had a strongly chelating nature at low acidity with the two nitrogen atoms in its structure. The elution order for transition metal ions was Mn(II)<Ni(II)<Cd(II)<Zn(II)<Pb(II)<Cu(II), with Cu(II) being virtually completely retained at pH 1. The separation of Mn(II), Cd(II) and Pb(II) at pH 2.2 is shown as Figure 2.18. At this low pH, with a retention of <5 minutes, the Pb(II) peak is very broad, demonstrating the slow kinetics of dissociation between this metal and PAR.

Another important consideration was the change in selectivity for the alkaline earth metals, eluting in the order Mg(II)<Ba(II)<Sr(II)<Ca(II). On the previous four dye loaded columns, Mg(II) was the most strongly retained, whereas on the PAR column it has the weakest affinity. This might result from the Mg(II) being too hard an acid to complex strongly with the two soft base nitrogen atoms. A separation of Mg(II), Sr(II) and Ca(II) at pH 9 is shown as Figure 2.19. At this pH, Ba(II) would co-elute with Mg(II). A separation of the trivalent metal ions, Al(III), Ga(III) and In(III) was also achieved at pH 1.4 (Figure 2.20). The rapid broadening of the In(III) peak in this separation profile again illustrates the strong chelating nature of PAR, and its affect on reaction kinetics. The k' vs. pH plot for selected metal ions on this substrate is given in Figure 2.21.

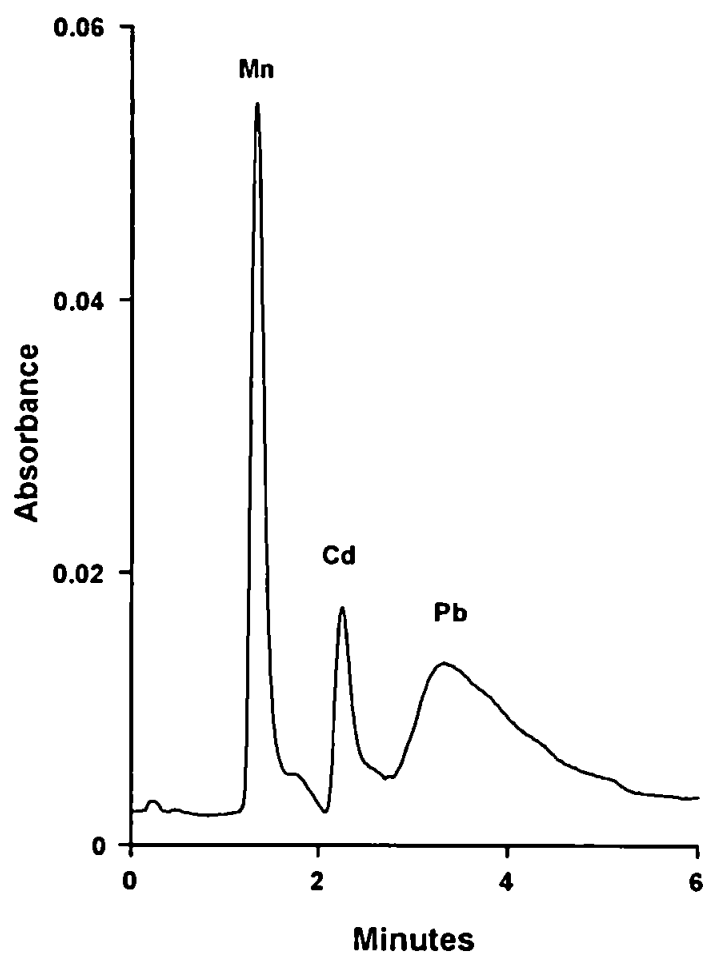


Figure 2.18. Separation of Mn(II) 0.5mg l^{-1} , Cd(II) 10mg l^{-1} and Pb(II) 5mg l^{-1} , on the 100 \cdot 4.6mm PAR column. Eluent: 1M KNO_3 50mM acetic acid at pH 2.2. Detection: PAR at 490nm.

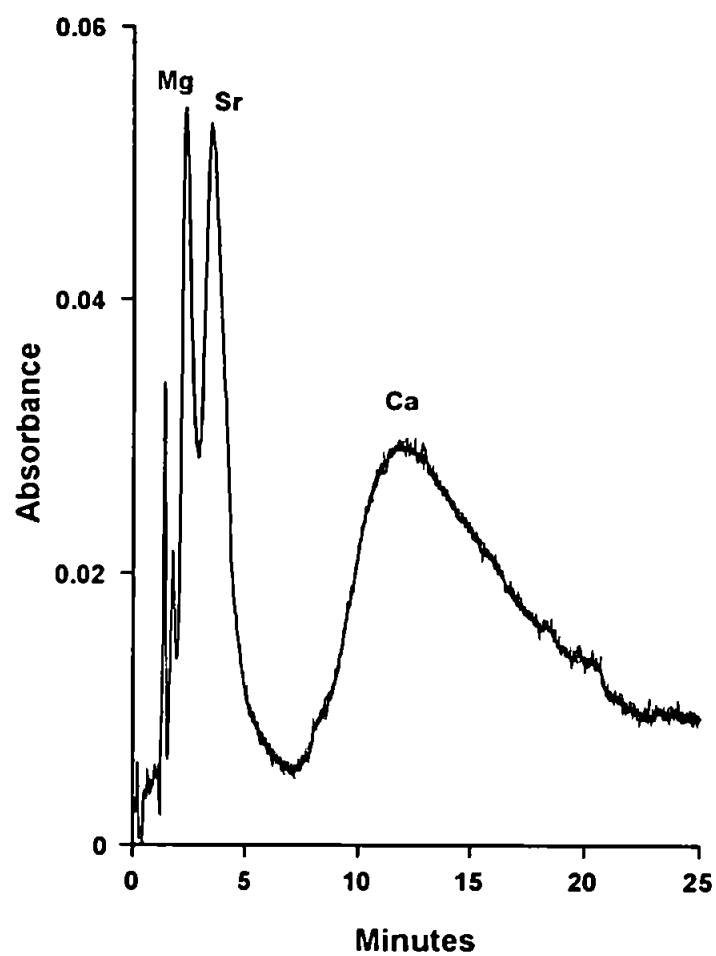


Figure 2.19. Separation of Mg(II) 1 mg l^{-1} , Sr(II) 5 mg l^{-1} and Ca(II) 10 mg l^{-1} , on the 100 \cdot 4.6mm PAR column. Eluent: 1M KNO_3 50mM acetic acid at pH 9. Detection PAR/ Zn-EDTA at 490nm.

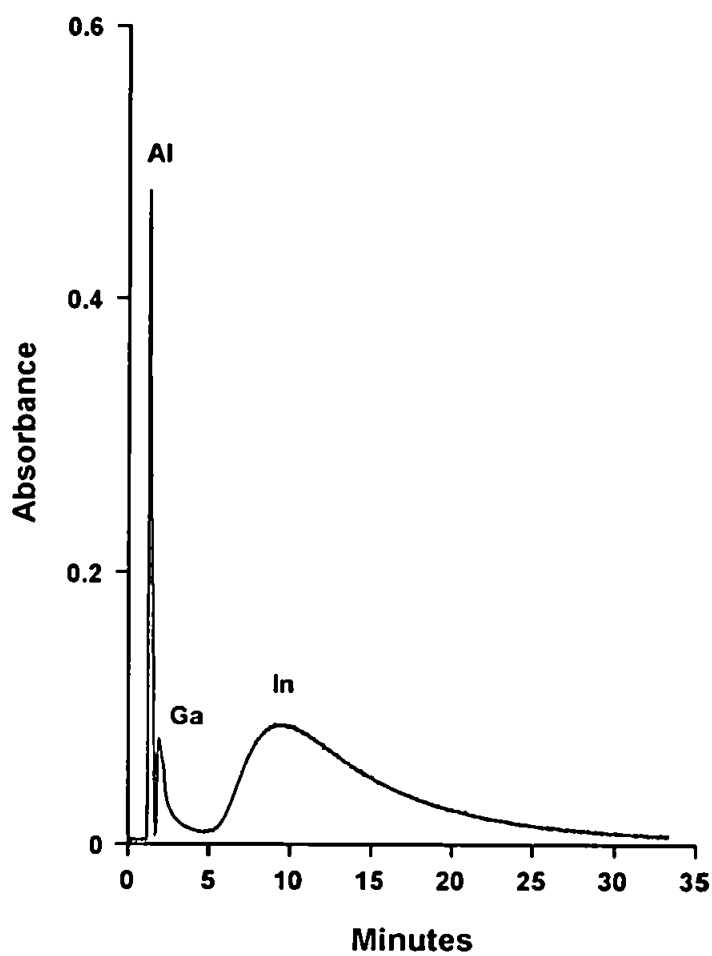


Figure 2.20. Separation of Al(III) 0.2mg l^{-1} , Ga(III) 10mg l^{-1} and In(III) 80mg l^{-1} , on the $100 \cdot 4.6\text{mm}$ PAR column. Eluent: 1M KNO_3 50mM acetic acid at pH 1.4. Detection: PCV at 580nm .

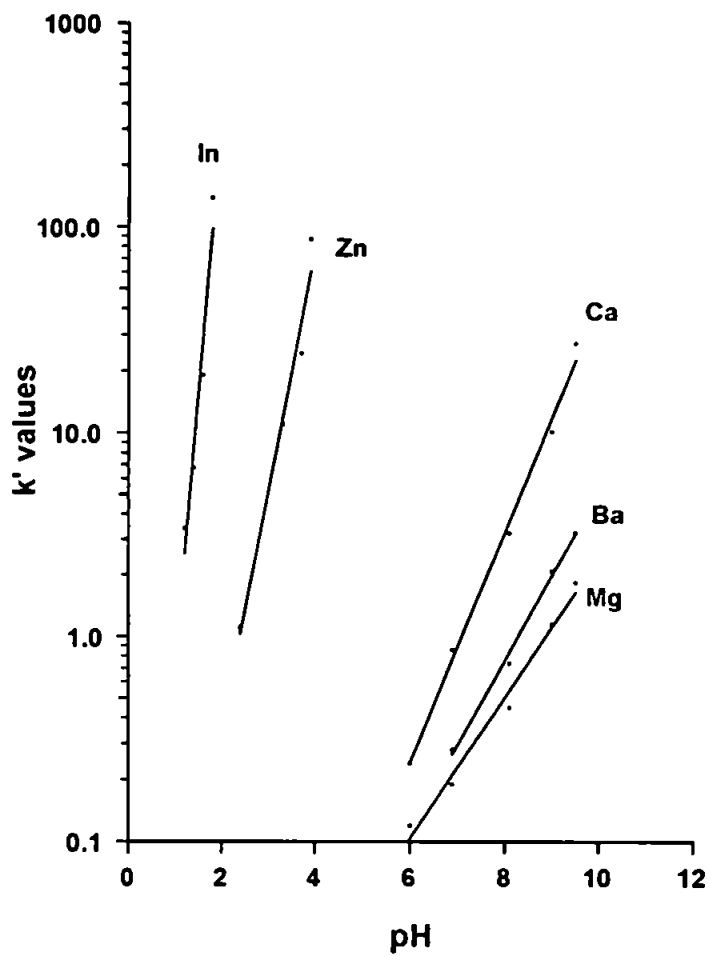
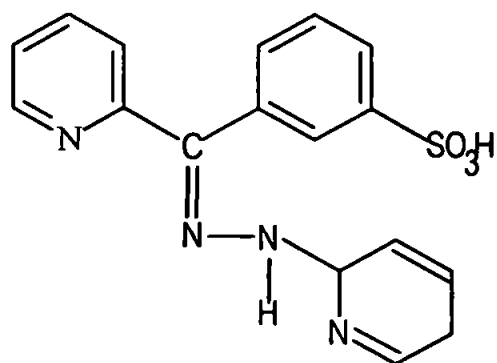


Figure 2.21. The dependence of capacity factors for selected metal ions on eluent pH, with the PAR loaded column. Eluent: 1M KNO₃ 50mM acetic acid.

2.3.6 2-(3-sulphobenzoyl)pyridine 2-pyridylhydrazone (SPP) Column



H_2L fw. 390.4 $pK_2 = 6.0$

This molecule is different from all the chelating dyes investigated previously, in that it contains no oxygen donor atoms. It has a hydrazone group $=C=N-N=$, which contains one nitrogen donor atom, the other ligating nitrogen atom on the pyridyl group, resulting in N,N chelation. This dye has previously been found to have no retention for the alkaline earth metals up to pH 11 because these ions are too hard to complex with the soft nitrogen groups [108]. This can provide advantages for inter-group separations.

N,N chelation is weaker than both O,O and N,O chelation, as explained previously, but again, in acidic eluents, the dissociation of the nitrogen donor atoms might somewhat counteract this. The acid dissociation constant of this molecule is low ($pK_2 = 6$) which means that it is not very strongly chelating, as expected. Going and Sykora found log stability constants of 6.6 for Zn(II), 5.6 for Cd(II) and 8.1 for Hg(II) [164], which confirms this reasoning.

An initial loading of 130mg /g resin (0.33mM dye) was immobilised onto the resin framework, but with elution of the mobile phase, column performance rapidly degraded, synonymous with dye bleed. This had been postulated previously [108], on another polymeric resin. For this reason, column capacity could not be ascertained to any degree of accuracy, and values were not recorded. The elution order for selected transition metals on this column was $Mn(II) < Pb(II) < Cd(II) < Zn(II)$, which demonstrates the weak affinity of

nitrogen ligands for Pb(II) ions. Before column performance deteriorated drastically, a separation of Pb(II), Cd(II) and Zn(II) at pH 3.2 (Figure 2.22), and Mn(II), Pb(II) and Cd(II) at pH 3.5 (Figure 2.23) was achieved. Figure 2.22 demonstrates the slow reaction kinetics for Zn(II) on this chelating column, resulting in a very broad, yet quite symmetrical peak.

With the short life-span of the impregnated SPP column, it was decided to add this ligand to the eluent, producing a dynamically loaded system. It was important to ensure that the stationary phase exhibited dominant metal retention characteristics. This can be achieved by minimising the concentration in the mobile phase, so that competition from the ligand in the eluent is negligible after equilibration. It is additionally important to reduce levels of ligand in the eluent to reduce interference with post column reagent sensitivity.

Considering these points, a concentration of 0.1mM SPP was added to the mobile phase, the column reaching a steady state equilibrium after 2-3 hours, deduced from the repeat injection of metal standards until reproducible retention times were recorded. The dynamically loaded column exhibited certain characteristics anomalous to the impregnated column. The most apparent was the shift in elution order between Cd(II) and Pb(II) with increasing pH. With increasing pH, Cd(II) demonstrated little change in retention over a range pH 2.5 – 3.5, whereas Pb(II) retention increased sharply, resulting in a cross-over at pH >3. The retention of Zn(II) also increased dramatically with pH on the dynamically loaded column, closely resembling the strong trivalent ion retention on other dye loaded columns. The k' vs. pH plot for selected metal ions on the dynamically loaded SPP column is shown in Figure 2.24. Zn(II) and Pb(II) exhibit strong retention on the stationary phase over the pH range studied, whereas Cd(II) apparently has a stronger affinity for the ligand present in the mobile phase. As expected, the hard Mg(II) has little affinity for this nitrogen chelating molecule.

Considering the very strong retention of the divalent transition and heavy metal ions on this column, with trivalent metals potentially able to form even stronger complexes, these

metals were not injected, as it was anticipated that very acidic eluents would be required for their elution.

The reaction kinetics on the dynamic system compared with the impregnated system were improved, demonstrated with a similar separation of Pb(II), Cd(II) and Zn(II) at pH 2.3 (Figure 2.25), nearly a pH unit less than the separation achieved on the impregnated column. The Zn(II) peak was still broad, but more symmetrical than found on the pre-coated column, indicative that the ligand in the mobile phase has a role in the separation of metal ions, at 0.1mM concentration.

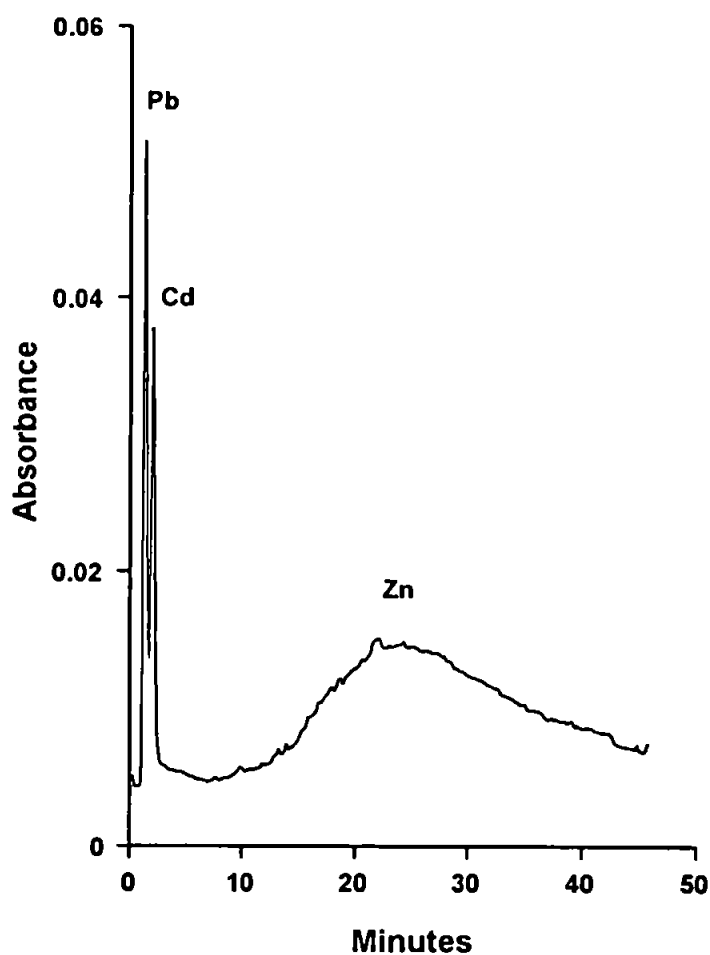


Figure 2.22. Separation of Pb(II) 5mg l⁻¹, Cd(II) 10mg l⁻¹ and Zn(II) 20mg l⁻¹, on the 100 · 4.6mm impregnated SPP column. Eluent: 1M KNO₃ 50mM acetic acid at pH 3.2.

Detection: PAR at 490nm.

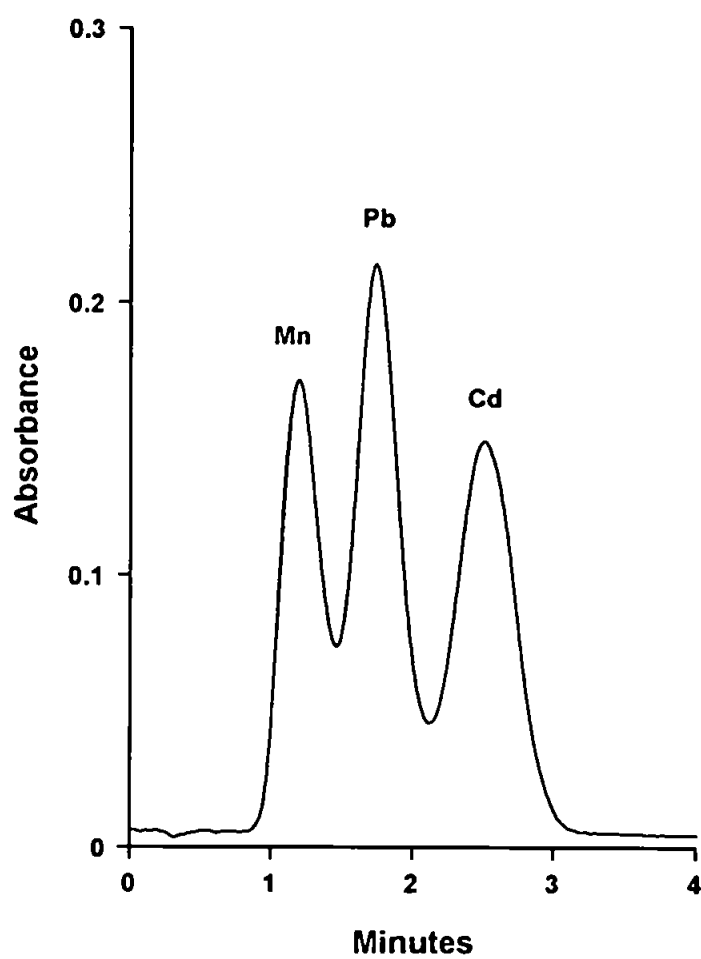


Figure 2.23. Separation of Mn(II) 2mg l⁻¹, Pb(II) 20mg l⁻¹ and Cd(II) 60mg l⁻¹, on the 100 · 4.6mm impregnated SPP column. Eluent: 1M KNO₃ 50mM acetic acid at pH 3.5. Detection: PAR at 490nm.

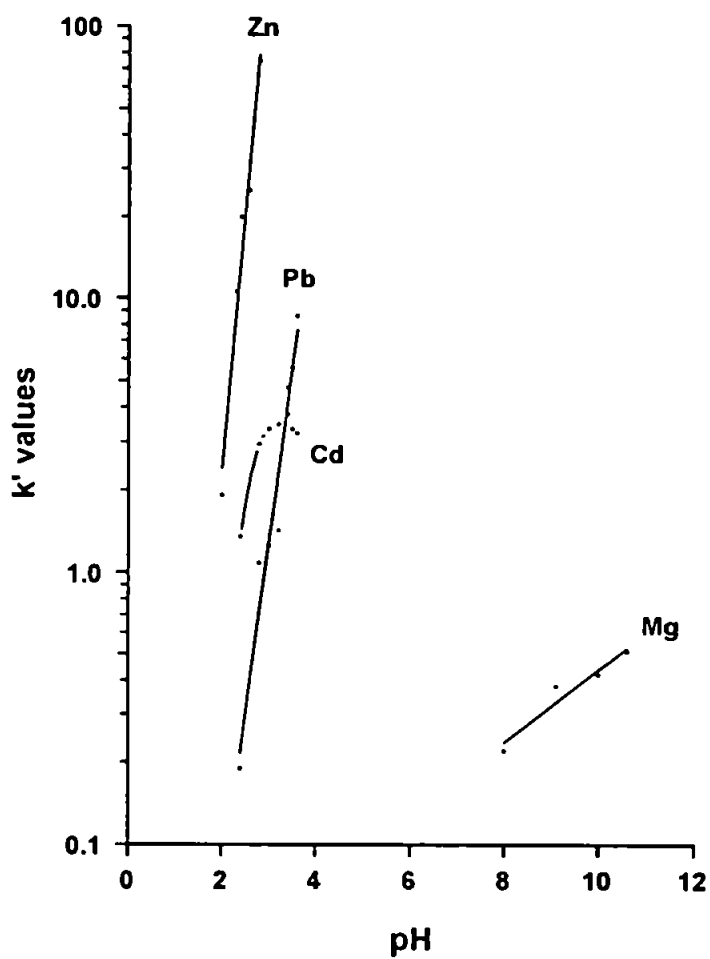


Figure 2.24. The dependence of capacity factors on the eluent pH, with the dynamically loaded SPP column. Eluent: 1M KNO_3 50mM acetic acid and 0.1mM SPP.

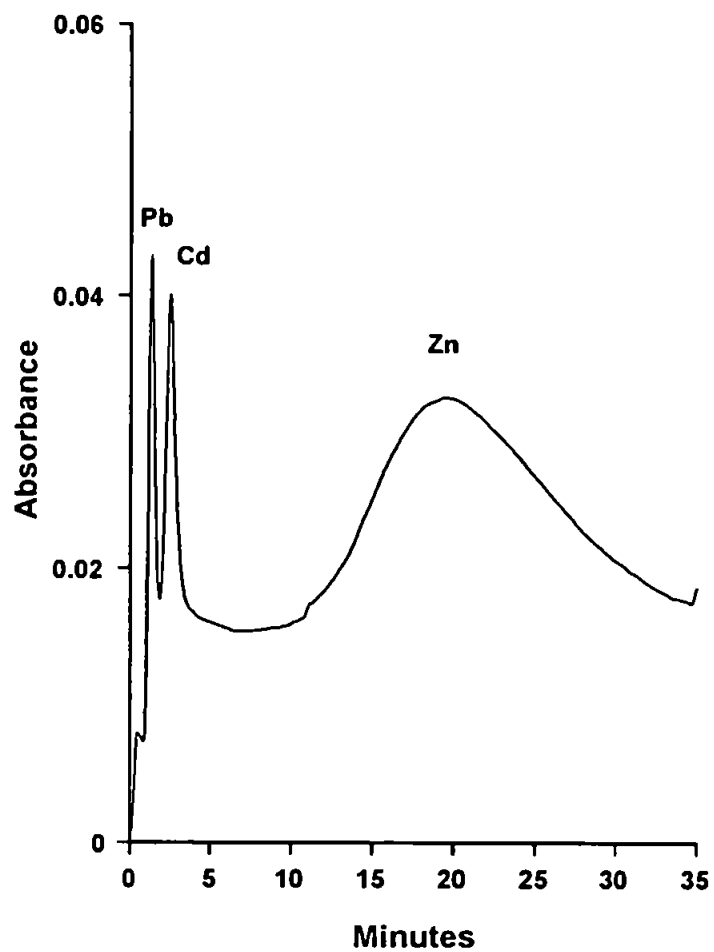


Figure 2.25. Separation of Pb(II) 5mg l⁻¹, Cd(II) 20mg l⁻¹ and Zn(II) 40mg l⁻¹, on the 100 · 4.6mm dynamically loaded SPP column. Eluent: 1M KNO₃ 50mM acetic acid, 0.1mM SPP at pH 2.3. Detection: PAR at 490nm.

2.3.7 Effect of System Parameters on Metal Ion Separations

It is important to understand the effects of various chromatographic parameters and experimental conditions on the separation of metal ions by HPCIC. The information derived, can provide the basis for a working framework around which a method can be developed, suitable for a particular analysis. In this study, various system characteristics were investigated: column length, column capacity, concentration of complexing buffer in the mobile phase, and mobile phase ionic strength. A short study on the metal retaining abilities of un-modified polymeric resins was also undertaken.

2.3.7.1 Column Length

All chromatographic techniques suffer from the problem of peak broadening. The longer the solute remains in the system, a greater degree of dispersion will occur. The more efficient the column, the smaller the dispersion, thereby more efficient columns produce sharper peaks compared with less efficient columns, for an equivalent retention time. As mentioned in the Introduction, increasing the length of a column will increase the number of effective plates, and thus improve separation efficiency.

Two 100mm CPC columns were connected with a minimal dead-time fitting, the first an older column with a re-checked capacity of 0.01mM Cu(II) /g resin, together with the column fabricated for this study (0.005mM Cu(II) /g resin). The dye had been immobilised onto 8.8µm PS-DVB (Dionex) to fabricate both columns.

The advantages of increasing column length can be illustrated with the peak shape for Zn(II), achieved on both 100mm and 200mm length columns (Figure 2.26). The same retention time, 2.6 minutes, can be achieved by using a lower pH for the longer column, which improves the rate of complex dissociation, thereby reducing the kinetic broadening effect and improving peak symmetry. A comparison of column efficiency at both lengths

was undertaken using Pb(II). Taking into consideration the different dead-times associated with each column, column efficiency was calculated at similar k' values for Pb(II) at each column length, using the number of effective plates (N_{eff}). The results are given in Table 2.6.

Table 2.6 Efficiency of analyte peak, Pb(II), with column length

Column Length /mm	pH	k'	N_{eff}
100	3.5	0.36	294
200	3.5	0.36	922
100	3.9	1.4	61
200	3.9	1.5	178

As apparent from the N_{eff} values, column length is an important parameter in increasing the efficiency of the column. Increasing the column length from 100 to 200mm, a factor of ~3 increase in the number of plates was observed, at two independent k' values. This increase in efficiency allowed the separation of four transition metals isocratically, demonstrated with the separation of Mn(II), Cd(II), Zn(II) and Pb(II) at pH 4.2 (Figure 2.27). Only three metals could be separated on the 100mm column using an isocratic elution program (Figure 2.15).

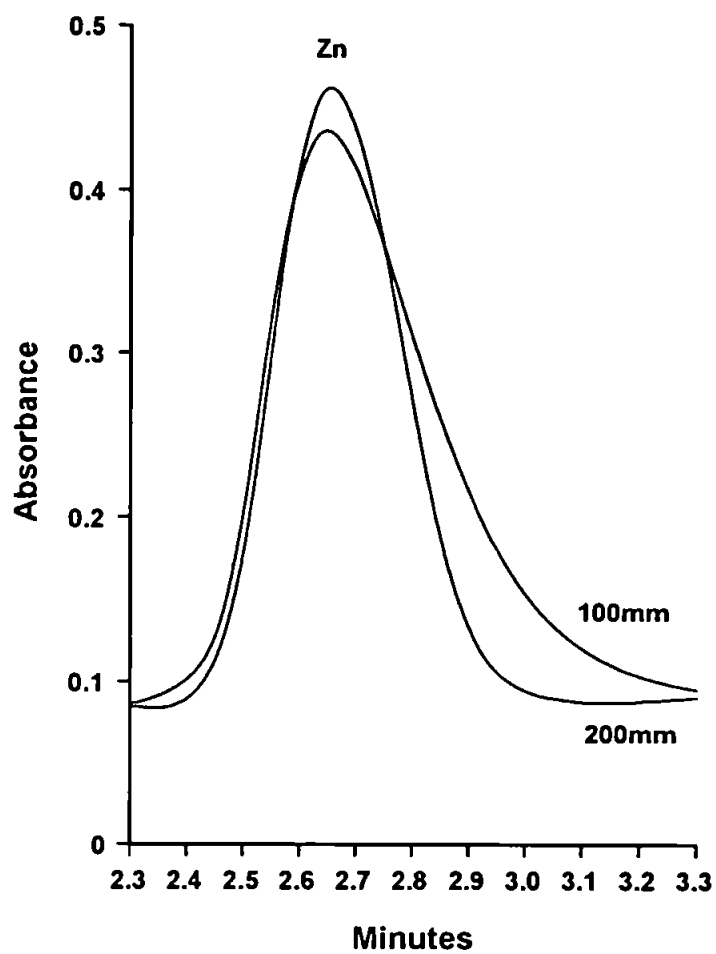


Figure 2.26. Zn(II) peak efficiency on CPC columns: retention time 2.6 minutes, achieved at pH 3.9 on 100mm column, and pH 3.3 with 200mm column length. Eluent: 1M KNO₃ 50mM acetic acid. Detection: PAR at 490nm.

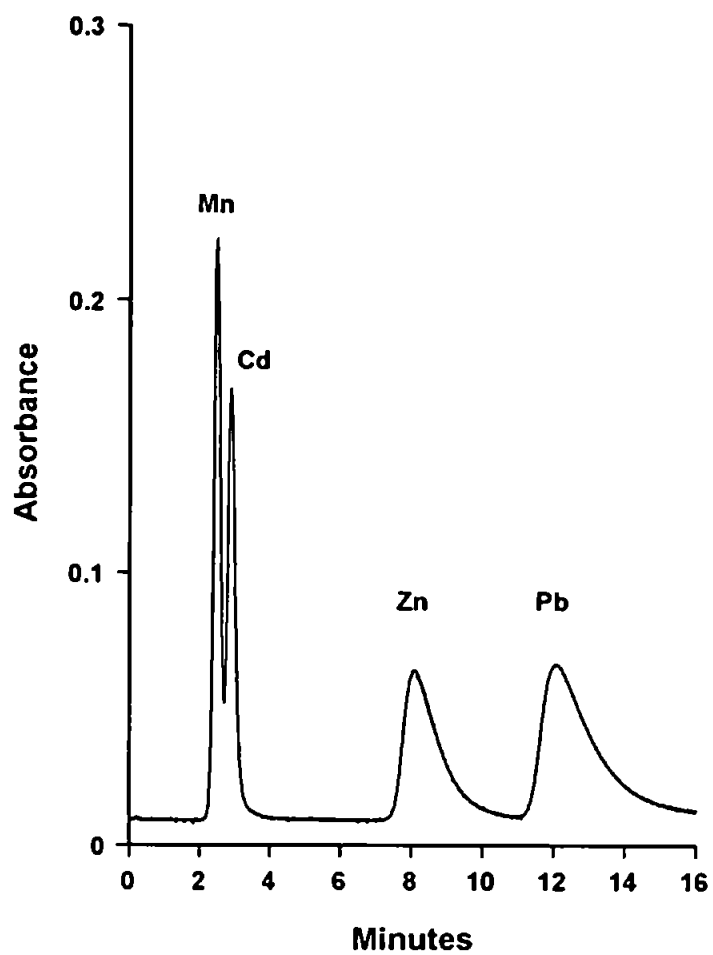


Figure 2.27. Separation of Mn(II) 2mg l^{-1} , Cd(II) 40mg l^{-1} , Zn(II) 10mg l^{-1} and Pb(II) 30mg l^{-1} , on a $200 \times 4.6\text{mm}$ CPC loaded column. Eluent: 1M KNO_3 50mM acetic acid at pH 4.2. Detection: PAR at 490nm .

2.3.7.2 Column Capacity

Investigations were undertaken to determine whether the capacity of a chelating column, related to the concentration of dye immobilised onto the substrate, can affect its metal separation capabilities.

Comparing the two CPC impregnated columns, it was found that a lower capacity reduces the retention times for eluting metals and consequently decreases the resolution between peaks, at an equivalent pH. This is illustrated with the separation of Cd(II), Zn(II) and Pb(II) at pH 3.9, on both columns (Figure 2.28 and Table 2.7).

Table 2.7. Change in the Selectivity factors with column capacity

At an equivalent pH.

Capacity mM Cu(II) /g resin	Retention Time / minutes		Selectivity Factor
	Zn(II)	Pb(II)	
0.005	1.97	2.83	1.1
0.01	2.63	4.33	2.3

This was the expected outcome, as an increased number of available chelating sites should retain metals more strongly, dependant upon their conditional stability constants, culminating in improved separation characteristics because of the increased k' values. The resolution on a reduced capacity column can be improved by increasing the eluent pH, thereby increasing the conditional stability constants, but unfortunately this can reduce peak symmetry due to the slower kinetics of complex dissociation.

In addition, column capacity appeared to have some effect upon k' values for metal ions over the pH range investigated. Figure 2.29 demonstrates this occurrence, with the CPC columns. Both Zn(II) and Mg(II) are retained more weakly on the lower capacity

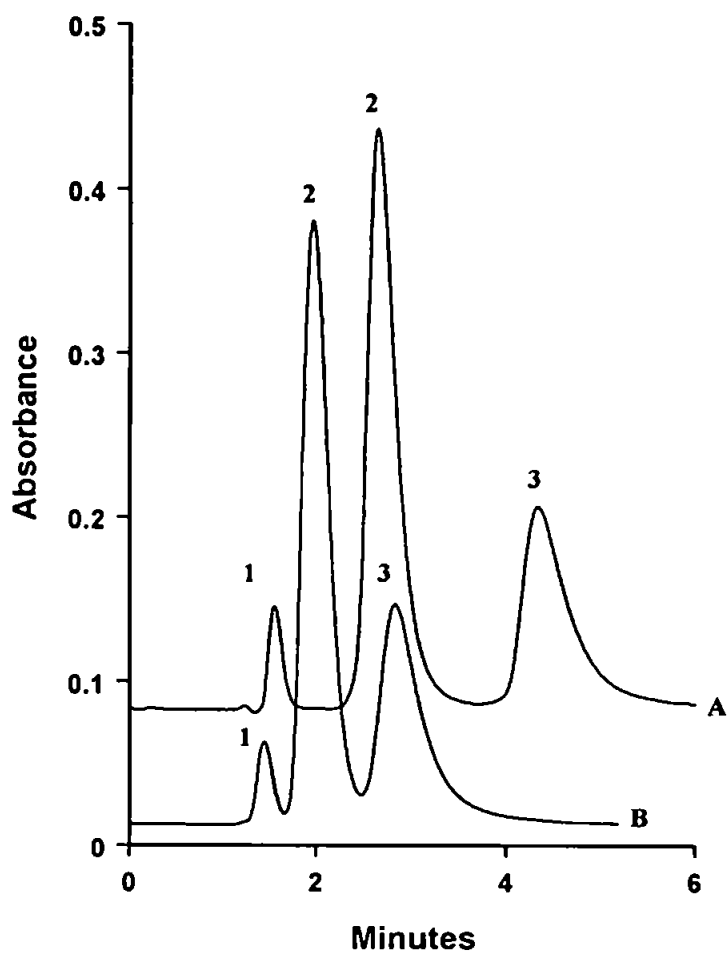


Figure 2.28. Effect of column capacity on metal ion separations. Columns: 100 · 4.6mm impregnated with CPC. Capacity: A: 0.01mM Cu(II) /g resin, B: 0.005 mM Cu(II) /g resin. 1: Cd(II) 10mg l⁻¹, 2: Zn(II) 20mg l⁻¹ and 3: Pb(II) 20mg l⁻¹. Eluent: 1M KNO₃ 50mM acetic acid at pH 3.9. Detection: PAR at 490nm.

Column, although there was not a corresponding twofold increase in metal ion retention with the twofold increase in capacity. This was also demonstrated using another chelating dye, CAL. A second azo dye column, prepared using a more impure source of this molecule (BDH), was immobilised onto 9 μ m PS-DVB (Dionex). This column had a very low capacity, 0.0004mM Cu(II) /g resin, in comparison with the high purity CAL loaded substrate (0.02mM Cu(II) /g resin), used to achieve metal separations in section 2.3.4. Although there was a 50 times difference in these column capacities, there was not a corresponding 50 times difference in the retention for Zn(II), Pb(II) or Cd(II) on the two columns, as shown in Figure 2.30. It would appear, therefore, that column capacity is an important factor to increase the retention of metal ions at an equivalent pH, but is not as significant as might be anticipated.

Another important aspect of applying low capacity columns for high efficiency separations, is the aspect of introducing sample solutions into the system. A complex sample matrix, even after dissolution procedures and dilution, can contain high concentrations of matrix metals, which could theoretically 'swamp' the limited chelation-exchange sites available, particularly at the beginning of the column, upsetting the chromatography. The pH and ionic strength can also interfere with the chromatographic performance on a low capacity column. This can be demonstrated with the injection of Cd(II), at varying sample pH, onto the low capacity CPC column (0.005mM Cu(II) /g resin). The eluent was 1M KNO₃, 100mM acetic acid, at pH 4.5. A 40mg l⁻¹ Cd(II) standard, prepared in Milli-Q water, was adjusted to the appropriate pH with dilute NH₃ and HNO₃. Figure 2.31 shows the results. An acidic sample caused the Cd(II) peak to split, the majority of this metal unretained on the column. Indeed, the sample had to be buffered to the eluent pH to suppress this splitting mechanism, which was not found with the higher capacity CPC column. Further study is required to assess the affect of sample ionic strength on the retention and peak disturbance of metal ions. Buffering samples to perform good chromatography is not ideal, possibly leading to the introduction of contaminants into

the solution. It is the author's viewpoint that low capacity columns are not suitable for high efficiency trace determinations of metal ions in complex samples, though they might prove useful for the analysis of relatively dilute samples.

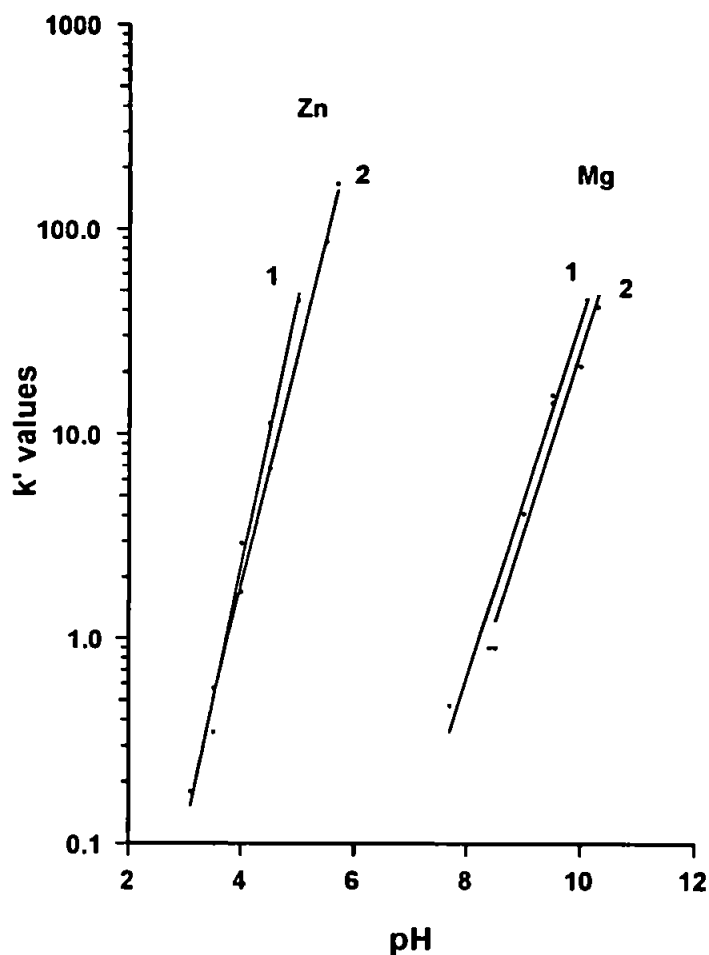


Figure 2.29. The dependence of capacity factors on pH, as a function of column capacity. Columns: 100 · 4.6mm impregnated with CPC. Capacity: 1: 0.01mM Cu(II) /g resin, 2: 0.005mM Cu(II) /g resin. Eluent: 1M KNO₃ 50mM acetic acid.

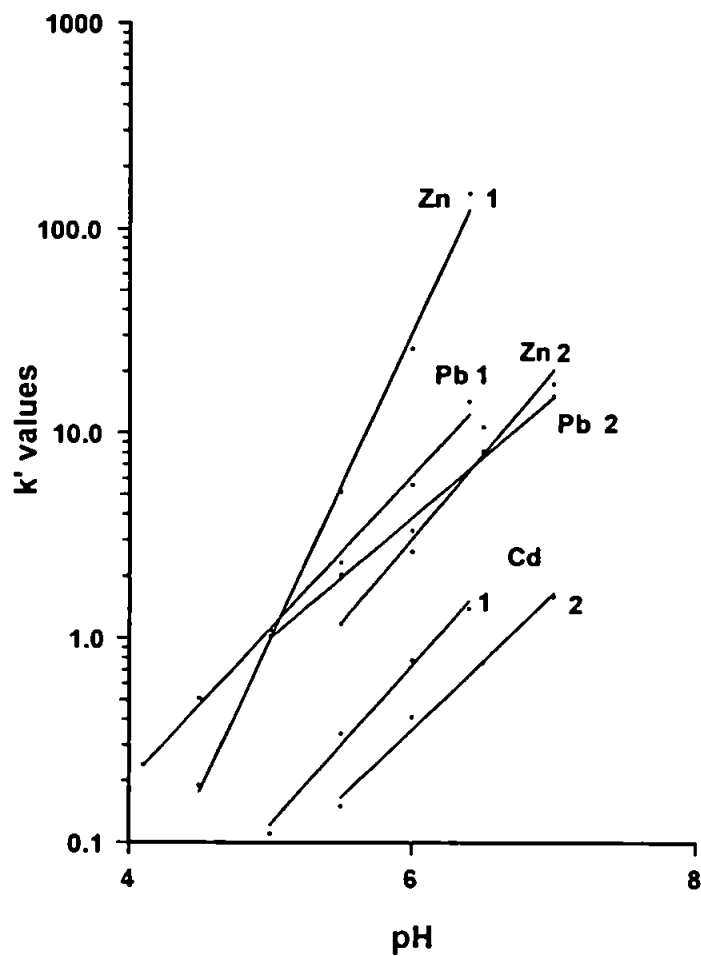


Figure 2.30. The dependence of capacity factors on eluent pH, as a function of column capacity. Columns: 100 · 4.6mm impregnated with CAL. Capacity: 1: 0.02mM Cu(II) /g resin, 2: 0.0004mM Cu(II) /g resin. Eluent: 1M KNO₃ 50mM acetic acid.

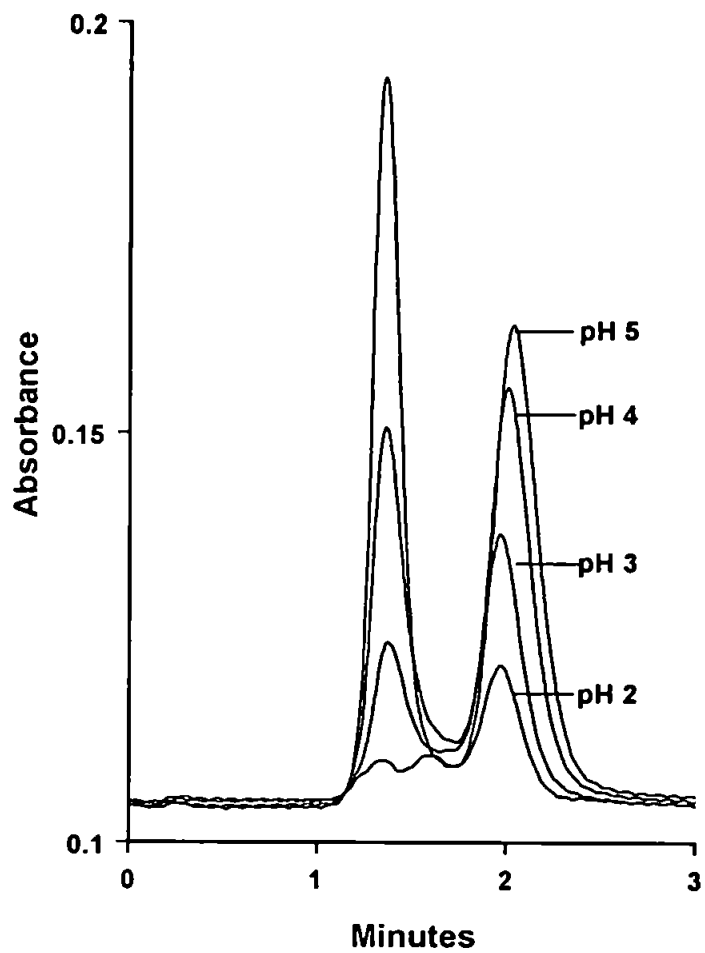


Figure 2.31. Effect of sample pH on Cd(II) peak with low capacity CPC column, 0.005mM Cu(II) /g resin. Eluent: 1M KNO₃ 50mM acetic acid at pH 4.5.

2.3.7.3 Mobile phase ionic strength

It is essential to ensure that simple ion-exchange interactions are suppressed during HPCIC separations, allowing chelation to become the dominant retention mechanism. This can be simply achieved by adding a salt to the mobile phase, increasing its ionic strength. Typically, HPCIC methods have utilised KNO_3 , at a concentration of 0.5 – 1M, to swamp ion-exchange sites on the resin [8]. To date, the effect of eluent ionic strength upon metal ion retention, using a chelating stationary phase, has not been fully characterised.

This was undertaken using the 100mm ATA column. The retention of selected transition metal ions was observed when varying the mobile phase ionic strength from 0.25 – 2M KNO_3 , over a designated pH range, pH 2.8 – 4.5. Selected results are shown as Figures 2.32 and 2.33

For the transition metals, Mn(II), Co(II), Zn(II) and Cd(II), it would appear that an ionic strength of 0.25M is sufficient to suppress ion-exchange interactions, the elution order unchanged over the range studied. For the more strongly retained metals, Pb(II) and Cu(II), an ionic strength >0.7M was required to provide the retention pattern associated with chelation-exchange.

Again, dependent upon column capacity, which will dictate the number of ion-exchange sites on the substrate, it appears that typical concentrations of 0.5 – 1M KNO_3 in the eluent, will suffice to ensure chelation is dominant. A check of each new fabricated column, prior to analysing samples by HPCIC, is advisable nonetheless.

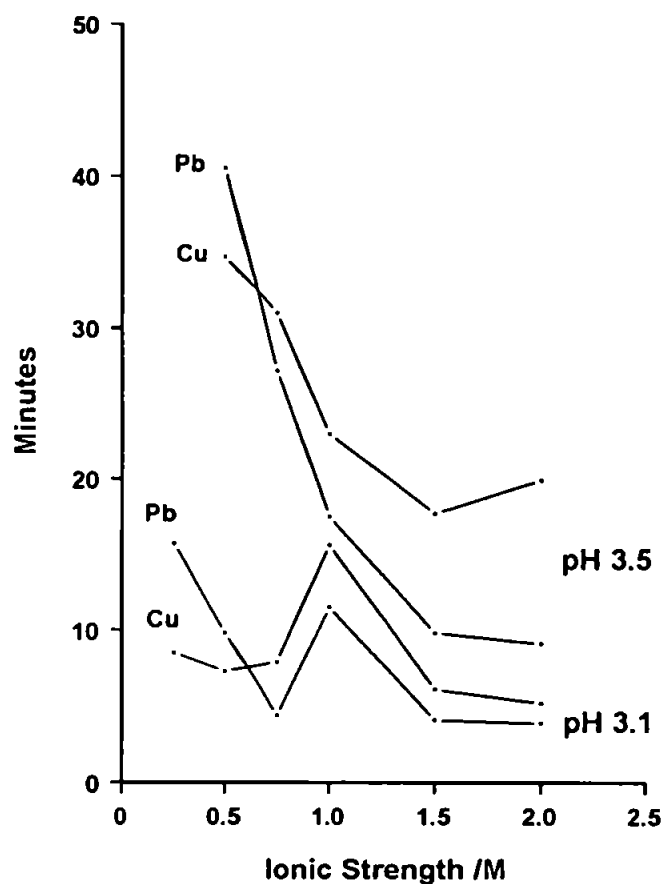


Figure 2.32. Effect of mobile phase ionic strength (KNO_3) on retention of Pb(II) and Cu(II) with the 100 · 4.6mm ATA column. Eluent contained 50mM acetic acid, adjusted to pH 3.1 or 3.5.

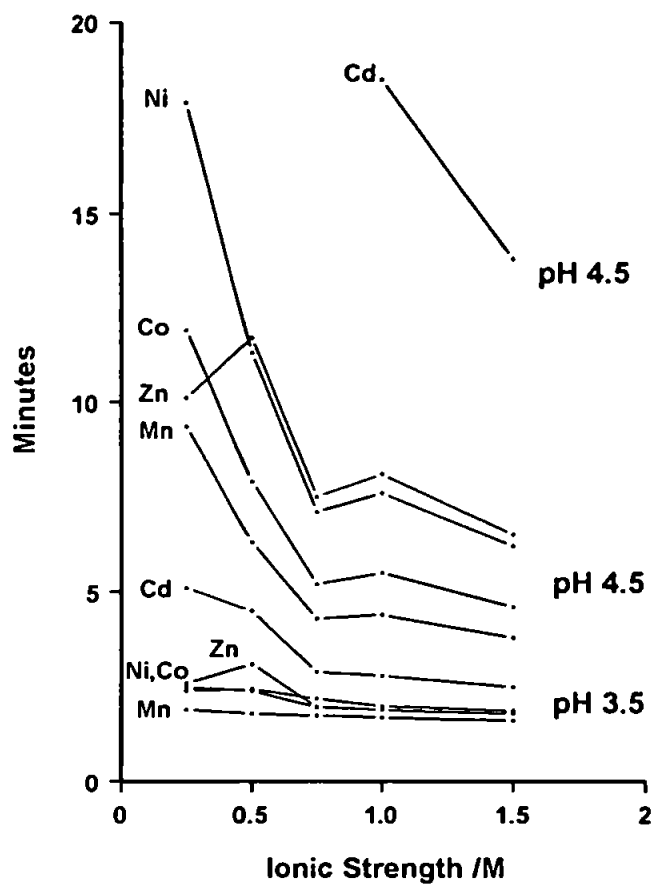


Figure 2.33. Effect of mobile phase ionic strength (KNO_3) on the retention of selected transition metal ions with the 100 · 4.6mm ATA column. Eluent contained 50mM acetic acid, adjusted to pH 3.5 or 4.5.

2.3.7.4 Complexing eluent effects

A weak complexing agent, typically acetic acid, is often added to the mobile phase for the separation of metal ions on dye immobilised resins to adjust to the pH required to separate metals exploiting their different conditional stability constants. The addition of acetic acid to the eluent also ensures the maintenance of metal solubility in less acidic solutions as weak acetate complexes. However, even weak complexing eluents will compete a little with the chelating substrate, so affecting retention. The effect, therefore, of the complexing agent concentration on the retention of metal ions formed the basis of this investigation. It had previously been determined that an acetate buffer reduced the affinity of Zn(II) on an azo dye, Sudan Orange G impregnated column [109].

The results of two acetate concentrations in the eluent, on the retention of selected transition and lanthanide metal ions, with the oxygen chelating ATA column are summarised in Table 2.8.

Table 2.8. Affect of Acetate Concentration on Metal Retention

100mm ATA column, 0.5M KNO₃ eluent.

[acetate] mM	Retention time / minutes							
	pH 3.1					pH 3.5		
	Cd(II)	Pb(II)	Cu(II)	La(III)	Lu(III)	Cd(II)	Pb(II)	Cu(II)
50	2.3	9.8	7.3	13	18	4.5	40.5	34.7
200	2.4	7.8	6.1	10.5	11.5	3.7	26	22.4

As anticipated, increasing the acetate concentration in the eluent has a significant effect on metal ion retention with the immobilised ligand. Adjusting the concentration of complexing agent in the mobile phase could, therefore, be used as an additional parameter

to optimise metal separations, by decreasing analysis time, the separation still dependant upon the dominant immobilised chelating agent characteristics.

2.3.7.5 Bare resin characteristics

It was proposed to evaluate the potential metal retaining abilities of bare substrates prior to investigating the chelating dyes studied, as a previous study concluded that a polymeric macronet resin, with high cross-linkages, (MN200, Purolite), was capable of retaining metal ions and achieving separations [109]. It is important to have confidence that metal separations achieved from this work are due to the chelating nature of immobilised dyestuffs, with minimal interference from the resin backbone.

To this end, a short investigation was initially undertaken to determine whether two low crosslinked resins used during this study had any metal retaining characteristics. The results for 100mm columns packed with the bare substrates are shown in Table 2.9.

Table 2.9. Retention of selected transition metals on Dionex resins

Eluent: 1M KNO₃ 50mM acetic acid (9 μ m PS-DVB) or 100mM acetic acid (8.8 μ m PS-DVB).

8.8 μ m PS-DVB		9 μ m PS-DVB							
		Retention time / minutes							
pH	Cu(II)	pH	Ni(II)	Co(II)	Mn(II)	Zn(II)	Cd(II)	Pb(II)	Cu(II)
4	1.8	4	1.15	1.17	1.15	1.15	1.15	1.28	1.55
4.5	1.9	5	1.17	1.18	1.18	1.17	1.18	1.77	3.55
5.5	3.8	6	1.2	1.25	1.23	1.88	1.75	3.53	14.95
6.2	6	6.5	1.23	1.35	1.27	-	-	-	-

- signifies peak splitting

It does indeed appear that there is a certain degree of metal retention on these un-modified resins, albeit very small with the exception of Cu(II). Indeed, the 9 μ m Dionex substrate apparently had a capacity of 0.0002mM Cu(II) /g resin.

The reason for metal retention on these un-modified substrates is unclear, as they are supposedly neutral with no functional groups. Retention could possibly be attributed in part to an ion – pair mechanism, metals held on the column as acetate complexes. Peak shapes were poor, and retention insignificant to that achieved with immobilised chelating dyes, however. Therefore, it can be concluded that resin backbone effects on metal retention can be essentially ignored in the presence of immobilised chelating dyes.

2.4 Summary

A range of chelating functionalities have been characterised, in terms of k' values, metal ion selectivity and separation efficiency, using dye immobilised substrates. An overview of the results obtained in this chapter are given in Table 2.10 and Table 2.11.

Table 2.10. Dye immobilised resin characteristics

Dye	Amount impregnated		Capacity mM Cu(II) /g resin	Mole % available sites for chelation
	mg /g resin	mM /g resin		
ATA	107	0.253	0.01	3.8
PCV	46.4	0.120	0.006	4.6
CPC	62.7	0.093	0.005	5.0
CAL	184	0.513	0.019	3.7
PAR	167.8	0.780	0.036	4.6
SPP	130	0.333	-	-

Table 2.11. Metal selectivity on each dye column

Dye	Chelation	Alkaline earth metals	Transition metals	Trivalent metals
ATA	O,O	Ba<Sr<Ca<Mg	Mn<Co<Zn<Ni<Cd<Pb<Cu	Al<Ga<In
PCV	O,O	Ba<Sr<Ca<Mg	Mn<Cd<Co<Ni<Zn<Pb<Cu	Al<Ga<In
CPC	N,O,O	Ba<Sr<Ca<Mg	Mn,Ni,Cd<Co<Zn<Pb<Cu	Al<Ga<In
CAL	N,O	Ba,Sr<Ca<Mg	Mn<Cd<Co<Pb<Zn<Cu	Al<In
PAR	N,N,O	Mg<Ba<Sr<Ca	Mn<Ni<Cd<Zn<Pb<Cu	Al<Ga<In
SPP	N,N	unretained	Mn<Pb<Cd<Zn	-

Differences in metal ion retention order were observed, dependant upon the ligating atoms attached to the dye molecule. This was noticed on columns containing both different and similar chelating groups. The ATA column (O,O chelation), exhibited a unique strong affinity for Cd(II), not repeated on the PCV coated column which also contains oxygen (O,O) donor atoms. Cd(II) was also weakly retained on the nitrogen, oxygen chelating dyes studied. The nitrogen (N,N) chelating molecule, SPP, retained Pb(II) weakly in comparison with Zn(II), not repeated on any other column with the exception of the CAL loaded resin. Significant differences in selectivity coefficients were also noted, for example the elution of the alkaline earths on the PAR and CAL loaded columns, which can be attributed to differences in the ligand base strength.

Table 2.11 illustrates the diverse range of elution profiles observed for the groups of metal ions studied, indicative of the scope of HPCIC to tailor specific chelating columns to determine metal ions in differing sample types.

All of the fabricated columns had a similar percentage of chelating sites available to complex metal ions, but large differences in selectivity coefficients arose. Of the six dye loaded columns, only the ATA and CPC molecules were capable of isocratically separating

the alkaline earth metals. For the transition and heavy metals, optimum resolution and peak efficiency was also observed with these two columns, but only three metals could be separated isocratically on a 100mm column. The ATA column also gave the best trivalent metal ion separation, although slow reaction kinetics gave very broad peaks.

Many of the other columns exposed the significant disadvantage of HPCIC with rapidly broadening asymmetric peaks with increasing elution time – the kinetic broadening effect. This can be seen with the Zn(II) peak on the SPP column (Figure 2.22), or Mg(II) peak on the CAL column (Figure 2.16).

Nevertheless, this study has established that both azo and triphenylmethane based dyes, with different chelating functionalities, can achieve analytical separations as demonstrated in previous work [147]. An advantage of dye immobilised columns, is the inter – group selectivity between transition and trivalent metal ions and the alkaline earth metals, which could facilitate the use of these columns to determine trace metals in concentrated brines and highly mineralised samples. A possible disadvantage is the poor intra – group selectivity exhibited by many columns, but this could possibly be overcome by increasing column length, column capacity and using pH gradient elution programs.

Other system parameters investigated, namely column length and capacity, together with mobile phase characteristics including ionic strength, ligand concentration in the mobile phase and complexing buffer concentration can result in more efficient separations by HPCIC.

This is the first thorough study undertaken to determine the effect of various chelating dyes and ligand groups for the high performance separation of metal ions. Early work has been of an ‘empirical’ nature, developing dye columns specifically to apply them for the separation and determination of trace metals in samples of interest, including seawater.

It is very useful to investigate different chelating groups, as they can provide unique selectivity coefficients, which can then ‘feed’ into other studies to develop systems for determining specific analytes. Chelating dye immobilised substrates provide a quick,

simple and easy solution to perform these comparisons. Promising ligand groups can then be bonded to high efficiency sorbents to improve the capacity, or the dye columns themselves employed for analytical purposes.

In the light of previous and current research to apply chelating dye columns to determine metal ions, it was decided to study other chelating systems for the remainder of this work.

It should be noted that dye loaded columns will be applied in future work for the analysis of more complex samples.

Chapter 3. Chelating Exchange Separation Properties of Aminophosphonate Functionalised Silica.

3.1 Introduction

The primary aim of HPCIC is to combine intergroup and intragroup selectivity, whilst still enabling the individual determination of metal ions, which remains a significant problem for ion chromatography.

An example of this 'ideal', would involve the separation of transition metals from the alkaline earths in a complex sample matrix including brine solutions (intergroup selectivity), for their individual determination (intragroup selectivity).

The dye loaded substrates investigated in Chapter 2, although useful for establishing the general metal retention properties of various ligands, and capable of achieving intergroup selectivity, are predominantly unsuitable for multi-element (>3-4 metal ions) isocratic separations of transition and alkaline earth metals, due to large differences in conditional stability constants and slow reaction kinetics. Multi-element separations could be achieved with these chelating columns, but would involve complex gradient elution strategies. An exception to this are dyes which contain iminodiacetate (IDA) functional groups (XO, MTB, CPC), which have been applied for multi-element separations in various samples, as mentioned in the preceding chapter. Iminodiacetate has a soft nitrogen atom and two hard oxygen donor atoms, enabling it to chelate metal ions over a wide pH range.

The IDA ligand has been immobilised onto many low efficiency sorbents for preconcentration purposes. A wide variety are available commercially, including Amberlite IRC-718 (Rohm and Haas), Dowex A-1 (Dow Chemical) and S-930 (Purolite), for the extraction of transition and heavy metals from aqueous solutions. The equilibria of sorption of H^+ and transition metals on an IDA substrate (silica) have been studied by Kholin *et al* [165].

Studies have also been undertaken to investigate the selectivity and adsorption mechanism of trivalent metal ions on IDA chelating resins [166,167]. Results indicate that the IDA functionality in a polymer phase can often not reproduce their aqueous phase metal – ligand configurations, due to steric effects which make it difficult for the ligands to orient themselves spatially around receptor metal ions. Increasing the spacer arm length between the functional group and polymer matrix can improve this situation. Recently, Noresson *et al* investigated the effects of capacity for trace metal preconcentration using an IDA chelating sorbent, concluding that a low specific capacity was optimal for the removal of matrix elements from aqueous solutions [168].

The alkali and alkaline earth metals have also been separated using an iminodiacetic acid bonded silica substrate, applied to the ion chromatographic determination of these metals in various water samples [169,170].

With regards to HPCIC, the IDA functional group produces good performance because it generates reasonably fast kinetics, combined with selectivity coefficients that are not too large. Table 3.1 illustrates the closeness of the stability constants for metal ions with this ligand, which will determine the selectivity coefficients on an IDA chelating substrate. Exceptions are Cu(II) and Fe(III), both with large stability constants, which would be retained strongly on such a substrate.

Table 3.1. Log stability constants of selected metal complexes with iminodiacetate [162].

M^{n+}	$\log K_1$	M^{n+}	$\log K_1$
Pb^{2+}	7.45	UO_2^{2+}	8.93
Ni^{2+}	8.19	Fe^{3+}	10.72
Zn^{2+}	7.27	In^{3+}	9.54
Co^{2+}	6.97	Al^{3+}	8.10
Cd^{2+}	5.73	La^{3+}	5.88
Cu^{2+}	10.63	Th^{4+}	10.66

The good performance of this ligand for metal ion separations has been demonstrated with other IDA functionalised high efficiency substrates, including iminodiacetic acid bonded silica [77], and polymethacrylate iminodiacetate column Tosoh chelate 5PW [76], both mentioned in Chapter 1. Nevertheless, isocratic separation on chelating phases containing IDA groups is presently still limited to 5-6 metals, and gradient steps may be required for strongly binding metals including Cu(II) and Fe(III). Although isocratic separation of 14 metal ions has been achieved for the lanthanides on an IDA phase [79], this was exceptional due to the relatively small differences in conditional stability constants between individual members of this series.

There is a certain conflict, therefore, between the advantages of having high selectivity with respect to one or two metals on chelating ion – exchangers, and the development of HPCIC as a multi-component method of analysis. Consequently, there is a need to continue searching for 'ideal' functional groups similar to or better than IDA, which will fulfil the criteria for both inter- and intragroup selectivity and metal ion determination within an isocratic run.

A possible candidate is aminophosphonic acid. This molecule is also a tridentate ligand which can bind metals through a nitrogen and two oxygen donor atoms (N,O,O). The substitution of the IDA carboxyl groups (CO_2^-) with phosphonate groups (PO_3^{2-}), generally increases the stability of metal complexes, due to the increase in basicity on the co-ordinating group [171]. Log stability constants for selected metals with the homogeneous analogue of this ligand are given in Table 3.2. The stability constants for this analogue of aminophosphonic acid are smaller than those found with the IDA ligand, though still closely spaced. Cu(II) has a large stability constant on both IDA and aminophosphonate, but there are differences between these two N,O,O chelators, noticeably in the larger stability constant of Ni(II) on IDA in comparison with Zn(II), which has a larger stability constant on the aminophosphonate ligand.

Table 3.2 Log stability constants of selected metals with 2-aminoethylphosphonic acid [163].

M^{n+}	$\log K_1$
Cu^{2+}	8.35
Ni^{2+}	5.18
Zn^{2+}	5.67
Co^{2+}	4.58
Mn^{2+}	3.5
Mg^{2+}	1.84
Ca^{2+}	1.43

Resins bearing aminophosphonic acid also represent a well-established class of chelating ion – exchangers, having an increased selectivity for transition and heavy metal ions [172]. A number of them under the trade names Lewatit OC 1060 (Bayer), Duolite C467 (Rohm and Haas), S940 and S950 (Purolite) and Chelite P (Serva), are available commercially, and have been applied to the preconcentration of toxic metals from natural and industrial waters [173,174]. Yebra-Biurrun *et al* [175], synthesised aminophosphonic acid onto Amberlite XAD-4, for the preconcentration of transition metal ions prior to AAS determination in natural waters [176] and mussel tissue [177].

Vaaramaa and Lehto [178], and Nesterenko *et al* [179] have investigated the ion – exchange properties of aminophosphonate sorbents. Vaaramaa and Lehto found that aminophosphonate, bound to a polymeric resin (Duolite C467) greatly prefers H^+ ions in neutral and acidic solutions, when the resin is present in its sodium form, affecting the exchange of other metal ions. Nesterenko *et al*, synthesising aminophosphonate onto a silica matrix, found changes in alkali metal selectivity dependant upon the acid concentration in the eluent, which would affect the dissociation of the phosphonic acid groups. In weak acid solution, the phosphonic acid is mono-dissociated (only one OH

group is dissociated), leading to the following selectivity: $\text{Li}^+ < \text{Na}^+ < \text{NH}_4^+ < \text{K}^+ < \text{Rb}^+ < \text{Cs}^+$, which changed to $\text{Cs}^+ < \text{Rb}^+ < \text{K}^+ < \text{Na}^+ < \text{Li}^+$ in neutral or alkaline eluents, where two OH groups are dissociated.

The suitability of an aminophosphonic ion exchanger as a stationary phase for HPCIC has not yet been investigated. The main aim of this study, therefore, was to characterise aminophosphonate functional groups, bonded to small particle size silica gel, in terms of metal selectivity and separation efficiency, using eluents of high ionic strength. This data could then be compared with a synthesised O,O chelating phenylphosphonic acid silica substrate, to assess the effect of the nitrogen donor atom on metal selectivity and column performance.

3.2 Experimental

3.2.1 Instrumentation

The HPCIC system used throughout these studies is described in section 2.2.1, with the exception that column length was either 150 · 4.6mm I.D. or 250 · 4.6mm I.D.

A short study on the ion exchange properties of phenylphosphonic acid (150 · 4.6mm I.D. column length) with the alkali metals was performed, where detection was achieved using a Waters 431 conductivity detector (Waters, Milford, MA, USA).

3.2.2 Reagents

All reagents were of Analar grade (BDH), with the exception of PAR and Zn-EDTA (Fluka). The post column photometric reagents used in these studies were PAR and PAR/ Zn-EDTA, detailed in section 2.2.2. Detection was achieved at 490nm.

An aqueous solution of either 0.5 or 1M KNO₃ was used as an eluent, adjusted to the required pH with HNO₃. The eluent and PCR were delivered at 1ml min⁻¹.

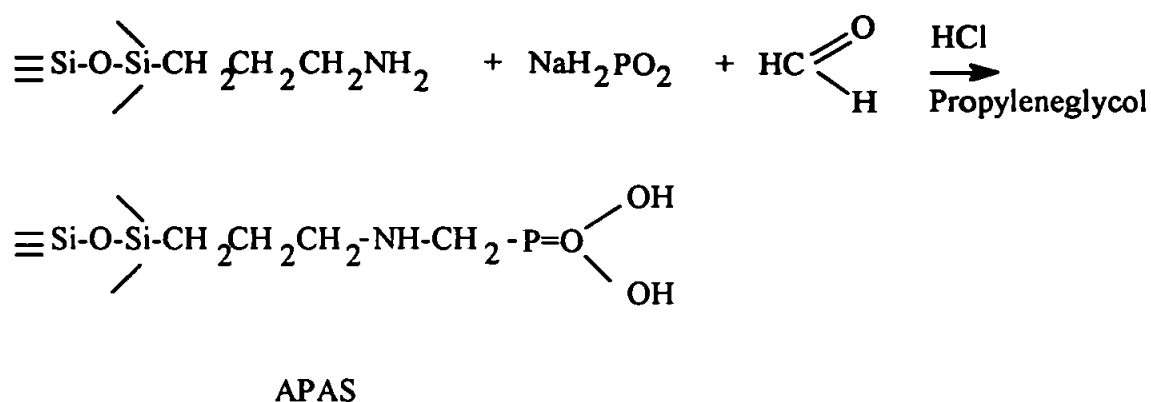
An aqueous solution of HNO₃ was used as an eluent for the ion – exchange of metal ions on the phenylphosphonic acid bonded silica column.

3.2.3 Sorbent Preparation

Dr. P.N. Nesterenko of Moscow State University, Russia, prepared both of the following sorbents.

3.2.3.1. Silica Bound Aminophosphonic acid (APAS)

The 5 μ m silica gel containing aminophosphonic functionality was synthesised as described earlier [179], by a Mannich type reaction of aminopropylsilica with hypophosphorous acid and formaldehyde:



From data obtained by CHN analysis and potentiometric titration, APAS contains 0.35mM g⁻¹ unreacted aminopropyl groups and 0.1mM g⁻¹ aminophosphonic acid functional groups at the surface [179].

3.2.3.2 Silica Bound Phenylphosphonic Acid (PPAS)

The phosphonic ion exchanger was obtained by a two step synthesis in accordance with Kudryavtsev *et al* [180]. 5g of commercially available phenylsilica (Serva, Heidelberg, Germany) was reacted with phosphorous trichloride in the presence of anhydrous aluminium trichloride, followed by acid hydrolysis of the phosphorous – chloride bonds and oxidation using potassium permanganate in an acid medium.

Both substrates were slurry packed into analytical columns using the Shandon packer, with a 2-propanol solvent at 2000psi.

3.3 Results and Discussion

3.3.1 Chelating Mechanism of Aminophosphonate Functional Groups

The aminomethylphosphonic acid chelating group (H_2L), is potentially a tridentate ligand, having two possible bonding sites at a phosphonic group and one co-ordination site at the secondary nitrogen atom, yielding a N,O,O chelating system. This has been determined by Kertman *et al* [181], using a calorimeter to measure enthalpy variations during the process of transition metal sorption onto aminophosphonic acid groups.

It is more probable that bidentate O,O chelation exists at low pH, due to protonation of the amino group. Thus, dependent upon pH, several possibilities for the co-ordination of divalent metal ions are likely, as presented in Figure 3.1.

Although several stoichiometries of metal complexes can be formed with aminophosphonate ion – exchangers, a 1:1 metal:ligand stoichiometry is the most stable [182]. The most favourable mode of chelation of this phosphonic acid group is formation of a four membered ring through deprotonation of the two P-OH groups (denoted VIII in Figure 3.1), though formation of a four membered ring (VII) through bonding of one of the hydroxyl groups and co-ordination of the oxygen atom P=O has been stated as possible [183].

Normally, the amino nitrogen does not participate under acidic conditions because of its strongly protonated nature, and only phosphonic groups chelate with metal ions. Nevertheless, as the pH increases into the weak acid region, the formation of N,O,O chelation cannot be ruled out, depending on the magnitude of the individual metal stability constants.

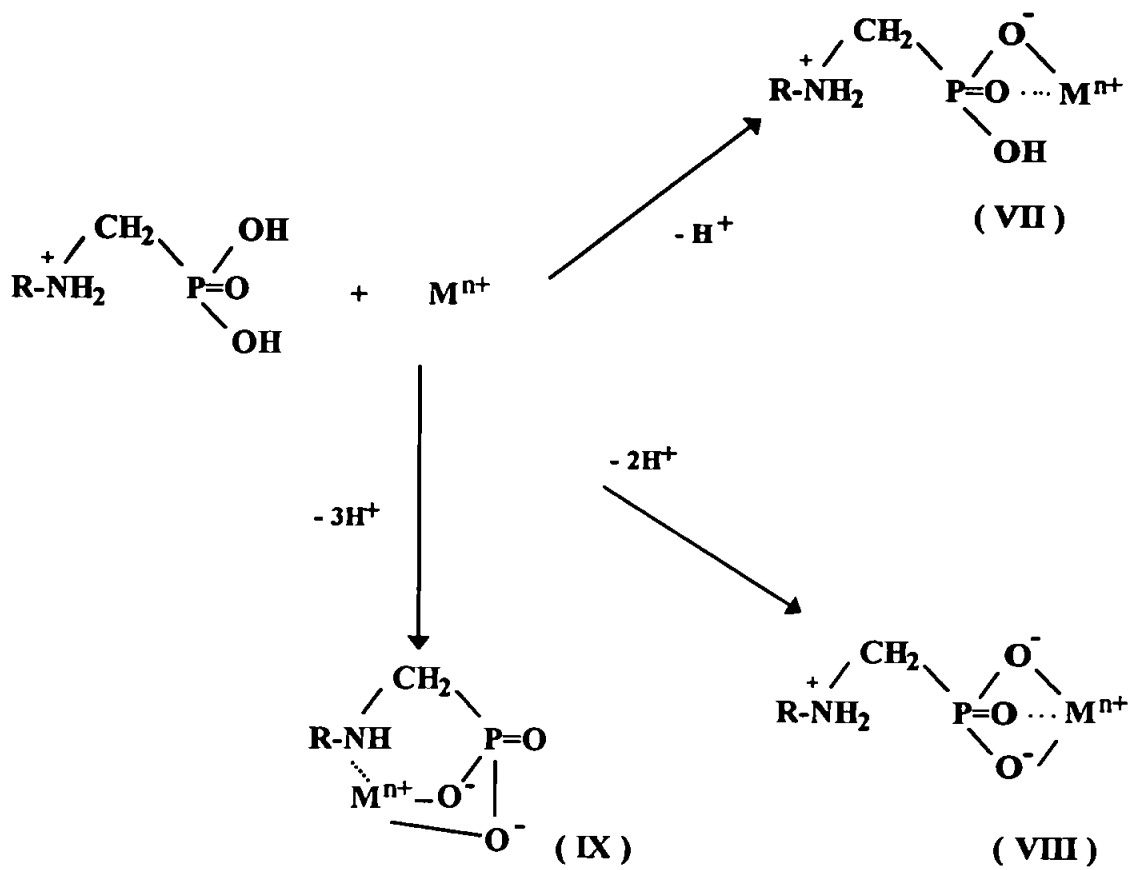


Figure 3.1 Possible Structures of Complexes Formed at the Surface of APAS

3.3.2 APAS Column Selectivity

The APAS substrate capacity was determined to be $0.027\text{mM Cu(II) g}^{-1}$ resin (pH 5.1), which is higher than that achieved with the dye loaded resins investigated (Table 2.9 Chapter 2).

As the eluent was un-buffered, primarily to determine the effect of the aminophosphonate group on metal retention without possible complexing agent interferences from the mobile phase, the time required to obtain column pH equilibration increased. With a 150mm column length, a pH change from 2 – 4.5 equilibrated within 3 hours, deduced by monitoring the column effluent. This is most probably due to the high column capacity, APAS groups competing for H^+ ions. Gradual pH increments of 0.5 units, however, reached equilibrium after approximately 30 minutes in the acid region.

Initial studies on the 150mm column found there to be an unusual elution pattern with this sorbent, most noticeably in the strong retention of Mn(II). This has not been observed on any of the chelating substrates investigated previously, and is a significant development in terms of separating this ion from other metals. This can be illustrated with the separation of 5 metals at pH 1.5 (Figure 3.2), Mn(II) being the most strongly retained. This chromatogram also demonstrates the increased efficiency of this column in comparison with the dye immobilised resins, which could generally only separate 4 metals isocratically. An initial plot of capacity factors against pH, using Zn(II) and Mg(II), resulted in S-shaped curves in the acid range. This curvature has not been observed before, the majority of metal ion : ligand complexes demonstrating a linear dependence of $\log k'$ with pH, as illustrated with the chelating dyes in Chapter 2. For this reason, a 250mm column was packed with the APAS substrate, to improve column efficiency and obtain a more detailed k' plot. Additional metal ions were studied, to ascertain whether this S-shaped curve was a general phenomenon on this phase. The capacity factor vs. pH plots for

12 metal ions are shown in Figures 3.3 and 3.4, and except for Cu(II), all display the S-shape effect.

From the previous discussion concerning the chelating mechanism of APAS, it was proposed that these S-shaped curves are a reflection of a change in metal co-ordination on the substrate with increasing pH. This could be in terms of a change in denticity and/or a change in ligand type from O,O to N,O,O. Using the pK_a values shown in Figure 3.5 for aminophosphonate [163,184], and taking into account the high ionic strength (1M), it can be shown that the change from the first to second deprotonation in APAS occurs in the pH range 2-3, which is close to the minimum of the S-shaped curves in Figures 3.3 and 3.4. Changes in protonation of a polydentate ligand frequently coincide with the formation of complexes with larger stability constants, which is reflected in the steeper slopes after the minimum.

The formation of protonated or acid complexes of structures VII and VIII have been established for alkaline earth metals [184,185]. Considering the much less favourable co-ordination between these metals and amino groups, the change in the slope of $\log k'$ against pH for these metals is probably connected to the second acid dissociation step of the phosphonic group and change in O,O co-ordination from VII to VIII.

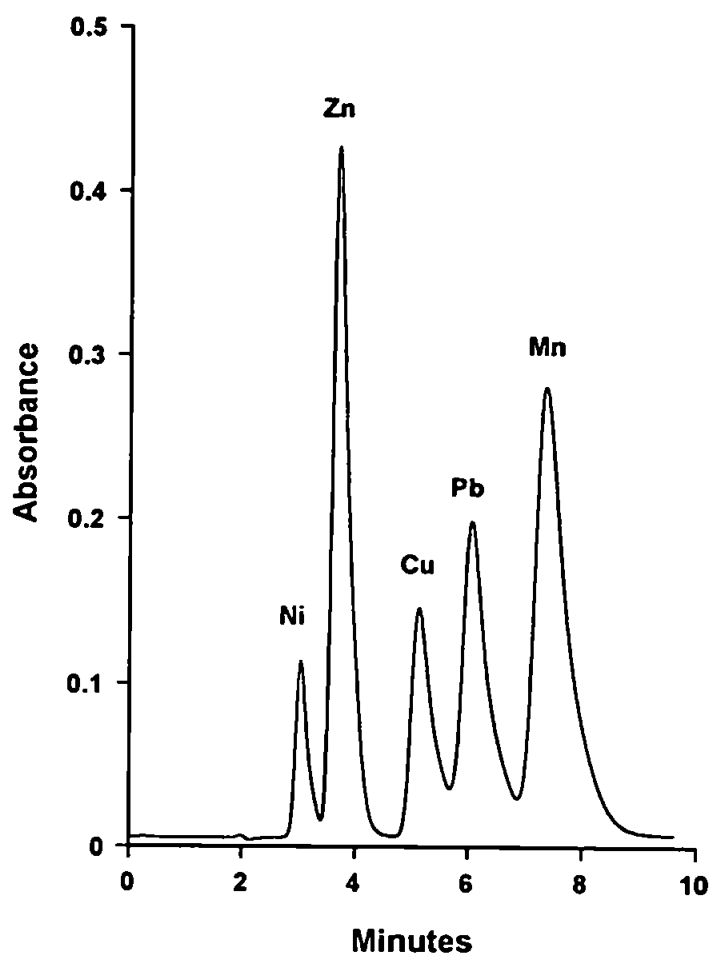


Figure 3.2. Separation of Ni(II) 1mg l^{-1} , Zn(II) 10mg l^{-1} , Cu(II) 2mg l^{-1} , Pb(II) 25mg l^{-1} and Mn(II) 5mg l^{-1} , on the $150 \cdot 4.6\text{mm}$ APAS column. Eluent: 0.5M KNO_3 at pH 1.5. Detection: PAR at 490nm.

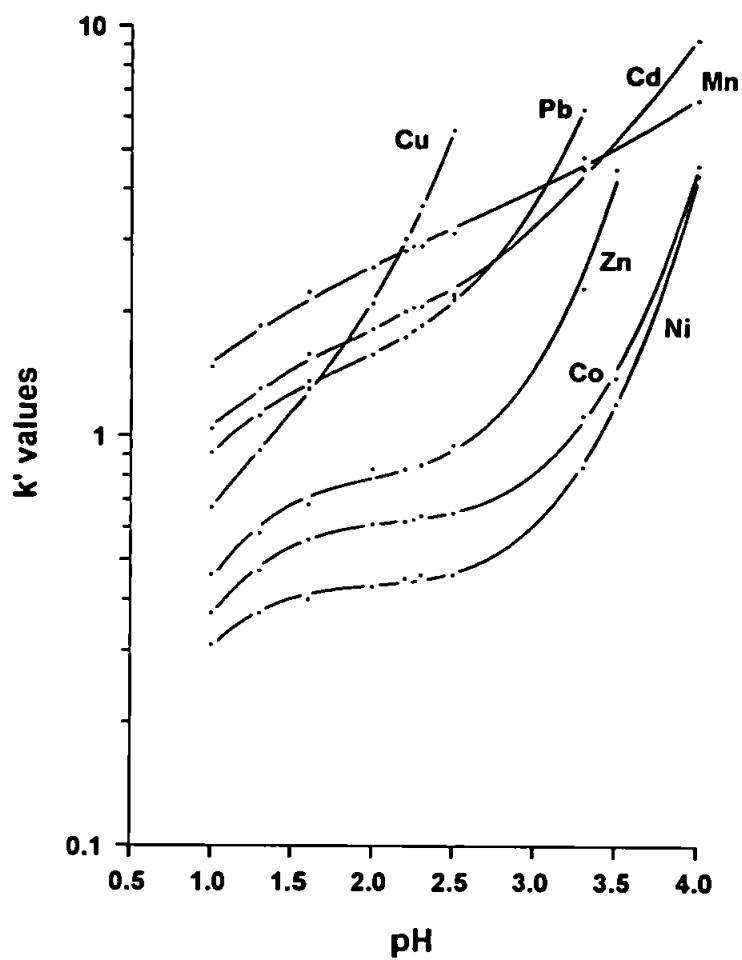


Figure 3.3. The dependence of capacity factors for transition metals on eluent pH, with the APAS column. Eluent: 1M KNO_3 adjusted to the appropriate pH with HNO_3 .

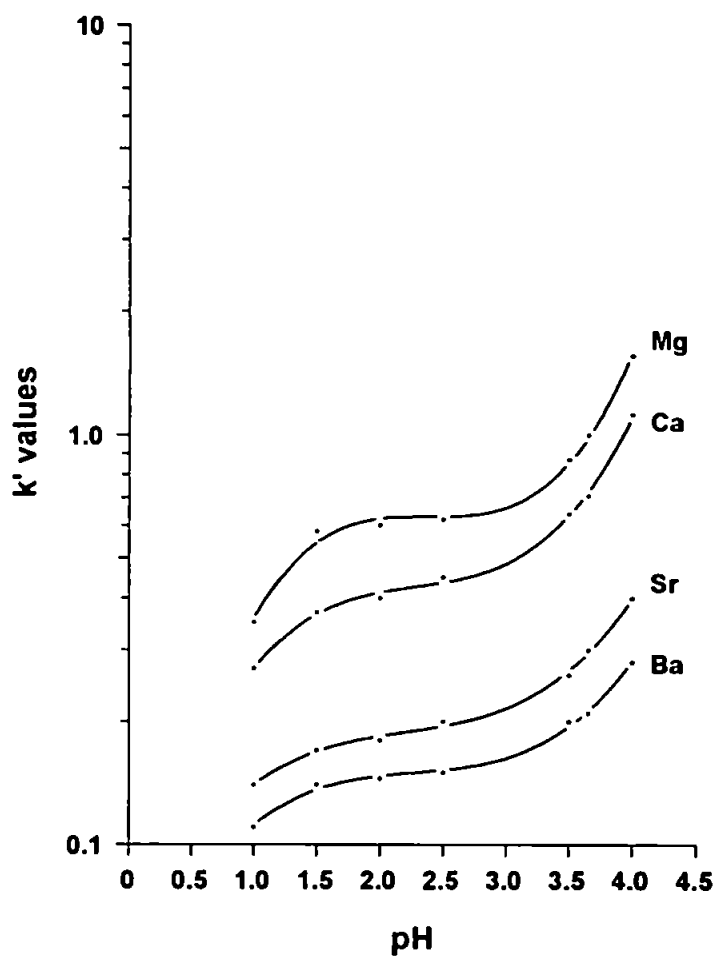


Figure 3.4. The dependence of capacity factors for alkaline earth metals on eluent pH, with the APAS column. Eluent: 1M KNO₃ adjusted to the appropriate pH with HNO₃.

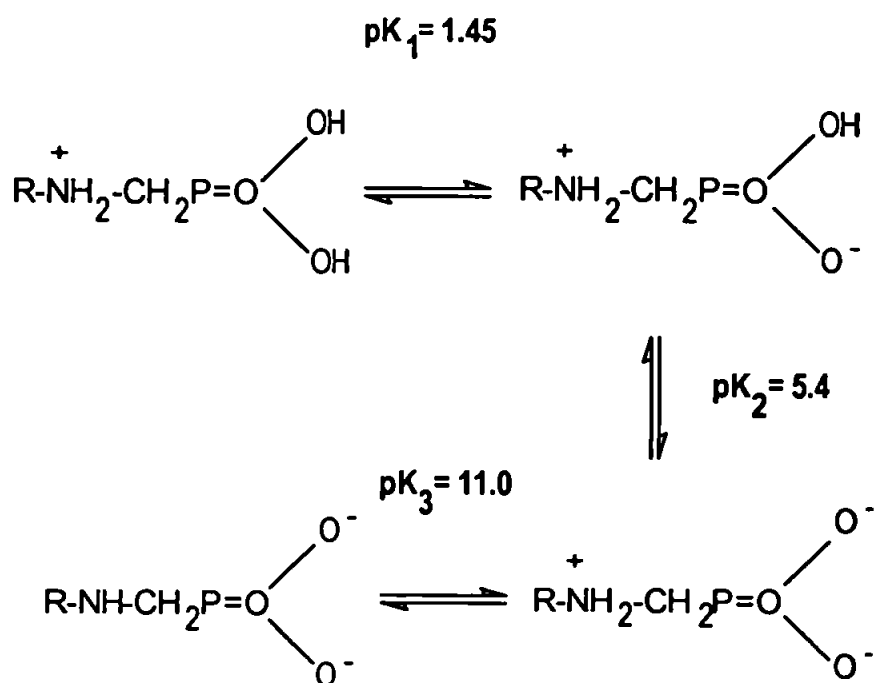


Figure 3.5. Dependence of aminophosphonate functionality on eluent pH.

Based on the acid dissociation constants for β -propylaminophosphonic acid (homogeneous analogue of APAS) [163,184]

The transition and heavy metals, with the exception of Cu(II), follow a similar S-shaped pattern to the alkaline earth metals. The slopes, however, are generally steeper and more varied, with some crossover. These metals have the possibility of complexation with aminophosphonic acid, including co-ordination on the amino group, as emphasised by other studies [183,186].

It was, therefore, suggested that structure IX, be considered to start to form as the pH was raised. The possibility of complexation of transition metals with two aminopropyl groups present at the surface of APAS is very low in accordance with [187]. Data on stability constants of aminophosphonates in homogeneous solution are sparse, particularly when extended to acid conditions. A study by Mohan and Abbott [185], however, covered most

of the transition metals examined here. They obtained stability constants for both structure IX (ML) and structure VIII (MHL). As expected, the values of K_{stab} for ML are much greater than those for MHL. Thus, some ML complexes can be expected to start forming in weak acid media, despite the large pK_a value of the amino nitrogen. It was suggested that the steeper and more varied slopes above pH 3-3.5 reflect the appearance of structure IX, which co-exists with structure VIII and eventually becomes more dominant. The ML complex for Cu(II) is particularly strong and speciation calculations show it actually forms at the same pH as the MHL complex. For Cu(II) complexes on APAS, therefore, structure VIII is 'swamped' or overtaken by structure IX, and could explain its steeply increasing slope and lack of discernible S shape. Speciation diagrams for Cu(II), Mn(II) and Zn(II) with the homogeneous analogue of APAS, aminoethanephosphonic acid are shown as Figures 3.6, 3.7 and 3.8, demonstrating the different rates of change of conditional constants as a function of pH. The Cu(II) ML complex can be seen to form below pH 3, in conjunction with the MHL complex, ML becoming dominant above pH 4. The formation of both complexes in the same pH region is probably why Cu(II) does not follow the S-shaped dependence witnessed with the other transition metals studied. The Zn(II) speciation diagram displays very different characteristics. With this metal, the MHL complex forms at around pH 3 – 4, whilst the ML complex appears at around pH 5, hence the S-shaped curve associated with a change from MHL to ML. Interestingly, the Zn(II) MHL complex is present over a much wider pH range (3.5 – 9) than the Cu(II) MHL complex (pH 3.5 – 6). The Mn(II) speciation diagram has also been included as it illustrates why this metal is the most strongly retained at low pH. This metal has the largest gap between the formation of the MHL and ML complexes, ML not forming in any significant concentration until after pH 6. It is the absence of the ML complex at low pH, with MHL the dominant species, which results in Mn(II) being the most strongly retained metal. The Mn(II) MHL complex is also present over a wide pH range, as apparent with the Zn(II) MHL complex.

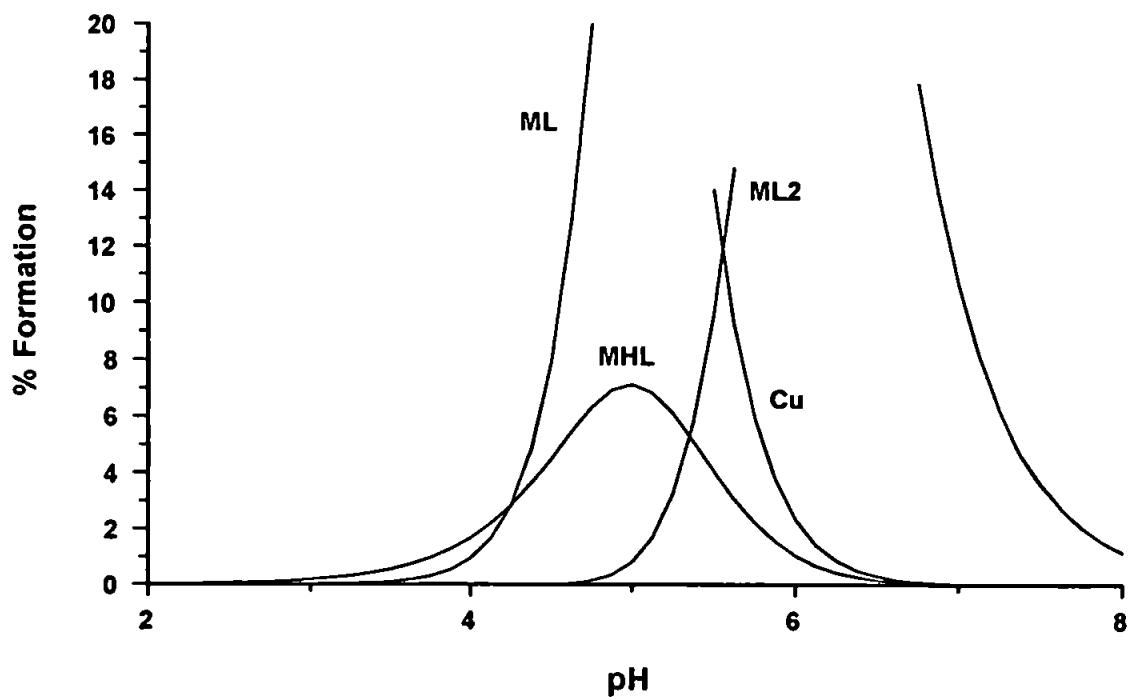
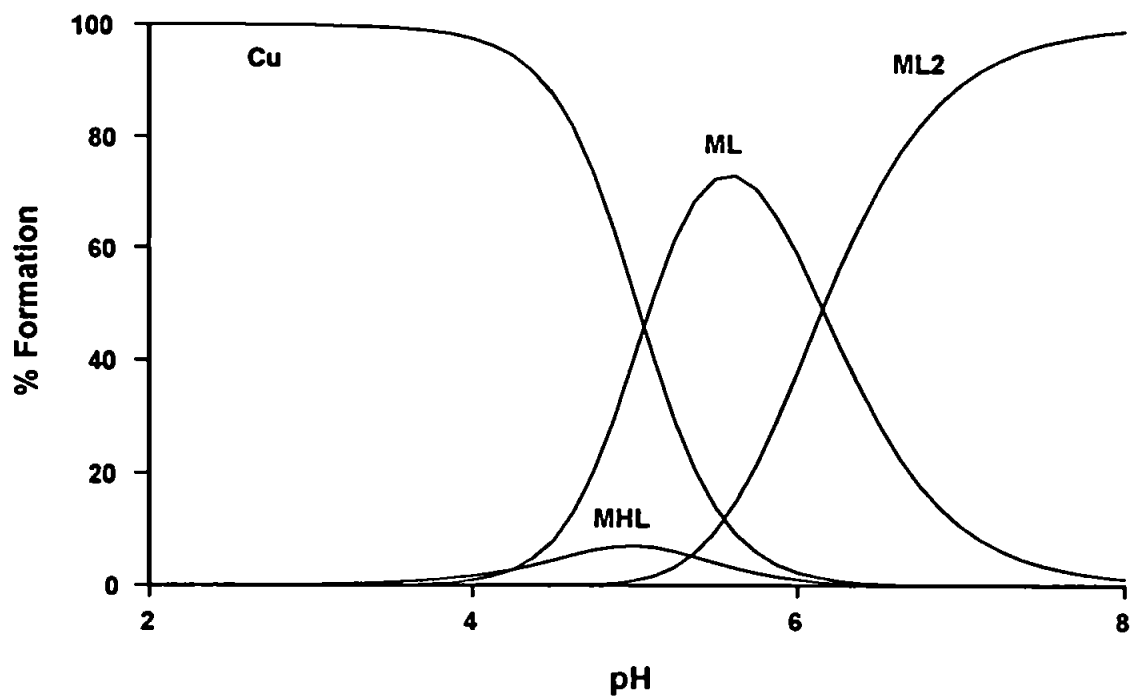


Figure 3.6 Speciation diagram of Cu(II) with aminoethanephosphonic acid [163].

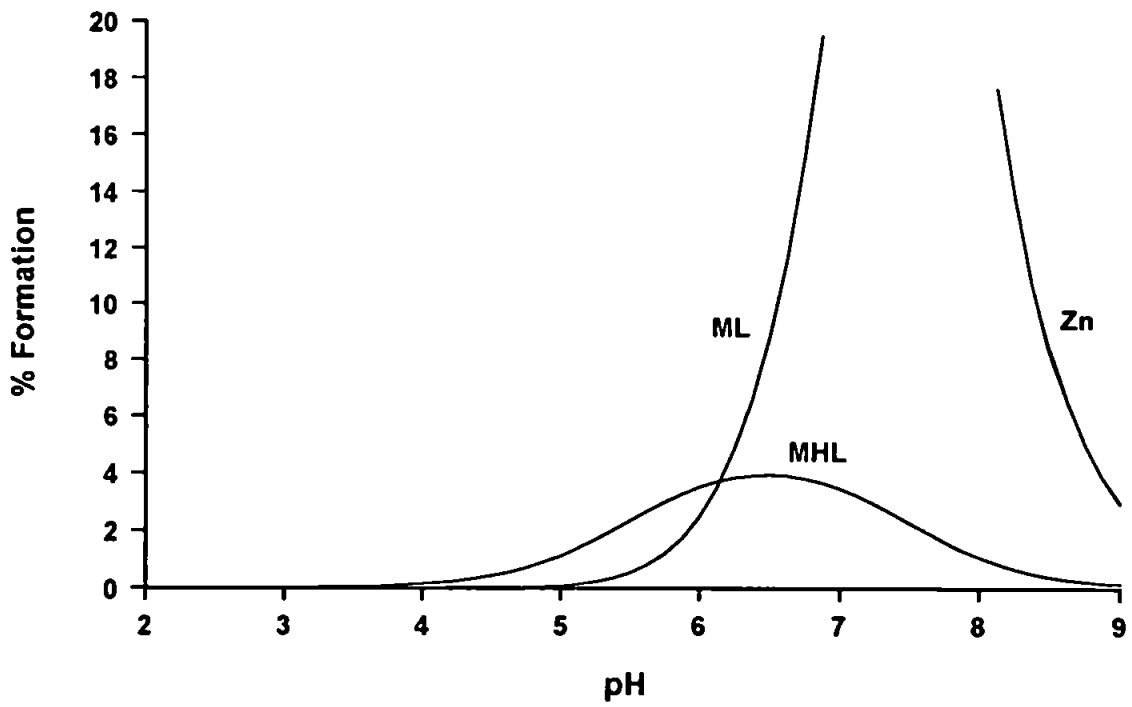
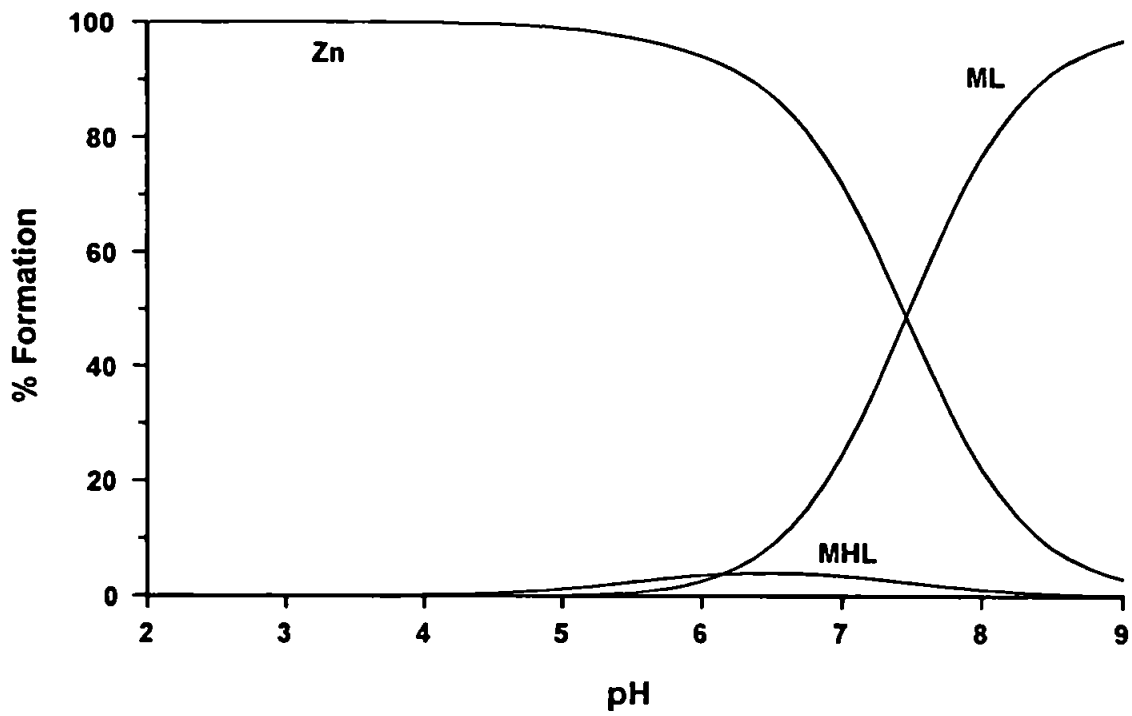


Figure 3.7. Speciation diagram of Zn(II) with aminoethanephosphonic acid [163].

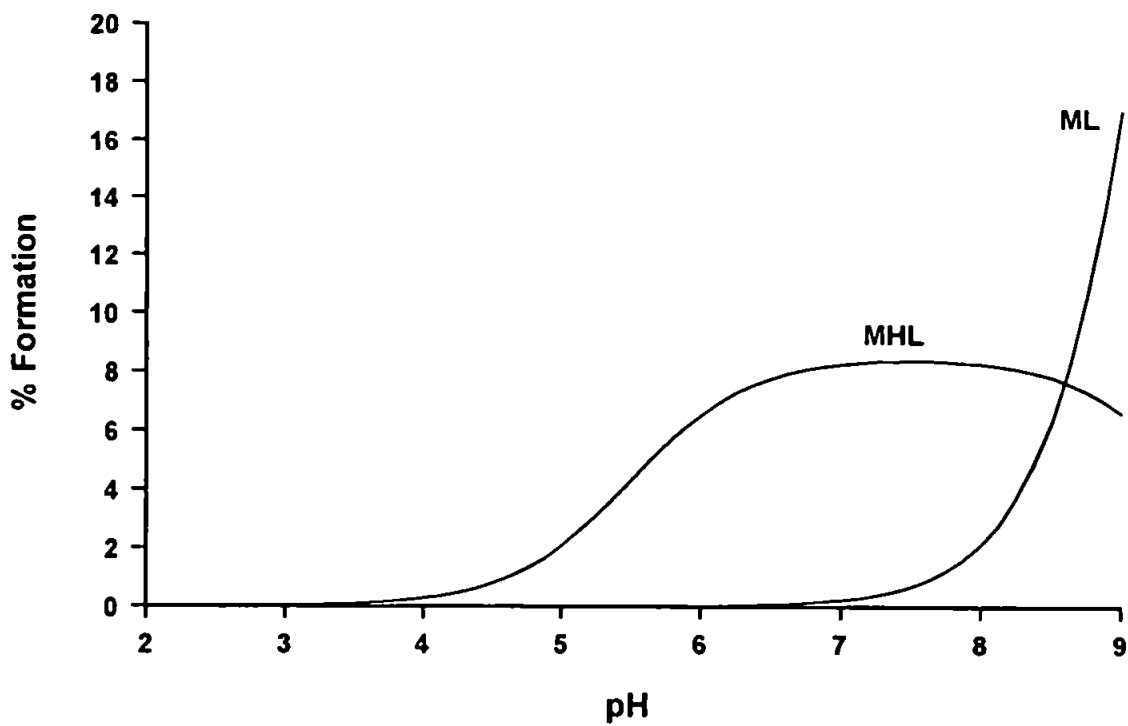
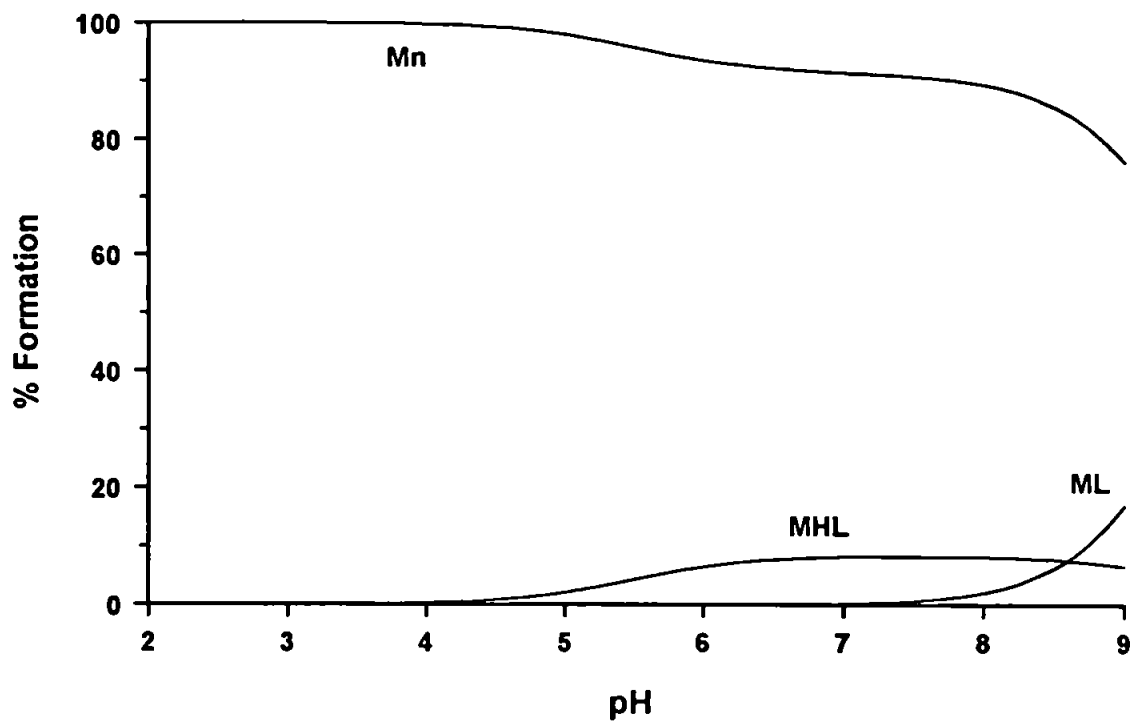


Figure 3.8. Speciation diagram of Mn(II) with aminoethanephosphonic acid [163].

As illustrated in Figure 3.3, under suppressed ion – exchange, the order of elution of transition metals on APAS varied with pH. At pH 1, the retention order was Ni(II)<Co(II)<Zn(II)<Cu(II)<Pb(II)<Cd(II)<Mn(II). A similar ion – exchange selectivity was observed at the same pH:

Ni(II)<Co(II)<Zn(II)<Cu(II)<Mn(II)<Cd(II)<Pb(II), as found in a previous study [179]. This similarity means that even in the absence of suppression of ion – exchange interactions between metal ions, and negatively charged phosphonic groups, the complexation at the surface of APAS remains the dominant separation mechanism.

The high selectivity of Mn(II), retained most strongly at low pH, agrees closely with the order of stability constants for MHL complexes of aminomethylphosphonate, measured by Mohan and Abbott [185], namely Ni(II)<Mg(II)<Co(II)<Zn(II)<Mn(II)<Cu(II). The position of Cu(II) is the only significant difference, but the high value for Mn(II) and the low value for Ni(II) are clearly evident.

As the pH was increased, the order of retention on APAS changed with Pb(II) and Cu(II) in particular becoming the most strongly retained. This reflects the change in co-ordination from O,O to N,O,O chelation as discussed previously. This is also noted in Mohan and Abbotts stability constant data [185], where the order for ML complexes is very different from that for MHL complexes, and similar to the more typical Irving – Williams order of Mn<Fe<Co<Ni<Cu>Zn [181,182]. If this is the case, one would expect the retention order on APAS to continue changing with pH until the Irving – Williams order is obtained. Referring again to Figure 3.3, the change in retention sequence is very noticeable as pH 4 is reached, and indeed appears to be moving towards the Irving – Williams order. The curve for Mn(II) is much shallower and has already been overtaken by Cu(II), Pb(II) and Cd(II). Zn(II), Ni(II) and Co(II) are increasing very steeply, and look as though they also will overtake Mn(II) and Cd(II) at higher pH. Likewise, the Mg(II) curve, shallower than the Co(II) and Ni(II) curves, is overtaken and becomes the most weakly retained metal ion at pH 4, with the exception of the other alkaline earth metals. Unfortunately, measurement

of retention times above pH 4 was not practical, except for the alkaline earth metals, as elution times became extremely long and peaks far too broad.

The retention behaviour of metal ions on APAS at low pH has an important bearing on its applicability to HPCIC determinations. The chromatogram in Figure 3.9 illustrates the high selectivity for Mn(II) at pH 1, eluting last after Cu(II) on the 250mm column. The small differences in selectivity coefficients under acidic conditions also means that high performance separations of a relatively large group of metal ions are possible without gradient elution, using the 250mm column. This is illustrated by the chromatogram in Figure 3.10, showing the high efficiency separation of eight metal ions at pH 2.3, with Cu(II) eluting last. Figure 3.11 shows the separation of four alkaline earth metals at pH 5. This figure emphasises the concept of inter- and intragroup selectivity on chelating phases. APAS shows a very high selectivity between the alkaline earth group and the +2 transition and heavy metal group at high pH, while still achieving good resolution between individual members of each group at selected pH values.

With chelation ion – exchange interactions dominant even in low ionic strength solutions, a short study examining the retention of metal ions in an eluent of 0.5M KNO₃ was undertaken. Solution viscosity can interfere with column efficiency by affecting the mass transfer of solute ions diffusing into the stationary phase, and thus the velocity of solute elution. Decreasing the ionic strength and therefore the eluent viscosity should ensure metal ions elute earlier with sharper peaks.

The k' vs. pH plot for selected transition metal ions in an eluent of 0.5M ionic strength is given in Figure 3.12. The general S-shaped trend is followed, but the slopes appear more shallow with an increase in pH. Another dissimilarity is the noticeable absence in a crossover between Cd(II) and Pb(II) over the pH range investigated. At 1M ionic strength, Pb(II) elutes before Cd(II) at high eluent acidity, becoming more strongly retained above pH 2.5. At 0.5M ionic strength, however, Pb(II) is more strongly retained over the pH range 1 – 3.5. Whether this anomaly is associated with solution viscosity or ionic strength

effect on the mode of chelation is unclear. The other transition metals, however, elute as observed with a 1M ionic strength mobile phase. The separation of 8 metal ions, at pH 2.3 in 0.5M KNO₃, illustrating the change in elution for Cd(II) and Pb(II), is given in Figure 3.13. Column efficiency measurements (Table 3.3) showed that there was not any significant advantage in reducing the ionic strength, other than to change the selectivity coefficients for Cd(II) and Pb(II). The peak asymmetry of the Cu(II) peak was similar at each ionic strength also, being 4.71 at 0.5M KNO₃ and 4.79 at 1M KNO₃ (a symmetrical peak has a value of 0).

Table 3.3 Column efficiency (N) on the APAS substrate at 0.5 and 1M KNO₃ (pH 2.3)

LS. /Molar	Ba(II)	Zn(II)	Mn(II)	Cu(II)
0.5	878	852	816	477
1	784	843	803	437

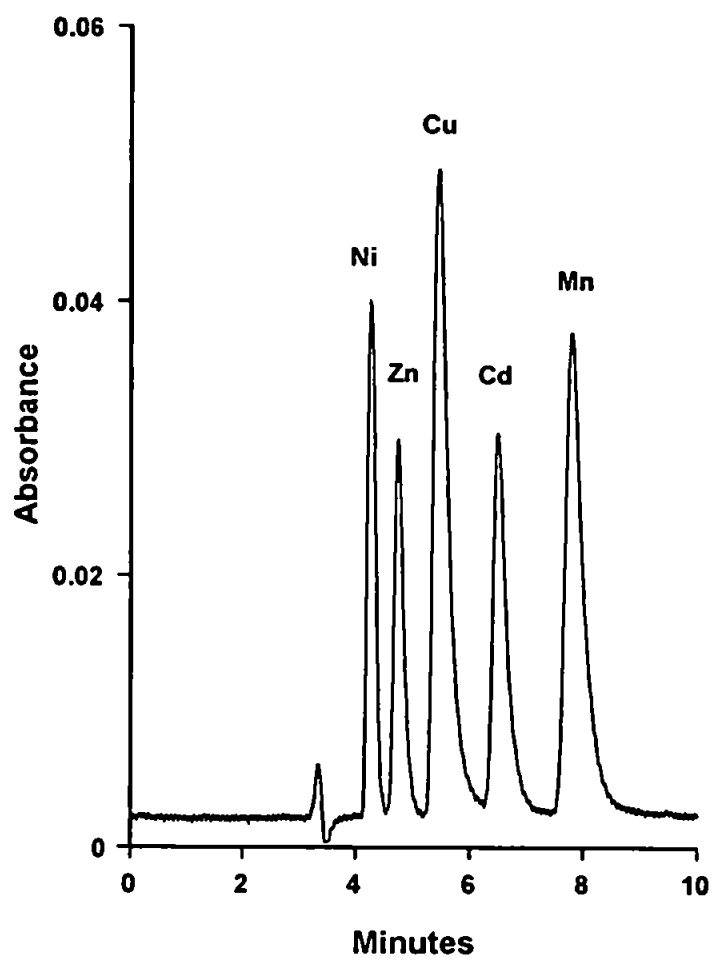


Figure 3.9. Separation of Ni(II) 1mg l^{-1} , Zn(II) 2mg l^{-1} , Cu(II) 1mg l^{-1} , Cd(II) 1mg l^{-1} and Mn(II) 1mg l^{-1} on the 250mm \cdot 4.6mm APAS column. Eluent: 1M KNO_3 100mM HNO_3 (pH 1). Detection: PAR at 490nm.

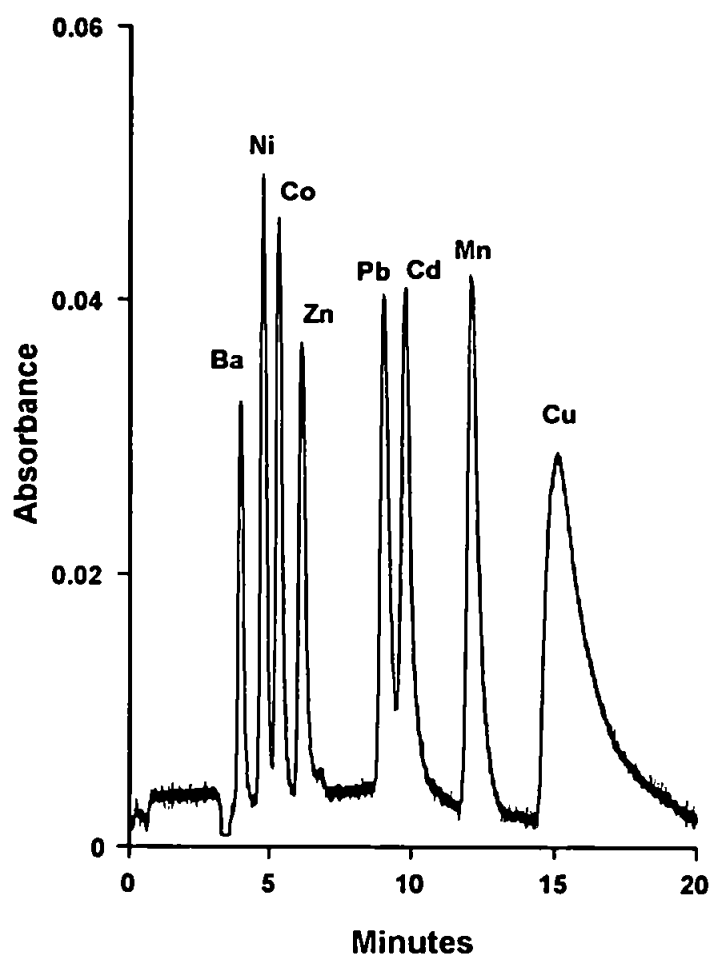


Figure 3.10. Separation of Ba(II) 1.5mg l^{-1} , Ni(II) 1mg l^{-1} , Co(II) 2mg l^{-1} , Zn(II) 1mg l^{-1} , Pb(II) 5mg l^{-1} , Cd(II) 2.5mg l^{-1} , Mn(II) 1.5mg l^{-1} and Cu(II) 5mg l^{-1} , on the $250 \cdot 4.6\text{mm}$ APAS column. Eluent: 1M KNO_3 5mM HNO_3 (pH 2.3). Detection: PAR / Zn-EDTA at 490nm .

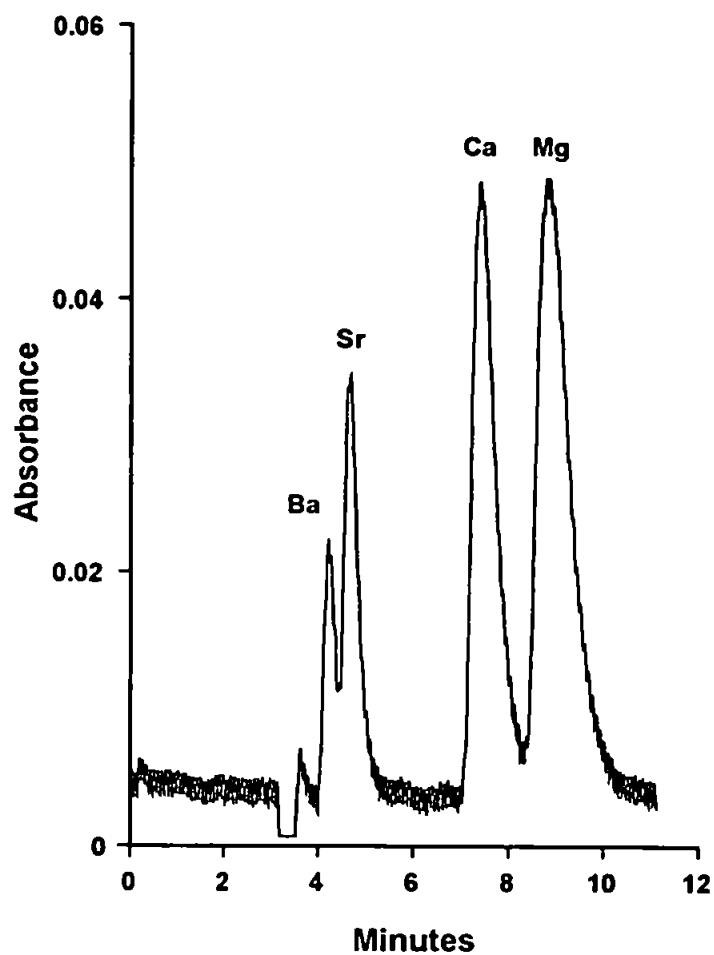


Figure 3.11. Separation of Ba(II) 1 mg l^{-1} , Sr(II) 1 mg l^{-1} , Ca(II) 1 mg l^{-1} and Mg(II) 1 mg l^{-1} on the $250 \times 4.6\text{ mm}$ APAS column. Eluent: 1 M KNO_3 at pH 5. Detection: PAR / Zn-EDTA at 490nm.

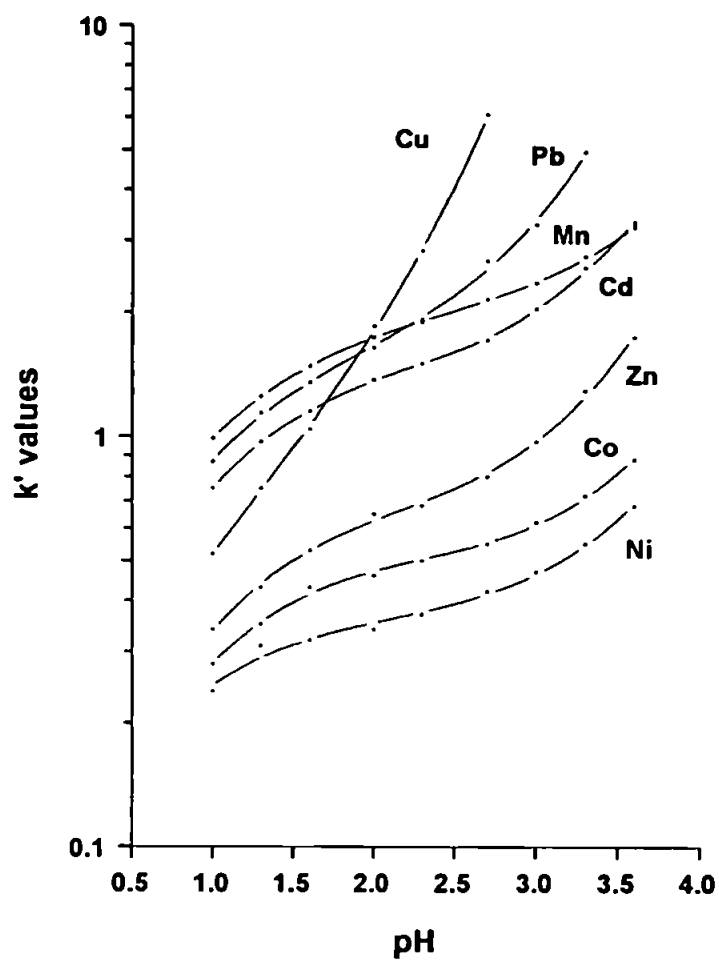


Figure 3.12. The dependence of capacity factors for transition metals on eluent pH, with the APAS column. Eluent: 0.5M KNO_3 adjusted to the appropriate pH with HNO_3 .

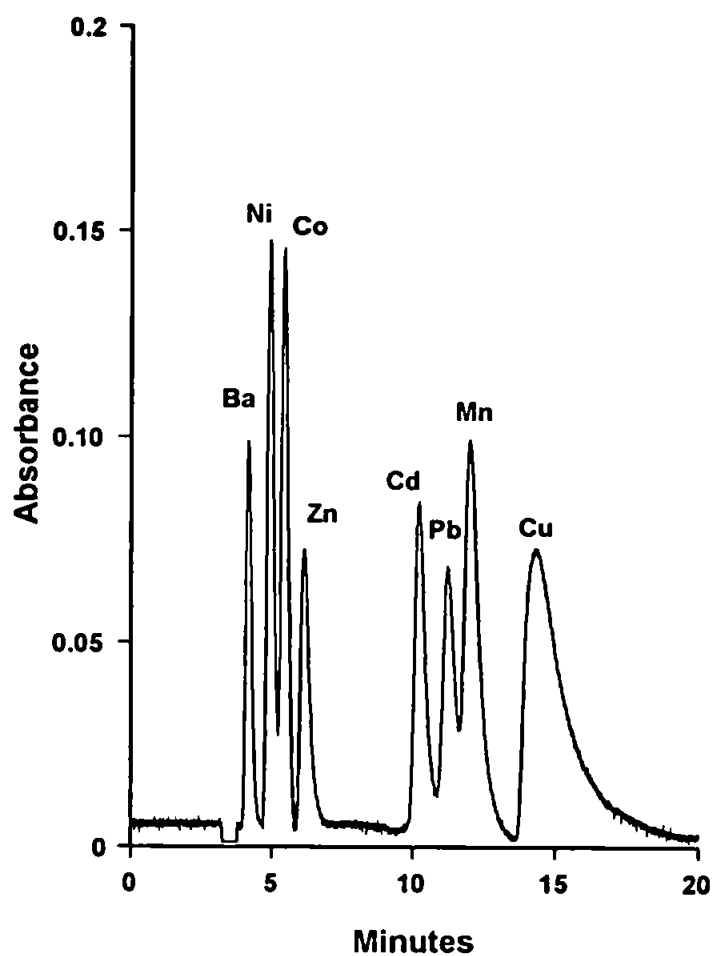


Figure 3.13. Separation of Ba(II) 1.5mg l^{-1} , Ni(II) 1mg l^{-1} , Co(II) 2mg l^{-1} , Zn(II) 1mg l^{-1} , Pb(II) 5mg l^{-1} , Cd(II) 2.5mg l^{-1} , Mn(II) 1.5mg l^{-1} and Cu(II) 5mg l^{-1} , on the $250 \times 4.6\text{mm}$ APAS column. Eluent: 0.5M KNO_3 5mM HNO_3 (pH 2.3). Detection: PAR / Zn-EDTA at 490nm.

3.3.3 Phenylphosphonic Acid Column Selectivity

To attribute the influence of the amino nitrogen on the chelation of metal ions by APAS experimentally, a 150mm phenylphosphonic acid functionalised silica column (PPAS) was investigated. On this substrate, metals can only bind with oxygen atoms on the phosphonate group (O,O). Phosphonic acid is a weak acid, and a high pH is required to dissociate the hydroxyl groups. It was postulated that this molecule would be more weakly chelating in acidic media than APAS, which contains mixed base character with its hard oxygen atoms and soft nitrogen. Nitrogen is de-protonated in weak acid solutions, allowing APAS to chelate metals within this pH region.

In an eluent of 1M KNO₃ 50mM acetic acid, all the transition metal ions investigated, namely Mn(II), Pb(II), Cd(II), Zn(II), Ni(II), Co(II) and Cu(II), remained virtually un-retained over the pH range 1.5 – 5.3. Only a slight retention of Pb(II) (k' 0.6) and Cu(II) (k' 0.4) was achieved at pH 5.3, indicative that the phosphonate group has only a weak complexing character in the absence of the amino group in the acidic pH range. It was, however, unclear as to whether the column capacity was low, which would influence the retention of metal ions, as discussed in Section 2.3.7.2, Chapter 2. Due to the poor retention of Cu(II), a capacity measurement was not made. Retention of lanthanide ions was also very poor on this column, with k' values of 0.4 for La(III) and 1.4 for Lu(III) at pH 3.5. There was, however, complexation with Fe(III) (k' 8.8) and UO₂²⁺ (k' 1.6) at pH 1.5, both peaks broad, signifying that the PPAS substrate demonstrated some chelating properties. A tentative elution order on this column, with 1M ionic strength, was Fe(III)<U(VI)<Lu(III)<La(III)<+2 metals at pH 1.5, and Pb(II)<Zn(II)<Cu(II)<Cd(II)<Mn(II)<Ni(II), Co(II) at pH 5.3.

On the assumption that column capacity was low, the ionic strength was reduced to 100mM KNO₃, to determine whether a limited suppression of ion – exchange interactions would benefit the retention of metal ions on the phosphonate ligand. At pH 3.5, however, all the transition metals still eluted on the solvent front, with only a weak retention of La(III) (k' 0.5) and Lu(III) (k' 1.2). To estimate whether sufficient phenylphosphonic acid groups had bonded to the silica matrix, the ion – exchange properties of this substrate were examined, using the alkali metal ions. The retention of these metals could be compared with data achieved on untreated silica, retention in this case due predominantly to reactive silanol groups ($-\text{Si}-\text{O}^-\text{H}^+$). A k' vs pH plot for Na⁺ on untreated silica is given in a book by Lederer [188]. The k' vs. pH plots for K⁺, Na⁺ and Li⁺ on the PPAS column are given in figure 3.14. It would appear that retention is due to the phenylphosphonate ligand, in comparison with the k' plot for Na⁺ given in [188]. On untreated silica, Na⁺ is not retained below pH 6, whereas on the PPAS substrate, retention of this metal was achieved at pH 2.8. A separation of these three metals was possible at pH 3.4, illustrated in Figure 3.15.

It would, therefore, appear from these preliminary findings, that the phosphonate group has only a weak complexing character in acid solutions, due to having only hard oxygen donor atoms. The chelating strength at low pH would improve with an increase in basicity derived from addition of an amino group, as witnessed with APAS. Other factors should be considered, however, most notably the unknown capacity of the column, which would considerably influence the retention of metal ions. Ideally, another batch of PPAS should be synthesised, and fully evaluated to determine its capacity, prior to investigating its metal retention properties.

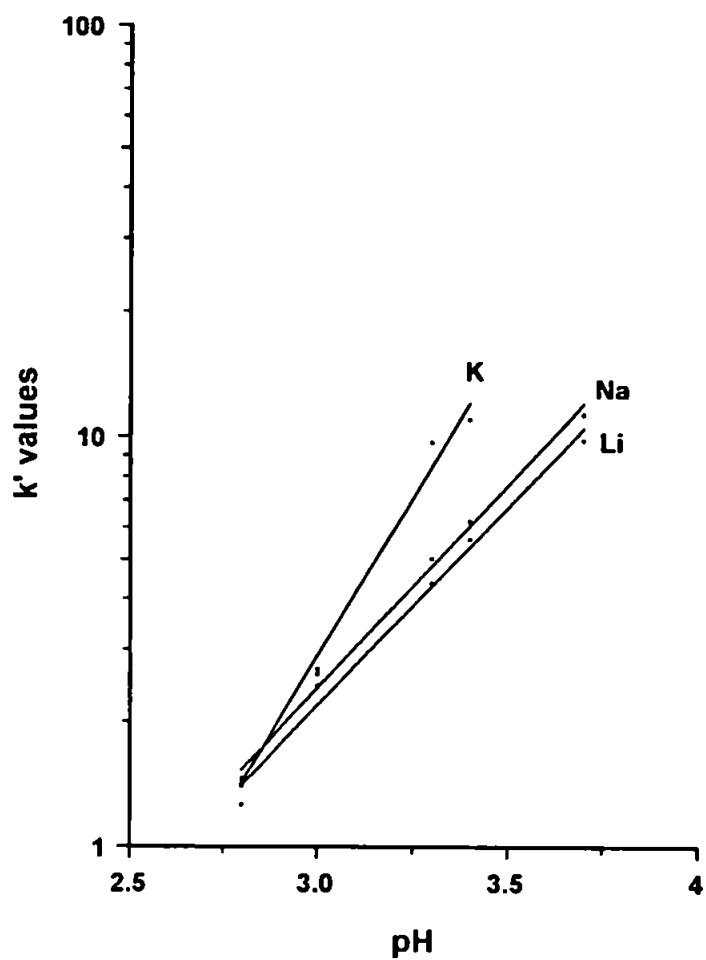


Figure 3.14. The dependence of capacity factors on eluent pH for selected alkali metals on the PPAS column. Eluent: Milli-Q water adjusted to the appropriate pH with HNO₃.

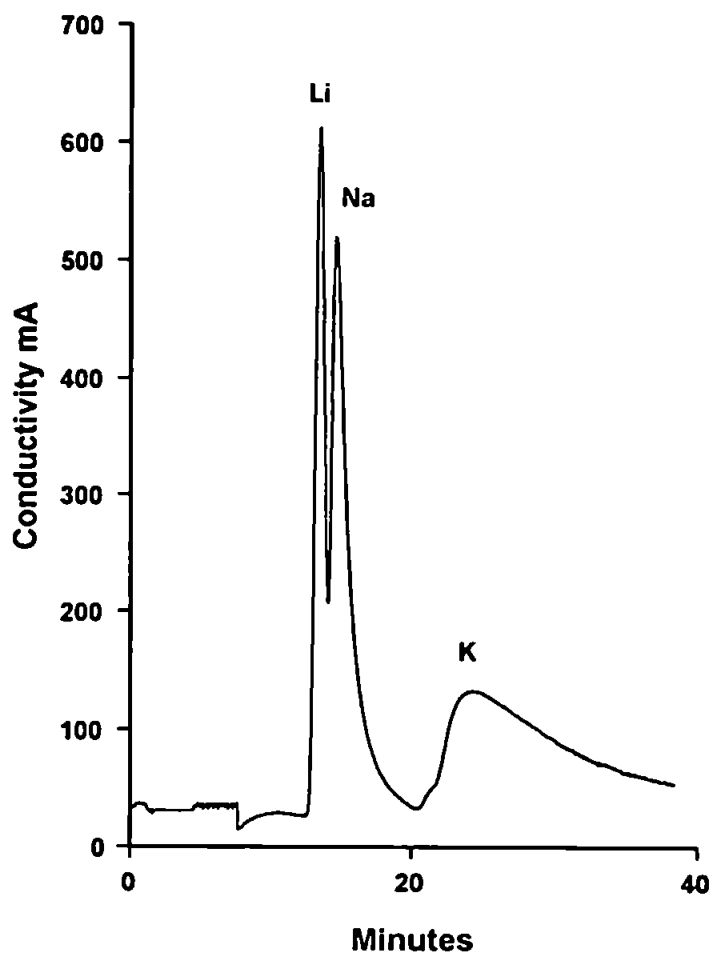


Figure 3.15. Separation of Li(I) 1mg l^{-1} , Na(I) 5mg l^{-1} and K(I) 30mg l^{-1} on the 150 · 4.6mm PPAS column. Eluent: 0.4mM HNO_3 (pH 3.4). Detection: Conductometric.

3.4 Summary

This study has shown that aminophosphonic acid bonded to silica is potentially a more efficient and versatile phase than IDA based substrates. The kinetics of complexation for metal ions are as good as achieved with IDA, and the more closely spaced selectivity coefficients under acidic conditions allow the high efficiency isocratic separation of a greater number of metals in a reasonable time, notably the separation of eight metal species in under 16 minutes. The ability to separate transition and heavy metal ions at low pH makes APAS particularly suitable for the analysis of samples prepared by acid digestion or fusion, where ionic strength is also likely to be high. The intergroup selectivity is significantly improved also with increasing pH. At low pH, however, Mg(II) and Ca(II) interfere with the early eluting transition metals, namely Co(II) and Ni(II), necessitating the requirement for a one step pH gradient, if these metals are to be determined in samples containing high concentrations of alkaline earth metals. Low concentrations of Mg(II) and Ca(II) would not constitute a problem due to their poor sensitivity with PAR detection. The chelating ability of the phenylphosphonate group cannot be fully resolved without further study, though preliminary findings indicate that this ligand has an expected weak complexing nature in acid solutions, though this could be partially attributed to a low capacity.

The APAS column additionally demonstrated a very strong affinity for the alkaline earth metal Be(II), which formed the basis of the next chapter. Further studies were also undertaken to assess the retention of various trivalent metal ions on this column, the results being reported in Chapter 4.

Chapter 4. The Determination of Trace Beryllium in a Stream Sediment.

4.1 Introduction

Beryllium, Be(II), is a group IIa alkaline earth metal, with atomic number 4, atomic mass 9.013, ionic radius 0.031nm and a density of 1.85g cm^{-3} [189]. It has the lowest atomic number and density of any metal that is stable in the air. This element is as electronegative as Al(III), and therefore, easily forms covalent compounds. The Be^{2+} ion, although too highly polarised to exist singly in an ionic lattice, can form the aquo ion $[\text{Be}(\text{H}_2\text{O})_4]^{2+}$, which functions as a Lewis acid in strongly acidic solutions [15].

The Be(II) content of the earth's crust is estimated at $2\text{-}3.5\ \mu\text{g g}^{-1}$, widely dispersed in common rock-forming minerals because of its ability to replace silicon, which has a similar ionic radius (0.041nm). One of the few mineral ores in which Be(II) is a major component is Beryl ($\text{Be}_3\text{Al}_2\text{Si}_6\text{O}_{18}$). Water contains very little Be(II) due to clay mineral capture during rock weathering and adsorption onto mineral grain surfaces during soil formation. The content in the open ocean is only about $0.0002\ \mu\text{g l}^{-1}$ in the form of $\text{Be}(\text{OH})^+$ and $\text{Be}(\text{OH})_2$ [189]. In surface waters, concentrations are usually about $0.01 - 1\ \mu\text{g l}^{-1}$ [190].

The low abundance of this metal in the earth's crust poses no environmental concern, but release from anthropogenic sources can cause problems. Beryllium is used as a hardening agent in alloys, as a moderator in atomic energy reactors and as a compact fuel element for rockets. It is also released by the combustion of coal, which was the original route for Be(II) to enter the environment.

Unfortunately, Be(II) is an exceedingly toxic metal [15]. It is known to cause mutagenic and carcinogenic illnesses, through its binding to specific regulatory proteins in cells and subsequent accumulation in mammalian tissues. Inhalation of this element can lead to beryllosis, a serious disease of the lungs, which can be fatal.

The continued use of this toxic element and its compounds by the nuclear, aerospace and metallurgical industries, its emission during the combustion of fossil fuels and its release into the aquatic environment by acidification of lakes and streams, has therefore led to a requirement for analytical methods suitable for the determination of this trace metal in environmental samples.

Many techniques have been developed for the determination of beryllium at low concentrations, including spectrophotometry [191-194] and fluorimetry [195,196], flow – injection [197,198], ion - selective electrode [199] and X-ray microanalysis [200]. From the literature, atomic spectrometry appears to be the method of choice, because of its simplicity and potential for high sensitivity and accuracy. Trace and ultra – trace Be(II) has been determined in many environmental matrices using atomic absorption spectrometry (AAS) [190,201-208] and inductively - coupled plasma atomic emission spectrometry [209,210]. Nevertheless, complex samples can cause matrix interferences that require preconcentration and/or separation steps to be incorporated into the analysis.

In contrast, there are very few methods available for the determination of Be(II) by liquid chromatography. Shoupu *et al* [211], used reverse - phase HPLC with a C₁₈ silica stationary phase and buffered methanol:water eluent to determine Be(II) in water, rice, flour and human hair samples as a chromotrope 2C chelate. Ion chromatographic techniques have also been developed. Kondratjonok and Schwedt [212], used a polybutadiene – maleic acid coated silica column and a citric acid / dipicolinic acid eluent to determine Be(II) and other cations in drinking water and wine samples, with conductivity detection. Betti and Cavalli [213], used an Ionpac CS3 column (Dionex) and a HCl eluent to determine Be(II) in sediment and water samples, with spectrophotometric detection. Sulimanov *et al* [214], developed an IC procedure to separate Be²⁺ and BeOH⁺ using a carboxyl cation exchanger and HNO₃ mobile phase, BeOH⁺ eluting first. Recently, Takaya used micellar electrokinetic chromatography to separate and determine Be(II) in airborne dust using a sodium dodecyl sulfate buffer [215].

Unfortunately, many chromatographic techniques also suffer from the problems associated with complex samples. As already stated, however, these matrix problems can often be overcome using high performance chelation ion chromatography.

An earlier paper detailing the determination of Be(II) in environmental matrices using HPCIC is given by Voloschick *et al* [216]. The method incorporated a chelating iminodiacetate sorbent together with an acidified complexing eluent containing dipicolinic acid with direct conductimetric detection. However, the selectivity of this chromatographic system was not too high, and Be(II) eluted just after the alkaline earth metals, restricting the variety of possible samples for analysis.

Initial studies undertaken on a 50mm column found that Be(II) was strongly retained on the APAS substrate. The ability of the aminophosphonate functional groups to serve as an O,O ligand, a type favoured by small highly charged metal ions, potentially makes APAS a useful and versatile new phase for the HPCIC of Be(II).

The aim of this study was to continue studies into the retention behaviour of selected metals on APAS using a high ionic strength eluent with varying pH, and subsequently develop a method for the determination of Be(II) in a certified stream sediment.

4.2. Experimental

4.2.1 Instrumentation

The HPCIC system used throughout these studies is described in section 2.2.1, with the exception that column length was 50 · 4.6mm I.D.

4.2.2. Reagents

The optimised post-column reagent (PCR) used in this study was a mixture of 0.008% Chrome Azurol-S (CAS), 1M hexamine and 10mM ethylenediaminetetraacetic acid (EDTA) buffered at pH 6, detection being achieved at 560nm. A 1M KNO₃, 0.5M HNO₃ and 0.08M ascorbic acid solution was used as the eluent. Both the eluent and PCR were delivered at 1ml min⁻¹.

All reagents were of AnalaR grade (BDH, Poole, U.K), with the exception of CAS (65% dye content) (Aldrich, Gillingham, U.K).

1000mg l⁻¹ metal stock solutions (BDH) were diluted to working standards using distilled deionised water (Milli-Q, Millipore, Milford, MA, U.S.A), and stored in poly-(propylene) bottles (BDH).

4.2.3 Sample pre-treatment

The certified sediment sample, GBW07311 (National Research Centre Certified Reference Material) was obtained from LGC, Middlesex, UK.

The sample was prepared using sodium hydroxide fusion. From a previous study [217], and our own investigations, HF digestion with borate addition is not suitable for the

determination of Be(II) by IC, due to the formation of a stable beryllium fluoride complex which elutes early.

For the fusion procedure, a known amount of accurately weighed sample (0.5g) was added to a nickel crucible (BDH) in which 5g of NaOH (Aristar, BDH) had been fused and allowed to cool. The crucible was heated to fusion and a temperature of about 500°C maintained for 45 minutes, after which it was ice-cooled. The fusion melt was treated with ice cooled Milli-Q water and transferred to a volumetric flask. Sufficient nitric acid was added to attain approximately 0.5M after neutralisation of the alkali and final dilution to 50ml.

4.3 Results and Discussion

4.3.1 Choice of Chelating Column

A short investigation was undertaken to assess the retention of Be(II) on the dye loaded chelating columns studied in Chapter 2. Be(II) displays hard acid characteristics due to its small highly charged nature, and should, therefore, complex most strongly with ligands containing a hard base donor atom, such as oxygen.

As anticipated, this expected outcome was realised. Using a mobile phase of 1M KNO₃ 1mM HNO₃ (pH 3), Be(II) was not retained on any of the N,O containing chelating dye columns *viz.* PAR, CAL and CPC, which display both soft and hard character in weak acid solutions. In contrast, this metal was retained on the O,O ligating ATA column, resulting in a *k'* value of 1.7 at pH 3. The chromatogram of Be(II) on the 100mm ATA column at pH 3 is given in Figure 4.1, and shows that it is quite broad with tailing.

The retention of Be(II) on the APAS substrate, however, was far greater than with the ATA column at an equivalent pH. This should improve its separation from large

concentrations of matrix metals present in many environmental matrices. It was therefore decided to continue studies into the determination of this metal in environmental samples using the aminophosphonate bound silica column.

4.3.2 Retention Characteristics and Selectivity of Be(II) and Selected Trivalent Metal Ions on APAS.

As already discussed in Chapter 3, the aminomethylphosphonic acid group has a number of chelating possibilities. At low pH the acidic P-OH groups would be the principal chelating ligands, whilst at higher pH the basic amino nitrogen could become additionally involved. However, APAS can also act as a cation exchanger in weak acid or neutral solutions through dissociation of its phosphonic groups [179]. This is the reason why a high concentration of KNO_3 was used within the mobile phase, to suppress any retention that may arise due to simple ion exchange and ensure that 'chelation exchange' was the dominant retention mechanism.

A detailed study of the retention of Be(II) on APAS was carried out, and the $\log k'$ vs. pH plot shown as Figure 4.2, follows the same trend for the other group IIa alkaline earth metals investigated in the previous chapter, in that an S-shaped dependence was observed. As Be(II) has a greater affinity for oxygen than for nitrogen, with the stability of complexes containing N,O ligands being lower than those of O,O donors [103,218], this change in the curve is probably due to the onset of the second acid dissociation step of the methylphosphonic acid group on APAS, which occurs in the pH range 2 – 3. It is proposed that this dissociation results in a change in the co-ordination between the phosphonic acid group and the metal, from two oxygen atoms on the phosphonic acid group, to all three.

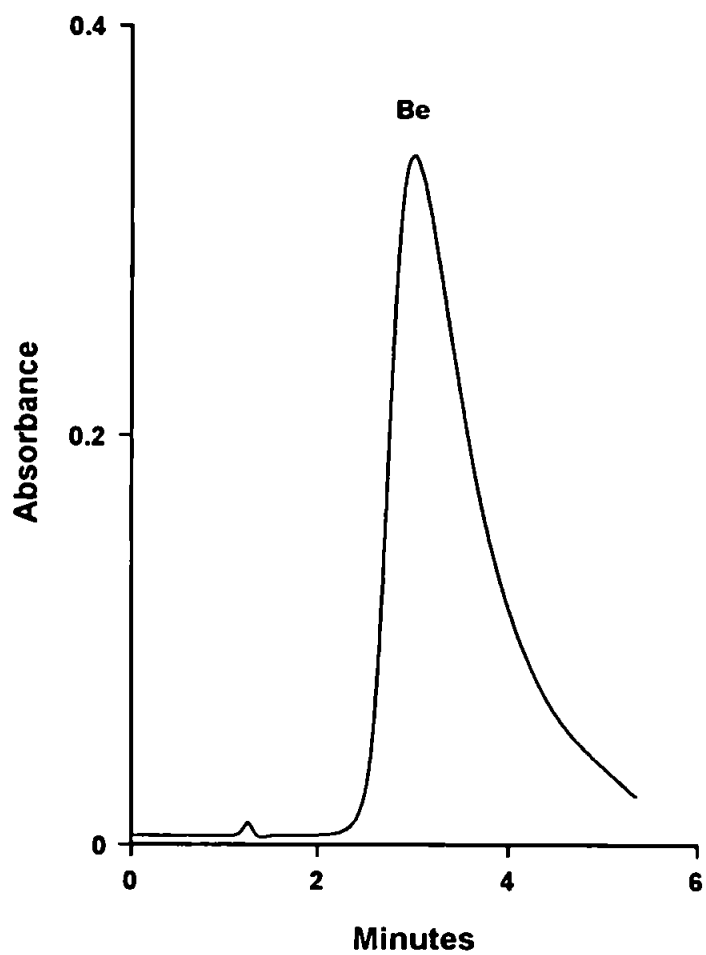


Figure 4.1. Chromatogram of Be(II) 20mg l⁻¹ on the 100 · 4.6mm ATA Column. Eluent: 1M KNO₃ 1mM HNO₃ (pH 3). Detection: CAS at 560nm.

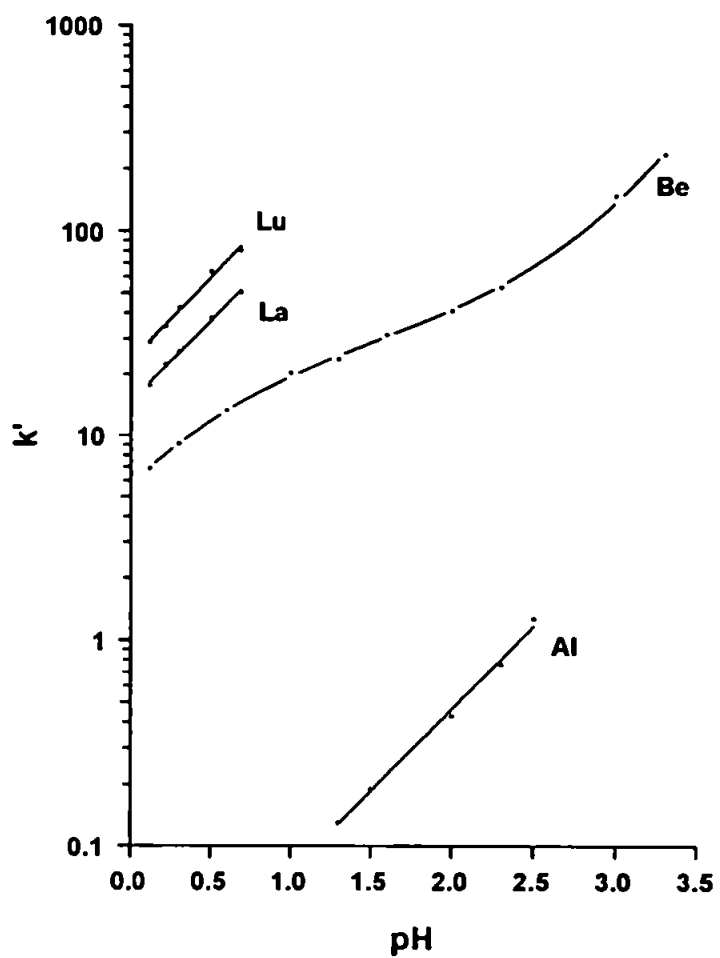


Figure 4.2. Dependence of Capacity Factors on Eluent pH for Be(II), La(III), Lu(III) and Al(III), with the APAS Column. Eluent: 1M KNO_3 adjusted to the required pH with HNO_3 .

This was similarly postulated for the other alkaline earth metals in the previous chapter.

Be(II) is more strongly retained on APAS than the other alkaline earth metals, which could be attributed to its small size and highly charged nature.

When considering the stability constants for metal ions complexing with methylphosphonic acid in homogeneous solution, which should be analogous to the APAS bonded group at low pH, the log stability constant for Be(II) is relatively large compared to other divalent metal ions, as shown in Table 4.1.

Table 4.1. Log Stability Constants of Selected Metals with Methylphosphonic Acid [163]

M^{n+}	K_1	M^{n+}	K_1
Cu^{2+}	3.5	Mn^{2+}	2.48
Ni^{2+}	2.25	Co^{2+}	2.24
Zn^{2+}	2.6	Be^{2+}	6.3
Cd^{2+}	2.9	Fe^{3+}	9.05

This finding is reflected in the Be^{2+} ion behaviour on APAS, giving a much stronger retention than all the +2 metal ions, including Cu(II), which is normally the most strongly retained.

The trivalent metals would be expected to show a stronger affinity for APAS compared to the divalent ions including Be(II), but interestingly, as shown in Figure 4.2, although the lanthanides show the expected increase in affinity, Al(III) is rather weakly retained. This could be due to the fact that the very small size of the Al(III) ion does not allow a 'good fit' into the rather rigid structure of the P-O bonds of the phosphonate group. Fe(III), has a much larger log K_1 value than Be(II) (Table 4.1), which reflects the special affinity of ferric ions for P-O bonds. This strong interaction of Fe(III) for the APAS substrate at low pH was proven experimentally, using a PCV PCR at 580nm (detailed in section 2.2.2). No Fe(III) peak was seen using the 50 · 4.6mm column, therefore a small 15 4.6mm

column was packed with APAS. Even in an eluent of 1M KNO₃, 1M HNO₃, a peak for Fe(III) (50 mg l⁻¹) was not seen, instead a rising baseline occurred. A similar pattern emerged for UO₂²⁺ (50 mg l⁻¹) on this small column. Using the same eluent conditions, this metal was not eluted as a visible peak after 100 minutes, using an Arsenazo III PCR (0.15mM in 62mM acetic acid) with detection at 658nm. It would appear, therefore, that U(VI) also has a very strong affinity for the APAS substrate.

A rather unexpected characteristic of beryllium retention on APAS is the peak shape.

Virtually all studies involving HPCIC show peak shapes that are quite sharp close to the solvent front, but rapidly broaden with increase in retention time. This phenomenon has been termed 'kinetic broadening'. The rapid broadening is as a result of slower kinetics of dissociation of the metal complexes on the chelating substrate as conditional stability constants increase. Furthermore, the increase in broadening is accompanied by an increase in peak asymmetry. However, for beryllium, the peak shape does not show this trend. Firstly, the peak is broader than normal at short retention times and doesn't broaden too drastically with increase in retention time and secondly, good peak symmetry is maintained regardless of the retention time, with a peak asymmetry measurement of 0 at both 750mM and 5mM HNO₃ concentration in the eluent. These characteristics are surprising and difficult to explain from the thermodynamic and kinetic properties of complex formation and dissociation. The Be(II) peak shape as a function of eluent pH is shown in Figure 4.3.

4.3.3 Method Development

4.3.3.1 Effect of Sample Ionic Strength on Metal Retention Characteristics

A short study was undertaken to determine whether the ionic strength of the sample would have an effect upon the metal retention characteristics. This was investigated through the injection of a standard transition metal mixture of Ni(II), Zn(II), Cd(II) and Mn(II) prepared in solutions of widely varying ionic strength, at pH 2.3. The resultant overlaid chromatograms of the metal mixture in deionised water and 2 M KNO₃, as illustrated in Figure 4.4, show that the retention times for each metal remain virtually unchanged in spite of a massive change in ionic strength. In addition, peak broadening does not appear to occur, with each metal peak remaining sharp and fully resolved. This result is a good example illustrating the insensitivity of HPCIC to large changes in ionic strength and also indicates that any possible simple ion exchange interaction is strongly suppressed.

4.3.3.2 Separation Conditions

As discussed previously, the special selectivity of APAS for Be(II) means that the peak should be well separated from other divalent metal ions. When considering sediment samples, however, there will also be large amounts of Al(III) and Fe(III) after digestion. Figure 4.2 shows that Be(II) should be completely separated from Al(III) as it is essentially unretained at low pH. The main problem is the presence of Fe(III). It is very strongly

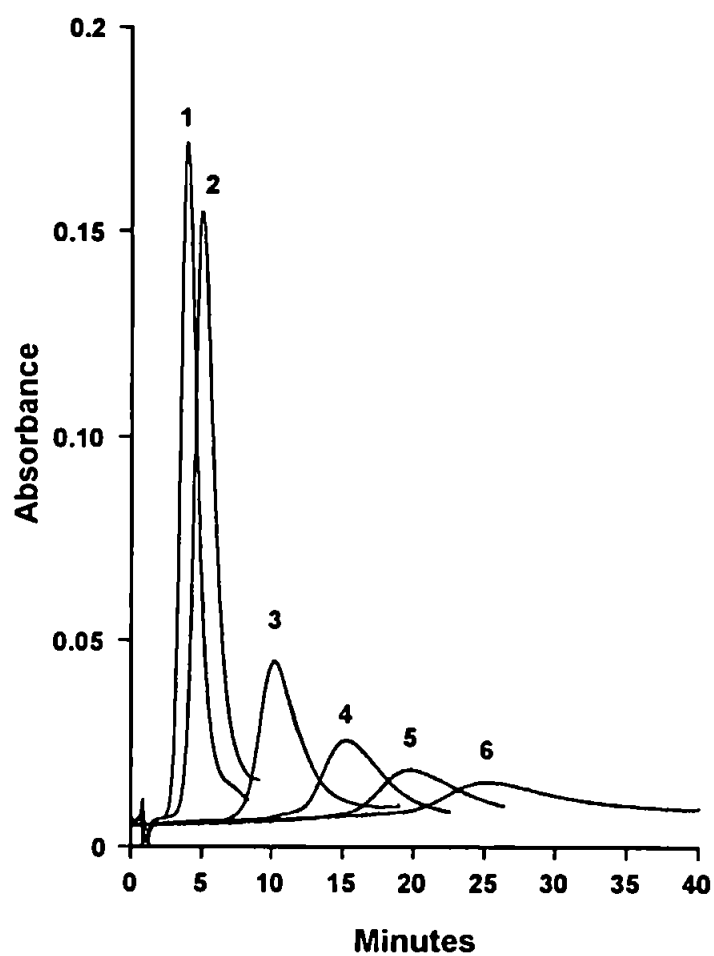


Figure 4.3. Effect of Eluent pH on the Be(II) (10mg l^{-1}) Peak Shape with the $50 \cdot 4.6\text{mm}$ APAS Column. Eluent: 1M KNO_3 adjusted to the required pH with HNO_3 (1: 750mM , 2: 500mM , 3: 100mM , 4: 25mM , 5: 10mM and 6: 5mM HNO_3). Detection: CAS at 560nm .

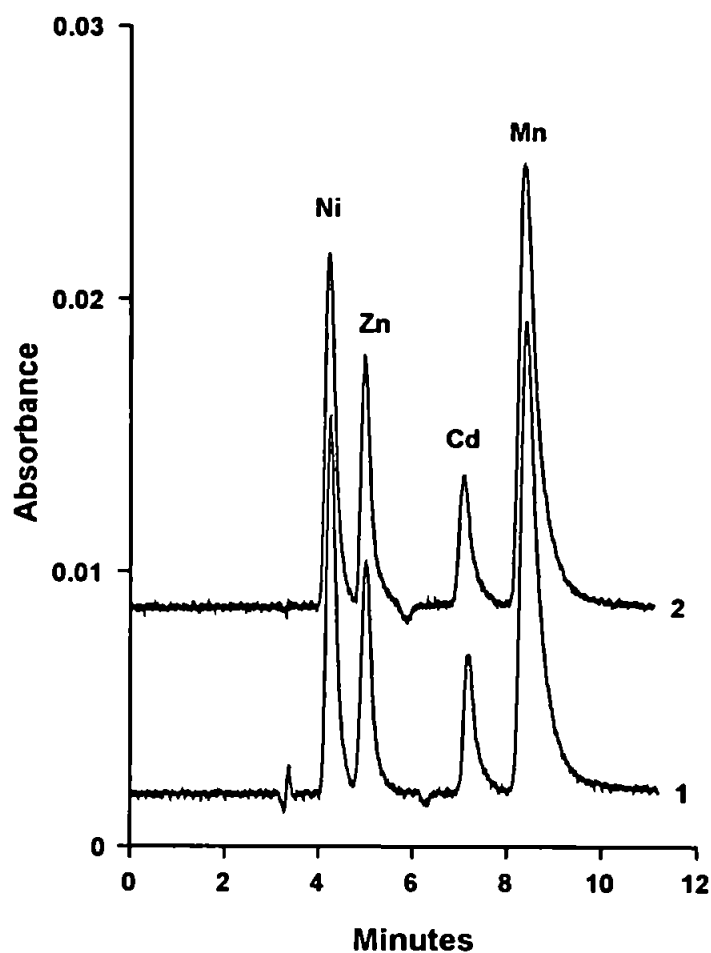


Figure 4.4. The Effect of Sample Ionic Strength: 1: Milli-Q, 2: 2M KNO₃, on the Separation of a Group of Metals, Ni(II) 0.5mg l⁻¹, Zn(II) 0.5mg l⁻¹, Cd(II) 2mg l⁻¹ and Mn(II) 0.5mg l⁻¹ with the 250 · 4.6mm APAS Column. Eluent: 1M KNO₃ 5mM HNO₃. Detection: PAR at 490nm.

retained even at high acidities, eluting slowly from the column giving rising baselines. To solve this problem, ascorbic acid was added to the mobile phase so that any Fe(III) injected with the sample would be reduced to Fe(II) on-column and elute close to the dead volume. Various studies have been undertaken to determine the kinetics and mechanism of Fe(III) reduction by ascorbic acid [219-221]. In aqueous solution, the aquo ion $\text{Fe}(\text{H}_2\text{O})_6^{3+}$ complexes with the oxygen chelating ascorbate ligand (H_2L) in a kinetically fast two step reaction, yielding the divalent complex species illustrated in Figure 4.5. It is the 'bite' distance (~ 0.3 nm) between the co-ordinating oxygen atoms which creates the sterically favourable interaction of ascorbate with Fe(III) [221]. Hseih and Hseih [222], investigated the complexation of Fe(III) by ascorbic acid over the pH range 2.6 – 6. They found that 2 mol Fe(III) was reduced by 1 mol ascorbic acid within this pH range, but that the rate of reduction decreased drastically as the pH was increased. In addition, the ferric ion could only be reduced below a certain pH limit, between pH 6 – 6.8. The addition of EDTA, giving a 1:1 Fe(III): EDTA species, prevented the ascorbic acid complex from forming, thereby Fe(III) was not reduced.

A concentration of 0.08M ascorbic acid was added to the eluent as this had previously been found sufficient to suppress the interference of Fe(III) at a concentration up to 500 mg l^{-1} [109].

An acid concentration in the mobile phase of 0.5M was finally chosen, as this gives a retention time of about 5 minutes for Be(II), ensuring an efficient analysis time. In addition, from results given in this and the previous chapter, the transition and heavy metals, the alkaline earth metals and Al(III) are unretained on the APAS substrate at this pH. The lanthanides, although more strongly retained than Be(II), should not be present in significant amounts and in any case do not react with the post column reagent, CAS [104,223].

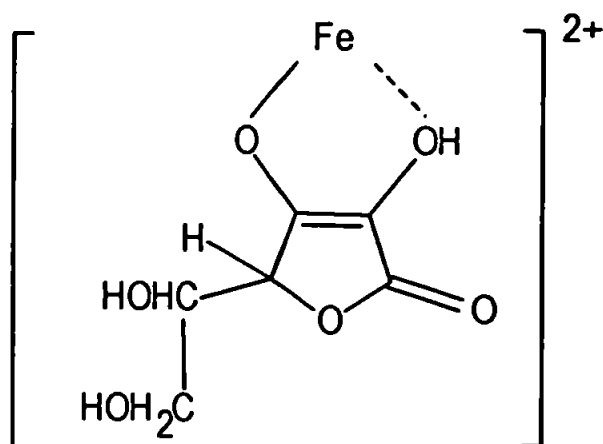


Figure 4.5. Structure of the Ascorbate : Iron(III) Complex [219]

4.3.3.3 Detection Conditions

CAS was chosen as the post column reagent as it is one of the most sensitive chromogenic ligands for the determination of Be(II), forming a 1:1 complex in the pH range 3.5 – 5 [104]. The absorbance spectra for Be(II) with CAS is given in Figure 4.6.

To establish the feasibility of using CAS in this system, a calibration of Be(II) over the concentration range $20\mu\text{g l}^{-1}$ to 5mg l^{-1} was performed. The PCR conditions were 0.008% CAS, 1M hexamine buffered to pH 6, which when combined with an eluent composed of 1M KNO_3 and 0.5M HNO_3 , resulted in an effluent pH of 5.3. The linearity of the system was good with a regression coefficient of $R^2 = 0.9986$ using peak area. The relative standard deviation (RSD) for the repeat injection ($n=6$) of a 1mg l^{-1} working standard was 1.24%, and the detection limit was calculated as $13\mu\text{g l}^{-1}$ using two times the average peak to peak noise.

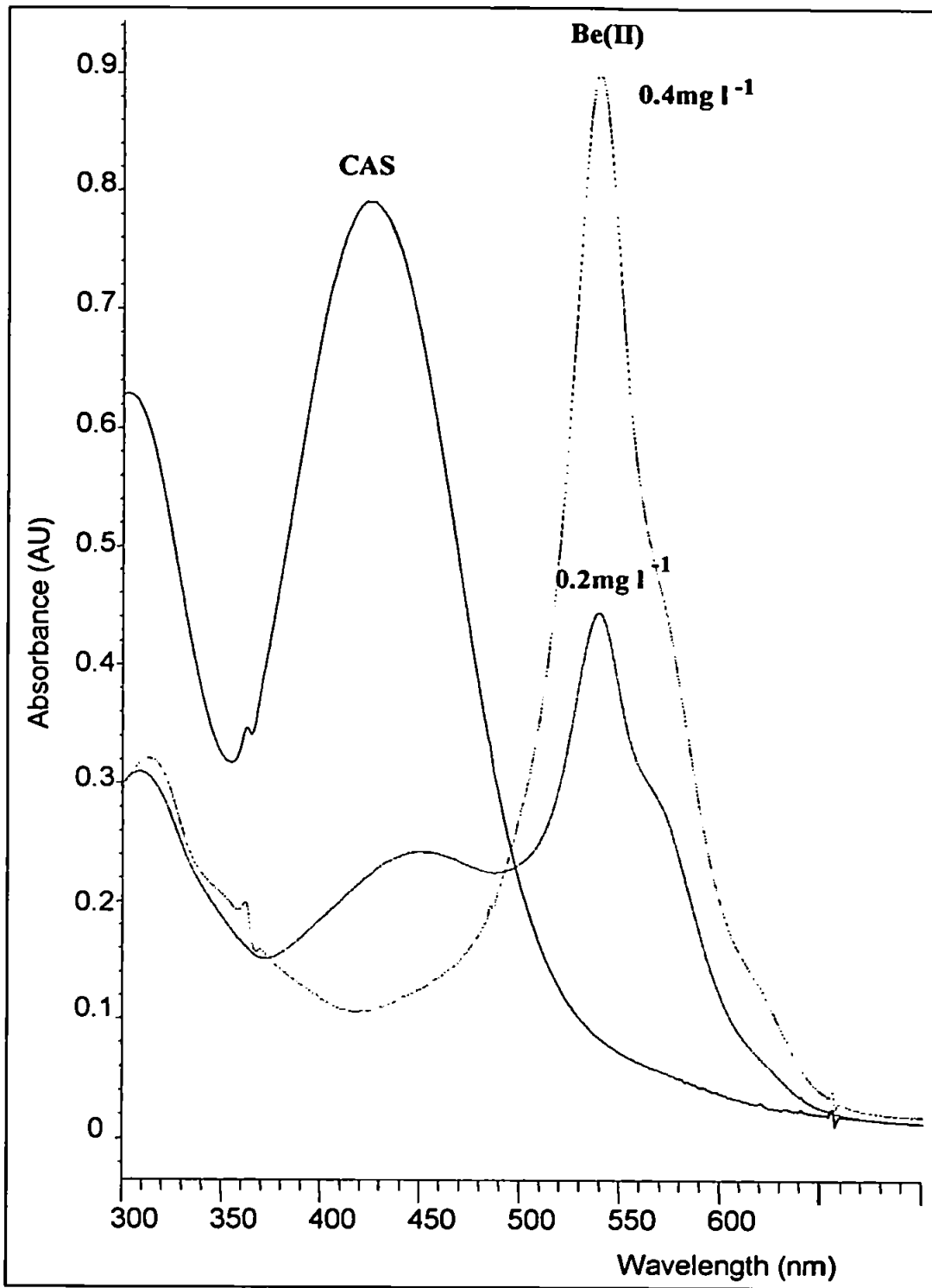


Figure 4.6. Absorbance Spectra for Be(II) with the CAS Post Column Reagent.

In spite of the good selectivity of APAS for Be(II), the very high concentration of metals present in the sample, even after the 100 times dilution during pre-treatment, meant the Be(II) peak became partly obscured with the accumulated massive tailing of these unretained metals. To solve this problem and still allow the sensitive detection of Be(II), EDTA was added to the PCR as a masking agent. EDTA complexes rather weakly with this alkaline earth metal, but much more strongly with those metals reacting with CAS, including Al(III), Fe(III) and Zn(II), due to the mixed soft and hard character of this N,O chelator. The speciation diagram for Be(II) with EDTA is given as Figure 4.7. This illustrates that at the effluent pH of ~5, Be-EDTA complexes have formed in solution, but the free metal percentage is still around 85%. The effect of EDTA concentration in the PCR on the signal for a 1 mg l^{-1} Be(II) sample is shown in Figure 4.8.

Although there is a loss of the Be(II) signal with EDTA present in the PCR, this was offset by the severe reduction in the signal from the unretained matrix metals eluting on the solvent front. Injecting large amounts ($\sim 500\text{ mg l}^{-1}$) of matrix metals into the chromatographic system with Be(II), a concentration of 10mM EDTA in the PCR was found sufficient to reduce the peak and subsequent tailing of a suite of metals which would elute on the solvent front and interfere with the Be(II) peak. At this concentration, in the presence of matrix metals, there was a minimal reduction in detector response for Be(II). A calibration of Be(II) over the range $50\mu\text{g l}^{-1}$ to 5 mg l^{-1} , in the presence of a suite of unretained metals in the proportions as found in the diluted reference material, namely Al(III) 500 mg l^{-1} , Fe(III) 300 mg l^{-1} , Mn(II) 25 mg l^{-1} , Zn(II) 4 mg l^{-1} and Cu(II) 1 mg l^{-1} , resulted in a regression coefficient of $R^2 = 0.9994$ using peak area. The RSD for the repeat injection ($n=6$) of a 1 mg l^{-1} Be(II) standard in the presence of the unretained metal suite (880 mg l^{-1}) was 4.81%. A detection limit of $35\mu\text{g l}^{-1}$ was calculated, using the same method as before. A typical separation of 5 mg l^{-1} Be(II) from the unretained metal suite is shown in Figure 4.9.

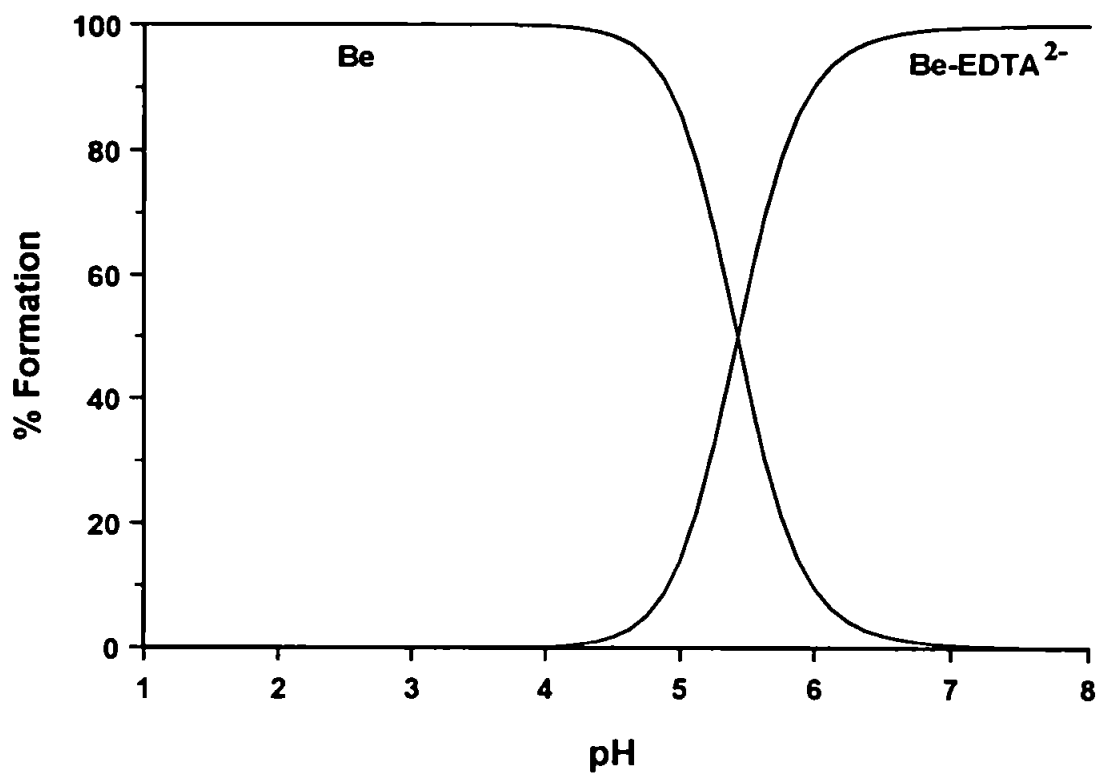


Figure 4.7. Speciation Diagram of Be(II) with EDTA [163]

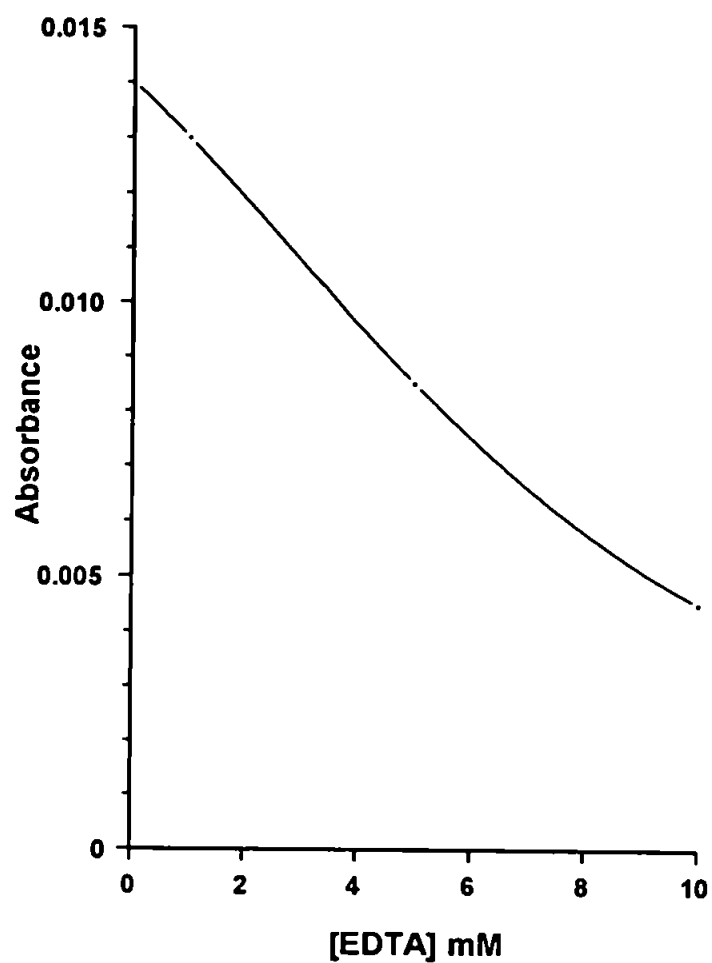


Figure 4.8. Effect of EDTA Concentration in Post Column Reagent (CAS) on Signal for 1 mg l^{-1} Be(II) at 560nm.

The effect of fluoride concentration in the sample on the Be(II) signal was also investigated, as the complex ion $[\text{BeF}_4]^{2-}$ can exist in acid solution. The speciation diagram for Be(II) with F^- is given in Figure 4.10. It is apparent that Be(II) forms a strong complex with excess F^- at low pH, which is why HF digestion was unsuitable to prepare the sample for analysis. From the very poor recovery of Be(II) in samples obtained by HF digestion, a Be(II) peak not visible, it was postulated that $[\text{BeF}_4]^{2-}$ is very stable, and kinetically slow to release Be(II) with competition from the aminophosphonate ligand on the column, thereby this metal would elute unretained with the matrix metals on the solvent front.

The fluoride concentration in the reference material was certified at $1250 \pm 61 \mu\text{g g}^{-1}$, and it was thought that this might also interfere with the Be(II) peak. In the presence of 500mg l^{-1} $[\text{F}^-]$ in the sample, the signal for a 1mg l^{-1} Be(II) standard, under optimum eluent and PCR conditions, was reduced by more than 50%, from $\sim 0.01 \text{AU}$ to $\sim 0.003 \text{AU}$.

At 50mg l^{-1} fluoride concentration in the sample, however, there was no noticeable reduction in the signal for Be(II). Taking into consideration the dilution factor during sample pre-treatment, and the presence of other matrix elements which could possibly complex with the fluoride ion, it was decided that the presence of this halide in the sample as a source of analyte loss would be negligible. However, fluoride levels should be taken into consideration when applying this method to other sample types.

A $200 \mu\text{l}$ loop was briefly investigated to try and improve system sensitivity, but with the increase in dead volume, the Be(II) peak became too broad. This idea was therefore abandoned, with samples analysed using the $100 \mu\text{l}$ injection loop.

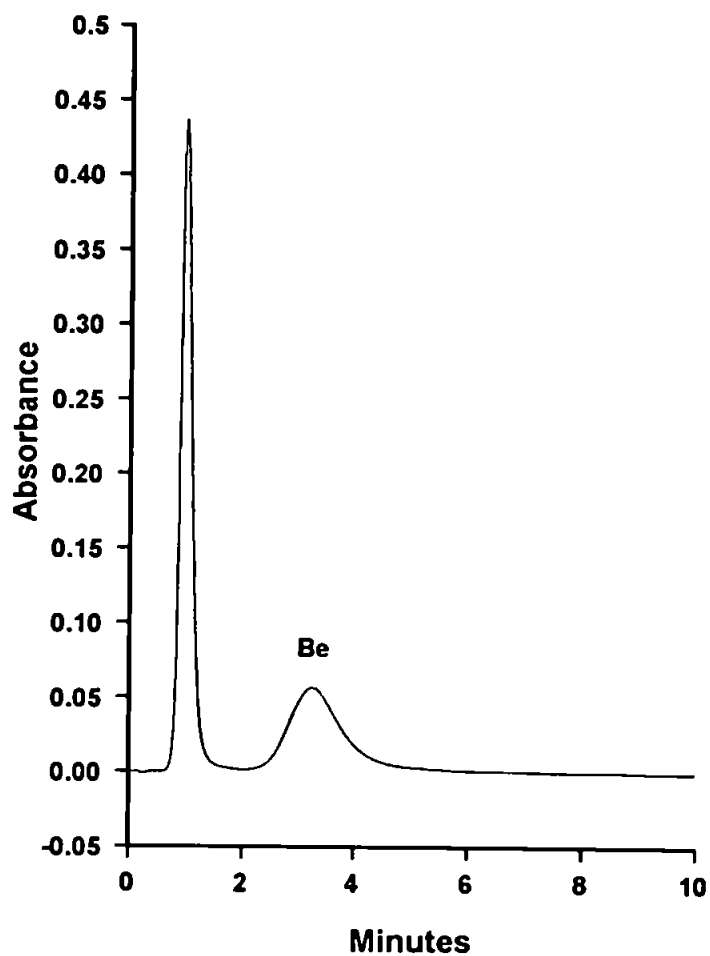


Figure 4.9. Separation of Be(II) 5mg l^{-1} , from Al(III) 500mg l^{-1} , Fe(III) 300mg l^{-1} , Mn(II) 25mg l^{-1} , Zn(II) 4mg l^{-1} and Cu(II) 1mg l^{-1} on the $50 \times 4.6\text{mm}$ APAS Column. Eluent: 1M KNO_3 0.5M HNO_3 and $0.08\text{M Ascorbic Acid}$. Detection: CAS at 560nm .

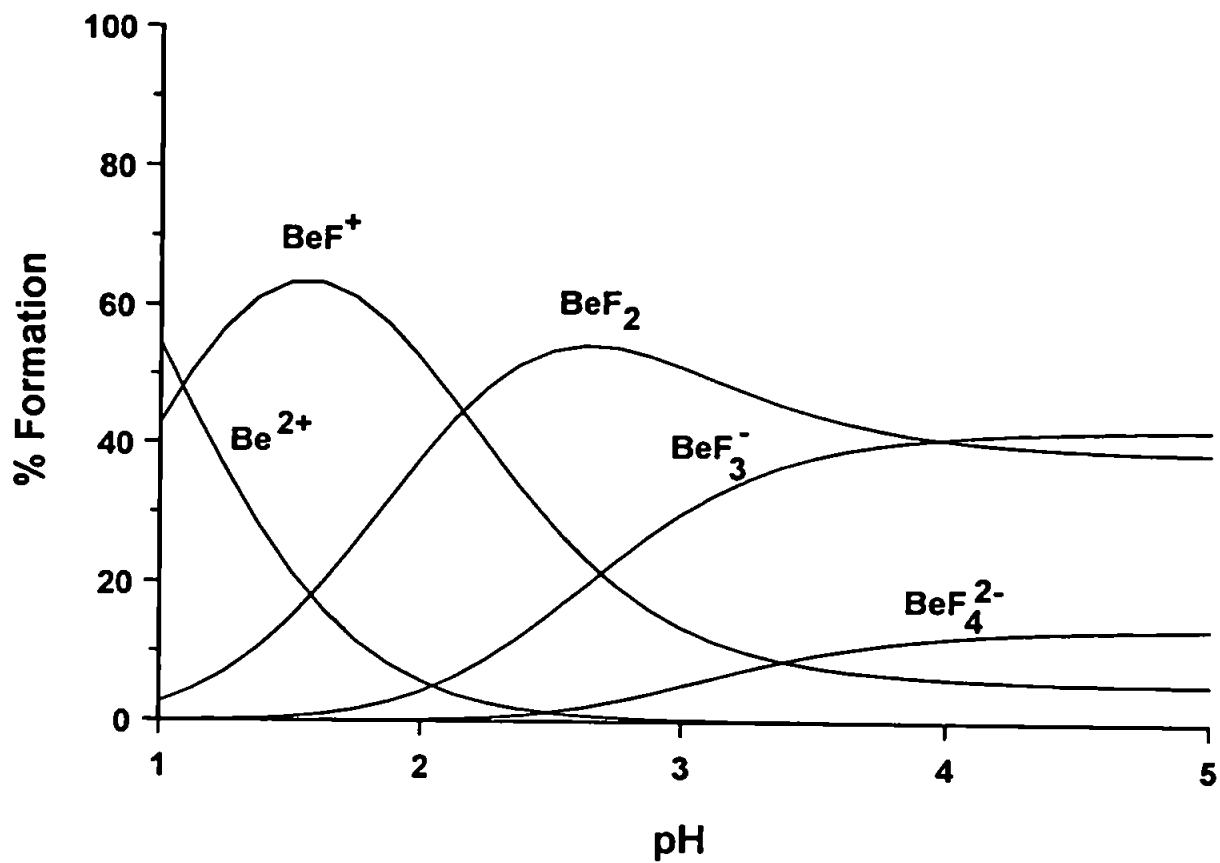


Figure 4.10. Speciation Diagram of Be(II) with the Fluoride ion [163].

4.3.4 Analytical Performance Characteristics

The accuracy of the proposed method was tested by the determination of Be(II) in a certified stream sediment, GBW07311, ($26 \pm 4\mu\text{g g}^{-1}$ certified concentration). Replicate sample analysis was achieved using standard addition calibration plots, an example given in Figure 4.11.

The results are given in Table 4.2.

Table 4.2. Analytical Characteristics of Be(II) Determination

Sample	Line equation	R ²	[Be] $\mu\text{g g}^{-1}$
1	$Y=569638.8X + 151558.6$	0.9999	26.6
2	$Y=319817.2X + 83781.3$	0.9979	26.2
3	$Y= 351652.6X + 91460.4$	0.9996	25.8
4	$Y= 352214.4X + 94203.9$	0.9993	26.7

Repeat sample analysis ($n=4$) gave a mean result of $26.3 \pm 0.4\mu\text{g g}^{-1}$, which compared well with the certified value. An analytical method is considered to perform well if the experimentally derived mean value lies within ± 2 method standard deviations of the certified value [224]. Thus, the mean value of $26.3\mu\text{g g}^{-1}$ lies within the limits of $26 \pm 0.8\mu\text{g g}^{-1}$, showing that this method is viable as a technique for the analysis of Be(II) in complex matrices.

The reproducibility (%RSD) of the method was ascertained with the repeat injection ($n=6$) of a sample, and was found to be 2.05% using peak area. A chromatogram of a sample injection is shown as Figure 4.12.

A blank fusion was also analysed to determine the system blank, but there was no apparent signal at the retention time for Be(II), indicating that sample pre-treatment was not a source of contamination.

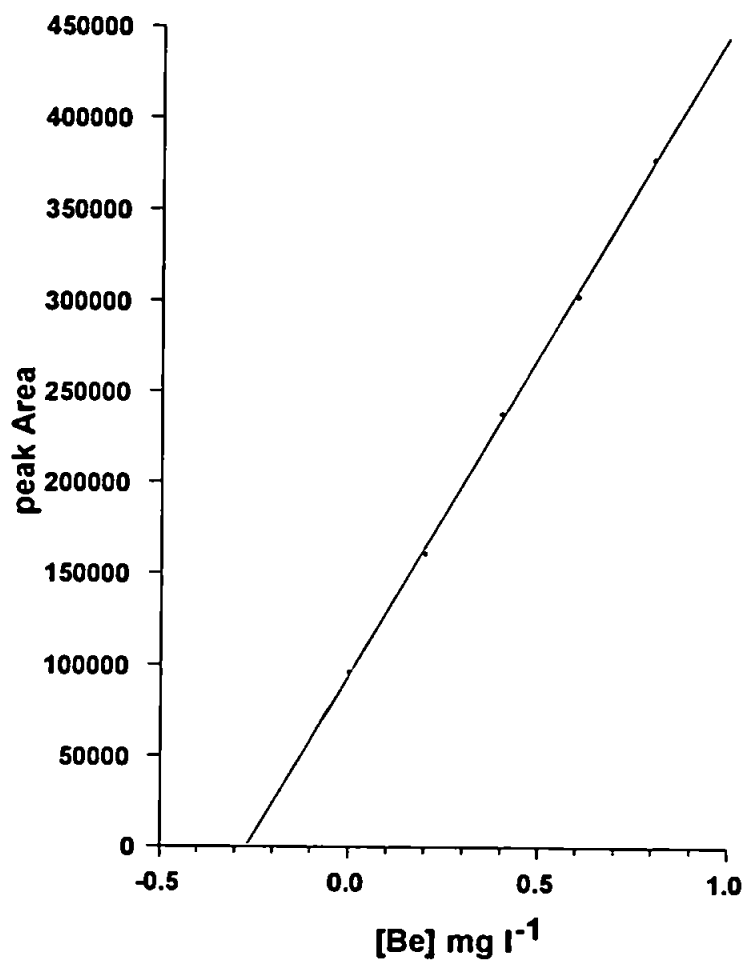


Figure 4.11. Sample 4 Standard Addition Curve.

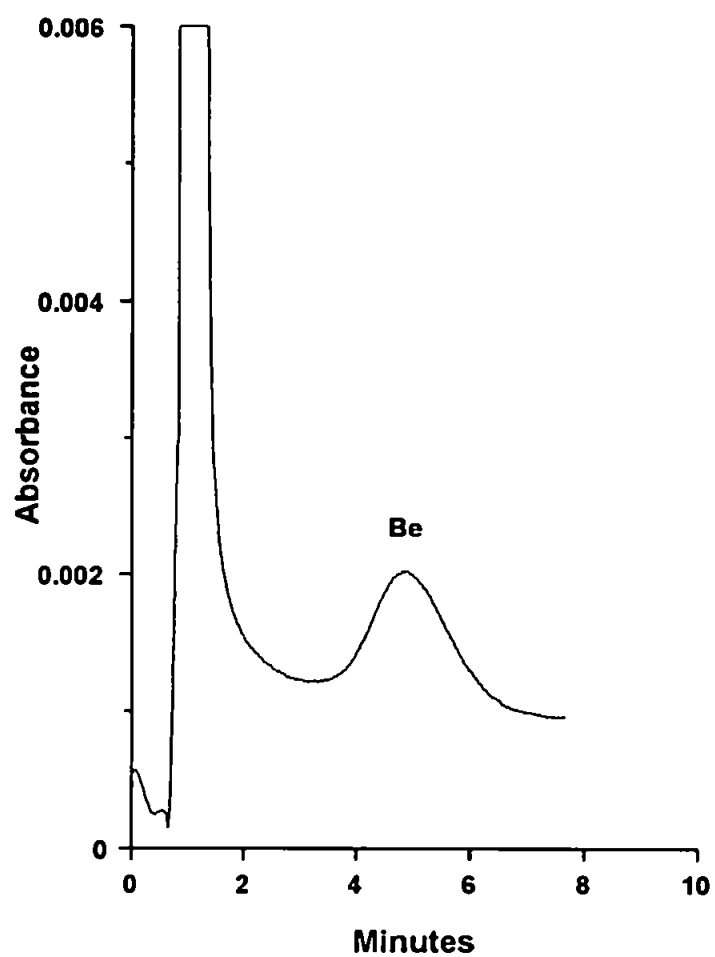


Figure 4.12. Separation of Be(II) from Matrix Metals in a Certified Reference Material (GBW07311)

4.4 Summary

A selective and sensitive HPCIC method for the determination of Be(II) in complex sample matrices has been developed. Using a small particle size silica, chemically modified with aminomethylphosphonic acid as a chelating substrate, trace concentrations of Be(II) could be separated from a massive excess of matrix metals ($>880\text{mg l}^{-1}$) using isocratic elution, in under six minutes. A detection limit of $35\mu\text{g l}^{-1}$ Be(II) was found with development of the post column reaction system and eluent conditions.

The results achieved for the stream sediment sample compared well with the certified value, which shows that this system is a useful alternative to atomic spectrometric techniques.

The limit of detection should be improved in samples containing less matrix metal ions, due to a reduction in the concentration of EDTA required to suppress the combined signal from these unretained elements. This HPCIC system is open to further development to improve sensitivity, possibly by increasing the column length and reducing the eluent pH further to determine whether the Be(II) peak will sharpen. It must be taken into consideration, however, that the silica matrix is susceptible to degradation at very low pH, which would reduce column capacity. Further optimisation of the PCR system, perhaps by reducing the CAS concentration to minimise background interference, and altering the buffer concentration to change the effluent pH, might also improve sensitivity.

It is also important to determine the fluoride concentration in the sample, which has been shown to complex with Be(II) and reduce the signal of this metal, when present in excess.

Chapter 5. Separation of Metal Ions using Neutral Substrates Dynamically Modified with Low Molecular Weight Chelating Molecules

5.1. Introduction

Thus far, investigations have focused on covalent bonding or physical impregnation of chelating groups onto high efficiency substrates for metal separations. As mentioned previously, the covalent attachment of a chelating group to any substrate matrix is generally a demanding synthetic task, which can influence the number of chelating adsorbents suitable for HPCIC. Impregnation of chelating dyes onto polystyrene resins provides a quick assessment of the metal separation properties of different ligand groups, but these fabricated columns are generally unsuitable for multi-element (>4 metals) analysis. This can often be overcome by incorporating gradient elution strategies by manipulation of eluent pH, but this can upset the system baseline, interfering with detection sensitivity. Improvements in metal selectivity and separation efficiency have been achieved when the chelating dye is a component of the mobile phase, creating a dynamically loaded system, as discussed in Sections 2.1.3 and 2.3.6.

Dynamic modification involves creating a chelating surface by having a ligand continuously present in the eluent. Using this method, an equilibrium is established between a sorbed layer of ligand on the surface of the substrate and the concentration of the ligand in the mobile phase. Altering such parameters as the concentration of ligand in the eluent, mobile phase pH, and the nature of the stationary phase, allows the dynamic equilibrium to change, which can affect metal selectivity.

In addition to the use of relatively large metallochromic molecules to form a dynamically sorbed layer, the potential for small hydrophobic molecules including organic acids to act as a chelating agent on hydrophobic microparticles has also been demonstrated.

Sutton *et al* [225], separated U(VI) from Th(IV), La(III) and Fe(II) using a macronet resin

(Purolite MN200) dynamically coated with dipicolinic acid. Elchuk *et al* [226], used mandelic acid in the eluent together with a C₁₈ silica column for the separation of certain transition metals, lanthanides, uranium and thorium, whilst Glennon *et al* [227], separated Ni(II), Cd(II), Pb(II) and Cu(II) using a porous graphitic carbon (PGC) column with oxalic acid in the mobile phase. The order of retention shown for the metal ions and the response to pH changes suggest that a sorbed layer of either mandelic acid or oxalic acid was present. Both findings are worthy of further investigation to establish if dynamic modification is occurring under the conditions used by these authors.

Small complexing organic molecules of course have been included in the mobile phase to improve the separation of metal ions using ion exchange substrates, as mentioned in Chapter 1. However, when ion exchange stationary phases are involved it has always been assumed that metal complexation only occurs in the mobile phase and not on the surface of the substrate. As discussed in Chapter 1, dipicolinic acid has been extensively applied for this purpose in conjunction with both cation and anion exchange resins for the analysis of transition and alkaline earth metals. A recent example is given by Chen and Adams, who used an anion exchange column to separate Mg(II) and Ca(II) from various anions as dipicolinic complexes [228]. Nesterenko *et al* have also undertaken investigations using picolinic acid [229] and quinaldic acid [230], in conjunction with silica columns for the on-column complexation and separation of transition metals.

Elefterov *et al* [231], investigated adding dipicolinic acid to the eluent to affect the separation of transition metals using an IDA bonded silica substrate.

There appeared to be no indication in any of these studies that the complexing acid in the mobile phase was forming a chelating surface on the stationary phase, the ion-exchange mechanism of the substrate groups being more dominant. However, when using neutral substrates there is evidence as discussed above that a chelating surface could result when using small organic carboxylic acids in the eluent.

The principal aim of this study, therefore, was to carry out further study into this relatively novel approach to metal ion separation. Three selected heterocyclic carboxylic acids, picolinic acid, quinaldic acid and dipicolinic acid, were each added to the mobile phase to evaluate the extent of dynamic modification of neutral substrates and the resulting chelation exchange properties. Dipicolinic acid was additionally chemically modified with a chloride ion, to assess the impact of adding a π -electron accepting functional group in the pyridine ring to the dynamic modification of π -electron donating polystyrene resins.

Two other chelating molecules were also studied; the carboxylic acid α -hydroxyhexadecanoic acid and the amino acid L-tryptophan.

Additional parameters were also investigated for their effect on selectivity and efficiency, namely eluent pH, ionic strength, ligand concentration in the mobile phase, substrate type and particle size on the separation of selected metals.

5.2. Experimental

5.2.1 Instrumentation

The HPCIC system is described in section 2.2.1. For this study, the analytical column was a PEEK 100 · 4.6mm i.d. or 250 · 4.6mm i.d. casing, packed with either PLRP-S 8 μ m or 5 μ m PS-DVB (Polymer Labs), PRP-1 7 μ m PS-DVB (Hamilton) or 9 μ m PS-DVB (Dionex). A stainless steel (100 · 4.6mm i.d.) casing contained Hypersil 5 μ m C₁₈ silica (Shandon HPLC, Runcorn, Cheshire, UK).

5.2.2 Reagents

The post column reagent used was PAR, described in section 2.2.2. The eluent was prepared using 1M KNO₃, adjusted to the required pH with HNO₃. The eluent and PCR were delivered at 1ml min⁻¹.

All reagents were of AnalaR grade (BDH), with the exception of PAR (Fluka), picolinic acid (99% purity), dipicolinic acid (99% purity) and quinaldic acid (98% purity) (Aldrich), L-tryptophan (99% purity) (BDH Biochemicals) and 2-hydroxyhexadecanoic acid (98% purity) (Avocado Research Chemicals Ltd, Lancs., UK).

5.2.3 4-Chlorodipicolinic acid synthesis

Dr. P.N. Nesterenko of Moscow University, Russia, kindly synthesised this compound.

The synthesis involved a one step reaction of chelidamic acid (0.5mol) and phosphorous pentachloride (2mol) in chloroform, in accordance with the procedure described by Bradshaw *et al* [232]. The crude product was hydrolysed by addition to ice cold water, refluxed with an excess of thionyl chloride and re-crystallised from hexane.

5.2.4 Preparation of the mobile phase

The required concentration of ligand was added to a nominal amount of 1M KNO₃ (100ml) in a covered glass beaker and stirred with heating until complete dissolution. This solution was then made up to the correct volume with addition of 1M KNO₃ and HNO₃ to give the appropriate pH.

5.3 Results and Discussion

5.3.1 Measurement of the dynamic loading of each carboxylic acid

Dynamic modification of a substrate involves adding a chelating compound to the mobile phase where the substrate initially has no chelating surface. Eventually, an equilibrium is established between the sorbed layer of chelating compound on the substrate and the chelating compound in the mobile phase. This is termed dynamic modification, as when the eluent is changed to contain none of the chelating compound, the sorbed layer will eventually leach off.

It was anticipated that for reasonable separation of metal ions to take place, the dynamically sorbed layer has to be significantly higher in concentration than the amount in the mobile phase. An indication of the amount sorbed can be obtained by determining the capacity factor for the organic acid, derived from the retention time for a discrete amount (1-10mM) injected onto the un-modified substrate. The higher the value of k' , the higher the 'concentration' of the organic acid in the stationary phase relative to that in the mobile phase. Thus, k' values for each carboxylic acid provide an indication of the potential chelating ability of the 'coated' substrate under dynamic conditions.

The absorbance spectrum of each organic acid solution was recorded to determine the optimal detection wavelength required for the k' injections.

With the C_{18} silica gel column, k' values of 0.79, 8.45 and 24.3 were recorded for picolinic acid, dipicolinic acid and quinaldic acid respectively, when using an eluent of 1M KNO_3 at pH 2. It is apparent that picolinic acid is the most weakly sorbed and quinaldic acid the most strongly sorbed to the silica. Quinaldic acid would be expected to have the highest k' value as the extra aromatic ring should give rise to stronger sorption on the C_{18} bonded surface. It is not so clear why dipicolinic acid should have a higher k' value than picolinic acid unless some of the 'bare' silica surface is strongly attracting the more polar molecule.

Table 5.1. k' values for the three heterocyclic carboxylic acids on neutral polystyrene resin with varying ionic strength. Eluent, KNO_3 at pH 2, column 100 · 4.6mm i.d. Detection : UV-Visible. Picolinic acid (265nm), dipicolinic acid (272nm) and quinaldic acid (314nm).

ACID	Fractional charge on the acid*	k' Values at Different Ionic Strengths			
		1M	0.5M	0.1M	0.01M
Picolinic ¹	+0.1	1.32	1.20	1.19	1.14
Dipicolinic ¹	-0.4	17.60	16.10	21.10	23.98
Quinaldic ²	+0.45	91.98	89.94	92.38	-

* Calculated using the protonation constants of the pyridyl nitrogen and carboxyl group.

1: PLRP-S 8 μm PS-DVB. 2: PRP-1 7 μm PS-DVB.

In other words some adsorption interactions could be occurring in combination with reversed-phase.

However, this k' order is repeated for the polystyrene resins (Table 5.1) where adsorption interactions should not be taking place. If this is the case, then the differences in degree of sorption between these three acids is certainly unexpected. Normally, for small polar organic molecules it would be assumed that the least charged or near neutral species would be the strongest sorbed. However, looking again at Table 5.1, where the degree of ionisation of the acid or basic group at pH 2 is shown, the degree of sorption is actually inversely related to the extent of ionisation. Another point to note is that each carboxylic acid has a higher absolute k' value on the polystyrene resin than on the C_{18} silica column at the same ionic strength and pH. This finding seems reasonable as additional π - π interactions, discussed earlier, should occur between the aromatic groups on the carboxylic acids and the benzene groups on the resin.

5.3.2 Effect of ionic strength on dynamic loading

It was considered that the ionic strength of the mobile phase would have an important affect on the k' values, as a 'salting - out' effect would operate, whereby a high concentration of KNO_3 should result in the carboxylic acids being 'forced' out of solution onto the stationary phase, producing a higher loading. However, although this appears to hold true for picolinic acid (Table 5.1), with the k' values increasing with increasing ionic strength, the pattern is not repeated for dipicolinic acid and quinaldic acid, where retention of these acids on polystyrene does not show any apparent trend with ionic strength. It would appear, therefore, that the ionic strength does not play a significant role in determining the concentration of ligand sorbed onto the stationary phase.

5.3.3 Effect of particle size on dynamic loading

Table 5.2. Effect of substrate particle size on k' values for heterocyclic carboxylic acids.

Eluent: 1M KNO_3 . Column dimensions: 100 · 4.6mm i.d. Detection : UV-Visible dipicolinic acid (272nm) and quinaldic acid (314nm).

Resin		k'		
Particle size μm	Pore size Å	Dipicolinic acid		Quinaldic acid
		pH 1	pH 2	pH 2
8	120	-	17.6	66.4
7	100	31.4	19.3	92.0
5	120	33.7	22.2	-

It was thought possible that resin particle size might influence the degree of dynamic modification. A reduced particle size could result in a higher loading of each ligand onto

the stationary phase, due to both an increased number of pores and therefore surface area amenable to sorption per column length, and the increase in substrate hydrophobicity attracting the hydrophobic molecules. From the preliminary data shown in Table 5.2, this appears to be the case. The k' values for both dipicolinic acid and quinaldic acid increased with a decrease in particle size. However, it is also possible that each manufacturer's resin has a different hydrophobicity dependent upon its preparation. Further study is necessary to fully evaluate this affect.

5.3.4 Reproducibility of dynamically modified substrates

Table 5.3. The reproducibility of selected metal ion retention times on a quinaldic acid coated polystyrene resin column (PRP-1 $7\mu\text{m}$) repeatedly stripped and recoated over a 5 day period. Mobile phase, $1 \cdot 10^{-4}$ M quinaldic acid in 1M KNO_3 . Column dimensions, 100 · 4.6mm. Detection: PAR at 490nm.

Day	Retention Time (min)		
	Zn	Co	Ni
1	2.9	4.3	19.3
2	2.8	4.0	17.8
3	2.8	4.1	18.2
4	2.8	4.1	17.2
5	2.9	4.4	20.4
Mean	2.84	4.18	18.58
RSD (%)	1.8	3.8	6.8

A significant factor, which expands the potential of adding small organic molecules to the mobile phase as a separation system, is the ability to recover the bare substrate for other uses after dynamic modification. For each carboxylic acid, a dynamic equilibrium was obtained between the substrate and eluent after 2-3 hours pumping of the carboxylic acid containing eluent. This was found to be reversible since this dynamically sorbed layer

could be leached off from the column using dilute HNO_3 (pH 2), again over a period of about 3 hours. The recovery of the original bare substrate was shown by injecting a strongly chelating metal such as copper throughout the leaching process, until there was no retention.

A trial was carried out where a column was washed daily and then re-coated dynamically. Metal retention times were found to be very consistent (Table 5.3), showing not only that the resin properties were essentially unaltered by the re-coating procedure, but also the level of dynamic coating was reproducible. Therefore, the ability to re-use a substrate after washing that is amenable to further dynamic modification by the same or other compound, or even for some other chromatographic application is a major advantage and obviously very cost effective.

5.3.5 Chelating exchange properties of the dynamically coated carboxylic acids

Both picolinic acid and quinaldic acid are N,O chelators, the metals complexing with the nitrogen of the pyridine ring and oxygen on the carboxyl group. With the addition of a second carboxyl group, dipicolinic acid potentially becomes a N,O,O chelator. The presence of a basic nitrogen and acidic oxygen should signify that these molecules can chelate metals over a wide pH range.

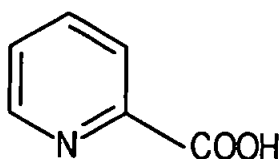
An important consideration with this approach to HPCIC, is that the concentration of chelating compound in the eluent has to be tailored to provide a sorbed layer on the substrate which will give dominant metal retention characteristics with minimal interference or competition from the same ligand in the eluent. Therefore, the concentration of each of these acids in the mobile phase was varied from 1 to 0.01mM, to evaluate the optimal concentration providing maximum chemisorption onto the substrate with minimal complexing capability in the eluent. From these initial studies, it appears that a concentration of between 1 – 0.1mM is required to obtain a dynamically modified

substrate capable of providing significant metal selectivity. The elution order for the metal cations investigated did not change with decreasing carboxylic acid concentration, but the retention times did decrease, both for the silica gel and polystyrene resins. Furthermore, for each of the acids investigated, the order of elution was the same on both the silica and resin substrates, over the pH range investigated.

All studies involving chelating surfaces, where the ligand is an acid or basic group, should consider the possibility of ion exchange effects, which could occur at the same time as chelation. As with the previous studies undertaken in this thesis, all eluents contain a high concentration of KNO_3 to swamp any ion exchange sites.

Another important consideration, unconnected with the chromatography is the effect of the presence of these acids in the eluent on detection. These carboxylic acids are relatively strong complexing agents, particularly dipicolinic acid, so could compete with PAR or other post column reagent. Detection sensitivity did in fact increase with decreasing carboxylic acid concentration. Changing from an eluent containing 1mM to 0.1mM dipicolinic acid at pH 1.5, sensitivity increased fourfold for Pb(II), about threefold for Co(II) and Ni(II) and approximately doubled the Cd(II) signal. This emphasises the need to keep the levels in the eluent as low as possible, consistent with good chromatography.

5.3.5.1 Picolinic Acid



2-pyridinecarboxylic acid

RMM 123.1 HL pK_a 0.85 [162]

Picolinic acid is partially protonated in moderately acid aqueous media [233], which might beneficially affect its potential to form a chelating surface. The mobile phase pH should be

kept as low as possible thus minimising ionisation of each organic acid, otherwise metal ions could be eluted as carboxylate complexes by an ion – pair mechanism, the ligand concentration in the mobile phase becoming important in retention, which could reduce metal selectivity on the column.

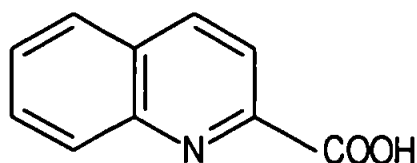
Zagorodni *et al* [234] synthesised a picolinic acid bonded chelating resin for the separation of Cu(II) and Zn(II), which produced slow kinetics, impairing the separation profile.

In our study, due to the low dynamic loading of this molecule (Table 5.1) all the metals investigated were not too far from the solvent front, many being split, presumably due to interactions with the stronger complexing eluent. Cu(II) was the exception, being retained very strongly on both silica gel and PS-DVB with an eluent containing 1M KNO₃ 1mM picolinic acid: k' 36.3 at pH 1.1 and 51.2 at pH 1.5, on a 100mm 9 μ m PS-DVB column, and $k' >75$ at pH 2 on the silica gel column.

The retention of Cu(II) was reduced drastically when the eluent contained 0.1mM picolinic acid, giving a k' value of 2.3 at pH 1.5 on the same PS-DVB column, and $k' = 0.5$ at pH 2 on the silica column.

A tentative elution order at pH 2 was Mn(II)<Cd(II)<Pb(II)<Zn(II)<Co(II)<Ni(II)<Cu(II). La(III) and U(VI) were also very weakly retained with substrates modified with picolinic acid.

5.3.5.2 Quinaldic acid



2-quinolinecarboxylic acid

RMM 173.17 HL pK_a 4.96 [162]

Quinaldic acid is a well known reagent for the gravimetric determination of Cu(II), Cd(II) and Zn(II) [103], though Ali *et al* also investigated the chelate compounds of selected trivalent rare earth metals with this reagent [235]. More recently, Moberg and Weber grafted quinaldic acid onto low efficiency polystyrene supports to extract metal ions from aqueous sulfate solutions at low pH [236]. It was found that there was a high preference for Cd(II) ions. Li *et al* bonded quinaldic acid to macroporous PS-DVB to selectively remove Al(III) from aqueous acidic solutions (pH 3.5) in the presence of selected divalent metals and Cr(III) [237].

The acid dissociation constant of quinaldic acid is greater than the corresponding value for picolinic acid, thereby it is a weaker acid with a subsequent stronger conjugate base, which indicates that it should form more stable complexes with metal ions. The additional aromatic group also improved the 'capacity' of the quinaldic acid chelating substrate, which should increase the retention of metal ions dependant upon the ligand concentration in the eluent.

Both of these assumptions were proven correct, in that metal retention was significantly improved on the quinaldic acid loaded column. As with picolinic acid, Cu(II) was also very strongly held by quinaldic acid. At a concentration of 0.1mM quinaldic acid in an eluent of 1M KNO₃, Cu(II) was retained for 10 minutes at pH 1.5, increasing to 70 minutes at pH 1.7 on the 100mm PRP-1 7 μ m PS-DVB column, a remarkable increase over a small pH

range. The retention times and selectivity coefficients using quinaldic acid are far greater than for picolinic acid, reflecting the higher dynamic loading. The elution order found for quinaldic acid was $Mn(II) < Pb(II) < Cd(II) < Zn(II) < Co(II) < Ni(II) < Cu(II)$ for the divalent metal ions, and $La(III) < Lu(III) < U(VI) < Fe(III)$ for the other metals investigated. A separation of $Pb(II)$, $Cd(II)$, $Co(II)$ and $Ni(II)$ and $Mn(II)$, $Pb(II)$, $Zn(II)$ and $Co(II)$ on the 100mm PLRP-S $8\mu m$ column are shown in Figures 5.1 and 5.2 respectively, with the separation of $Pb(II)$, $Cd(II)$, $Co(II)$ and $Ni(II)$ on the silica gel shown in Figure 5.3. Because of the reduced dynamic loading of quinaldic acid on the silica gel, a higher pH was required to achieve a similar separation to that possible on a polystyrene resin. The peak symmetries are similar between both substrates, but the peaks observed for the silica gel are slightly broader, due to this increase in pH slowing the kinetics of dissociation. What is interesting to note from Figures 5.1 and 5.3 is the very broad yet apparently symmetrical peak shape for $Ni(II)$, implying slow kinetics between this metal and the dynamically coated substrate. This good symmetry is unusual, as slow kinetics usually produces bad tailing of analyte peaks. Indeed, the symmetry of the $Ni(II)$ peak appears superior to that obtained with $Be(II)$ on the APAS substrate, which also demonstrated this unusual behaviour.

A $\log k'$ against pH plot was obtained for seven metal ions using a quinaldic acid eluent at a concentration of 0.1 mM, shown in Figure 5.4. From the observed linearity of the plots it was considered that chelation on the substrate was the dominant retention system. The concentration of quinaldic acid in the eluent was insufficient to provide any significant competition for metal chelation, which is the desired outcome for this type of separation process. It is interesting to note the markedly different slope for $Pb(II)$, implying that this metal does not have that high an affinity for a N,O chelating system.

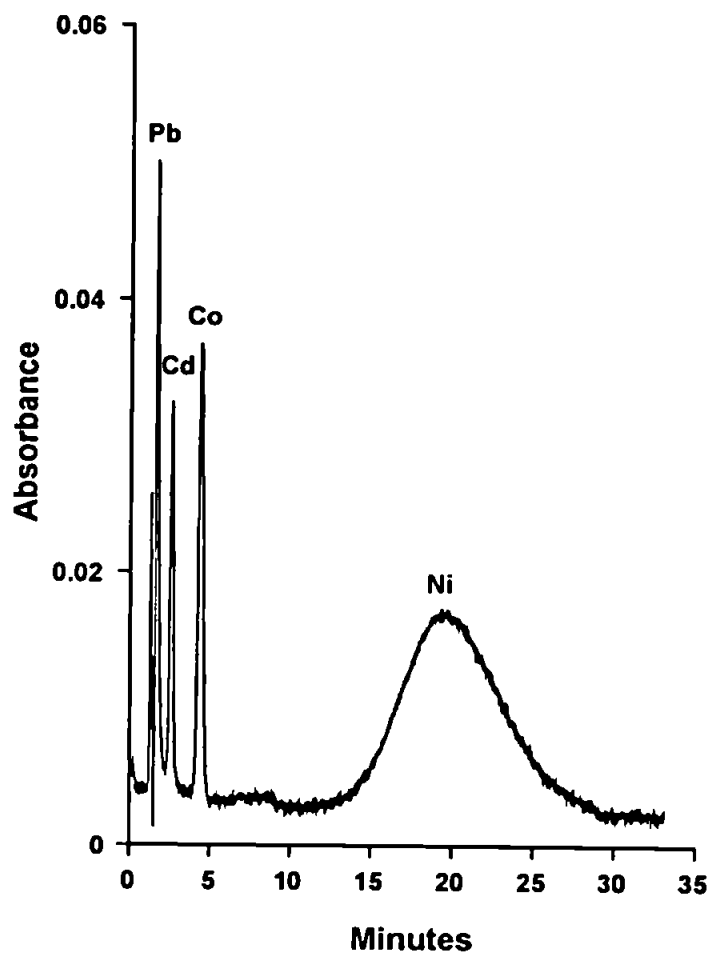


Figure 5.1. The separation of Pb(II) 4 mg l⁻¹, Cd(II) 10 mg l⁻¹, Co(II) 1 mg l⁻¹ and Ni(II) 10 mg l⁻¹ on a 100 · 4.6mm PLRP-S 8µm PS-DVB Column. Eluent: 1M KNO₃, 1mM quinaldic acid at pH 1.5. Detection: PAR at 490nm.

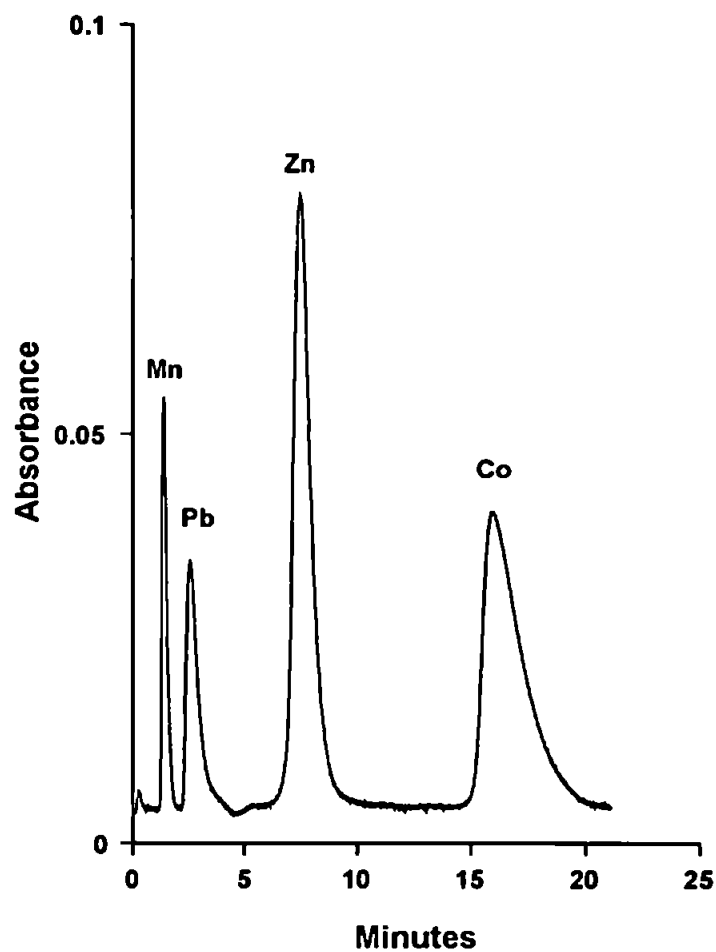


Figure 5.2. The separation of Mn(II) 0.5 mg l^{-1} , Pb(II) 5 mg l^{-1} , Zn(II) 15 mg l^{-1} and Co(II) 5 mg l^{-1} on a $100 \times 4.6 \text{ mm}$ PLRP-S $8 \mu\text{m}$ PS-DVB Column. Eluent: 1 M KNO_3 , 0.1 mM quinaldic acid at pH 2.6. Detection: PAR at 490 nm .

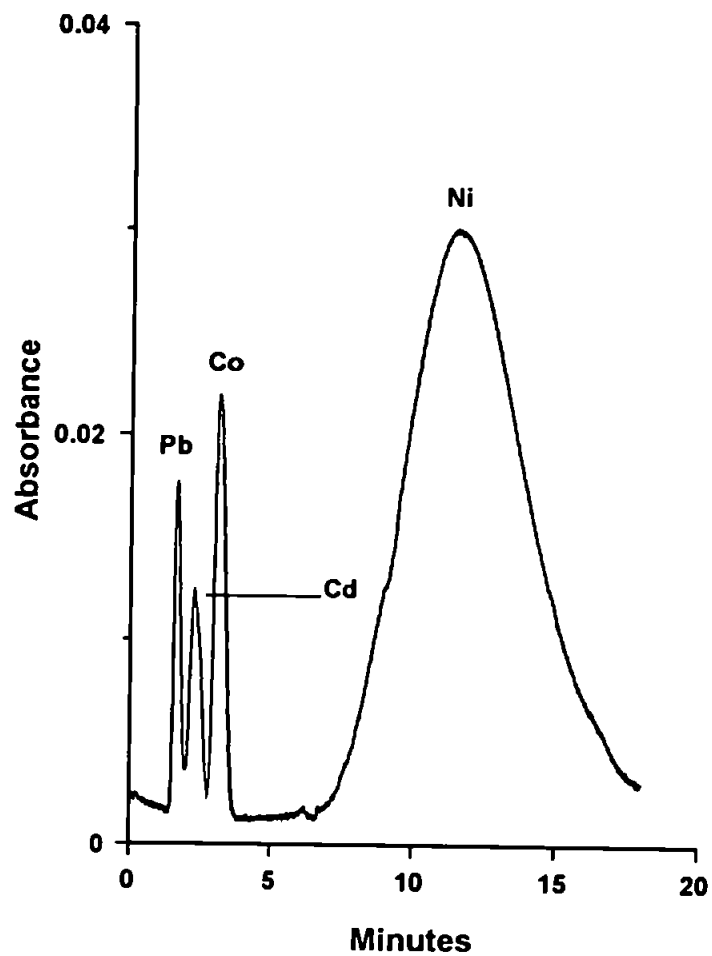


Figure 5.3. The separation of Pb(II) 2 mg l⁻¹, Cd(II) 10 mg l⁻¹, Co(II) 1 mg l⁻¹ and Ni(II) 20 mg l⁻¹ on a 100 · 4.6mm C₁₈ silica column. Eluent: 1M KNO₃, 1mM quinaldic acid at pH 2. Detection: PAR at 490nm.

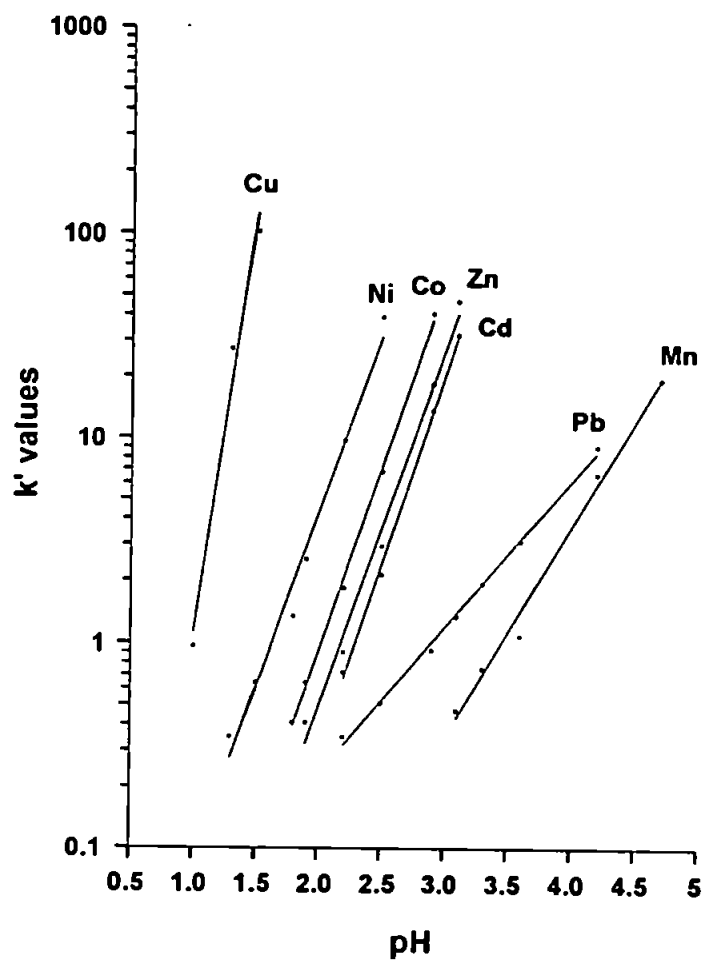
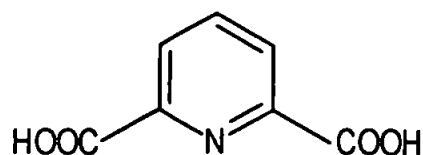


Figure 5.4. The dependence of capacity factors for transition and heavy metal ions on eluent pH. Eluent: 1M KNO₃ 0.1mM quinaldic acid.

5.3.5.3 Dipicolinic acid



2,6-pyridinedicarboxylic acid

RMM 167.1 H₂L pK₁ 2.16 pK₂ 4.76

This carboxylic acid has been used as a spectrophotometric reagent for Mn(II) at 510nm [103]. Chessa *et al* [238] prepared a dipicolinic acid bonded polystyrene phase for the selective separation of Pd(II) from Pt(II) or Pt(IV) at pH 6, and the separation of Au(III) from Pd(II) and Pt(IV) at pH 0, as chloro-complexes.

In this study, the addition of a second carboxyl group to the pyridine moiety, giving possible N,O,O chelation, altered the elution order of metal ions markedly. The order for dipicolinic acid at pH 1.5 was:

Mn(II)<Cu(II)<Co(II),Ni(II)<Zn(II)<Pb(II)<Cd(II)<Fe(III)<U(VI).

What is interesting to note here, is that Cu(II) is very weakly retained at this pH, which seems to indicate a preference of a N,O system for this metal. In contrast, U(VI) is very strongly retained on the dipicolinic acid modified column, this metal being very weakly held on both the N,O chelating columns. In addition, the retention times for the transition metal ions decreased slightly with increasing pH above 1.5, whereas for Fe(III) and U(VI) the situation was reversed. The strikingly different elution order for divalent metal ions with dipicolinic acid in comparison with picolinic acid and quinaldic acid, emphasises the different chelating properties of mono- and dicarboxylic acids.

The dramatic change in Cu(II) retention between picolinic acid and dipicolinic acid is difficult to explain, as the stability constants for Cu(II) are the largest of the dipositive

metal ions for both ligands ($\log K_1 = 8.73$ with picolinic acid and 9.15 with dipicolinic acid [163]).

The separation of selected metals using dipicolinic acid are shown in Figures 5.5 and 5.6.

Although the retention of transition metal ions were close to the solvent front, k' plots are given in Figures 5.7 and 5.8 with 1 and 0.1mM dipicolinic acid present in the eluent respectively. It was clear that retention increased for most metals up to pH 1.2-1.5, before decreasing again, dramatically so above pH 2. This indicates that strong competition from the dipicolinic acid in the mobile phase occurs at this higher pH, possibly due to a dissociation of one of the carboxyl groups (pK_1 2.16).

This observation is in stark contrast to the linear relationship shown with quinaldic acid, and indicates that dicarboxylic acid – metal interactions are more complicated than with simple monocarboxylic acids.

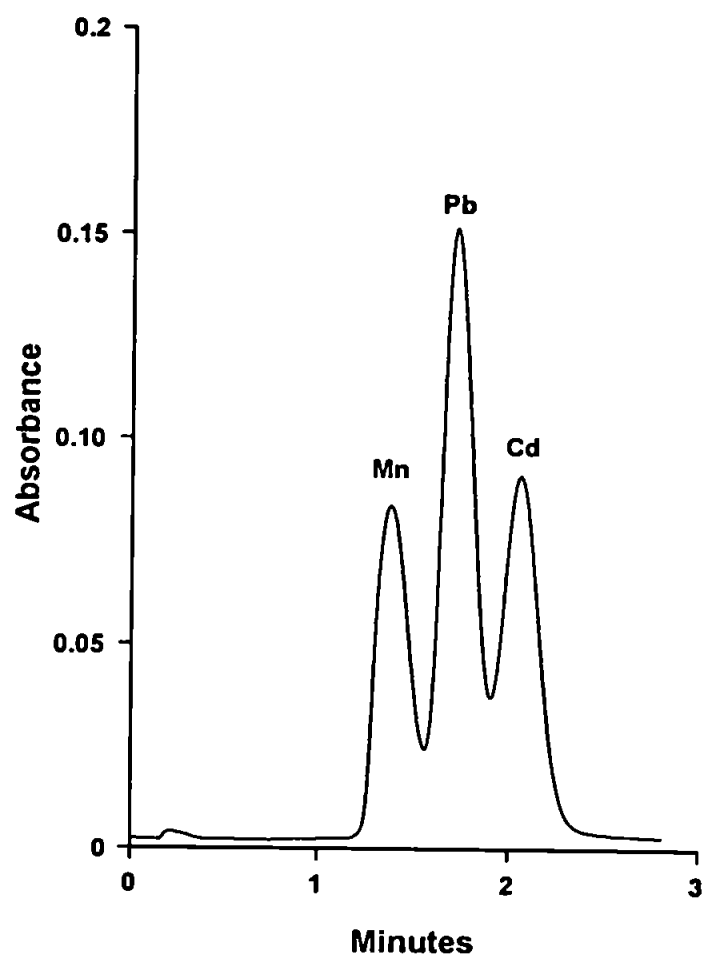


Figure 5.5. The separation of Mn(II) 2 mg l⁻¹, Pb(II) 70 mg l⁻¹ and Cd(II) 80 mg l⁻¹, on a 100 · 4.6mm PLRP-S 8µm PS-DVB Column. Eluent: 1M KNO₃, 1mM dipicolinic acid at pH 1.5. Detection: PAR at 490nm.

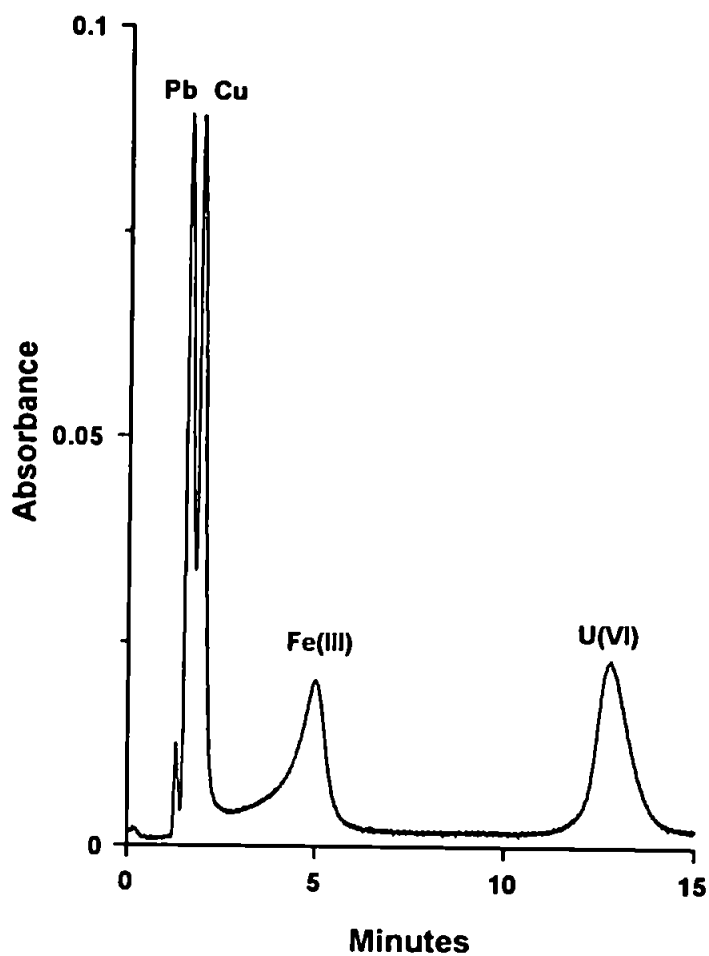


Figure 5.6. The separation of Pb(II) 5 mg l⁻¹, Cu(II) 1 mg l⁻¹, Fe(III) 1 mg l⁻¹ and U(VI) 40 mg l⁻¹, on a 100 · 4.6mm PLRP-S 8µm PS-DVB Column. Eluent: 1M KNO₃, 1mM dipicolinic acid at pH 1.5. Detection: PAR at 490nm.

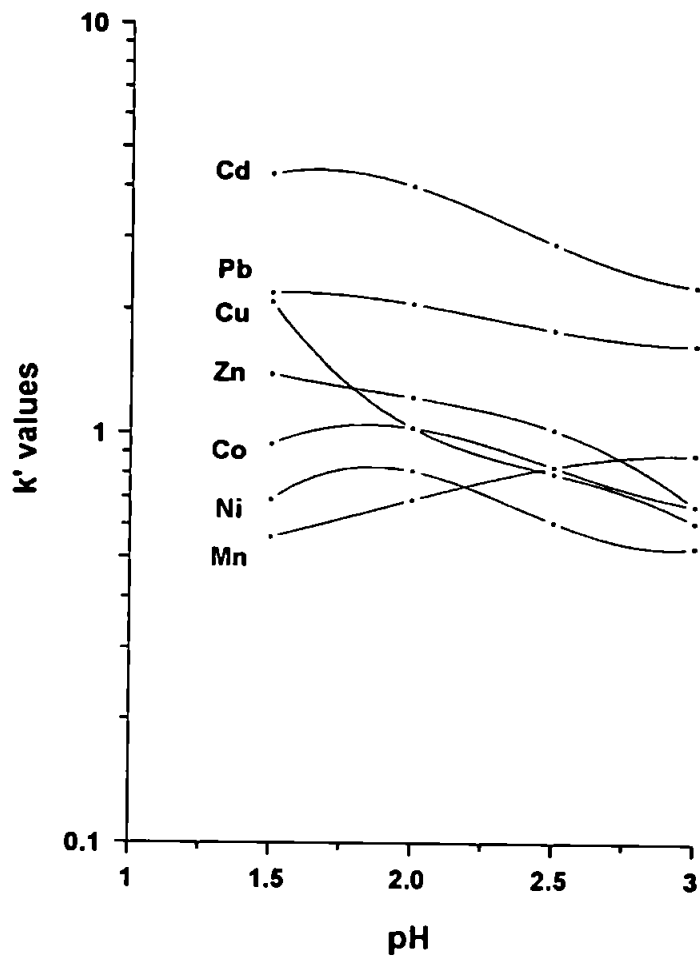


Figure 5.7. The dependence of capacity factors for transition and heavy metal ions on eluent pH. Eluent: 1M KNO_3 1mM dipicolinic acid.

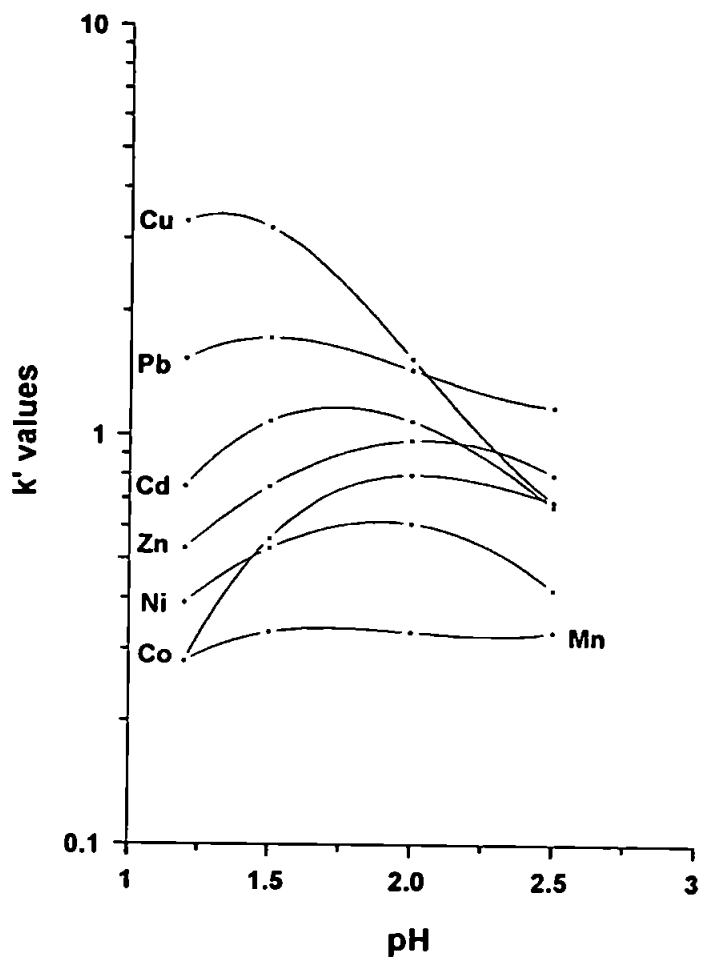
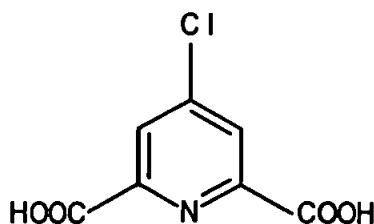


Figure 5.8. The dependence of capacity factors for transition and heavy metals on eluent pH. Eluent: 1M KNO_3 0.1mM dipicolinic acid.

5.3.5.4 4-Chlorodipicolinic acid



RMM 201.57 H₂L pK₁ 1.7 pK₂ 3.75 [239]

As stated in section 5.3.5.3, dipicolinic acid, under conditions of high pH, had a dynamically sorbed layer that was insufficient and possibly unstable, resulting in low resolution between most metal ions. Strong competition from the dipicolinic acid in the mobile phase additionally made it more difficult to provide an explanation of the separations obtained, and could limit its potential for the analysis of real samples.

To improve this situation, as mentioned previously, it is necessary to considerably increase the concentration of the sorbed layer relative to that in the mobile phase. This can be achieved by two methods. One is to use more hydrophobic chelating molecules having the same functional groups. Unfortunately, there are no commercially available or easily synthesised analogs of dipicolinic acid with high hydrophobicity. Alternatively, as the π -electron donating properties of the PS-DVB matrix are well known [240], a more stable dynamic modification of the PS-DVB surface can be obtained by using derivatives of dipicolinic acid having π -electron accepting functional groups in the pyridine ring, an example being 4-chlorodipicolinic acid. It should be especially outlined that this organic molecule will preferably be co-ordinated on the flat outer surface of the resin due to the stronger π - π interactions. Thus, not only will the capacity of the sorbed layer be increased, but also the accessibility of the chelating functional groups to metal ions will be improved,

which as a consequence, should enhance the performance of this modified stationary phase.

Oehlke *et al* [241], found that 5-chloropicolinic acid had an increased affinity for Cu(II) than picolinic acid, giving stability constants of $\log K_1$ 8.5 and 7.5 respectively.

5.3.5.4.1 Preliminary 100mm PS-DVB column investigations

To ascertain the metal retention properties of chlorodipicolinic acid, initial studies were performed using the PRP-1 7 μ m Hamilton resin, packed into a 100mm PEEK column.

The adsorption of organic molecules having oppositely charged functional groups onto the surface of a hydrophobic resin must be at a maximum at an eluent pH close to the isoelectric point. According to the pK values for the carboxylic groups and pyridine nitrogen, the isoelectric point for both dipicolinic acid and chlorodipicolinic acid must be achieved within a pH range of 1-1.5. At pH 1.5 in 1M KNO₃, the retention of chlorodipicolinic acid ($k' = 229$) was almost nine times greater than the retention of dipicolinic acid ($k' = 26$).

As the retention of these organic molecules is proportional to their distribution coefficients in this heterogeneous system, it can reasonably be assumed that a more concentrated chelating exchanger is obtained by dynamic modification with chlorodipicolinic acid.

When mixtures of metal ions were injected onto the 100mm chlorodipicolinic acid modified column, it was immediately apparent that a more concentrated and stable chelating surface was present compared to that produced by dipicolinic acid, since longer retention times and larger selectivity coefficients were obtained at equivalent pH. The retention order found for selected metal ions using an eluent consisting of 1M KNO₃, 0.5mM chlorodipicolinic acid at pH 1.2 was:

Mn(II)<Co(II)<Ni(II)<Zn(II)<Cu(II)<Pb(II)<Cd(II)<lanthanides<Fe(III)<U(VI).

A change in the concentration of chlorodipicolinic acid in the mobile phase should affect the amount sorbed onto the polystyrene resin, thus affecting metal ion retention times. Figure 5.9 shows this to be the case where retention times generally increased with chlorodipicolinic acid concentration, up to 1mM. This is further illustrated by the chromatograms shown in Figure 5.10 and 5.11, demonstrating the effect of chlorodipicolinic acid concentration on metal ions separations at an equivalent pH. These chromatograms also indicate reasonable efficiencies, considering the column length was 100mm, as well as symmetrical peak shapes. Better resolution should be obtained with a longer column.

The log k' vs. pH plot for selected transition metal ions in an eluent containing 1mM chlorodipicolinic acid is shown in Figure 5.12, and generally follows the complex pattern demonstrated with dipicolinic acid (Figures 5.7 and 5.8). Indeed, the retention order is generally the same at an equivalent pH. Although Figure 5.12 is useful for establishing the pH required for optimum selectivity and separation, these complicated patterns are difficult to interpret.

It was postulated that three possible retention mechanisms could operate within a dynamic system: ion-exchange or chelation-exchange on the substrate surface, and/or an ion-interaction system whereby the ligand in the eluent complexes metal ions in conjunction with interactions on the substrate surface, thereby affecting retention.

Due to the high ionic strength eluent, it is believed that ion exchange interactions are suppressed. Therefore, it is thought that a mixed mode mechanism is operating, which changes in proportion with pH. It is proposed that in moderately acidic eluents (<pH 1.5) complexation at the substrate surface is dominant. Then as the pH is raised, complexation in the mobile phase becomes more important as the chlorodipicolinic acid molecules deprotonate, and start to compete effectively with complexation on the surface of the stationary phase.

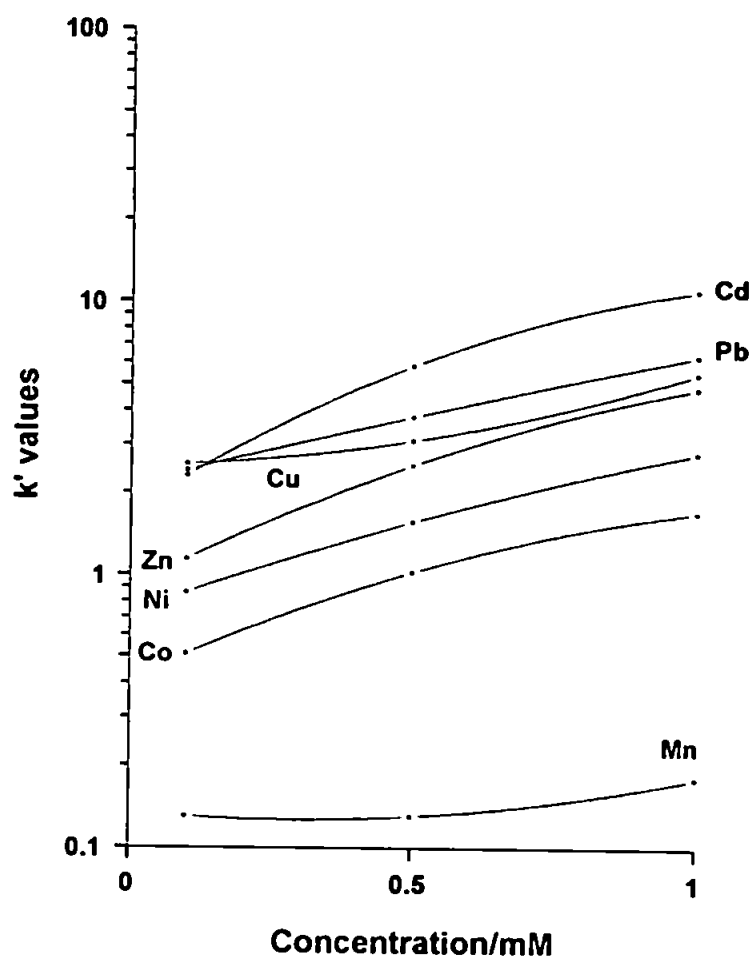


Figure 5.9. The dependence of capacity factors for transition and heavy metals on the concentration of chlorodipicolinic acid in the eluent. Eluent: chlorodipicolinic acid in 1M KNO_3 at pH 1.2.

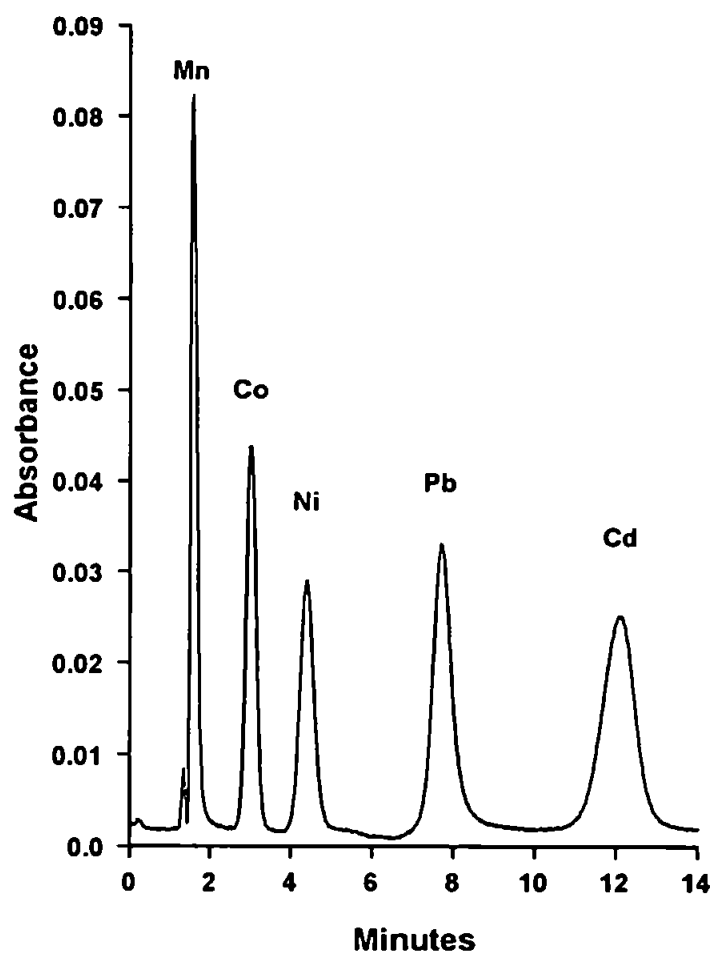


Figure 5.10. The separation of Mn(II) 0.5 mg l⁻¹, Co(II) 0.5 mg l⁻¹, Ni(II) 0.5 mg l⁻¹, Pb(II) 10 mg l⁻¹ and Cd(II) 20 mg l⁻¹, on a 100 · 4.6mm PRP-1 7µm PS-DVB Column. Eluent: 1M KNO₃, 1mM chlorodipicolinic acid at pH 1.2. Detection: PAR at 490nm.

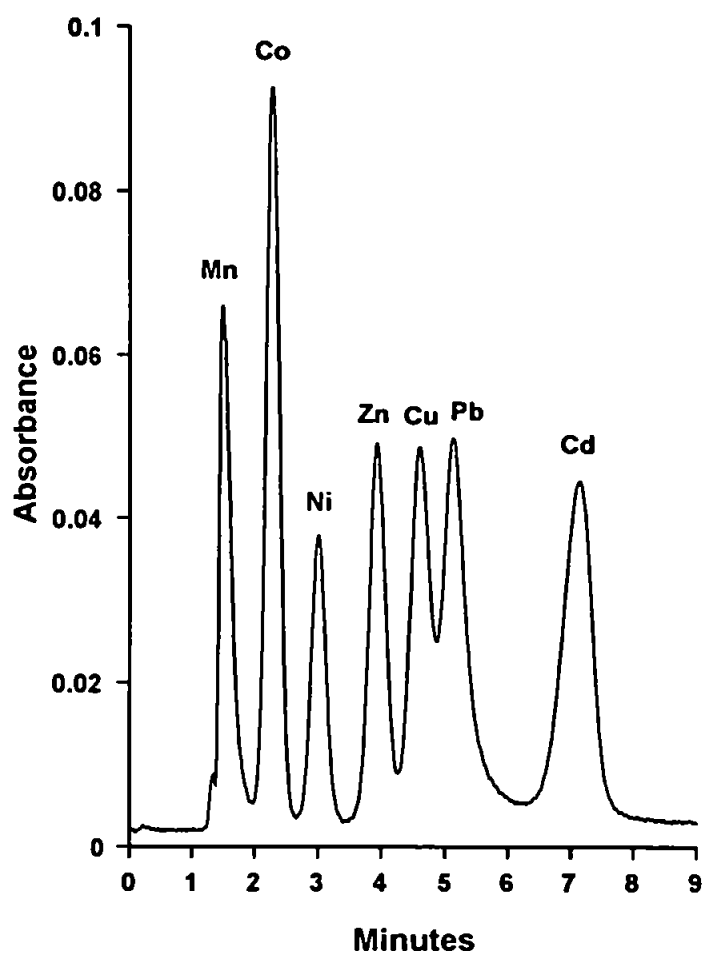


Figure 5.11. The separation of Mn(II) 0.5 mg l⁻¹, Co(II) 1 mg l⁻¹, Ni(II) 0.5 mg l⁻¹, Zn(II) 2 mg l⁻¹, Cu(II) 1 mg l⁻¹, Pb(II) 10 mg l⁻¹ and Cd(II) 20 mg l⁻¹, on a 100 · 4.6mm PRP-1 7µm PS-DVB Column. Eluent: 1M KNO₃, 0.5mM chlorodipicolinic acid at pH 1.2.

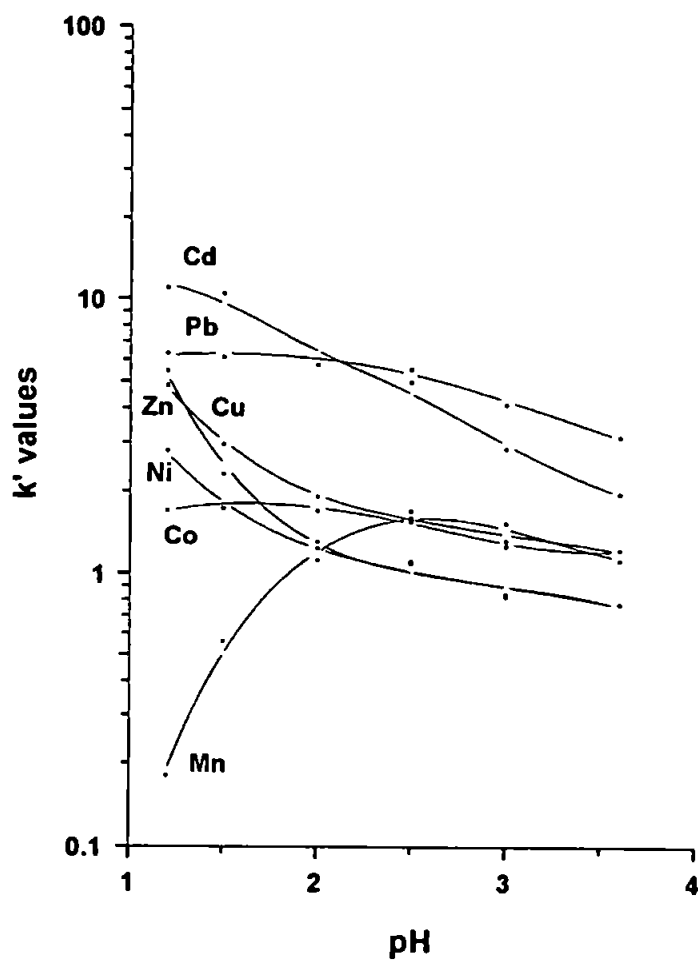


Figure 5.12. The dependence of capacity factors for transition and heavy metals on eluent pH. Eluent: 1M KNO_3 1mM chlorodipicolinic acid.

This would indicate why metal ion retention generally decreases above pH 2. In addition, the amount of ligand dynamically coated onto the resin decreases with increasing pH, reaching a maximum near the isoelectric point, as shown in Figure 5.13. Thus, as the pH increases, dipicolinic acid becomes increasingly negatively charged due to deprotonation, which will reduce its adsorption capacity onto a neutral hydrophobic resin.

Furthermore, it is also possible that neutral chlorodipicolinic acid complexes in the mobile phase could be retained by a hydrophobic mechanism in accordance with previously published data [229]. Nevertheless, as long as the dynamic system is stable and reproducible, as has already been demonstrated (Table 5.3), this complex relationship can be exploited for unusual selectivity control.

The preliminary investigations undertaken resulted in some interesting observations concerning the selectivity and analytical performance of the chlorodipicolinic acid column. Firstly, Cd(II) was retained more strongly than other common transition metals, including Cu(II) at low pH, which is unusual and could be exploited for its selective determination. Secondly, the Ni(II) peak has a good symmetrical peak shape, much sharper than obtained with the quinaldic acid column at an equivalent pH, which indicates that this metal is ideally suited to separation using a dynamically modified system. As already mentioned, the peak shape is unusual, as this metal is considered kinetically slow in complexation.

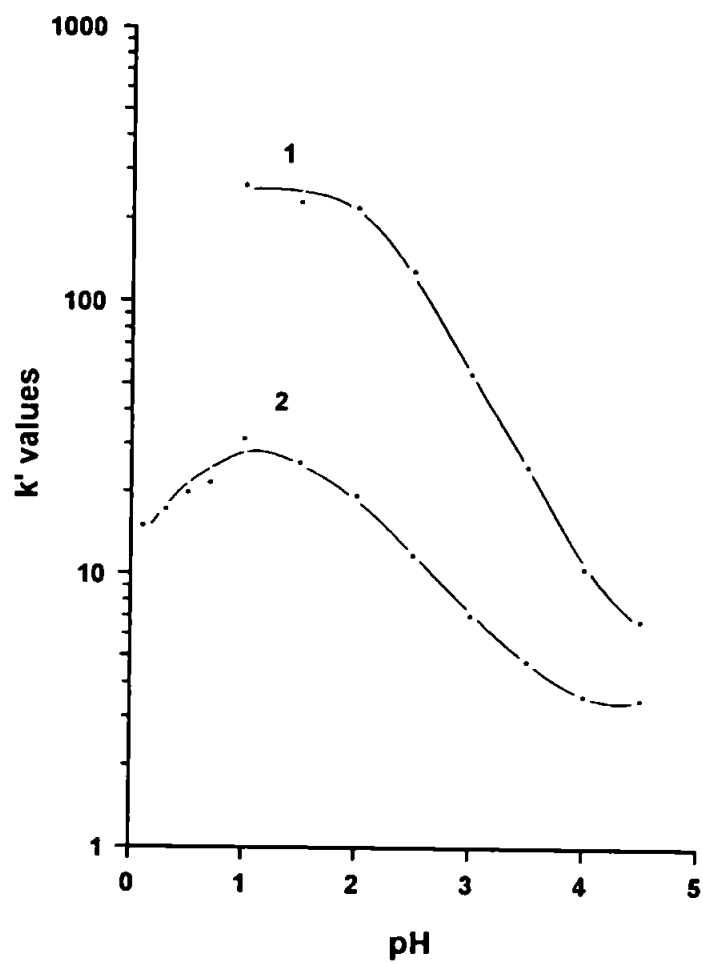


Figure 5.13. The dependence of capacity factors for chlorodipicolinic acid (1) and dipicolinic acid (2) on eluent pH. Eluent: 1M KNO₃.

5.3.5.4.2 250mm PS-DVB column investigations

An attempt to improve the selectivity and performance of the chlorodipicolinic acid system was made by increasing the column length to 250mm, and further investigating the effect of ligand concentration in the eluent on metal retention characteristics with pH. More detailed k' plots were produced over a wider pH scale, and more metal ions investigated, namely U(VI), Fe(III), Al(III), Lu(III) and La(III). From these investigations, it appeared that a concentration of 0.25 – 0.5mM ligand in the eluent was optimal for the separation of transition metal ions. The k' vs. pH plot for metal ions at 0.5mM chlorodipicolinic acid concentration in the eluent is given in Figure 5.14, with the separation of seven metals at pH 2 given in Figure 5.15. The equivalent k' plot with 0.25mM chlorodipicolinic acid in the mobile phase is given in Figure 5.16, the best separation of a transition metal suite achieved at pH 2.2 (Figure 5.17). As with the dipicolinic acid column, it is apparent that U(VI) is very strongly retained. Fe(III) is also strongly retained which is in contrast to Al(III), which is more weakly retained than the divalent metal ions at low pH.

From the k' plots and chromatograms shown, complete resolution of the transition metals was not feasible with a 250mm column length, due to complex retention behaviour, most noticeably with the reduction in Cu(II) retention at a low pH (<2) whilst other metal ions were increasing in retention in this region. Whether this is due to the ligand present in the mobile phase is uncertain. Nevertheless, this complex retention pattern of overlapping and interfering between metal ions, complicated the separation profile, especially between Cu(II), Pb(II) and Cd(II).

To overcome this problem and obtain a virtually complete resolution of the transition metal mixture, column efficiency was increased further by addition of a 50 · 4.6mm column, resulting in a total column length of 300mm. Figure 5.18 illustrates the separation of seven transition metal ions at pH 2.2, in a mobile phase containing 0.25mM chlorodipicolinic acid.

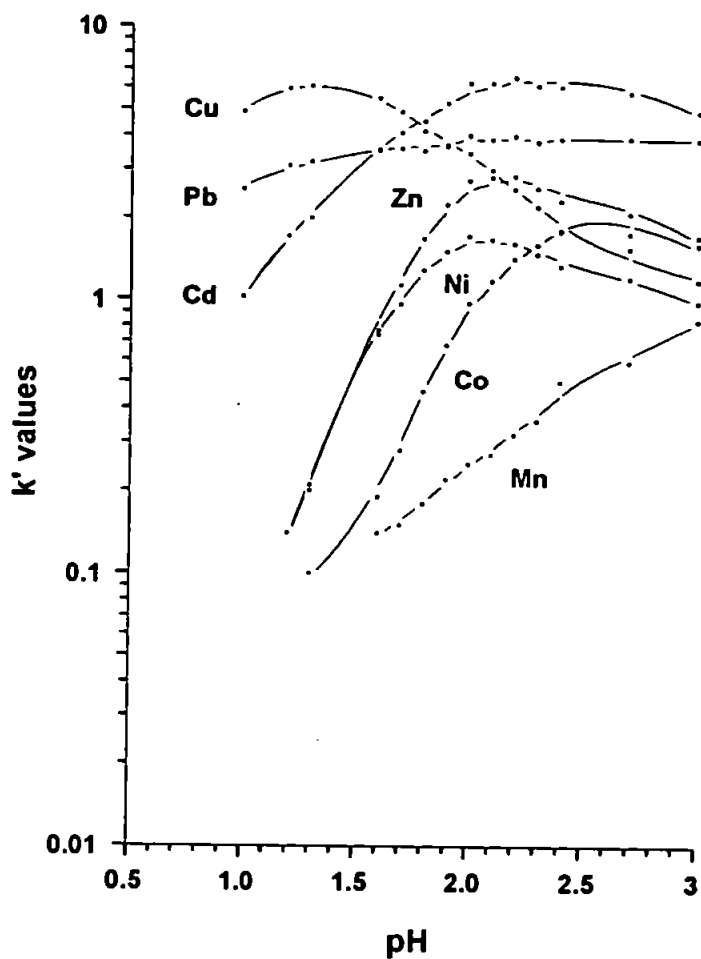


Figure 5.14. The dependence of capacity factors for transition and heavy metal ions on eluent pH. Eluent: 1M KNO_3 , 0.5mM chlorodipicolinic acid.

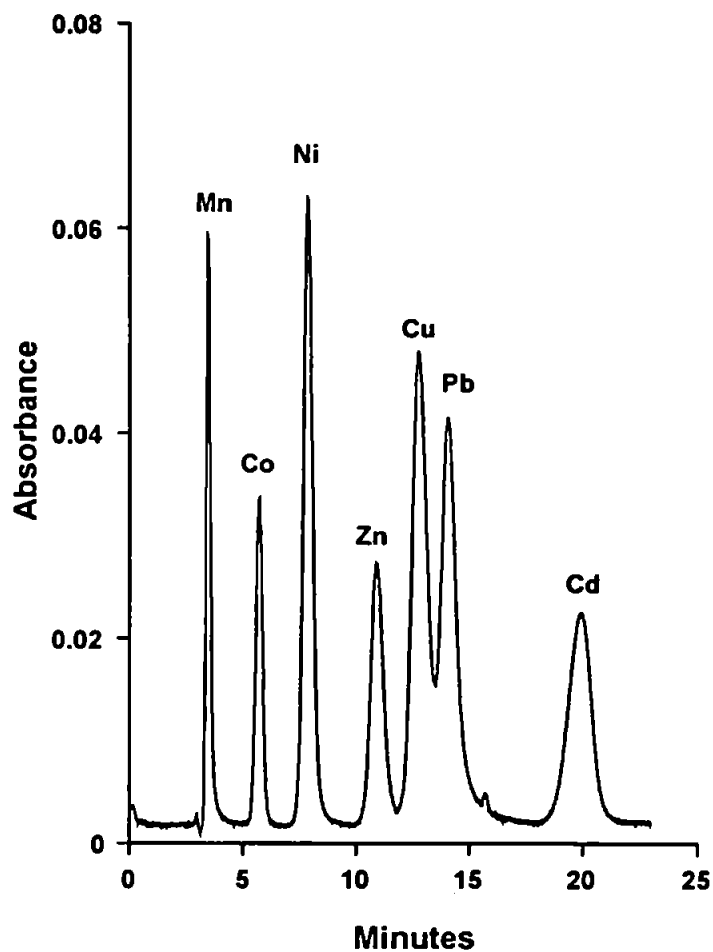


Figure 5.15. The separation of Mn(II) 0.5 mg l⁻¹, Co(II) 0.5 mg l⁻¹, Ni(II) 0.5 mg l⁻¹, Zn(II) 2 mg l⁻¹, Cu(II) 2 mg l⁻¹, Pb(II) 10 mg l⁻¹ and Cd(II) 20 mg l⁻¹ on a 250 · 4.6mm PRP-1 7µm PS-DVB Column. Eluent: 1M KNO₃, 0.5mM chlorodipicolinic acid and 10mM HNO₃ (pH 2). Detection: PAR at 490nm.

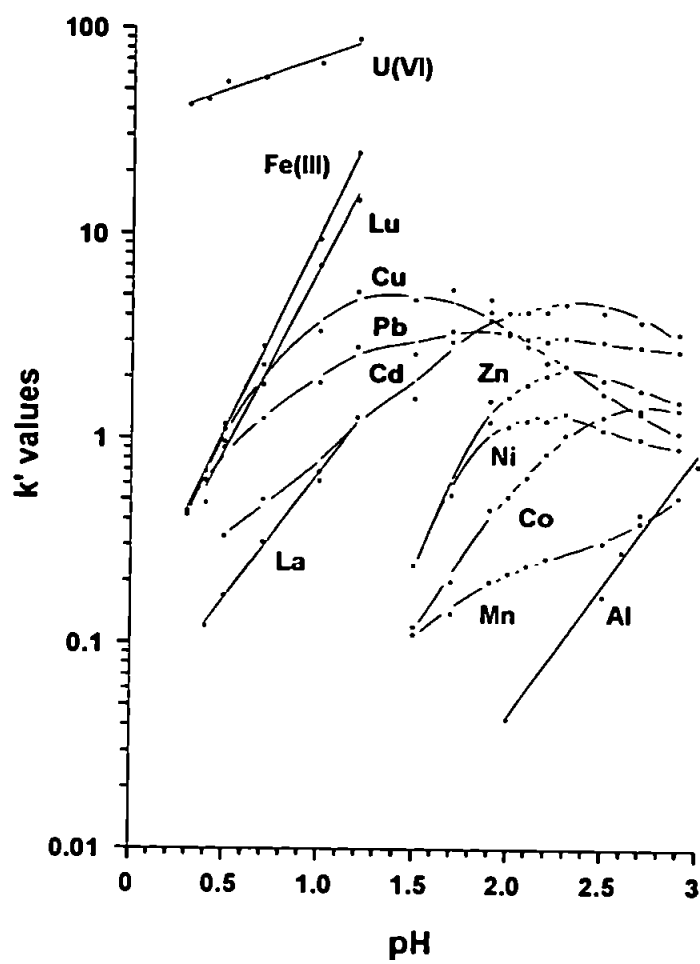


Figure 5.16. The dependence of capacity factors for selected metals on eluent pH. Eluent: 1M KNO_3 , 0.25mM chlorodipicolinic acid.

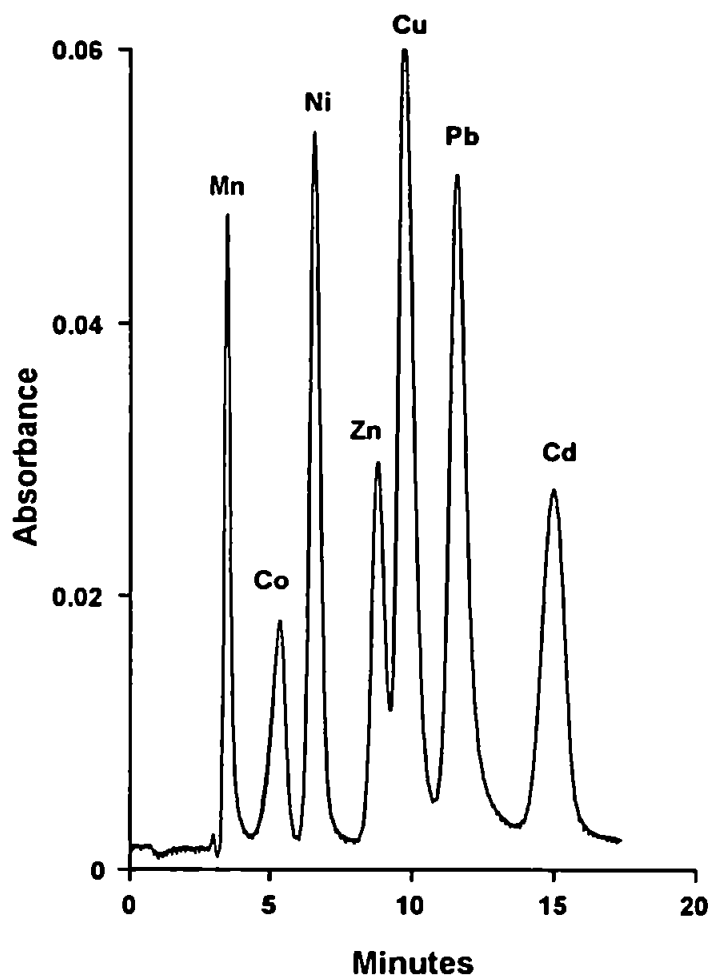


Figure 5.17. The separation of Mn(II) 0.5 mg l⁻¹, Co(II) 0.5 mg l⁻¹, Ni(II) 0.5 mg l⁻¹, Zn(II) 2 mg l⁻¹, Cu(II) 2 mg l⁻¹, Pb(II) 10 mg l⁻¹ and Cd(II) 20 mg l⁻¹ on a 250 · 4.6mm PRP-1 7µm PS-DVB Column. Eluent: 1M KNO₃, 0.25mM chlorodipicolinic acid and 6mM HNO₃ (pH 2.2). Detection: PAR at 490nm.

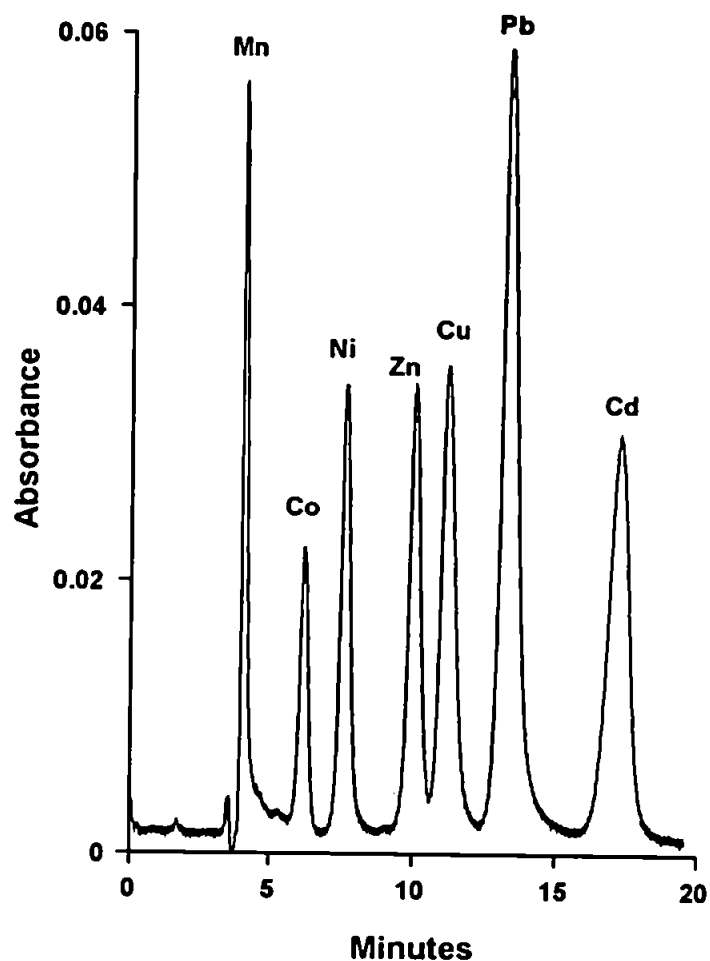
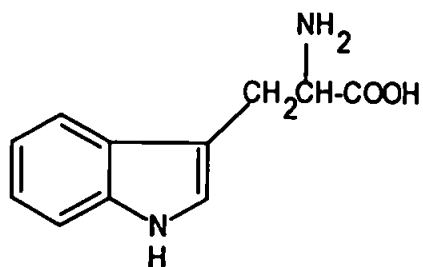


Figure 5.18. The separation of Mn(II) 0.5 mg l⁻¹, Co(II) 0.5 mg l⁻¹, Ni(II) 0.5 mg l⁻¹, Zn(II) 2 mg l⁻¹, Cu(II) 1 mg l⁻¹, Pb(II) 10 mg l⁻¹ and Cd(II) 20 mg l⁻¹ on a 300 · 4.6mm PRP-1 7µm PS-DVB Column. Eluent: 1M KNO₃, 0.25mM chlorodipicolinic acid and 6.25mM HNO₃ (pH 2.2). Detection: PAR at 490nm.

5.3.6 L -Tryptophan



RMM 204.2 HL pK_a 9.57 [163]

In addition to the study of heterocyclic carboxylic acids as chelating agents in dynamic systems, other molecules were investigated.

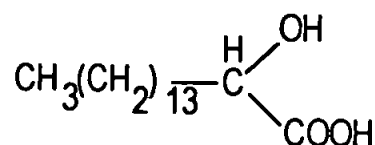
L - tryptophan is an amino acid that can act as a N,O chelator, through its carboxyl group and amino nitrogen. The acid dissociation constant of this molecule is high, making it a very weak acid, weaker than any of the organic acids investigated thus far. It should therefore have a very strong conjugate base, and complex metal ions actively. From the sparse stability constant data available, it does form a strong complex with Fe(III) ($\log K_1 = 9.0$) though this is weaker for Fe(II) ($\log K_1 = 3.4$) [163].

Upon adding this ligand to the mobile phase (1M KNO₃) at a concentration of 1 or 0.1mM, however, there was very little retention of any metal ions over the pH range 1.5 – 4.5. A noticeable exception on a 100mm PS-DVB column was Cu(II) ($k' = 28.1$ at pH 2.7) and U(VI) ($k' = 6.0$ at pH 3.5), in an eluent containing 1mM L – tryptophan. Peak shapes were broad but quite symmetrical. A tentative elution order on this column was:

Mn(II)<Zn(II)<Cd(II)<Pb(II)<U(VI)<Cu(II) at pH 3.5. La(III) and Lu(III) were also very weakly retained. Due to the poor retention, metal ion separations were not feasible. This might be a result of the dynamic modification of the substrate, which is uncertain considering the aromatic group on this molecule, or it could be attributed to a strong influence from the ligand in the mobile phase. An attempt was made to assess the dynamic

modification of polystyrene by L – tryptophan, but a repeat injection of 0.1M was not detected as a peak at 280nm. Whether this could be the result of on-column degradation in the eluent (1M KNO₃ at pH 2) or very strong retention (> 100 minutes) is uncertain, though unlikely to be the latter based on the poor metal retention results.

5.3.5 2-hydroxyhexadecanoic acid



RMM 272.4

This carboxylic ‘fatty’ acid is an O,O chelator, and the weakest ligating system in acidic solutions of the types investigated in this chapter. The long alkyl chain might reduce steric effects associated with the resin backbone, moving the donor atoms away from this region to freely access the solute metals.

Unfortunately, it appeared that there was a critical H⁺ concentration above which this molecule formed micelles in aqueous solution, due to the insoluble hydrophobic long carbon chain and the polar hydrophilic carboxyl group. Thus, this acid is amphipathic, having both polar and non-polar ends. The critical point was reached at about pH 9, which made this molecule unsuitable as a chelating agent in a dynamic system. Indeed, the acid precipitated out of solution below about pH 5, confirming its status as insoluble in water [242].

It was therefore decided to try and impregnate this molecule onto PS-DVB. A 0.1mM solution of this acid was loaded overnight at pH 9.5 onto a 100mm column packed with 9µm PS-DVB. A high ionic strength acidic eluent might retain the fatty acid on the column, due to the ‘salting out’ principal. The retention of metal ions on this column, over

the pH range 3.5 – 5 was examined over a week. Retention was poor, but metals were held up after this period, indicating that a portion of this molecule was impregnated into the pore structures. In an eluent of 1M KNO₃, Cu(II) was retained the most strongly ($k' = 7.2$ at pH 3.5 and 15.9 at pH 4), with Pb(II) being retained at a higher pH ($k' = 4.7$ at pH 5). Peak shapes were also very poor, being extremely broad with bad tailing. The elution order was Mn(II)<Zn(II)<Cd(II)<Pb(II)<Cu(II) in 1M KNO₃. Lu(III) was very weakly retained on this column. The molar capacity of the column was very low, calculated at 0.002mM Cu(II) /g resin.

An attempt was made to dynamically load this acid onto the 100mm silica gel column, using a method devised by Cassidy and Elchuk [243]. In this instance, the acid (0.25mM) was loaded overnight using a mixture of Milli-Q water and acetonitrile (57:43ml) the solvent added to keep the reagent in solution. However, subsequent retention of metal ions was still very poor using an eluent of 1M KNO₃, most metals eluting near the solvent front at pH 3.5 – 4, with the exception of Cu(II) ($k' = 2.7$ at pH 3.5).

5.4 Summary

This study has demonstrated that an effective metal chelating substrate can be dynamically formed in the presence of low molecular weight carboxylic acids in the eluent, giving rise to the separation of selected transition metals, certain heavy metals and uranium with good efficiency.

Dynamic modification thus should allow the use of different chelating compounds to be temporarily sorbed onto a substrate to meet analysis requirements, with the substrate amenable to stripping and re-coating with another chelating agent if necessary.

The neutral polystyrene resins were found to be a better substrate for the purpose of dynamic coating than C₁₈ silica, though other bonded silica gel matrices might produce different characteristics.

The size and structure of the acid is very important, as shown by the very weak ability of picolinic acid to act as a dynamic chelating exchanger in comparison with quinaldic acid. The addition of π -electron accepting groups to the pyridine ring can also improve the dynamic loading, as illustrated with the bonding of a chloride atom to dipicolinic acid. It would appear that heterocyclic organic acids with aromatic characteristics are the most suitable for this type of chelation exchange process, based on the poor results achieved with L – tryptophan and 2-hydroxyhexadecanoic acid.

The concentration of the acid in the mobile phase is also a key factor for the attainment of optimum separating ability on the column.

Interesting selectivity differences were found between the different acid coatings with pH. For example, for divalent metal ions, the retention order on quinaldic acid was:

$\text{Mn(II)} < \text{Pb(II)} < \text{Cd(II)} < \text{Zn(II)} < \text{Ni(II)} < \text{Cu(II)}$ regardless of pH, indicating that retention on the substrate surface was dominant. However, with dipicolinic acid, the retention order altered with pH in a complex manner, being

$\text{Mn(II)} < \text{Co(II)} < \text{Ni(II)} < \text{Zn(II)} < \text{Cd(II)} < \text{Pb(II)} < \text{Cu(II)}$ near its isoelectric point. U(VI) was strongly held and Cu(II) weakly retained on a dipicolinic acid coated column, which was reversed when a carboxyl group was removed with picolinic and quinaldic acid, illustrating the varying affinities of metal ions for N,O and N,O,O chelating groups.

A separation of seven resolved transition metals within 20 minutes was achieved on a 300mm PS-DVB resin modified with chlorodipicolinic acid at pH 2.2, with good peak symmetry. These metals could be resolved in under 8 minutes on a 100mm column at pH 1.2, with the exception of Zn(II), Cu(II) and Pb(II), demonstrating the potential of this separation system.

The further study of this approach to metal ion separation, together with the development of systems for the analysis of real samples is given in the next chapter, including the effect of large concentrations of matrix metals such as the alkaline earths on the dynamically modified substrate.

Chapter 6. Determination of Trace Metals in Environmental Samples using Dynamically Modified Substrates.

Part 1. Determination of Uranium in a Stream Sediment and Complex Aqueous Matrices.

6.1 Introduction

Uranium, the fourth member of the actinide series, has the atomic number 92, atomic mass 238.03, and oxidation states ranging from +2 to +6, though the dominant state is U(VI), usually in the form of the linear uranyl ion UO_2^{2+} . It is also one of the densest metals, being 19.07g cm^{-3} at 25°C [218].

It is a ubiquitous element, being one of only a few actinides present in the upper layers of the earth in amounts sufficient for practical extraction. The earth's crust contains about $2.4\mu\text{g g}^{-1}$ of this metal [189], the chief ores being uraninite (pitchblende) U_3O_8 and carnotite [$\text{K}_2(\text{UO}_2)_2(\text{VO}_4)_2 \cdot 2\text{H}_2\text{O}$] [244]. The abundance of uranium in ocean water with a salinity of 35‰ is given as $3.3\mu\text{g l}^{-1}$, with a residence time of $5 \cdot 10^5$ years, possibly dissolved as $\text{UO}_2(\text{CO}_3)_3^{4-}$ [245].

Uranium has two long-lived isotopes which occur naturally, ^{235}U ($T_{1/2} = 7.04 \cdot 10^8$ years) and ^{238}U ($T_{1/2} = 4.46 \cdot 10^9$ years) eventually decaying to the stable lead isotopes ^{206}Pb and ^{207}Pb respectively [189]. It is ^{235}U which is the only naturally occurring nucleus that can be split when bombarded by neutrons. This fissionable nucleus constitutes only 0.72% of natural uranium, and so is separated from the bulk ^{238}U (99.27%) by various techniques including laser irradiation, which can break a $^{235}\text{U-F}$ bond while leaving a $^{238}\text{U-F}$ bond intact, resulting in a mixture of solid $^{235}\text{UF}_5$ and gaseous $^{238}\text{UF}_6$ [246].

The main use of uranium is as a nuclear fuel, other minor applications including addition to ship ballast's, aeroplane counterweights and glass colourings.

Due to the radioactive nature of uranium and its decay products, together with its continued role in the nuclear industry, this metal instils environmental concern. It is a highly toxic metal, as are its salts, able to readily complex with the phosphate containing mineral matrix of bone, and bind to a multitude of biomolecules including proteins [189]. This can lead to renal damage and acute arterial lesions, a lethal intake stated as 36mg in rats [246].

Emissions of uranium during mining and processing are generally low, but significant increases above natural levels can occur in local aquatic systems via accumulative input from waste streams. Another significant source of pollution is posed by the sudden (Chernobyl 1986, Three Mile Island 1978) or insidiously gradual (leaching of disposed waste) release of radioactive material into the local environment.

Due to these risks, and requirements for environmental monitoring, a number of chromatographic techniques have been developed to determine this metal in various sample types. Using ion chromatography with a cation exchange column, Byerley *et al* determined U(VI) in process liquors using an ammonium sulfate/ sulphuric acid eluent [247], Beer and Coetzee separated and determined U(IV) and U(VI) in uranium compounds using a magnesium sulfate/ sulphuric acid eluent [248], whilst Al-Shawi and Dahl determined uranium and thorium in nitrophosphate fertiliser solution using either hydrochloric acid or nitric acid together with ammonium sulfate in the eluent [249].

Another system utilised a preconcentration step on an IDA functionalised chelating resin, followed by cation exchange with a hydrochloric acid/ sodium sulfate, for the determination of uranium and thorium in natural waters and geological materials [250].

Investigations with reversed phase liquid chromatography (RP-HPLC), using complexing agents in the eluent as a method to separate and determine uranium and other actinides, has also received particular interest.

Cassidy and co-workers [251-253], reported using α -hydroxyisobutyric acid (HIBA) to study fission products in uranium dioxide, thorium – uranium fuels and uranium ore

refining processes. Similar methods have been demonstrated by Barkley *et al* to determine uranium and thorium in mineral ores [254], and by Haddad *et al* [255], for uranium and thorium in mineral sands [256], nitrophosphate solution [257] and spiked seawater [258]. Other complexing agents which have been studied include mandelic acid [226], glycolic acid [259] and *bis*(salicylaldehyde)propylenediimine [260].

All these methods incorporated post-column spectrophotometric detection with either PAR [247] or Arsenazo III [248-259], with the exception of [260], which utilised UV detection of the uranium complex species at 260nm.

Many of the IC and RP-HPLC systems mentioned above displayed good separation and detection qualities for uranium and other actinides. However, when determining these metals in complex matrices, for example in the presence of large amounts of other metals, some of the systems lose their capacity, which can result in the column being unable to resolve analyte peaks. An example of this is the HIBA system with a reversed phase column [251]. In the presence of a high concentration of Fe(III), the system loses its ability to separate uranium from thorium. This problem can often be overcome using matrix elimination steps, but these can be either time consuming or increase the complexity of the adsorption or separation system.

As already illustrated in Chapter 4, HPCIC can be used to determine one metal in a vast excess of matrix metals, without upsetting the chromatographic system and performance characteristics.

Low efficiency chelating substrates have been used to preconcentrate and extract uranium from various sample matrices. These include commercial resins such as U/TEVA.spec [261-265] and TRU-spec [266] (EiChrom, IL, USA) which contain diphosphonic groups attached to a polystyrene matrix. Other chelating sorbents which have been investigated include lanthanum ammonium oxalate [267], TAR immobilised onto polystyrene [268] and phosphonic acid derivatised polystyrene [269].

Few studies using HPCIC, however, have centred on the heavy elements such as the actinides. A PS-DVB column was impregnated with the chelating dyestuff methylthymol blue (IDA functionality) to determine the trace uranyl ion in saline samples [270]. Similarly, two neutral polystyrene resins were impregnated with either calmagite or PAR, both azo dyestuffs, to separate uranium from thorium [225].

In addition to using hydrophobic dyes as chelating ligands, a short study was undertaken using a hypercrosslinked polystyrene resin, MN200, dynamically modified with dipicolinic acid [225]. Using this column, U(VI) was successfully separated from Fe(III), La(III) and Th(IV), which illustrated the potential of dynamic modification using this organic acid as a tool for the separation and determination of U(VI) in complex matrices. Results given in the preceding chapter, using a standard low crosslinked polystyrene polymer dynamically coated with dipicolinic acid also displayed promising properties for separating uranium from other metal ions.

The aim of this study was to further investigate this system of dynamic modification of a neutral substrate with dipicolinic acid, together with the development of a method for determining uranium as the uranyl ion in complex matrices, including sea water, and a certified stream sediment.

6.2 Experimental

6.2.1 Instrumentation

The isocratic HPCIC system is described in section 2.2.1, with the exception that the PEEK sample loop size was 500 μ l. The analytical column was a PEEK (100 · 4.6mm I.D) casing, packed with PRP-1 7 μ m PS-DVB (Hamilton).

6.2.2 Reagents

Two post-column reagents were used in this study.

- (a) A mixture of 0.15 mM Arsenazo III and 10mM urea in 1M HNO₃, with detection at 654nm (The UV-Vis spectrum of U(VI) with this PCR is given in Figure 6.1), and
- (b) A mixture of 0.12 mM 4-(2-pyridylazo)-resorcinol (PAR), 2.6 M ammonia and 0.85M ammonium nitrate (pH 10.2), with detection at 490nm.

The eluent consisted of 1M KNO₃, 0.5M HNO₃ and 0.1mM dipicolinic acid solution. Both the eluent and PCR were delivered at 1ml min⁻¹.

All reagents were of AnalaR grade (BDH, Poole, U.K), with the exception of Arsenazo III (95% dye content) (ICN Biomedicals Inc., Aurora, OH, USA), dipicolinic acid (99% purity) (Aldrich, Gillingham, UK) and PAR (Fluka, Glossop, UK).

1000mg l⁻¹ metal stock solutions (BDH) were diluted to working standards using distilled deionised water (Milli-Q, Millipore, Milford, MA, U.S.A), and stored in poly-(propylene) bottles (BDH).

6.2.3 Sample Pre-treatment

Mr D. Henon, of the University of Plymouth, UK, kindly performed the standard reference digestions.

The stream sediment sample, national research centre certified reference material (GBW07311, LGC, Middlesex, UK), was prepared using hydrogen fluoride digestion. The fluoride ion does not complex with uranium in solutions of high acidity so will not interfere with the separation and detection systems.

For the digestion procedure, a known amount of accurately weighed sample (approximately 0.5 g) was added to a PTFE vessel together with 10 ml HNO₃, capped and left on a hot-plate (120°C) for 24 hrs. 2 ml of HF was added and left on the hot-plate for a further 48 hrs. The vessel was uncovered, 4 ml HNO₃ added, and the HF and HNO₃ evaporated at 120°C. The residue was transferred to a volumetric flask with small quantities of 0.5M HNO₃, 0.9 g boric acid added to dissolve any insoluble fluorides, and then made up to a final volume of 50 ml using 0.5M HNO₃.

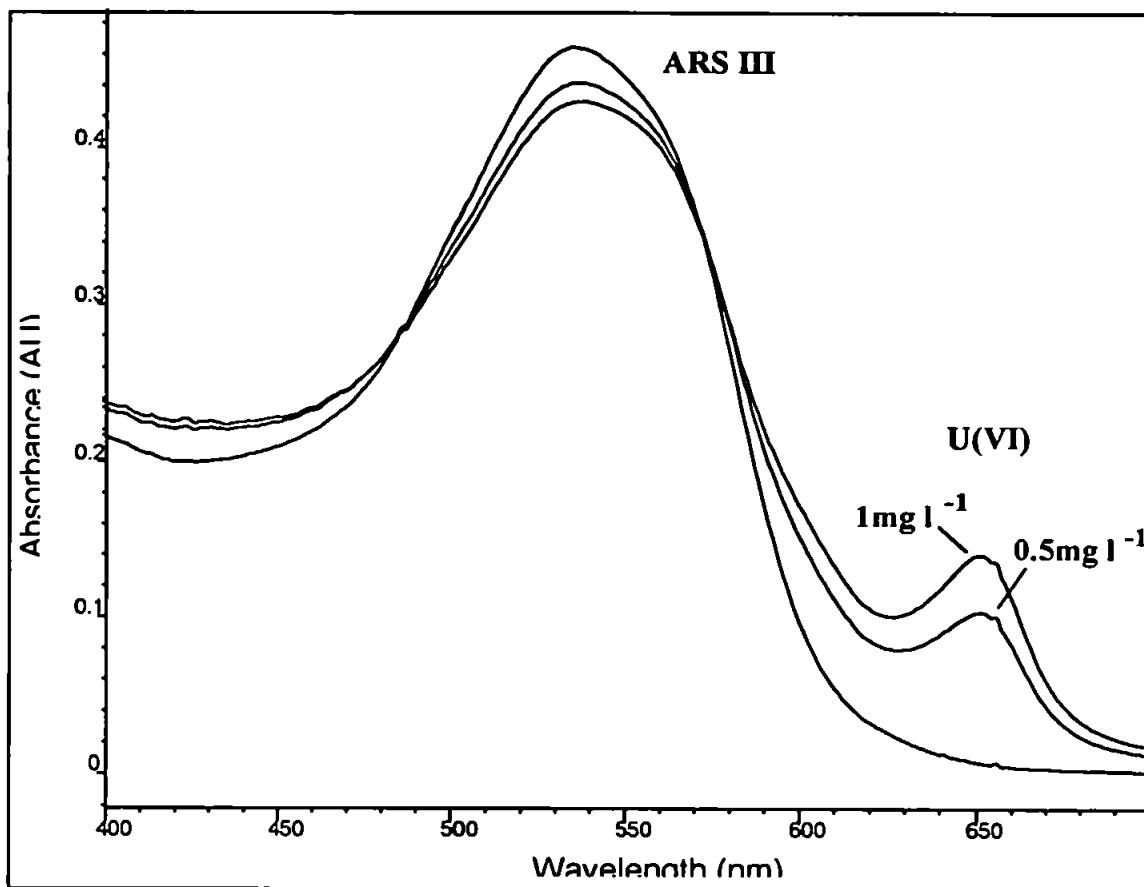


Figure 6.1. Absorbance spectra of U(VI) with the Arsenazo III post column reagent.

6.3 Results and Discussion

6.3.1 Retention Characteristics of Uranium on the Dynamically Modified Substrate

As previously mentioned, the N,O,O chelating dipicolinic acid dynamically adheres to the PS-DVB stationary phase through a combination of hydrophobic and π - π interactions between the aromatic group on the acid and the benzene groups on the resin.

An increase in the mobile phase pH will increase the complexation ability of this acid, in accordance with an increase in the dissociation of the carboxyl groups ($pK_1 = 2.1$, $pK_2 = 4.68$ [162]). U(VI) is known to form a much stronger complex with this ligand than Th(IV) [225] and most of the transition and heavy metals investigated in Chapter 5.

To determine the concentration of chelating agent required in the eluent so that the sorbed layer on the substrate would exhibit dominant metal retention characteristics, with minimal interference from the same ligand in the mobile phase, $\log k'$ plots were studied. These are given in Figure 6.2, for U(VI) and Fe(III), altering the dipicolinic concentration from 0.01mM to 1mM in the eluent. Other trivalent ions such as the lanthanides and aluminium are not shown as they exhibited minimal retention over the pH range studied.

Figure 6.2 shows some particularly interesting features. As illustrated throughout this thesis, chemically bonded or impregnated chelating phases usually give linear or S shaped k' curves, but dynamic modification provides a more complex picture. The first factor associated with this effect is that the concentration of the dynamically sorbed layer does not stay constant with change in pH (Figure 5.13). The second, equally important factor is that the concentration of the chelating agent in the mobile phase has a potential for competing with the sorbed layer for the metal ion. This is most likely to be a maximum at high pH, when the acidic groups on the ligand become highly dissociated. Referring again

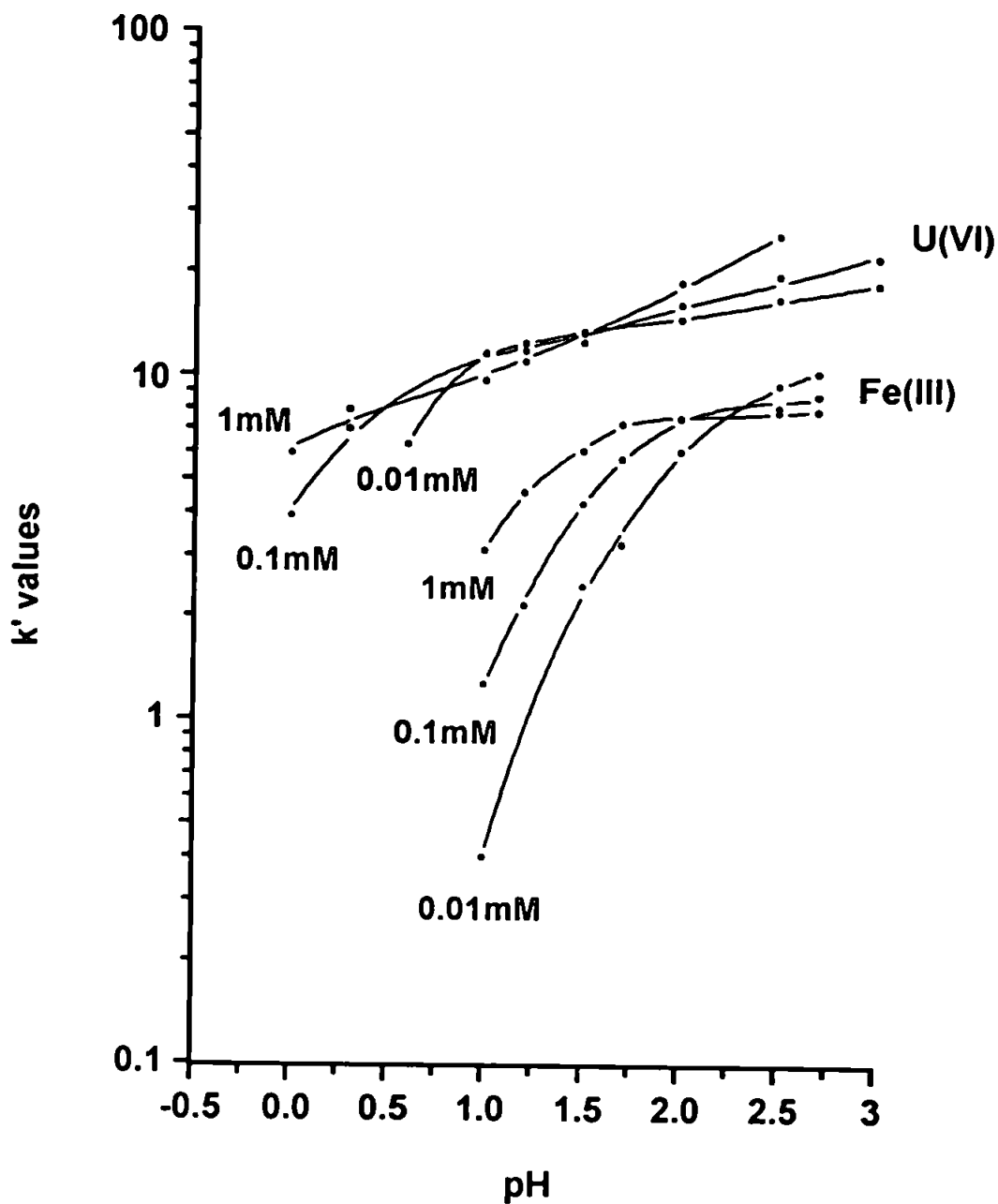


Figure 6.2 The dependence of capacity factors for U(VI) and Fe(III) on eluent pH. Eluent: 1M KNO_3 with various concentrations of dipicolinic acid adjusted to the appropriate pH with HNO_3 .

to Figure 6.2, it can be seen that there is a fairly rapid increase in $\log k'$ in strong acid, where the conditional stability constants will be very low. However, rather than continuing to increase steeply with pH, as normally expected, both Fe(III) and U(VI) plots become very shallow and almost horizontal in some cases. Furthermore, the plots for the different concentrations of dipicolinic acid show 'crossovers' which are also unexpected. Clearly, these plots reflect the fact that the situation with dynamic coating is very complex, as demonstrated for the transition and heavy metals in Chapter 5.

As the pH is raised above the isoelectric point, the sorbed layer concentration will decrease. At the same time the conditional stability constants are increasing both on the substrate and in the mobile phase. It appears that these effects more or less balance each other above about pH 1.5, so that there is not much change in retention with further increase in pH.

Nevertheless, as long as the chromatography is stable and reproducible at the specified pH, as already demonstrated in the preceding chapter, then these $\log k'$ plots are useful for finding the parameters for optimum separation and selectivity.

It is clear that dipicolinic acid loaded columns show a special selectivity for U(VI) against virtually all other +2 and +3 metal ions, particularly below pH 1, and therefore this can be exploited for uranium determination in complex samples. Figure 6.3 shows the separation of Fe(III) and UO_2^{2+} demonstrating the good selectivity of the dynamically loaded column at pH 1.

6.3.2 Method Development – Separation Conditions

As already mentioned in Chapter 5, the resin particle size can have an affect on the dynamic loading of dipicolinic acid due to changes in hydrophobicity. However, the relative hydrophobicity might alter, dependant upon the resin manufacturer and

polystyrene divinylbenzene synthesis procedure. Table 6.1 illustrates the k' values for dipicolinic acid and the corresponding retention of U(VI) on three resins.

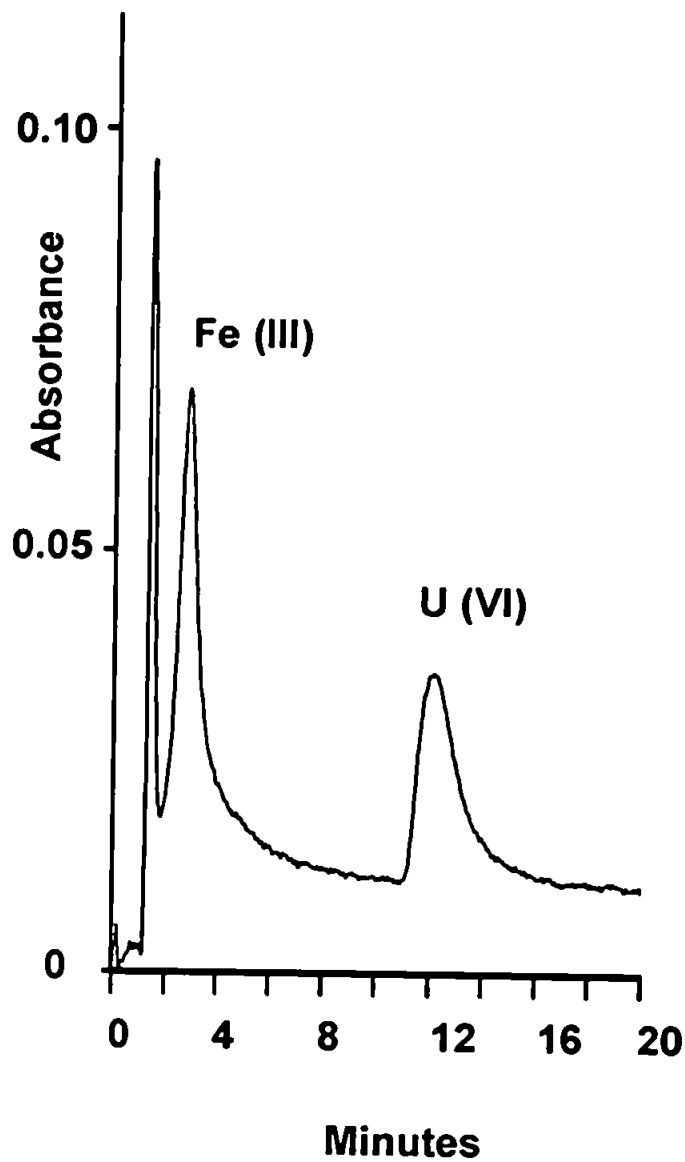


Figure 6.3 The separation of U(VI) 20mg l^{-1} from Fe(III) 2mg l^{-1} on a $100 \cdot 4.6\text{mm}$ PRP-1 $7\mu\text{m}$ PS-DVB column. Eluent: 1M KNO_3 , 0.1M HNO_3 (pH 1) and 0.1mM dipicolinic acid. Detection: PAR at 490nm .

Table 6.1 Effect of particle size on the dynamic loading of dipicolinic acid and corresponding retention for U(VI) on the modified substrate. Column length 100 · 4.6mm. Eluent: 1M KNO₃, including 0.1mM dipicolinic acid for the U(VI) studies.

Manufacturer	Particle size μm	Pore size \AA	k' Dipicolinic acid		k' U(VI)		
			pH 1	pH 2	pH 1	pH 1.5	pH 2
Polymer Labs	8	120	-	17.6	-	11.0	-
Hamilton	7	100	31.4	19.3	11.5	13.0	16.0
Polymer Labs	5	120	33.7	22.2	11.0	11.7	13.6

The results provide some confusing parallels. Although it appears that the dynamic loading does indeed increase as a result of decreasing particle size, there is not a similar trend with the retention of U(VI), as would be anticipated. This could be due to the structure of the resins dependant upon the manufacturer, and possibly the different pore sizes affecting the passage of U(VI) through the column. It is also possible that the different k' values are merely a result of statistical variation, as the variations are not too large. A more detailed study is advised to fully evaluate the affect of resin type and particle/ pore size on the degree of dynamic modification and subsequent metal retention. Due to availability, the Hamilton PRP-1 7 μm polystyrene divinylbenzene column was used as the stationary phase.

A concentration of 0.1mM dipicolinic acid was deemed sufficient for producing a stable dynamic layer on the polystyrene resin. The reasons for this are twofold. Firstly, U(VI) was strongly retained on the substrate at this concentration, with competition from the ligand in the eluent being relatively small, and secondly, as found in the previous chapter, the concentration of ligand in the eluent can adversely affect detection sensitivity using a chromogenic post column reagent.

With a concentration of 0.1mM dipicolinic acid in the mobile phase, a stable layer of this molecule on the substrate could be obtained within 2 hours, confirmed through repeat injections of a uranium standard. When the eluent was changed to one containing none of the chelating ligand, the dynamic coating was quickly lost through leaching of dipicolinic acid into the effluent, with virtually complete removal after 3 hours. This is also shown with the repeat injection of U(VI), given in Figure 6.4.

An acid concentration in the eluent of 0.5M HNO₃ (equivalent pH 0.3) was chosen, as this resulted in a retention time of under 10 minutes for uranium, ensuring an efficient analysis time. As found in previous studies [225] and in Chapter 5, this level of acidity produced excellent selectivity from all the common +2 and +3 charged metal ions and Th(IV). Thus, Fe(III), the lanthanides and Th(IV) all elute close to the solvent front. This was a significant discovery in that these metals can be associated with uranium in mineral and environmental samples, potentially causing problems in isolation and determination procedures.

As with all HPCIC studies, the eluent also contained a high concentration of KNO₃ to suppress ion-exchange interactions.

6.3.3 Method Development – Detection Conditions

The azo dye Arsenazo III (Figure 1.11) ($pK_8 = 10.9$ [163]) was selected as the post column reagent as it forms a sensitive 1:1 complex with uranyl ions in acidic solutions. Indeed, Arsenazo III is capable of forming coloured complexes with uranium at acid concentrations between 0.01 – 10M HCl, giving a molar absorption coefficient, ϵ , approaching $10^5 \text{ mol}^{-1} \text{ cm}^{-1}$ [102].

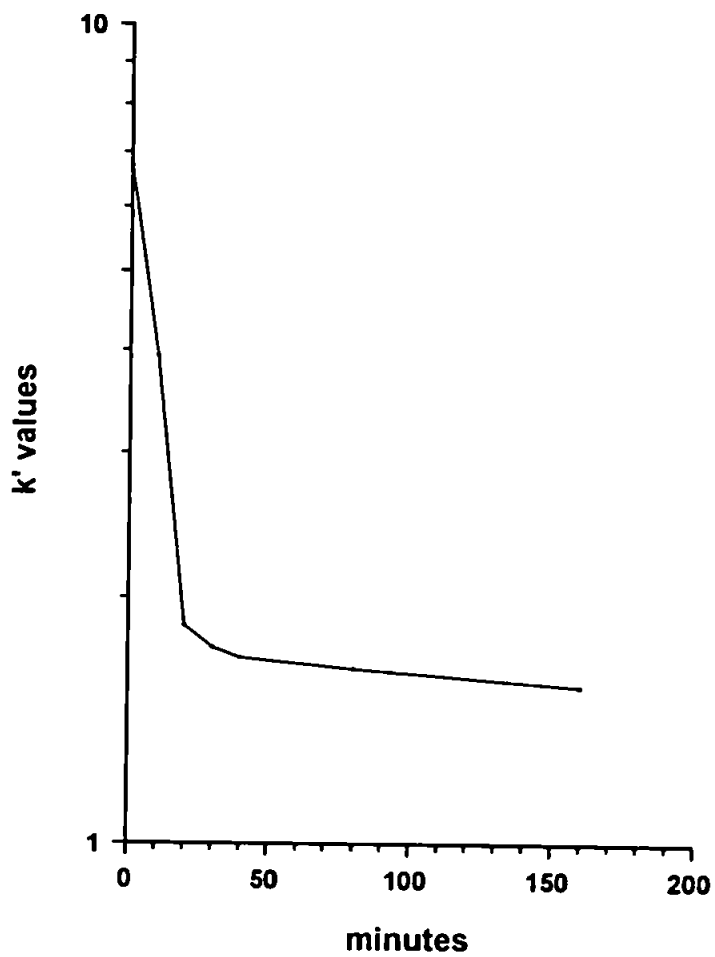


Figure 6.4 The leaching of dipicolinic from the 100 · 4.6mm PRP-1 7 μ m PS-DVB column, shown with the repeat injection of U(VI). Eluent: 1M KNO₃ 0.5M HNO₃.

An additional advantage of using this chromogenic ligand, is that with decreasing pH, the column selectivity towards uranium increases, reducing the interfering background absorbance due to other metals and so improving the sensitivity.

Initial studies utilised an Arsenazo III solution buffered with 10mM urea and 62mM acetic acid, as reported in a recent review on detection techniques for IC [106]. However, due to the highly acidic nature of the eluent, it was found that using a stronger acid solution of 1M HNO₃ in the PCR greatly improved the sensitivity of the chelating ligand for U(VI), giving an absorbance of 0.0005AU increasing to 0.0009AU for a 1mg l⁻¹ UO₂²⁺ standard with a 100µl sample loop. Arsenazo III is also very stable at this pH, which was demonstrated by the fact that the UV-Vis spectrum of the PCR changed very little over a three week period (a tenfold dilution gave an absorbance of 0.465AU freshly prepared, changing to 0.463AU with three weeks ageing. Detection at 535nm). A subsequent increase of acid in the PCR, to 2Molar, provided no additional benefits in sensitivity.

To further improve sensitivity, a short study on sample size optimisation was undertaken. A range of loop volumes were investigated, 100µl to 1ml, the results given in Figure 6.5. Changing from 100µl to a 1ml loop, a sixfold increase in sensitivity was recorded for uranium. Unfortunately, the 1ml loop volume exhibited significant tailing of the uranium peak. The 0.5ml loop provided the best compromise, giving a threefold increase in sensitivity without noticeably widening the uranium peak, taking into consideration the broadness of this metal in the dynamically modified system.

The affect of fluoride concentration in the sample is not as important for uranium, as it was for Be(II), due to the acidity of the mobile phase. The speciation diagram for U(VI) with F⁻ in acidic solutions is given in Figure 6.6, and essentially shows that U(VI) is not complexed at the very low eluent pH (by extrapolation). Therefore, uranium-fluoride species should not form in the mobile phase, which would otherwise elute the U(VI) on the solvent front, reducing the retained uranyl peak absorbance.

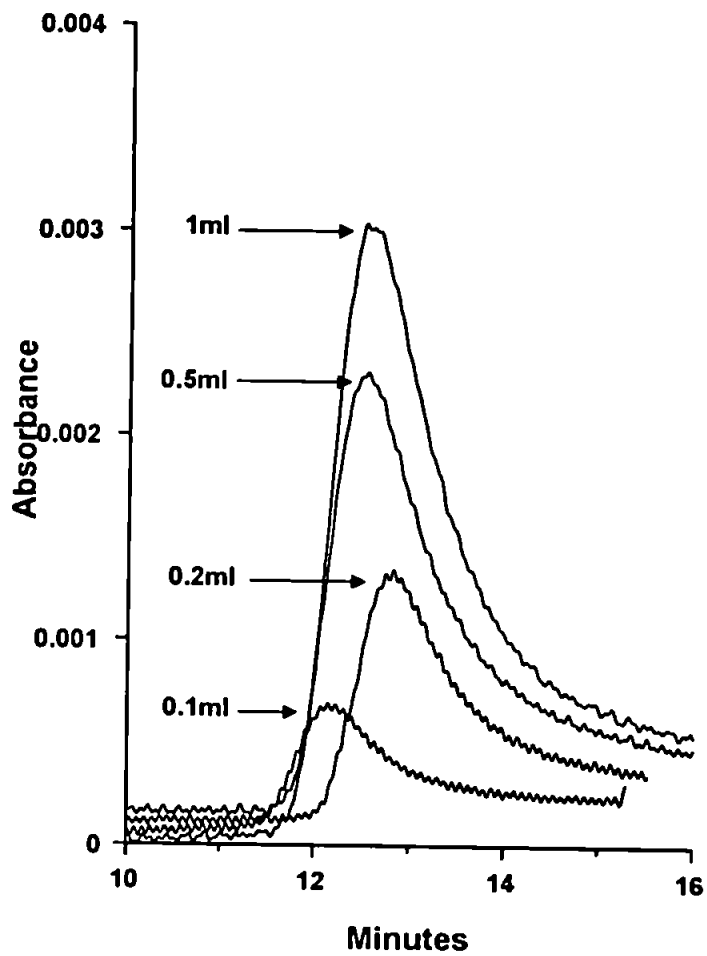


Figure 6.5 Effect of sample loop volume (100 μ l – 1ml) on the U(VI) peak, using a 100 . 4.6mm PRP-1 7 μ m PS-DVB column. Eluent: 1M KNO₃ 0.5M HNO₃ and 0.1mM dipicolinic acid. Detection: Arsenazo III at 654nm.

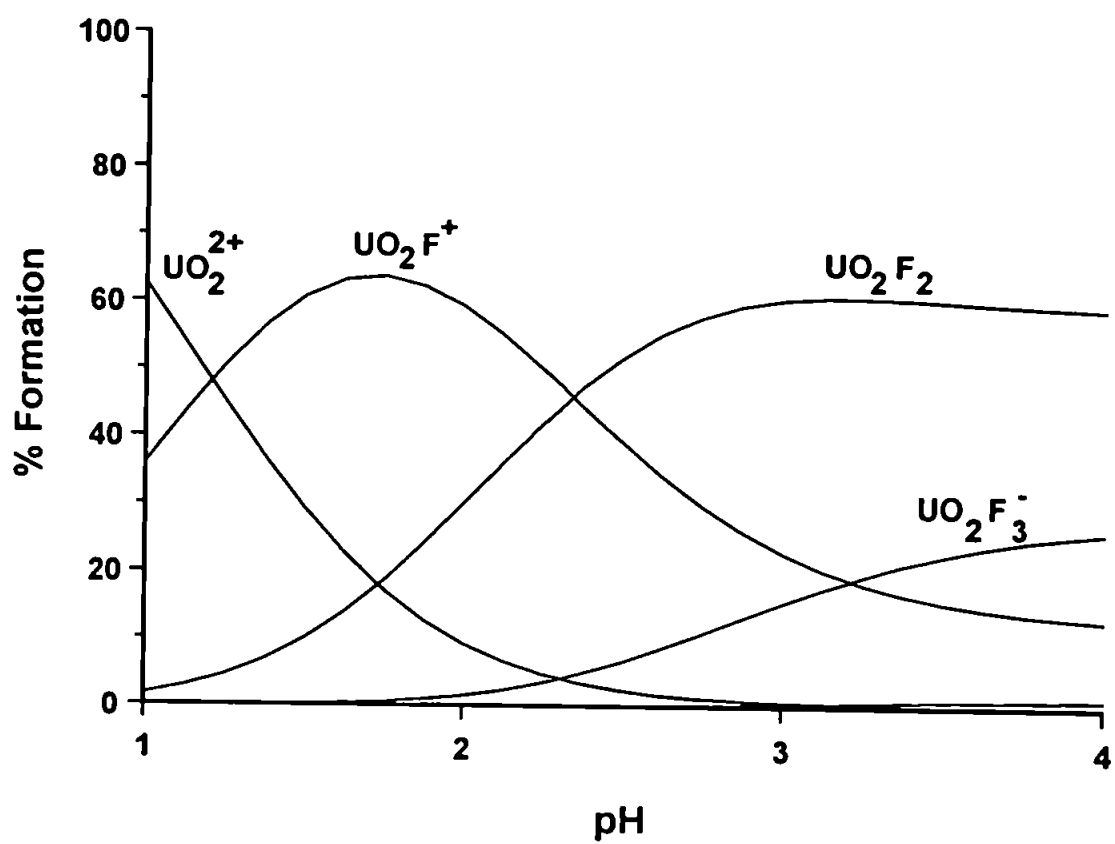


Figure 6.6 Speciation diagram of the uranyl ion UO_2^{2+} with the fluoride ion [163].

6.3.4 Analytical Characteristics for the Determination of Uranium

A calibration of U(VI) over the concentration range $25\mu\text{g l}^{-1}$ to 5mg l^{-1} , using the optimised eluent and PCR conditions, was undertaken to ascertain system performance. The linearity of the system was good with a regression coefficient of $r^2 = 0.9995$, using peak area. The detection limit was calculated as $20\mu\text{g l}^{-1}$, defined as 2 times the average peak to peak baseline noise.

To assess the accuracy of the method, a National Water Research Institute standard reference soft water sample, TMDA 54.2 (LGC) was analysed. A mean result ($n=6$) of $62.0 \pm 0.6\mu\text{g l}^{-1}$ was obtained for this work comparing well with the certified value of $62.3 \pm 13.1\mu\text{g l}^{-1}$. The reproducibility (%RSD) of the chromatographic method was calculated with repeat injections ($n=6$) of the certified sample and found to be 1.02% using peak area.

Although a good result was obtained for the certified reference soft water a more complex sample type was required to assess the affect of larger amounts of matrix metals. The proposed method was subsequently applied to more complex aqueous samples. There was a possibility that when analysing a sample containing a large concentration of matrix metals eluting close to the solvent front, the dynamically sorbed layer could be temporarily disturbed, leading to erroneous system peaks as the dynamic layer re-equilibrates, possibly interfering with the uranium peak. This was investigated by injecting various mixtures of Ca(II) and Mg(II) up to 1000mg l^{-1} of each into the eluent. No discernible effects upon either the baseline or uranium peak were noticed. A commercially available mineral water (Badoit, Danone, France) containing high concentrations of alkali and alkaline earth metals Ca(II) 190 mg l^{-1} , Mg(II) 85 mg l^{-1} , Na 150 mg l^{-1} and K 10 mg l^{-1} was spiked with $50\mu\text{g l}^{-1}$ uranium, and acidified with 0.5M HNO_3 . A standard addition calibration plot gave very good linearity, $R^2 = 0.9998$, producing a quantitative uranium recovery of

99.8%, which is indicative that the method is suitable for determining uranium in mineral water samples. A chromatogram of the spiked mineral water is shown in Figure 6.7.

Seawater was also selected to test the potential of this method, as it is an even more challenging matrix in terms of increased levels of alkaline earth metals and high ionic strength. With the production of waste samples containing this metal from the nuclear industry, uranium concentrations can fluctuate necessitating a requirement for methods to determine this actinide in brine solutions. As the open ocean seawater can contain about 3.5% total salts, most in the form of NaCl, many IC techniques have to incorporate complex matrix elimination and preconcentration steps to analyse these samples. However, utilising the HPCIC method, which can cope with high concentrations of salts, the uranium could be determined directly. An open ocean reference material NASS-4 (National research council certified reference material, LGC, Middlesex, UK), was spiked with 50 $\mu\text{g l}^{-1}$ giving a linear standard addition plot ($n=3$) of $R^2 = 0.9995$, with a uranium recovery of 95.6%. A chromatogram of the spiked seawater is shown in Figure 6.8.

As stated previously, for many of the commonly used techniques, the presence of large amounts of Fe(III) can cause problems with uranium determinations. To assess the ability of the dynamically loaded column to separate uranium from high concentrations of iron, a certified stream sediment, GBW07311, was analysed. Even with a 100 fold dilution after sample pre-treatment, the solution contained in excess of 800 mg l^{-1} matrix metals, namely Al(III) 500 mg l^{-1} , Fe(III) 300 mg l^{-1} , Mn(II) 25 mg l^{-1} , Zn(II) 4 mg l^{-1} and Cu(II) 1 mg l^{-1} . Nevertheless, with the optimised eluent conditions, these metals are unretained and co-elute on the solvent front with negligible tailing, causing minimal interference to the uranyl peak. Replicate sample analysis ($n=4$) with a standard addition calibration plot using peak area ($R^2 > 0.997$), gave a mean result of $8.6 \pm 0.3 \mu\text{g g}^{-1}$ which compared well with the certified value of $9.1 \pm 1.3 \mu\text{g g}^{-1}$.

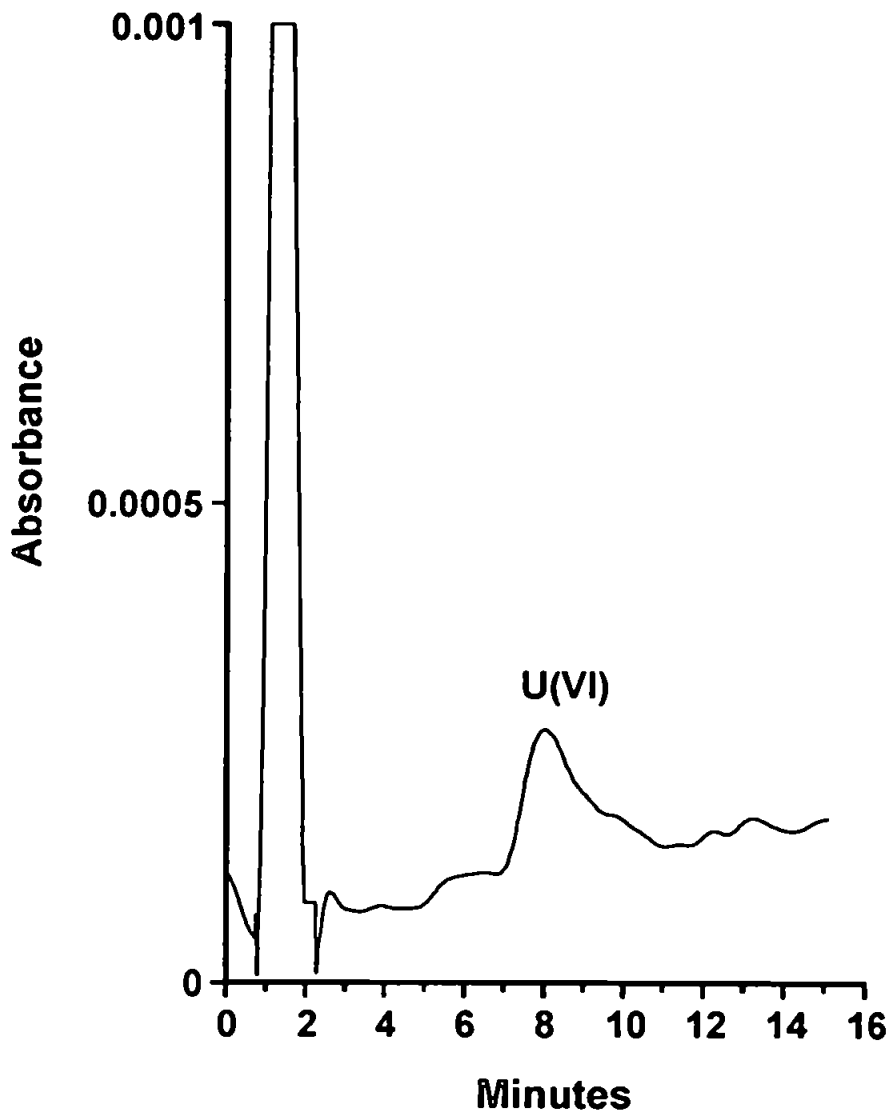


Figure 6.7 The separation of $50\mu\text{g l}^{-1}$ U(VI) from matrix metals in a spiked mineral water, on the $100 \times 4.6\text{mm}$ PRP-1 $7\mu\text{m}$ PS-DVB column. Eluent: 1M KNO_3 0.5M HNO_3 and 0.1mM dipicolinic acid. Detection: Arsenazo III at 654nm .

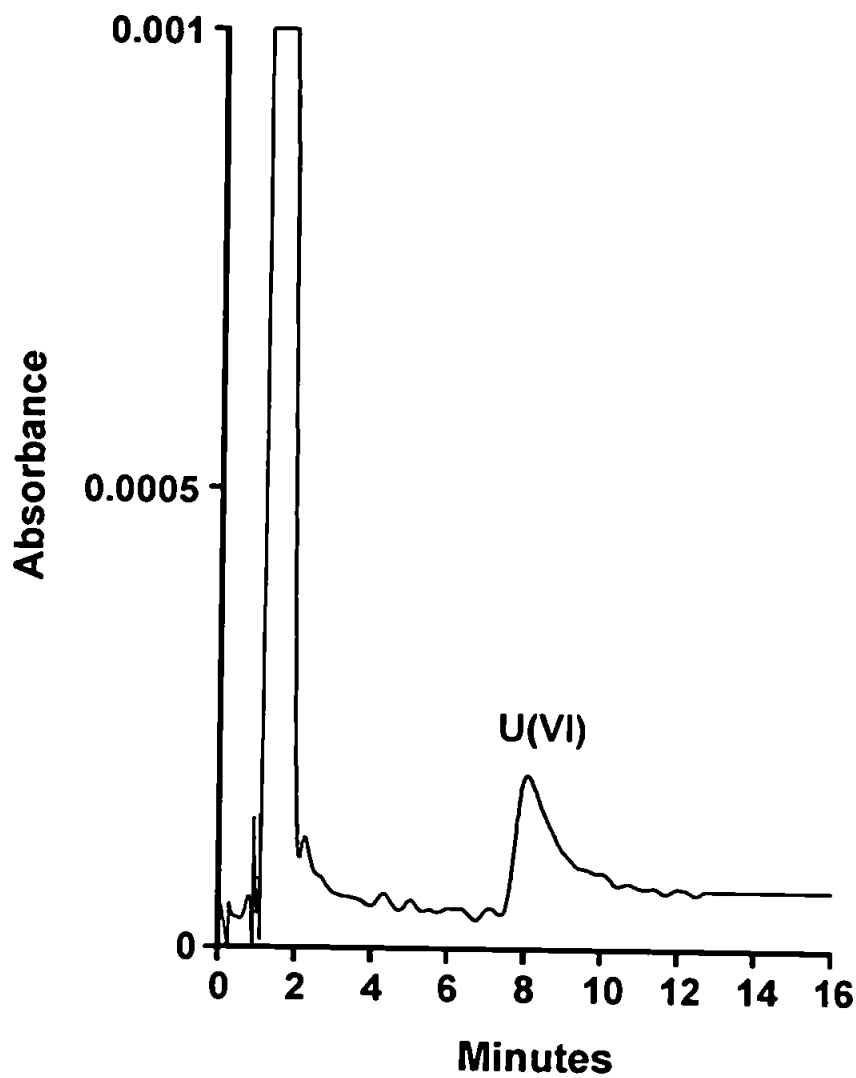


Figure 6.8 The separation of $50\mu\text{g l}^{-1}$ U(VI) from matrix metals in a spiked seawater on the $100 \cdot 4.6\text{mm}$ PRP-1 $7\mu\text{m}$ PS-DVB column. Eluent: 1M KNO_3 0.5M HNO_3 and 0.1mM dipicolinic acid. Detection: Arsenazo III at 654nm .

The reproducibility (%RSD) of the method was calculated with the repeat injection (n=6) of a sample, and found to be 3.5% using peak area. The analytical results for the sample analysis are given in Table 6.2. A typical standard addition curve is given in Figure 6.9.

Table 6.2. The analytical characteristics of the sediment analysis.

sample	Line equation	R ²	[UO ₂ ²⁺] µg g ⁻¹
1	309661x + 26304	0.9973	8.48
2	315007x + 27490	0.9975	8.72
3	318775x + 26871	0.9998	8.41
4	277812x + 25416	0.9996	9.14

The chromatogram of a typical sample injection is shown in Figure 6.10. As can be seen, a peak was observed with a later retention than uranium. This was not expected as it was known that divalent and trivalent ions usually found in environmental samples elute on or close to the solvent front. It was therefore assumed that the peak could be attributed to a metal in a higher oxidation state. Using the elements listed in the sample certificate which react with Arsenazo III as a guide, it was subsequently established that the unknown peak was due to the zirconyl ion ZrO²⁺, present in the sample certified as 153 ± 19mg l⁻¹. Hafnium also eluted after U(VI), and was partially separated from zirconium, which is an interesting development as these group IVa metals are not easily determined by traditional liquid chromatography techniques [271-275]. Using the optimised eluent (1M KNO₃ 0.5M HNO₃ and 0.1mM dipicolinic acid) together with the 100mm PRP-1 7µm column, k' values of 12.3 and 11.0 were recorded for Zr(IV) and Hf(IV) respectively, in comparison with 7.8 for U(VI) and 1.1 for Th(IV). A tentative k' of 1.7 was recorded for Tl(III), as it is unknown at this juncture whether this metal would be present as the aquo ion [Tl(H₂O)₆]³⁺ or other oxidation state in the acidic eluent.

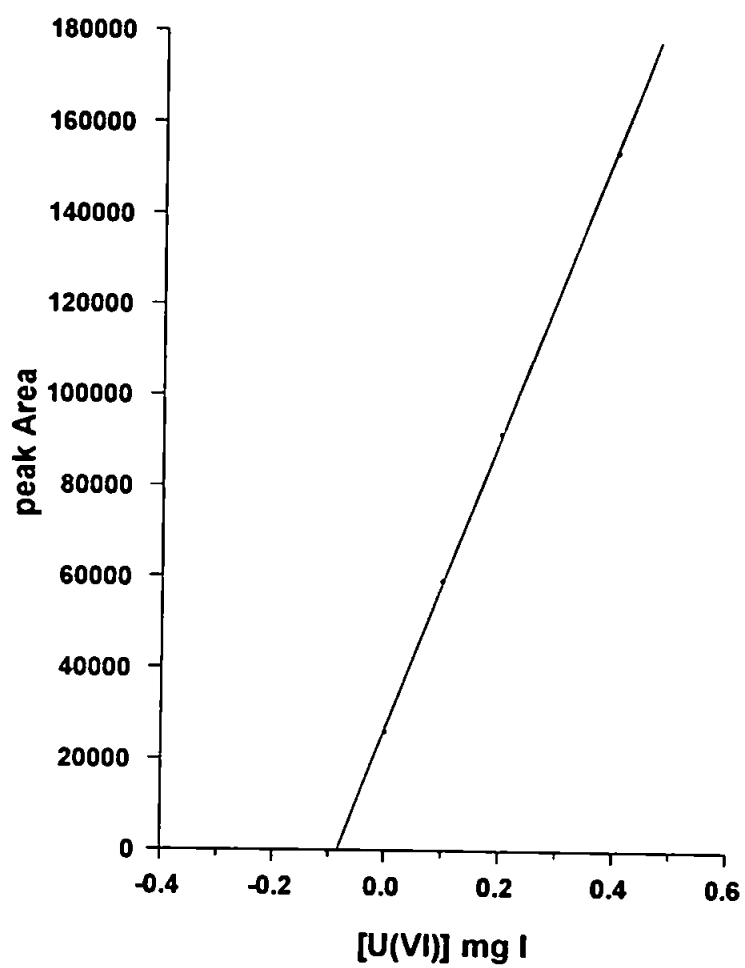


Figure 6.9 The standard addition calibration curve for sample 3.

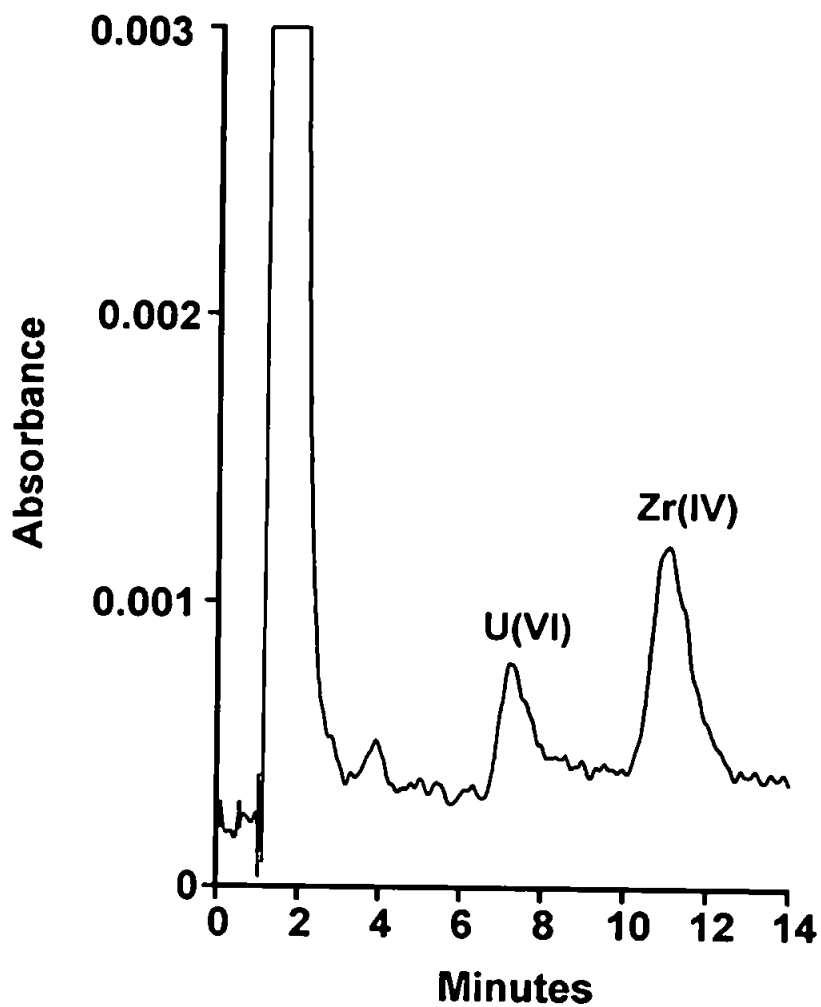


Figure 6.10 The separation of U(VI) from matrix metals in the certified sediment sample GBW07311, on a 100 · 4.6mm PRP-1 7 μ m PS-DVB column. Eluent: 1M KNO₃ 0.5M HNO₃ and 0.1mM dipicolinic acid. Detection: Arsenazo III at 654nm.

6.4. Summary

A selective and sensitive HPCIC system has been developed as a novel technique for the quantitative determination of U(VI) in complex matrices. Using a high efficiency PS-DVB resin, dynamically modified with dipicolinic acid, trace concentrations of the uranyl ion could be separated from large concentrations of matrix metals using isocratic elution, in under 10 minutes. Good recoveries were obtained from spiked mineral water and seawater, and the standard addition calibration curves produced good linearity ($R^2 > 0.997$), with a detection limit, calculated as twice baseline noise, of $20 \mu\text{g l}^{-1}$.

The results obtained for the soft water and sediment sample compared well with the certified values for uranium, which illustrates the potential for using dynamic modification of neutral substrates as a cost effective and reliable analytical technique for uranium determinations in various complex matrices.

The unexpected retention of hafnium and zirconium on the dipicolinic acid loaded column at low pH is also a significant discovery, which, with further development, could be exploited for the determination of these elements in complex samples.

Part 2. The Determination of Pb(II), Cd(II) and Cu(II) in Rice Flour

6.5 Introduction

Lead, atomic number 82, atomic mass 207.2 and density 11.34 g cm^{-3} , is located in group IVa of the periodic table. It is fairly abundant in the earth's crust, $16\mu\text{g g}^{-1}$ [189], and is generated as the stable end product of two natural radioactive decay series: $^{232}\text{Th} \rightarrow ^{208}\text{Pb}$ (52%) and $^{238}\text{U}, ^{235}\text{U} \rightarrow ^{206}\text{Pb}$ (24%) and ^{207}Pb (23%) respectively.

The most important Pb(II) minerals are Galena (PbS), Cerussite (PbCO_3) and Anglesite (PbSO_4).

The metal is used in car batteries, accounting for about 40% of all Pb(II) consumed [189], and as a component of solder. Lead based pigments are used as a protective coating for many exterior surfaces, and the metal is used for roofing and glazing, though these applications are in decline [244].

The production of organolead compounds, tetramethyl- and tetraethyl lead, which are used as anti-knock agents in gasoline, used to account for 10% of the world lead consumption, though this is also in decline due to recent environmental legislation.

This has been implemented due to the toxic nature of this metal. Lead compounds introduced into the environment by human activity are not decomposed and accumulate locally with transfer to biological organisms. A significant source of release into the environment results from the combustion of leaded fuel, which can result in levels of organolead compounds ranging from $5 - 200\text{ ng m}^{-3}$ in the urban atmosphere. With regards to the aqueous environment, lead can enter into rivers and lakes as dust fall-out with precipitation, or waste effluent from mining and smelting sites. The Pb(II) content of lake and river waters is typically $0.1 - 10\mu\text{g l}^{-1}$, and $0.01 - 0.03\mu\text{g l}^{-1}$ in surface ocean water [189]. Pb(II) can also enter the human food chain through uptake by plants, which in addition may be consumed by food – producing animals.

This metal is toxic due in part to its accumulation on enzyme thiol sites, which participate in the heme synthesis pathway. This inhibits the production of the haemoglobin molecule, resulting in anaemia. Organolead compounds are more toxic due to their lipophilic nature and ease with which they can pass the blood brain barrier. This metal is eventually deposited and accumulates in calciferous matter, with a $T_{1/2}$ of 10–20 years.

Cadmium, atomic number 48, atomic mass 112.4 and density 8.64g cm^{-3} , located in group IIb, is also a toxic metal, non-essential to life. It is a relatively rare element, occurring in the continental crust at an average concentration of $0.15\mu\text{g g}^{-1}$ [276]. Pure cadmium minerals are very rare, for example Greenockite (CdS) and Otavite (CdCO_3), this metal principally processed by the refining of Zn(II) ores, for instance Galmei (ZnCO_3) with Cd(II) contents up to 5%. This metal is used primarily for coatings, pigments, alloys and dry battery production, for example rechargeable Ni-Cd.

It is the localised release into the environment from human derived emissions that has created problems. Atmospheric discharges of Cd(II) can arise from the burning of fossil fuels or incineration of municipal waste. The largest source of Cd(II) emissions into water in Europe is thought to arise from process streams emanating from phosphate rock waste used to obtain fertilisers and detergents [277]. In 1995, the aquatic input of Cd(II) into the North Sea was estimated at 11.8 tonnes [277], the open ocean Cd(II) concentration given as approximately $<1\text{-}15\text{ng l}^{-1}$ [189]. Initial concern for this metals impact arose from an isolated incident termed 'itai-itai' disease (Japan, 1945), whereby a prolonged discharge of cadmium rich mining residues into the local river system, transferred to the local population via drinking water and contaminated rice from paddy fields, resulting in severe skeletal deformation and kidney damage.

Cd(II) uptake occurs by ingestion and inhalation, accumulating predominantly in the kidneys with a biological $T_{1/2}$ of >10 years. This metal is considered toxic as it can replace Zn(II) in enzymes and bind to sulfur atoms in thio proteins [244].

In complete contrast to Pb(II) and Cd(II), Cu(II) is essential to life, involved with many metabolic processes in living organisms.

This metal, atomic number 29, atomic mass 63, with a density of 8.93 g cm^{-3} , is present at a concentration of $55\mu\text{g g}^{-1}$ in the earth's crust and $\leq 0.3\mu\text{g l}^{-1}$ in the open ocean [189]. It is widely distributed as a metal, the commonest mineral being Chalcopyrite CuFeS_2 [15]. Industrial uses of Cu(II) include electrical applications, water piping, roofing material and pigments.

It is widely used by biological organisms as a component of many electron transfer enzymes, involving the redox potential of Cu(I)/Cu(II). The dietary requirement for human adults is around 5mg per day [189]. However, although Cu(II) is essential, it is also potentially toxic, necessitating a requirement to regulate discharges into the environment. Copper at concentrations exceeding 0.1 mg l^{-1} in water is toxic to fish, whilst ruminants are quite susceptible to copper toxicosis. Amongst humans, Cu(II) is essentially non-toxic. Gram quantities can lead to poisoning, but rarely death. An exception is Wilson's disease, whereby individuals display a life long deficiency of the plasma copper protein ceruloplasmin, and an excess of hepatic copper, which collects in the liver before release into the bloodstream, with potentially fatal consequences.

As a source of reference to assess the relative toxicity of these three metals, the UK Water Supply (Water Quality) Regulations 1989 stipulate maximum concentrations in drinking water of $3000\mu\text{g l}^{-1}$ Cu(II), $50\mu\text{g l}^{-1}$ Pb(II) and $5\mu\text{g l}^{-1}$ Cd(II).

Due to the relative toxicity of Pb(II) and Cd(II), it is surprising how few IC methods have been developed for their determination. This has been in part due to the poor sensitivity towards these metals of many chromogenic ligands used in post column systems, as mentioned in Chapter 1. Another problem has been to develop techniques whereby these elements can be separated from other more commonly occurring transition metal ions. A list of samples which have been analysed for Pb(II) and/or Cd(II) using IC, CIC or HPCIC, over the last decade, are given in Table 6.3.

The sum total is very few methodologies developed for the analysis of real samples to determine these key metals, especially Pb(II) and Cd(II) concurrently within the same method. More surprisingly, few liquid chromatographic techniques have been investigated for the determination of Cd(II) in foodstuffs, as the most important Cd(II) source for humans is through intake of food [189]. A recent review on Pb(II) analysis only cited four methods to selectively separate this metal using liquid chromatography, only one method implementing a chelating sorbent (PAR), the others using an ion-pair mechanism [278].

Based upon the promising preliminary results achieved with a chlorodipicolinic acid coated resin (Chapter 5), the aim of this study was to develop a method to selectively determine Pb(II) and Cd(II) in a food – rice flour, containing other matrix metals and a high organic content. Rice is a major dietary source for the Asian population, and there is concern over waste leaching from mines entering rivers and soil, potentially increasing the content of heavy metals in rice.

Table 6.3 Sample matrices that have been analysed to quantify concentrations of Pb(II) and Cd(II)

Technique	Sample	Cd(II)	Pb(II)	Reference
IC	Silicon wafer	✓	✓	44
IC	Vegetable oil	✓	✓	46
IC	Sewage water	✓	-	47
IC	Mineral water	✓	-	48
IC	Lead acid battery	✓	-	49
IC	Nitrate/phosphate fertiliser	✓	✓	51
IC	Mussel tissue	✓	-	53
IC	River water	✓	-	54
IC	Parenteral solution	✓	✓	59
CIC	Sea water	✓	✓	66
CIC	Coral skeleton	✓	-	68
CIC	Drinking water	✓	✓	69
CIC	Oyster tissue	✓	-	73
HPCIC	Sea water	✓	-	142
HPCIC	Sea water	✓	✓	143
HPCIC	River water	-	✓	85
HPCIC	Sea water	-	✓	145

6.6 Experimental

6.6.1 Instrumentation

The isocratic HPCIC system is described in section 2.2.1. The analytical column was either a 300 · 4.6mm I.D. PEEK casing packed with PRP-1 7µm PS-DVB (Hamilton) or 100 · 4.6mm I.D. packed with PLRP-S 5µm PS-DVB (Polymer Labs).

6.6.2 Reagents

The optimised mobile phase consisted of 1M KNO₃, 30mM HNO₃ (pH 1.5) and 0.25mM chlorodipicolinic acid.

The post column reagent was a mixture of 0.1mM PAR, 0.125M di-sodium tetraborate and 0.2M NaOH (pH 10.5), with detection at 520nm. The UV-Vis spectrum for selected metals with this PCR is given in Figure 6.11.

Both the eluent and PCR were delivered at 1ml min⁻¹. All reagents were of AnalaR grade (BDH) with the exception of NaOH (Aristar, BDH), PAR (Fluka) and chlorodipicolinic acid (in-house synthesis).

6.6.3 Sample Pre-treatment

The rice flour sample, National Research Centre Certified Reference Material (GBW08502, LGC) was prepared using microwave digestion.

A known amount of accurately weighed sample (approximately 0.5g) was added to a PTFE bomb together with 1ml 30% hydrogen peroxide (Fluka) and 4ml HNO₃ (Aristar, BDH), capped and left overnight (about 12 hours).

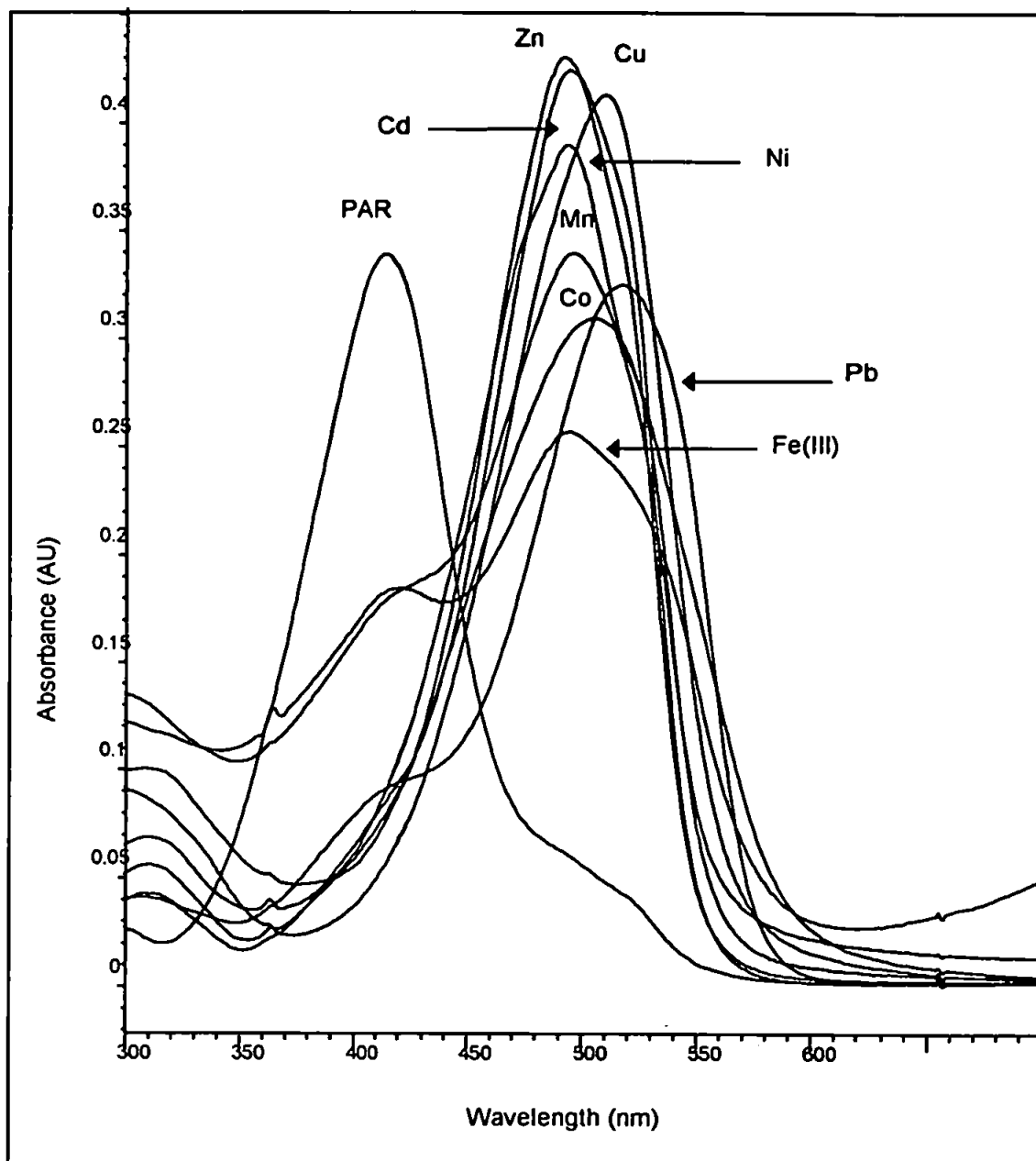


Figure 6.11 Absorbance spectra of selected transition metals (1 mg l^{-1}) with the PAR – borate post column reagent.

The pre-digested material was microwaved at 750W using a commercial microwave (Microchef SM11, Proline, UK) for five 2 minute cycles. The vessel was uncapped and the material evaporated to incipient dryness using a water bath. The residue was transferred to a volumetric flask with small quantities of eluent, made up to a final volume of 2ml and analysed within 2 hours.

A blank run was also performed to estimate system contamination. The moisture content of the rice flour was determined by oven drying 0.5g of the material at 80°C for 4 hours, before cooling in a vacuum dessicator, and found to be 2%.

6.7 Results and Discussion

6.7.1 Choice of Digestion Procedure

Microwave digestion techniques have gradually gained widespread acceptance as an effective method of sample preparation.

The advantage of using a closed system (bomb) is that the acid mixture can be heated to higher temperatures resulting in higher reactivity and oxidising power [279]. In a microwave oven this is more pronounced because heating takes place inside the mixture. This results in a reduced sample digestion time which is a significant benefit. Other advantages of using microwave digestion include reductions in contamination due to reduced volumes of reagents required, less sample usage, and minimising of analyte loss from volatilisation, in comparison with open wet digestion and dry ashing procedures.

Food samples generate problems due to lipids and proteins which generally require high dissolution temperatures for complete digestion. Proteins decompose at ~150°C, lipids at around 160°C [280]. HNO₃ normally boils at 120°C, but using a closed vessel to increase the pressure subsequently raises this boiling point, increasing the dissolution rate of these

organic matrices. For example, HNO₃ at 5 atmospheres in a closed container boils at 176°C when heated by microwaves [280].

Cd(II), Cu(II) and Pb(II) have been determined in rice flour using microwave digestion with HNO₃ prior to ICP-MS detection [281-282]. Pb(II) and Cu(II) were determined in rice flour using HNO₃ wet-ashing prior to HPLC separation with detection as hexamethylenedithiocarbamate complexes [283]. Reviews on microwave assisted sample preparation, with further examples of dissolution procedures for rice flour and other sample types are given by Kuss [284], Smith and Arsenault [280] and Lamble and Hill [285].

6.7.2 Method Development – Detection Conditions

The buffering system in the PAR post column reagent was changed from ammonia (NH₃) to boric acid (B(OH)₃), as borate complexes are comparatively weaker, enabling more metal ions to freely complex with PAR. The log stability constants of selected metal ions with ammonia and boric acid are given in Table 6.4.

Table 6.4. Log stability constants of selected metals with ammonia and boric acid [163]

M ⁿ⁺	Log K ₁ NH ₃	Log K ₁ B(OH) ₃
Cu ²⁺	4.18	3.48
Cd ²⁺	2.80	1.42
Zn ²⁺	2.14	0.9

The increased complexation of metal ions with PAR in the borate buffered system is illustrated in Table 6.5.

Table 6.5 The absorbance of selected transition metal ions (1mg l⁻¹) with PAR post column reagents (tenfold dilution) buffered with either ammonia or borate.

M ⁿ⁺	PAR - NH ₃		PAR - B(OH) ₃	
	490nm	520nm	490nm	520nm
Pb ²⁺	0.144	0.162	0.255	0.324
Cd ²⁺	0.165	0.134	0.419	0.352
Zn ²⁺	0.252	0.205	0.429	0.325
Co ²⁺	0.180	0.164	0.295	0.291
Ni ²⁺	0.261	0.194	0.386	0.289
Mn ²⁺	0.204	0.184	0.334	0.283
Cu ²⁺	0.230	0.234	0.366	0.384
Fe ³⁺	-	-	0.205	0.232

A change in the buffer conditions from ammonia to borate dramatically increased the sensitivity for many of the metal ions studied, with a near twofold increase in absorbance for Cd(II). The detection wavelength was altered to 520nm, providing a significant increase in sensitivity for Pb(II), traditionally a metal which does not form a strong chelate with PAR (log K₁ = 8.6) resulting in a weak response in comparison with other transition metal ions. At 520nm, a slight increase in sensitivity was additionally noticed for Cu(II).

A further advantage of increasing the detection wavelength, is that system noise declines due to a reduction in the absorbance of the background PAR. With the PAR-borate system, the noise was 0.0008AU at 490nm, diminishing to 0.0004AU at 520nm, which can improve analyte detection limits.

Ammonia has previously been added to the PCR mixture as it has a stronger buffering capacity than borate (ammonia: pK_a = 9.12, Borate: pK_a = 8.8 [162]). This has been advantageous when injecting highly acidic samples into the chromatographic system, or using pH based gradient elution, which could upset the baseline, interfering with analyte

peaks. For this work, however, incorporating isocratic elution, it was assumed that a PCR buffered with borate would suffice.

6.7.3 Method Development – Separation conditions

Initial investigations centred on the 300mm column with an optimised eluent of 1M KNO₃ 6.5mM HNO₃ (pH 2.2) and 0.25mM chlorodipicolinic acid, which had previously been found capable of separating seven transition and heavy metal ions (Section 5.3.5.4.2). It was thought that a method could be developed whereby multi-element (>5 metals) determinations were possible. For the most part, however, this proved unfeasible.

The main reason for this was the instability of the dynamically modified substrate at pH 2.2. Unless metal standards were prepared in the eluent, erroneous negative and positive system peaks resulted, interfering with the detection of Mn(II) and Zn(II). The possible explanations for this affect included leaching of either background metals present in the eluent reacting with PAR, a plug of chlorodipicolinic acid complexing with background metals, or a temporary pH imbalance resulting from sample metals displacing H⁺ ions from the chelating groups.

Increasing the buffering capacity of the PCR by reverting to the ammonia solution still resulted in system peaks, thereby this affect was not caused by pH changes. It was eventually concluded that the background metal contamination was the fundamental causative factor. The UV-Vis spectrum of a PCR/ eluent mixture showed a hump on the PAR spectra with a maximum at 485nm, synonymous with metal contamination. Increasing the ionic strength of the sample, thereby increasing the concentration of background metals, also reduced the severity of the system disturbance. Adding an excess of EDTA to the PCR (10mM), 'mopped up' these eluting background metals, suppressing the system affects totally, confirming this was the cause of the erroneous peaks.

To this end, subsequent studies involved using 'cleaned' KNO_3 . This was achieved through pumping a 2 molar solution through a high capacity chelating column (250mm XO Column with a capacity of 0.27mg Cu(II)/ g resin) at a pH which gave complete retention of metal ions, to a point before breakthrough occurred. This KNO_3 solution was then diluted to 1Molar with Milli-Q water, and the column regenerated with an acid wash.

A further and unfortunately unresolved problem, which occurred at pH 2.2 was the columns susceptibility to high concentrations of matrix metals in the sample. With a concentration of 1000mg l^{-1} alkaline earths present in the sample, a huge system disturbance was noted, an example given in Figure 6.12, though this system affect also occurred with lower concentrations of these metals in the sample. As already postulated in Chapter 5, at this pH, the dicarboxylic acid is partially deprotonated, with the ligand able to complex metal solute ions. In addition, as illustrated in Figure 5.13, there is an approximately twofold decrease in the 'concentration' of ligand on the stationary phase at pH 2.2, in comparison with the isoelectric point of chlorodipicolinic acid at pH 1.5. This would appear to confirm that as the pH is increased above a value of 1.5, the chlorodipicolinic acid in the eluent plays an increasingly dominant role in the separation of metal ions, possibly by separating these solutes by an ion-pair mechanism. This type of separation would be strongly influenced and adversely affected by large concentrations of unretained metal ions present in the eluting sample plug, which would swamp the system temporarily.

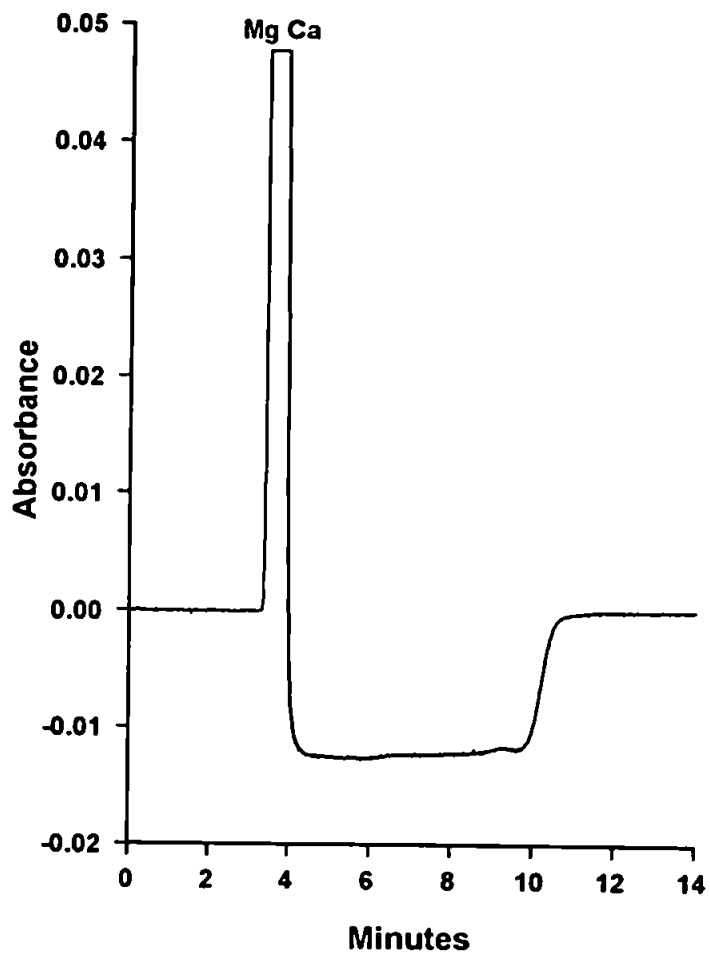


Figure 6.12 The effect of 500mg l^{-1} Ca(II) and Mg(II) on the dynamically modified substrate. Column: $300 \times 4.6\text{mm}$ PRP-1 $7\mu\text{m}$ PS-DVB. Eluent: 1M KNO_3 6mM HNO_3 and 0.25mM chlorodipicolinic acid (pH 2.2). Detection: PAR at 520nm .

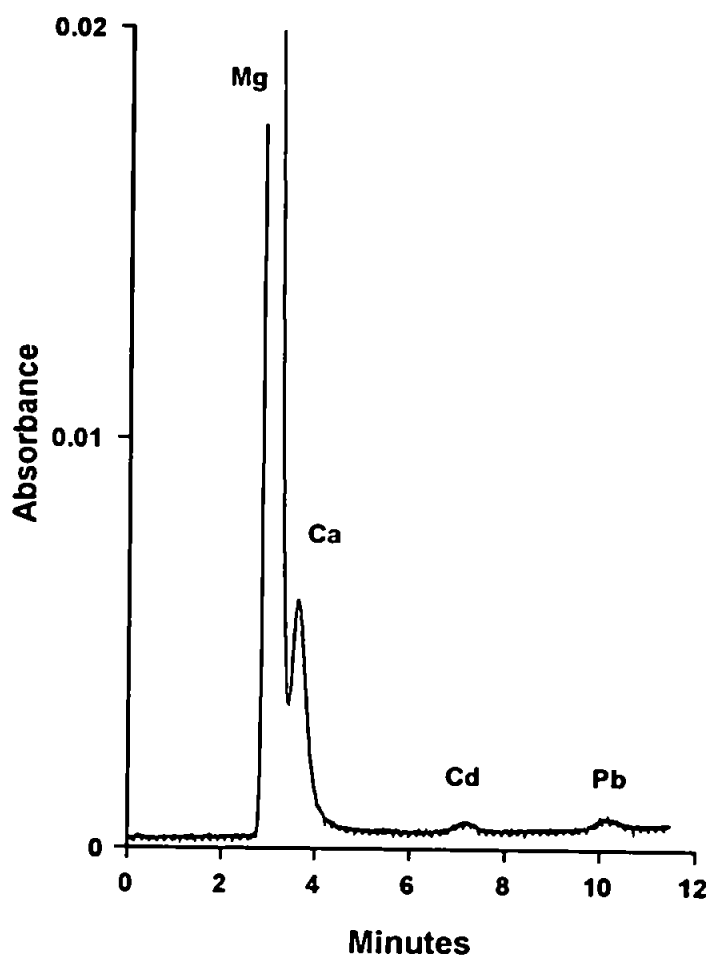


Figure 6.13 The effect of 500mg l^{-1} Ca(II) and Mg(II) on the dynamically modified substrate. Column: $300 \times 4.6\text{mm}$ PRP-1 $7\mu\text{m}$ PS-DVB. Eluent: 1M KNO_3 30mM HNO_3 and 0.25mM chlorodipicolinic acid ($\text{pH } 1.5$). Detection: PAR at 520nm .

When reducing the pH to 1.5, an addition of 1000mg l⁻¹ alkaline earths in the sample had no discernible affect on the system stability (Figure 6.13) confirming the supposition that chelation on the substrate is dominant at this low pH. The insensitivity to high concentrations of alkaline earth metals in acidic eluents was also noted with the dipicolinic acid modified column, illustrated earlier in this chapter. At pH 1.5, it was possible to separate only Pb(II), Cd(II) and Cu(II), the other transition metals eluting close to the solvent front. At pH 2.2, however, with the presence of alkaline earths in the sample, the resulting system disturbance prevented all but the determination of these three metals anyway.

Due to the long run time required to elute these metals at pH 1.5 on a 250mm column length, approximately 20 minutes, it was decided to revert back to a 100mm column length. In addition, the particle size of the resin was reduced from 7µm to 5µm, in an attempt to increase column efficiency. With an eluent of 1M KNO₃ 30mM HNO₃ and 0.25mM chlorodipicolinic acid, on the 100mm column, Pb(II), Cd(II) and Cu(II) were eluted within 10 minutes, ensuring an efficient analysis time. In addition, the other transition metals co-eluted on or near to the solvent front at this pH. A typical separation of Pb(II), Cd(II) and Cu(II) at pH 1.5 is given in Figure 6.14.

6.7.4 Analytical Characteristics of the Analysis

With the 300mm column, using an eluent composed of 1M KNO₃ 6mM HNO₃ and 0.25mM chlorodipicolinic acid, a calibration of seven transition and heavy metals was possible, standards prepared in a matrix matched solution. The results are given in Table 6.6. The reproducibility (%RSD) was calculated with the repeat injection (n=6) of a 10µg l⁻¹ standard or 100µg l⁻¹ standard for Pb(II). The limit of detection was calculated as twice baseline peak to peak noise, metal concentrations determined using peak area.

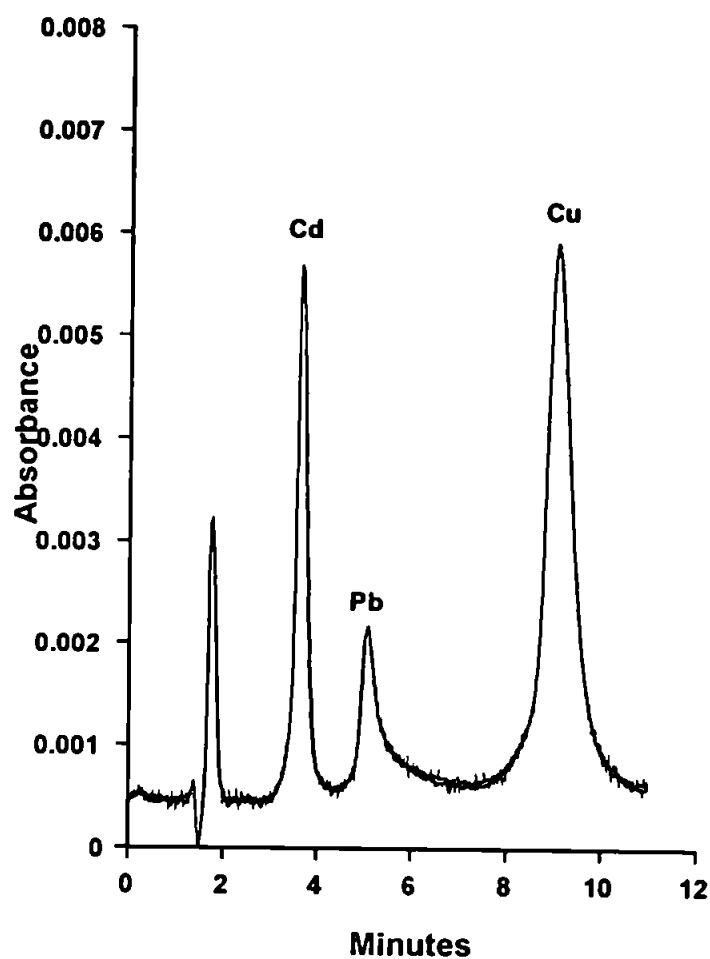


Figure 6.14 The separation of Cd(II) $100\mu\text{g l}^{-1}$, Pb(II) $500\mu\text{g l}^{-1}$ and Cu(II) $200\mu\text{g l}^{-1}$ on the $100 \times 4.6\text{mm}$ PLRP-S $5\mu\text{m}$ PS-DVB column. Eluent: 1M KNO_3 30mM HNO_3 and 0.25mM chlorodipicolinic acid (pH 1.5). Detection: PAR at 520nm .

Table 6.6 Analytical Characteristics achieved with the 300mm Column length with an eluent of 1M KNO₃ 6mM HNO₃ and 0.25mM chlorodipicolinic acid.

M⁺⁺	Range	Line equation	R²	% RSD	L.O.D
Mn(II)	5µg l ⁻¹ – 1mg l ⁻¹	Y=1.845·10 ⁶ x - 16210	0.9988	1.02	3.5µg l ⁻¹
Co(II)	5µg l ⁻¹ – 1mg l ⁻¹	Y=1.596·10 ⁶ x - 9559	0.9997	4.26	3.5µg l ⁻¹
Ni(II)	5µg l ⁻¹ – 2mg l ⁻¹	Y=571564x - 2428	0.9981	3.50	14µg l ⁻¹
Zn(II)	5µg l ⁻¹ – 2mg l ⁻¹	Y=1.362·10 ⁶ x - 31996	0.9986	4.31	5.5µg l ⁻¹
Cu(II)	5µg l ⁻¹ – 3mg l ⁻¹	Y=1.203·10 ⁶ x - 28106	0.9994	1.12	12.5µg l ⁻¹
Pb(II)	50µg l ⁻¹ – 30mg l ⁻¹	Y=2.165·10 ⁶ x - 72944	0.9987	1.51	82µg l ⁻¹
Cd(II)	5µg l ⁻¹ – 3mg l ⁻¹	Y=908404x - 6966	0.9997	4.13	15.5µg l ⁻¹

To assess the accuracy of this system, the National Water Research Institute Standard Reference soft water sample, TMDA 54.2 (LGC) was analysed. This water contains very low concentrations of alkali and alkaline earth metals, Ca(II) 9.2mg l⁻¹, Mg(II) 2.1mg l⁻¹, Na(I) 3.1mg l⁻¹ and K(I) 0.4mg l⁻¹, which should not interfere with the dynamic equilibrium. The water sample was diluted twofold, and analysed using standard addition curves, metals determined using peak area measurements. The %RSD for each metal was calculated with the repeat injection (n=6) of the diluted sample, the results given in Table 6.7.

Table 6.7 Results achieved with the certified soft water sample, TMDA 54.2

M²⁺	Certified conc. $\mu\text{g l}^{-1}$	Line equation	R²	%RSD	Actual conc. $\mu\text{g l}^{-1}$
Mn(II)	346 \pm 32.7	Y=3465900x + 626997	0.9998	1.55	362 \pm 5.6
Co(II)	276 \pm 21.9	Y=285589x + 38264	0.9996	3.52	268 \pm 9.4
Ni(II)	325 \pm 30.3	Y=315873x + 55325	0.9944	3.00	350 \pm 10.5
Cu(II)	460 \pm 41.9	Y=128700x + 307468	0.9967	1.07	477.5 \pm 5.1
Pb(II)	531 \pm 54.4	Y=75789x + 19159	0.9967	4.22	506 \pm 21.4
Cd(II)	165 \pm 16.1	Y=1066200x + 92079	0.9996	1.54	173 \pm 2.7

All the metals were within the certified limits, with the exception of Zn(II), which was not analysed due to interference by a system peak anomaly. A chromatogram of the diluted water sample is given in Figure 6.15.

Due to a susceptibility to interfering matrix metals at pH 2.2, the eluent pH was lowered to 1.5, ensuring that chelation on the dynamically modified substrate was the dominant retention mechanism. At this pH, on the 100mm PLRP-S 5 μm column, it was possible to calibrate Cd(II) to 1 $\mu\text{g l}^{-1}$, illustrating the sensitivity of this system with addition of borate as a buffering agent. A calibration of Cd(II) from 1-5 $\mu\text{g l}^{-1}$, using an eluent of 1M KNO₃ 30mM HNO₃ and 0.25mM chlorodipicolinic acid, was undertaken to assess the system sensitivity. The linearity of the system was good, with a regression coefficient of R² = 0.9982, using peak area. A detection limit of 0.8 $\mu\text{g l}^{-1}$ was calculated, using two times baseline noise. The chromatogram of Cd(II) from 1-4 $\mu\text{g l}^{-1}$ is given in Figure 6.16. The ability to quantify Cd(II) to these low levels could be applied to the analysis of drinking water.

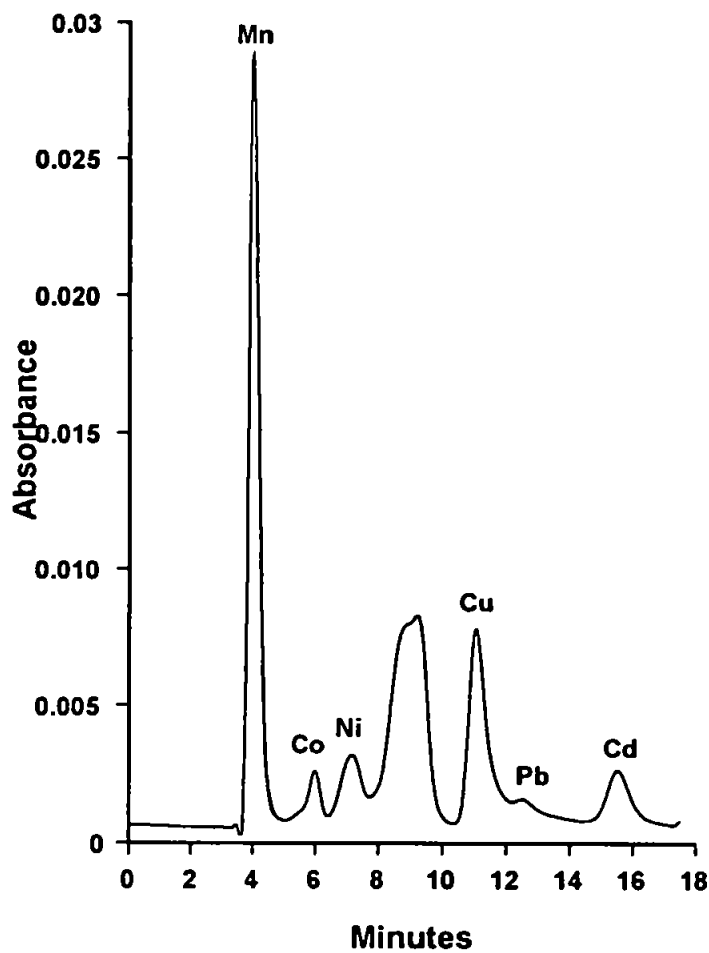


Figure 6.15 Chromatogram of the transition metal ions in the certified soft water sample TMDA 54.2 on the 300 · 4.6mm PRP-1 7 μ m PS-DVB column. Eluent: 1M KNO₃ 6mM HNO₃ and 0.25mM chlorodipicolinic acid. Detection: PAR at 520nm.

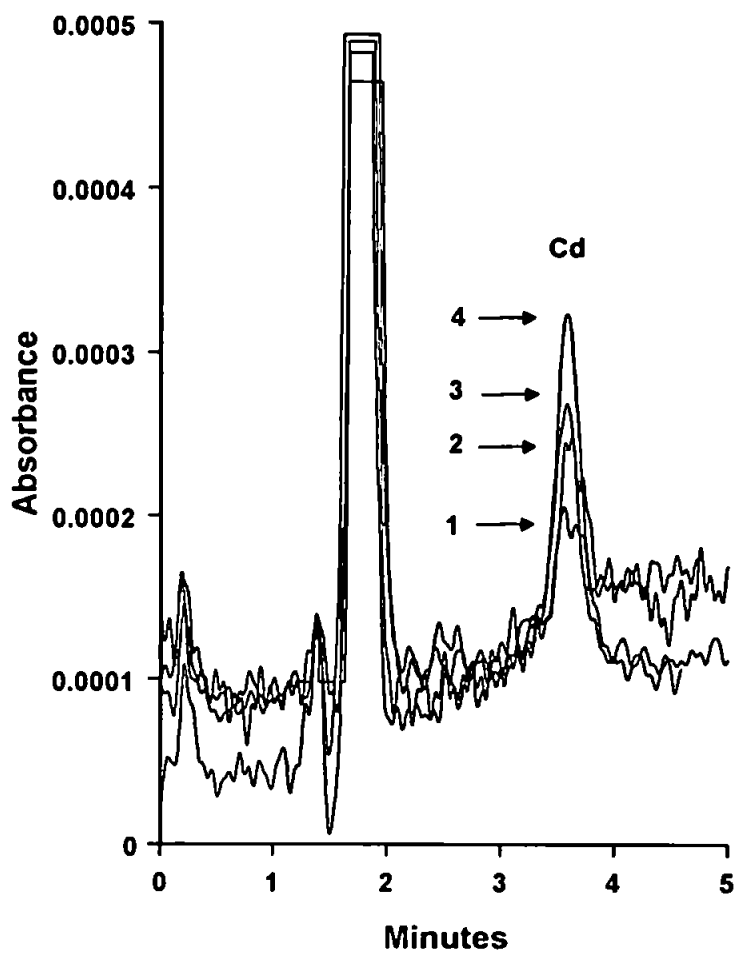


Figure 6.16 Determination of Cd(II) $1-4\mu\text{g l}^{-1}$ on the $100 \cdot 4.6\text{mm}$ PLRP-S $5\mu\text{m}$ PS-DVB column. Eluent: 1M KNO_3 30mM HNO_3 and 0.25mM chlorodipicolinic acid. Detection: PAR at 520nm .

A calibration of Pb(II), Cd(II) and Cu(II) in the eluent at pH 1.5 was undertaken to ascertain system performance. The reproducibility of the system was calculated with the repeat injection (n=6) of 100µg l⁻¹ Cd(II), 500µg l⁻¹ Pb(II) and 200µg l⁻¹ Cu(II). The detection limits were calculated as given previously. The results are shown in Table 6.8.

Table 6.8 Analytical Characteristics achieved with the 100mm Column with an eluent of 1M KNO₃ 30mM HNO₃ and 0.25mM chlorodipicolinic acid.

M ²⁺	Range µg l ⁻¹	Line equation	R ²	%RSD	L.O.D
Cd(II)	1-1000	Y=926386x - 5534	0.9987	0.48	0.8µg l ⁻¹
Pb(II)	5-5000	Y=139875x - 11421	0.9980	1.38	39µg l ⁻¹
Cu(II)	2-2000	Y=1175300x - 6589	0.9995	0.70	5.5µg l ⁻¹

To assess the affect of a more complex sample matrix on the system performance, a certified rice flour, GBW 08502 was analysed. Replicate sample analysis (n=5) was undertaken, one sample additionally analysed using a standard addition curve to determine system bias. The reproducibility of the method was calculated with the repeat injection (n=6) of a sample, and found to be 5.1% for Cd(II), 2.2% for Pb(II) and 1.7% for Cu(II). The results are given in Table 6.9.

Table 6.9 The Results obtained for the certified rice flour analysis.

Sample	Cd(II) $\mu\text{g l}^{-1}$	Pb(II) $\mu\text{g l}^{-1}$	Cu(II) mg l^{-1}
1	19.6	758.5	2.61
2	18.5	678.5	2.68
3	19.3	758.9	2.78
4	-	686.5	2.75
5	18.9	755.5	2.54
Mean	19.1 ± 0.5	727.6 ± 41.5	2.67 ± 0.1
certified	20 ± 3	750 ± 100	2.6 ± 0.3

The results compared well with the certified values for each metal. The chromatogram of a typical sample injection is shown in Figure 6.17.

6.8 Summary

Using a high efficiency neutral polystyrene divinylbenzene resin dynamically modified with 4-chlorodipicolinic acid, a novel technique has been developed to determine trace Cd(II), Pb(II) and Cu(II) in complex matrices. An isocratic separation system, using an eluent containing 1M KNO_3 30mM HNO_3 and 0.25mM chlorodipicolinic acid, allowed the three metals to be separated from other transition metal ions in under ten minutes. Detection was achieved using a PAR post column reagent buffered with borate, which increased the sensitivity towards the transition metals in comparison with the ammonia buffered reagent. The detection limits, calculated as twice baseline noise, were $0.8\mu\text{g l}^{-1}$ for Cd(II), $39\mu\text{g l}^{-1}$ for Pb(II) and $5.5\mu\text{g l}^{-1}$ for Cu(II). The procedure was applied to the determination of Pb(II), Cd(II) and Cu(II) in a standard reference rice flour. The results

obtained compared well with the certified values, with the system producing good calibration linearity (>0.998).

The ability of this system to quantify Cd(II) to very low concentrations (sub- $\mu\text{g l}^{-1}$) without preconcentration could be developed to determine this toxic metal in other foodstuffs and drinking water.

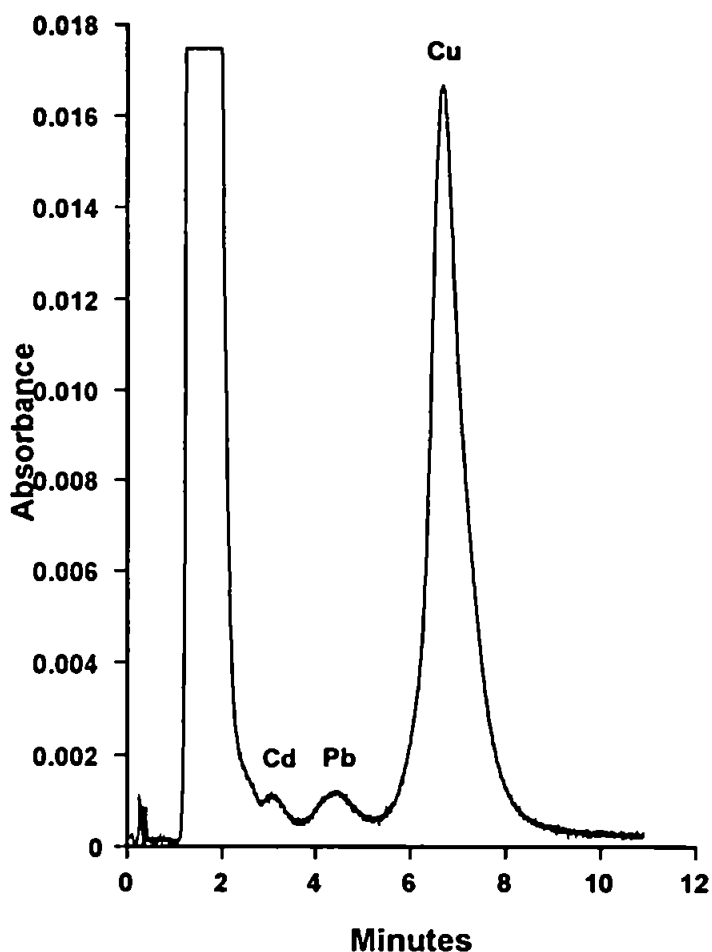


Figure 6.17 The separation of Cd(II), Pb(II) and Cu(II) from matrix interferences in the certified rice flour GBW08502 on the 100 · 4.6mm PLRP-S 5 μm PS-DVB column. Eluent: 1M KNO₃ 30mM HNO₃ and 0.25mM chlorodipicolinic acid. Detection: PAR at 520nm.

Chapter 7. Conclusions and Suggestions for Further Work

7.1 Conclusions

The studies detailed in this thesis have demonstrated the use of various chelating agents immobilised onto hydrophobic and hydrophilic substrates by three mechanisms: physical impregnation, covalent bonding and dynamic chemisorption, for the high efficiency separation and determination of metal ions in complex matrices, with a single column and isocratic elution.

Previous work had mainly concentrated on the use of dye immobilised polystyrene resins for the analysis of trace metals in a variety of samples including brine solutions and milk powder. This illustrated the advantages of High Performance Chelation Ion Chromatography, or HPCIC, in comparison with conventional ion chromatographic techniques. These include both the potential to alter metal selectivity, dependant upon the chelating system involved, to separate metal ions of interest, and an ability to determine one metal in a vast excess of matrix interferences. This is because the separation is based on the conditional stability constants of metal chelate species, which can be altered by manipulation of mobile phase pH, and not by simple ion-exchange interactions which can become swamped by high ionic strength samples, reducing column efficiency.

Initial work presented in this thesis involved undertaking a more detailed and thorough investigation into the effect of the chelating system on metal ion retention, using chelating dyes, as previous work had not extended beyond an empirical level.

With different combinations of nitrogen and oxygen donor ligands, unique metal selectivity profiles were observed, for the six dyes investigated. The O,O chelating Aurin Tricarboxylic Acid impregnated column demonstrated a strong preference for Cd(II) in

comparison with N,O type dyes, whilst the N,N,O chelating 4-(2-pyridylazo)resorcinol loaded column exhibited a uniquely weak retention for Mg(II) against the other alkaline earth metals. The Aurin Tricarboxylic Acid and *o*-cresolphthalein complexone (N,O,O chelation) columns displayed superlative separation characteristics in comparison with the other dyes investigated, for both the alkaline earth, transition and trivalent metal ions. Capacity factor (k') versus pH plots provided an indication of the relative strength of each chelating system, the general order being N,N>N,O>O,O under acidic eluent conditions. The mole percentage activity of each dye impregnated column was quite similar, values ranging from 3.7 – 5%. Even though this loading was apparently low, metal separations were possible on all six columns, the Aurin Tricarboxylic Acid and *o*-cresolphthalein complexone columns in particular displaying good efficiency. Indeed, the triphenylmethane based dyes provided more efficient column separations than the azo based dyes, which although providing significantly increased loadings, did not give a comparatively significant increase in capacity. This could be due in part to the dye structures and relative ease of impregnation into resin pores.

Various system parameters investigated, namely column length, capacity and mobile phase characteristics including ionic strength and concentration of complexing buffer, could also improve separations by HPCIC.

Even though the dye loaded columns displayed good inter-group selectivity between trivalent metal ions, the divalent transition metals and the alkaline earths, intra-group selectivity was generally poor using isocratic elution, with separations of >4 metals generally unfeasible, especially with respect to the transition metals.

Because of this fact, together with the knowledge that further studies by other researchers were in progress to separate metal ions using dye loaded columns, subsequent investigations concerned the development of novel substrates for this purpose.

The first examined was aminomethylphosphonic acid, covalently bound to a high efficiency silica substrate. Apart from the promising preliminary results shown with the Aurin Tricarboxylic Acid column, previous work had found that the best chelating group examined to date, in terms of separation efficiency, was iminodiacetate, a N,O,O chelating group. It was therefore decided to investigate another N,O,O chelating molecule with different substituent atoms attached to the ligating group, in this case phosphorus atoms. In addition, the nitrogen atom is sterically further distanced from the oxygen donors in the aminomethylphosphonate ligand, compared with iminodiacetate. This produced some interesting results, most noticeably S-shaped k' curves associated with a change in the mode of chelation as the pH increased. For the alkaline earth metals, this outcome resulted from a change in the type of O,O chelation occurring, whilst for the transition metal ions, a change from O,O to N,O,O chelation was postulated. Preliminary findings indicated that aminomethylphosphonate is potentially a more efficient and versatile chelating agent than iminodiacetate, demonstrated by the high efficiency separation of eight metal ions in under 16 minutes.

A further advantage of this substrate was a strong affinity for beryllium in acidic eluents. An isocratic chromatographic system was developed to determine this alkaline earth in the presence of large concentrations of matrix metals. Using a Chrome Azurol-S post column reagent and a mobile phase consisting of 1M KNO_3 0.5M HNO_3 and 0.08M ascorbic acid, trace Be(II) could be separated from an excess of 800mg l^{-1} matrix metals in under six minutes. A detection limit of 35 $\mu\text{g l}^{-1}$ Be(II) was found, and replicate analysis of a certified sediment sample gave a mean result which fell well within acceptable limits, implying that this method is viable for analytical determinations. A relative standard deviation of 2.05% for six replicate injections additionally indicated that the system was reproducible.

The final type of separation system studied was dynamic modification using small hydrophobic chelating molecules. A chelating surface was produced by having the ligand continuously present in the eluent. Eventually, an equilibrium was established between a sorbed layer of ligand on the surface of the substrate and the concentration of ligand in the mobile phase. It was proved necessary to use low concentrations of ligand in the mobile phase, consistent with good chromatography, both to minimise competition from the complexing eluent and reduce interference with post column chromogenic reagents used for detection purposes.

Of the chelating molecules and substrates studied, it appeared that heterocyclic carboxylic acids sorbed onto polystyrene resins provided the optimum separation profiles. This was due in part to an increased dynamic layer resulting from π - π interactions between the aromatic groups on the PS-DVB matrix and the pyridine group on the organic acid. The addition of a π -electron accepting group to the pyridine ring could significantly improve the dynamic modification further, illustrated with the bonding of a chloride ion to dipicolinic acid. The size and structure of the acid was also very important, demonstrated by the weak chelating potential of picolinic acid in comparison with quinaldic acid. Different chelating groups provided unique metal selectivity profiles, shown by the N,O chelation of metal ions by quinaldic acid and N,O,O chelation using dipicolinic acid. With the N,O,O system, mobile phase pH was additionally an important parameter in determining the elution order of metal ions, due to increased competition from the ligand in the mobile phase with decreasing eluent acidity. Unfortunately, this resulted in system instability above about pH 2, the separation profile prone to disturbance by matrix metals and ionic strength. Nevertheless, below about pH 1.5, dynamically modified substrates were found to be very stable, even in the presence of large concentrations of alkaline earth metals ($>1000\text{mg l}^{-1}$) injected into the system. This, together with the good separation

efficiency exhibited by some of these modified substrates towards certain metal ions, was subsequently exploited for the analysis of complex samples.

The first was the determination of U(VI) in a certified stream sediment, using a dipicolinic acid modified PS-DVB column, and Arsenazo III post column detection. An eluent of 1M KNO_3 0.5M HNO_3 and 0.1mM dipicolinic acid allowed the uranyl ion to be separated from matrix ions in under 10 minutes. The system was tested by standard addition to a sea water and mineral water matrix with good recoveries (>95%). The analysis of the sediment sample yielded a result well within the certified limits. The limit of detection was calculated as $20\mu\text{g l}^{-1}$ with good reproducibility (3.5%) obtained from six replicate injections.

The second application of these dynamically modified substrates was for the determination of Pb(II), Cd(II) and Cu(II) in rice flour using a 4-chlorodipicolinic acid coated PS-DVB column. Using a PAR post column reagent, buffered with borate, and a mobile phase of 1M KNO_3 , 30mM HNO_3 and 0.25mM chlorodipicolinic acid, the system was very sensitive towards these metals, with detection limits of $0.8\mu\text{g l}^{-1}$ for Cd(II), $39\mu\text{g l}^{-1}$ for Pb(II) and $5.5\mu\text{g l}^{-1}$ for Cu(II). The system reproducibility was good, with values of 5.1%, 2.2% and 1.7% recorded for Cd(II), Pb(II) and Cu(II) respectively.

The ability to determine key toxic metals such as Be(II), U(VI), Pb(II) and Cd(II) at trace levels in complex sample matrices by HPCIC is a significant breakthrough in metal ion analysis by chromatographic techniques. The chelating substrates examined during this study remained stable for long periods under the working conditions described, without a noticeable loss of efficiency. Ideas for continuing studies in HPCIC, relating to the work presented in this thesis are detailed in the following section.

7.2 Further Work

It is proposed that further study is undertaken to develop the chelating dye impregnation technique. Previous work plus that presented in Chapter 1, has shown that variations in loading can result dependant upon the resin used, dye structure and loading procedure. Work should be performed to fully evaluate the optimum resin to use, based on manufacturer, particle and pore size, and loading procedures optimised to improve both the degree of impregnation and level of reproducibility between columns. This could possibly be achieved by increasing the concentration of dye amenable to immobilisation, and sonicating a loose resin/ dye solution as opposed to the current procedure of pumping the dye solution through a packed column. This may result in a more reproducible even and concentrated coating.

The Aurin Tricarboxylic Acid molecule should be investigated further, as it demonstrated a unique affinity for Cd(II) and a strong preference for Pb(II) in acidic eluents. A system developed to determine these metals in the presence of matrix interferences such as the alkaline earth metals, whether by isocratic or gradient elution, could be applied to the analysis of brine solutions and highly mineralised samples.

Another N,N chelating molecule should be examined to assess whether a stable loading of this type of reagent is feasible. The strong retention of selected metals at low pH, as demonstrated on the 2-(3-sulphobenzoyl)pyridine 2-pyridylhydrazone loaded column, might provide a unique selectivity profile which could be exploited. To date, a dye containing N,S groups has not yet been immobilised onto a high efficiency substrate, therefore this is a possible avenue to explore regarding metal ions separations.

The aminomethylphosphonic acid functionalised silica column should be used to develop a system capable of multi-element (>5) transition metal separations in complex samples, as it demonstrated the best efficiency of the chelating systems examined in this thesis towards these metals. It is possible that a one step pH gradient will be required to separate the alkaline earth metals from the early eluting Co(II) and Ni(II) ions, if they are to be determined in samples containing high concentrations of these interfering metals. This could be a significant breakthrough in multi-element transition metal analysis.

Dynamic modification of neutral substrates is also open to further development. Different substrates including macroporous polystyrene resins or silica gels might improve the system efficiency and increase loading. An O,O chelating system should be examined to compare the metal retention characteristics obtained using N,O chelating molecules. This could be achieved, for example, by modifying substrates with the heterocyclic organic molecule mandelic acid, and might provide different and useful selectivity coefficients as a function of eluent pH.

Stronger π -electron accepting groups, for example NO_2 , could be synthesised onto dipicolinic acid to determine whether the dynamic loading could be improved further. It is possible, however, that stronger groups will withdraw electrons from the pyridine group, affecting the chelating donor atoms. An alternative would be to graft dipicolinic acid directly to a substrate backbone, negating the requirement to add the ligand to the mobile phase. This might provide very different and more straightforward k' plots to those achieved with dynamically modified substrates, which could provide benefits for metal selectivity. In addition, PCR sensitivity should improve due to the absence of complexing agents in the eluent.

It would be of interest to apply the quinaldic acid loaded column to the analysis of complex samples, possibly to determine Ni(II) and Co(II), or indeed Cd(II) and Pb(II). Investigations into the stability of this monocarboxylic acid system in the presence of matrix metals and changes in eluent pH could be compared to that achieved with dipicolinic acid.

The promising preliminary data concerning the retention of Zr(IV) and Hf(IV) in the dipicolinic acid loaded column could be exploited for the determination of these metals in various samples, which is not easily achieved by simple ion-exchange.

The existing methodologies developed for the determination of Be(II), U(VI), Pb(II) and Cd(II) in this thesis are open to further optimisation. The U(VI) peak especially tailed quite noticeably on the Hamilton substrate, but this was not noted on the Polymer Labs resin, therefore investigations into the peak shape on this latter type of resin might improve detection limits. The Be(II) peak was broad, and might sharpen by manipulating the eluent conditions. The Cd(II), Pb(II) and Cu(II) peaks observed on the chlorodipicolinic acid modified column also tailed somewhat, which is not ideal. In addition, the post column reaction systems were not fully optimised, and improvements could possibly be made to increase detection limits.

An important facet of HPCIC is the potential to analyse complex samples using a single column to determine levels of trace metals. High ionic strength matrices and those containing large concentrations of matrix metals including Fe(III), present in many environmental samples, can be analysed by HPCIC, whereas these conditions would normally swamp an IC column without incorporation of a pre-treatment step, for example preconcentration and batch extraction on low efficiency chelating resins, which can contaminate the sample from excess reagents used or lead to analyte loss. It is proposed

that more types of 'real' samples are analysed for metals of interest, using both existing chelating columns and developing systems, to illustrate the full scope and potential of this technique.

High Performance Chelation Ion Chromatography is a maturing approach to trace metal determinations, both practically simple and relatively inexpensive. The full possibility of this technique has yet to be realised, but development of existing methodologies and investigations into novel chelating systems could somewhat remedy this situation.

References

- [1] T.R. Dulski, Trace elemental analysis of metals, Marcel Dekker, New York, 1999.
- [2] H. Small, Ion Chromatography, Plenum Publishing, New York, 1989.
- [3] E. Katz, R. Eksteen, P. Schoenmakers & N. Miller (Eds.), Handbook of HPLC, Chromatographic Science Series Vol. 78, Marcel Dekker, New York, 1998.
- [4] W.J. Lough, I.W. Wainer (Eds.), High Performance Liquid Chromatography, Blackie, London, 1996.
- [5] T. Hanai, HPLC – A Practical Guide, RSC Chromatography Monographs, The Royal Society of Chemistry, Cambridge, 1999.
- [6] P.R. Haddad & P.E. Jackson, Ion Chromatography – Principle and Applications, Journal of Chromatography Library Vol. 46, Elsevier, New York, 1990.
- [7] H. Small, T.S. Stevens and W.C. Bauman, *Anal. Chem.*, **47** (1975) 1801.
- [8] P. Jones and P.N. Nesterenko, *J.Chromatogr. A*, **789** (1997) 413.
- [9] R. Harjula and J. Lehto, in A. Dyer, M.J. Hudson and P.A. Williams (Eds.), Ion – Exchange Processes: Advances and Applications, Royal Society of Chemistry, Cambridge, 1997, p 439.
- [10] A.R. Timerbaev and G.K. Bonn, *J. Chromatogr.*, **640** (1993) 195.
- [11] B.D. Karcher and I.S. Krull in I.S. Krull (Ed.), Trace Metal Analysis and Speciation, J. Chromatography Library Vol. 47, Elsevier, Amsterdam, 1991.
- [12] J. Weiss, Ion Chromatography, 2nd Ed., VCH, Weinheim, 1995
- [13] C.A. Vanderwerf, Acids, Bases, and the Chemistry of the Covalent Bond, Chapman and Hall, London, 1965.
- [14] I.M. Koltoff and P.J. Elving (Eds.), Treatise on Analytical Chemistry, Part 1 – Theory and Practice, 2nd Ed. Vol. 2, John Wiley & Sons, New York, 1979.
- [15] F.A. Cotton, G. Wilkinson and P.L. Gaus, Basic Inorganic Chemistry, 3rd Ed., John Wiley & Sons, New York, 1995.

- [16] C.F. Bell, Principles and Applications of Metal Chelation, Oxford University Press, 1977.
- [17] A.G. Sharpe, Inorganic Chemistry 3rd Ed., Longman Group Ltd, Essex, 1992.
- [18] K.M. Mackay, R.A. Mackay and W. Henderson, Introduction to Modern Inorganic Chemistry 5th Ed., Blackie, London, 1996.
- [19] D.A. Skoog, D.M. West and F.J. Holler, Fundamentals of Analytical Chemistry 6th Ed., Saunders College Publishing, New York, 1992, p289.
- [20] G.V. Myasoedova and S.B. Savvin, *CRC Crit. Rev. Anal. Chem.*, **17** (1986) 1.
- [21] S.K. Sahni and J. Reedijk, *Coord. Chem. Rev.*, **59** (1984) 1.
- [22] J.F. Biernat, P. Konieczka, B.J. Tarbet, J.S. Bradshaw and R.M. Izatt, *Separation and Purification Methods*, **23** (1994) 77.
- [23] C. Kantipuly, S. Katragadda, A. Chow and H.D. Gesser, *Talanta*, **37** (1990) 491.
- [24] R.A. Nickson, S.J. Hill and P.J. Worsfold, *Anal. Proc.*, **32** (1995) 387.
- [25] B.S. Garg, R.K. Sharma, N. Bhojak and S. Mittal, *Microchem. J.*, **61** (1999) 94.
- [26] M. Ahuja, A.K. Rai and P.N. Mathur, *Talanta*, **43** (1996) 1955.
- [27] X. Wang, Z. Zuang, C. Yang and F. Zhyu, *Spectrochim. Acta B*, **53** (1998) 1437.
- [28] V.G. Akerkar, N.B. Karalkar, R.K. Sharma and M.M. Salunkhe, *Talanta*, **46** (1998) 1461.
- [29] K. Dev, R. Pathak and G.N. Rao, *Talanta*, **48** (1999) 579.
- [30] D. Das, A.K. Das and C. Sinha, *Talanta*, **48** (1999) 1013.
- [31] K. Inoue, K. Yoshizuka and K. Ohto, *Anal. Chim. Acta*, **388** (1999) 209.
- [32] J. Chwastowska, A. Rogowska, E. Sterlinska and J. Dudek, *Talanta*, **49** (1999) 837.
- [33] H. Small, *J. Chromatogr.*, **546** (1991) 3.
- [34] M.L. Marina, J.C. Diez-Masa and M.V. Dabrio, *J. Liquid Chromatogr.*, **12** (1989) 1973.
- [35] W.T. Frankenberger, H.C. Mehra and D.T. Gjerde, *J. Chromatogr.*, **504** (1990) 211.

- [36] K. Robards, P. Starr and E. Patsalides, *Analyst*, **116** (1991) 1247.
- [37] P.L. Buldini, S. Cavalli and A. Trifiro, *J. Chromatogr. A*, **789** (1997) 529.
- [38] C. Sarzanini and E. Mentasti, *J. Chromatogr. A*, **789** (1997) 301.
- [39] C. Sarzanini, *J. Chromatogr. A*, **850** (1999) 213.
- [40] P.R. Haddad, P. Doble and M. Macka, *J. Chromatogr. A*, **856** (1999) 145.
- [41] C.A. Pohl, J.R. Stillian and P.E. Jackson, *J. Chromatogr. A*, **789**, (1997) 29.
- [42] J. Morris and J.S. Fritz, *J. Chromatogr.*, **602** (1992) 111.
- [43] N.T. Basta and M.A. Tabatabai, *Soil Sci. Soc. Am. J.*, **54** (1990) 1289.
- [44] K. A. Ruth and R.W. Shaw, *J.Chromatogr.*, **546** (1991) 243.
- [45] P. Janvion, S. Motellier and H. Pitsch, *J. Chromatogr. A*, **715** (1995) 105.
- [46] P.L. Buldini, D. Ferri and J.L. Sharma, *J. Chromatogr. A*, **789** (1997) 549.
- [47] N. Cardellicchio, P. Ragone, S. Cavalli and J. Riviello, *J.Chromatogr. A*, **770** (1997) 185.
- [48] N. Cardellicchio, A. Dell'atti, S. Giandomenico, A. Di Leo and S. Cavalli, *Annali Di Chimica*, **88** (1998) 819.
- [49] P.L. Buldini, A. Mevoli and J.L. Sharma, *Analyst*, **123** (1998) 1109.
- [50] E. Lane, A.J. Holden and R.A. Coward, *Analyst*, **124** (1999) 245.
- [51] A.W. Al-Shawi and R. Dahl, *Anal. Chim. Acta*, **391** (1999) 35.
- [52] N. Cardellicchio, S. Cavalli, P. Ragone and J.M. Riviello, *J.Chromatogr. A*, **847** (1999) 251.
- [53] H. Lu, S. Mou and J.M. Riviello, *J.Chromatogr. A*, **857** (1999) 343.
- [54] M.C. Bruzzoniti, E. Mentasti and C. Sarzanini, *Anal. Chim. Acta*, **382** (1999) 291.
- [55] P.N. Nesterenko, A.I. Elefterov, D.A. Tarasenko and O.A. Shpigun, *J. Chromatogr. A*, **706** (1995) 59.
- [56] K. Ohta, K. Tanaka, B. Paull and P.R. Haddad, *J.Chromatogr. A*, **770** (1997) 219.
- [57] K. Ohta, H. Morikawa, K. Tanaka, Y. Uryu, B. Paull and P.R. Haddad, *Anal. Chim. Acta*, **359** (1998) 255.

- [58] M.E. Fernandez-Boy, F. Cabrera, E. Madejon, M.J. Diaz, F. Moreno and J.P. Calero, *J.Chromatogr. A*, **823** (1998) 279.
- [59] A.A. Almeida, X. Jun and J.L.F.C. Lima, *Analyst*, **123** (1998) 1283.
- [60] S. Schnell, S. Ratering and K. Jansen, *Environ. Sci. Technol.*, **32** (1998) 1530.
- [61] A. Martin-Esteban, R.M. Garcinuno, S. Angelino and P. Fernandez, *Talanta*, **48** (1999) 959.
- [62] A.W. Al-Shawi and R. Dahl, *J.Chromatogr.A*, **671** (1994) 173.
- [63] M.C. Bruzzoniti, E. Mentasti, C. Sarzanini, M. Braglia, G. Cocito and J. Kraus, *Anal. Chim. Acta*, **322** (1996) 49.
- [64] M.C. Bruzzoniti, E. Mentasti and C. Sarzanini, *Anal. Chim. Acta*, **353** (1997) 239.
- [65] A. Siriraks, H.M. Kingston and J.M. Riviello, *Anal. Chem.*, **62** (1990) 1185.
- [66] N. Cardellicchio, S. Cavalli and J.M. Riviello, *J.Chromatogr.*, **640** (1993) 207.
- [67] R. Caprioli and S. Torcini, *J.Chromatogr.*, **640** (1993) 365.
- [68] W. Shotyk and I. Immenhauser-Potthast, *J.Chromatogr. A*, **706** (1995) 167.
- [69] H. Lu, S. Mou, Y. Yan, S. Tong and J.M. Riviello, *J.Chromatogr. A*, **800** (1998) 247.
- [70] H. Lu, S. Mou, Y. Hou, F. Liu, K.Li, S. Tong, Z. Li and J.M. Riviello, *J. Liq. Chrom. & Rel. Technol.*, **20** (1997) 3173.
- [71] H. Lu, S. Mou, Y. Yan, F. Lui, K. Li, S. Tong and J.M. Riviello, *Talanta*, **45** (1997) 119.
- [72] C. Lui, N. Lee and T. Wang, *Anal. Chim. Acta*, **337** (1997) 173.
- [73] C. Lui, N. Lee and J. Chen, *Anal. Chim. Acta*, **369** (1998) 225.
- [74] S. Motellier and H. Pitsch, *J.Chromatogr. A*, **739** (1996) 119.
- [75] M. Laikhtman, J. Riviello and J.S. Rohrer, *J.Chromatogr. A*, **816** (1998) 282.
- [76] P. Nesterenko and P. Jones, *J. Liq. Chrom. & Rel. Technol.*, **19** (1996) 1033.
- [77] P.N. Nesterenko and P. Jones, *J.Chromatogr. A*, **770** (1997) 129.
- [78] P.N. Nesterenko and P. Jones, *Anal. Commun.*, **34** (1997) 7.

- [79] P.N. Nesterenko and P. Jones, *J.Chromatogr. A*, **804** (1998) 223.
- [80] R.M.C. Sutton, S.J. Hill and P. Jones, *J.Chromatogr. A*, **789** (1997) 389.
- [81] K.H. Faltynski and J.R. Jezorek, *Chromatographia*, **22** (1986) 7.
- [82] G. Bonn, S. Reiffenstuhl and P. Jandik, *J.Chromatogr.*, **499** (1990) 669.
- [83] A.I. Elefterov, P.N. Nesterenko and O.A. Shpigun, *J. Anal. Chem.*, **51** (1996) 972.
- [84] M.G. Kolpachnikova, N.A. Penner and P.N. Nesterenko, *J.Chromatogr. A*, **826** (1998) 15.
- [85] M.P. O'Connell, J. Treacy, C. Merly, C.M.M. Smith and J.D. Glennon, *Anal. Lett.*, **32** (1999) 185.
- [86] Y. Inoue, H. Kumagai, Y. Shimomura, T. Yokoyama and T.M. Suzuki, *Anal. Chem.*, **68** (1996) 1517.
- [87] R.M. Silverstein, G.C. Bassler and T.C. Morrill, *Spectrometric Identification of Organic Compounds*, 5th Ed., John Wiley & Sons, New York, 1991
- [88] E. Gomez, J.M. Estela, V. Cerda and M. Blanco, *Fres. J. Anal. Chem.*, **342** (1992) 318.
- [89] E. Engstrom, I. Jonebring and B. Karlberg, *Anal. Chim. Acta*, **371** (1998) 227.
- [90] A.C. Co, A.N. Ko, L. Ye and C.A. Lucy, *J.Chromatogr. A*, **770** (1997) 69.
- [91] M.T. Vasconcelos and C.A.R. Gomes, *J.Chromatogr. A*, **696** (1995) 227.
- [92] S. Oszwaldowski and M. Jarosz, *Chem. Anal. (Warsaw)*, **42** (1997) 739.
- [93] C.A. Lucy and H.N. Dinh, *Anal. Chem.*, **66** (1994) 793.
- [94] S. Murakami and T. Yoshino, *Talanta*, **28** (1981) 623.
- [95] E.A. Gautier, R.T. Gettar, R.E. Servant and D.A. Batistoni, *J.Chromatogr. A*, **770** (1997) 75.
- [96] H. Onishi and K. Sekine, *Talanta*, **19** (1972) 473.
- [97] H. Rohwer, N. Collier and E. Hosten, *Anal. Chim. Acta*, **314** (1995) 219.
- [98] H. Rohwer and E. Hosten, *Anal. Chim. Acta*, **339** (1997) 271.
- [99] S. Abe and M. Endo, *Anal. Chim. Acta*, **226** (1989) 137.

- [100] Z. Li, Z. Zhu, Y. Chen, C. Hsu and J. Pan, *Talanta*, **48** (1999) 511.
- [101] T. Yamane and Y. Yamaguchi, *Anal. Chim. Acta*, **345** (1997) 139.
- [102] E.B. Sandell and H. Onishi, Photometric Determination of Traces of Metals, Part 1, 4th Ed., of Colorimetric Determination of traces of Metals, John Wiley, New York, 1978.
- [103] Z. Holzbecher *et al*, Handbook of Organic Reagents in Inorganic Analysis, John Wiley & Sons, New York, 1976.
- [104] F.D. Snell, Photometric and Fluorometric Methods of Analysis: Metals Part 1&2, John Wiley & Sons, New York, 1978.
- [105] R.M. Cassidy and B.D. Karcher in I.S. Krull (Ed.), Reaction Detection in Liquid Chromatography, Chromatographic Science Series Vol. 34, Marcel Dekker, New York, 1986.
- [106] W.W. Buchberger and P.R. Haddad, *J.Chromatogr. A*, **789** (1997) 67.
- [107] O.J. Challenger, Ph.D. Thesis, 1993.
- [108] B. Paull, Ph.D. Thesis, 1994.
- [109] R.M.C. Sutton, Ph.D. Thesis, 1996.
- [110] M.L. Marina, V. Gonzalez and A.R. Rodriguez, *Microchem. J.*, **33** (1986) 275.
- [111] M. Torre and M.L. Marina, *CRC Crit. Rev. Anal. Chem.*, **24** (1994) 327.
- [112] K. Brajter and E. Olbrych-Sleszynska, *Talanta*, **30** (1983) 355.
- [113] H.W. Handley, P. Jones, L. Ebdon and N.W. Barnett, *Anal. Proc.*, **28** (1991) 37.
- [114] L. Ebdon, H.W. Handley, P. Jones and N.W. Barnett, *Mikrochim. Acta*, **II** (1991) 39.
- [115] R. Kocjan and M. Garbacka, *Sep. Sci. Technol.*, **29** (1994) 799.
- [116] K. Brajter, E. Olbrych-Sleszynska and M. Staskiewicz, *Talanta*, **35** (1988) 65.
- [117] A.K. Singh and T.G. Sampath Kumar, *Microchem. J.*, **40** (1989) 197.
- [118] A.K. Singh and P. Rita, *Microchem. J.*, **43** (1991) 112.
- [119] A.K. Singh and S.K. Dhingra, *Analyst*, **117** (1992) 889.

- [120] R. Saxena and A.K. Singh, *Anal. Chim. Acta*, **340** (1997) 285.
- [121] Z. Molodovan and L. Vladescu, *Talanta*, **43** (1996) 1573.
- [122] K. Brajter and E. Dabek-Zlotorzynska, *Analyst*, **113** (1988) 1571.
- [123] A.T. Pilipenko, V.G. Safronova and L.V. Zakrevskaya, *Ind. Lab.*, **56** (1990) 152.
- [124] P. Su and S. Huang, *Anal. Chim. Acta*, **376** (1998) 305.
- [125] G. Chakrapani, D.S.R. Murty, P.L. Mohanta and R. Rangaswamy, *J. Geochem. Explor.*, **63** (1998) 145.
- [126] S.A. Morozko and V.M. Ivanov, *J. Anal. Chem.*, **50** (1995) 572.
- [127] S.A. Morozko and V.M. Ivanov, *J. Anal. Chem.*, **51** (1996) 580.
- [128] L. Cornejo-Ponce, P. Peralta-Zamora and M.I.M.S. Bueno, *Talanta*, **46** (1998) 1371.
- [129] S.L.C. Ferreira, C.F. de Brito, A.F. Dantas, N.M. Lopo de Araujo and A.C. Spinola Costa, *Talanta*, **48** (1999) 1173.
- [130] C.H. Lee, J.S. Kim, M.Y. Suh and W. Lee, *Anal. Chim. Acta*, **339** (1997) 303.
- [131] C.H. Lee, M.Y. Suh, K.S. Joe, T.Y. Eom and W. Lee, *Anal. Chim. Acta*, **351** (1997) 57.
- [132] S.L.C. Ferreira, H.C. dos Santos, J.R. Ferreira, N.M. Lopo de Araujo, A.C.S. Costa and D. Santiago de Jesus, *J. Braz. Chem. Soc.*, **9** (1998) 525.
- [133] O. Zaporozhets, N. Petruniok, O. Bessarabova and V. Sukhan, *Talanta*, **49** (1999) 899.
- [134] R. Kocjan, *Hung. J. Ind. Chem.*, **26** (1998) 263.
- [135] R. Kocjan and R. Swieboda, *Chem. Anal. (Warsaw)*, **44** (1999) 35.
- [136] S.L.C. Ferreira, J.R. Ferriera, A.F. Dantas, V.A. Lemos, N.M.L. Araujo and A.C. Spinola Costa, *Talanta*, **50** (2000) 1253.
- [137] R. Shah and S. Devi, *Talanta*, **45** (1998) 1089.
- [138] E. Morosanova, A. Velikorodny and Y. Zolotov, *Fres. J. Anal. Chem.*, **361** (1998) 305.

- [139] K. Huddersman, V. Patruno, G.J. Blake and R.H. Dahm, *J. Soc. Dyers & Colourists*, **114** (1998) 155.
- [140] P. Jones and G. Schwedt, *J. Chromatogr.*, **482** (1989) 325.
- [141] O.J. Challenger, S.J. Hill, P. Jones and N.W. Barnett, *Anal. Proc.*, **29** (1992) 91.
- [142] P. Jones, O.J. Challenger, S.J. Hill and N.W. Barnett, *Analyst*, **117** (1992) 1447.
- [143] O.J. Challenger, S.J. Hill and P. Jones, *J. Chromatogr.*, **639** (1993) 197.
- [144] P. Jones, M. Foulkes and B. Paull, *J. Chromatogr. A*, **673** (1994) 173.
- [145] B. Paull, M. Foulkes and P. Jones, *Analyst*, **119** (1994) 937.
- [146] B. Paull, M. Foulkes and P. Jones, *Anal. Proc.*, **31** (1994) 209.
- [147] B. Paull and P. Jones, *Chromatographia*, **42** (1996) 528.
- [148] R.M.C. Sutton, S.J. Hill and P. Jones, *J. Chromatogr. A*, **739** (1996) 81.
- [149] J.E. Dinunzio, R.W. Yost and E.K. Hutchison, *Talanta*, **32** (1985) 803.
- [150] J. Toei and N. Baba, *J. Chromatogr.*, **361** (1986) 368.
- [151] J. Toei, *Fres. Z Anal. Chem.*, **331** (1988) 735.
- [152] J. Toei, *Analyst*, **113** (1988) 247.
- [153] J. Toei, *Chromatographia*, **23** (1987) 583.
- [154] J. Toei, *Chromatographia*, **23** (1987) 355.
- [155] T.A. Walker, *J. Chromatogr.*, **602** (1992) 97.
- [156] B. Paull, P.A. Fagan and P.R. Haddad, *Anal. Commun.*, **33** (1996) 193.
- [157] B. Paull, M. Macka and P.R. Haddad, *J. Chromatogr. A*, **789** (1997) 329.
- [158] B. Paull, P. Nesterenko, M. Nurdin and P.R. Haddad, *Anal. Commun.*, **35** (1998) 17.
- [159] B. Paull, P. Nesterenko and P.R. Haddad, *Anal. Chim. Acta*, **375** (1998) 117.
- [160] B. Paull, M. Clow and P.R. Haddad, *J. Chromatogr. A*, **804** (1998) 95.
- [161] B. Paull and P.R. Haddad, *Trends Anal. Chem.*, **18** (1999) 107.
- [162] L.G. Sillen and A.E. Martell, Stability Constants of metal-ion complexes, Spec. Publ. N17 and N24, Chem. Soc., London, 1964 & 1971.

- [163] Stability Constants Database, SCQUERY, IUPAC and Academic Software, 1993.
- [164] J.E. Going and C. Sykora, *Anal. Chim. Acta*, **70** (1974) 127.
- [165] Y.V. Kholin, Y.V. Shabaeva and I.V. Khristenko, *Russ. J. Appl. Chem.*, **71** (1998) 407.
- [166] A. Yuchi, T. Sato, Y. Morimoto, H. Mizuno and H. Wada, *Anal. Chem.*, **69** (1997) 2941.
- [167] H. Kumagai, Y. Inoue, T. Yokoyama, T.M. Suzuki and T. Suzuki, *Anal. Chem.*, **70** (1998) 4070.
- [168] B. Noresson, P. Hashemi and A. Olin, *Talanta*, **46** (1998) 1051.
- [169] I.N. Voloshchik, B.A. Rudenko and M.L. Litvina, *J. Anal. Chem.*, **49** (1994) 1165.
- [170] A.I. Elefterov, P.N. Nesterenko and O.A. Shpigun, *J. Anal. Chem.*, **51** (1996) 887.
- [171] P. Buglyo, T. Kiss, M. Dyba, M. Jezowska-Bojczuk, H. Kozlowski and S. Bouhsina, *Polyhedron*, **16** (1997) 3447.
- [172] Chelation Systems, Purolite Technical Bulletin, 1997.
- [173] H. Leinonen, J. Lehto and A. Makela, *React. Polym.*, **23** (1994) 221.
- [174] J. Lehto, K. Vaaramaa and H. Leinonen, *React. Funct. Polym.*, **33** (1997) 13.
- [175] M.C. Yebra-Biurrun, A. Bermejo-Barrera and M.P. Bermejo-Barrera, *Anal. Chim. Acta*, **264** (1992) 53.
- [176] M.C. Yebra-Biurrun, A. Bermejo-Barrera, M.P. Bermejo-Barrera and M.C. Barciela-Alonso, *Anal. Chim. Acta*, **303** (1995) 341.
- [177] M.F. Enriquez-Dominguez, M.C. Yebra-Biurrun and M.P. Bermejo-Barrera, *Analyst*, **123** (1998) 105.
- [178] K. Vaaramaa and J. Lehto, *React. Funct. Polym.*, **33** (1997) 19.
- [179] P.N. Nesterenko, O.S. Zhukova, O.A. Shpigun and P. Jones, *J. Chromatogr. A*, **813** (1998) 47.

- [180] G.V. Kudryavtsev, D.V. Milchenko, S.Z. Bernadyuk, T.E. Vertinskaya and G.V. Lisichkin, Synthesis and Properties of Silica based Phosphonic Acid Cation-Exchangers, *Teor. Eksp. Khim.*, **28** (1987) 7.
- [181] S.V. Kertman, G.M. Kertman and Y.A. Leykin, *Thermochim. Acta*, **256** (1995) 227.
- [182] S.K. Sahni, R.V. Bennekorn and J. Reedijk, *Polyhedron*, **4** (1985) 1643.
- [183] V.D. Kopylova, T.V. Mekvabishvili and E.L. Gefter, Phosphor-Containing Ion-Exchangers, Voronezh University, 1992, p192.
- [184] M. Wozniak and G. Nowogrocki, *Talanta*, **26** (1979) 1135.
- [185] M.S. Mohan and E.H. Abbott, *J. Coord. Chem.*, **8** (1978) 175.
- [186] G.N. Zaitseva and O.P. Ryabushko, *Ukr. Khim. Zh.*, **58** (1992) 965.
- [187] P.N. Nesterenko, A.V. Ivanova, N.A. Galeva and J.B. Seneveratne, *Zh. Anal. Khim.*, **52** (1997) 814.
- [188] M. Lederer, Chromatography for Inorganic Chemistry, John Wiley & Sons, New York, 1994.
- [189] E. Merian (Ed.), Metals and Their Compounds in the Environment, VCH, Weinheim, 1991.
- [190] J. Koreckova-Sysalova, *Intern. J. Environ. Anal. Chem.*, **68** (1997) 397.
- [191] M.C. Valencia, S. Boudra and J.M. Bosque-Sendra, *Analyst*, **118** (1993) 1333.
- [192] N.K. Agnihotri, H.B. Singh, R.L. Sharma and V.K. Singh, *Talanta*, **40** (1993) 415.
- [193] E.P.C. Lai, B.D. Statham and K. Ansell, *Anal. Chim. Acta*, **276** (1993) 393.
- [194] H.B. Singh, N.K. Agnihotri and V.K. Singh, *Talanta*, **47** (1998) 1287.
- [195] M. de la Torre, F. Fernandez-Gamez, F. Lazaro, M.D. Luque de Castro and M. Valcarel, *Analyst*, **116** (1991) 81.
- [196] F. Capitan, E. Manzano, A. Navalon, J.L. Vilchez and L.F. Capitan-Vallvey, *Talanta*, **39** (1992) 21.
- [197] L. Kutsera, H. Ghaziaskar and E.P.C. Lai, *Anal. Lett.*, **25** (1992) 2289.

- [198] L.N. Moskvina, S.V. Drogobuzhskaya and A.L. Moskin, *J. Anal. Chem.*, **54** (1999) 272.
- [199] M.R. Ganjali, A. Moghimi and M. Shamsipur, *Anal. Chem.*, **70** (1998) 5259.
- [200] H. Kleykamp, *J. Anal. At. Spectrom.*, **14** (1999) 377.
- [201] L.C. Robles, C. Garcia-Olalla, M.T. Alemany and A.J. Aller, *Analyst*, **116** (1991) 735.
- [202] S.S. Bhattacharyya and A.K. Das, *J. Anal. At. Spectrom.*, **7** (1992) 417.
- [203] N. Goyal, P.J. Purohit, A.G. Page and M.D. Sastry, *Talanta*, **39** (1992) 775.
- [204] D.B. Do Nascimento and G. Schwedt, *Anal. Chim. Acta*, **283** (1993) 909.
- [205] T. Okutani, Y. Tsuruta and A. Sakuragawa, *Anal. Chem.*, **65** (1993) 1273.
- [206] L.C. Robles and A.J. Aller, *J. Anal. At. Spectrom.*, **9** (1994) 871.
- [207] T. Cernohorsky and S. Kotrly, *J. Anal. At. Spectrom.*, **10** (1995) 155.
- [208] T. Shimizu, K. Ohya, H. Kawaguchi and Y. Shijo, *Bull. Chem. Soc. Jpn.*, **72** (1999) 249.
- [209] S. Tao, Y. Okamoto and T. Kumamaru, *Anal. Chim. Acta*, **309** (1995) 379.
- [210] S. Recknagel, A. Chrissafidou, D. Alber, U. Rosick and P. Bratter, *J. Anal. At. Spectrom.*, **12** (1997) 1021.
- [211] L. Shoupu, Z. Mingqiao and D. Chunanyue, *Talanta*, **41** (1994) 279.
- [212] B. Kondratjonok and G. Schwedt, *Fres. Z. Anal. Chem.*, **332** (1988) 333.
- [213] M. Betti and S. Cavalli, *J. Chromatogr.*, **538** (1991) 365.
- [214] R.I. Suleimanov, T.G. Khanlarov and D.G. Gambarov, *J. Anal. Chem.*, **49** (1994) 754.
- [215] M. Takaya, *J. Chromatogr. A*, **850** (1999) 363.
- [216] I.N. Voloschik, M.L. Litvina and B.A. Rudenko, *J. Chromatogr. A*, **706** (1995) 315.
- [217] E.B. Sandell, *Ind. Eng. Chem., Anal. Ed.*, **12** (1940) 674.

- [218] F.A. Cotton and G. Wilkinson (Eds.), *Advanced Inorganic Chemistry*, 5th edn., Wiley, New York, 1988.
- [219] P. Martinez and D. Uribe, *Z. Naturforsch*, **37b** (1982) 1446.
- [220] M.J. Hines and D.F. Kelly, *J. Chem. Soc., Chem. Commun.*, **13** (1988) 849.
- [221] J. Xu and R.B. Jordan, *Inorg. Chem.*, **29** (1990) 4180.
- [222] Y.H.P. Hsieh and Y.P. Hsieh, *J. Agric. Food Chem.*, **45** (1997) 1126.
- [223] D. Chen, M. Bastian, F. Gregan, A. Holy and H. Sigel, *J. Chem. Soc., Dalton Trans.*, **10** (1993) 1537.
- [224] J.C. Miller and J.N. Miller, *Statistics for Analytical Chemistry*, 3rd Ed., Ellis Horwood, New York, 1993.
- [225] R.M.C. Sutton, S.J. Hill, P. Jones, A. Sanz-Medel and J.I. Garcia-Alonso, *J. Chromatogr. A*, **816** (1998) 286.
- [226] S. Elchuk, K.I. Burns, R.M. Cassidy and C.A. Lucy, *J. Chromatogr.*, **558** (1991) 197.
- [227] C. Merly, B. Lynch, P. Ross and J.D. Glennon, *J. Chromatogr. A*, **804** (1998) 187.
- [228] Z.L. Chen and M.A. Adams, *Chromatographia*, **49** (1999) 496.
- [229] P.N. Nesterenko, G.Z. Amirova and T.A. Bol'shova, *Anal. Chim. Acta*, **285** (1994) 161.
- [230] P.N. Nesterenko and G.Z. Amirova, *J. Anal. Chem.*, **49** (1994) 495.
- [231] A.I. Elefterov, S.N. Nosal, P.N. Nesterenko and O.A. Shpigun, *Analyst*, **119** (1994) 1329.
- [232] J.S. Bradshaw, G.E. Mass, J.D. Lamb, R.M. Izatt and J.J. Christensen, *J. Am. Chem. Soc.*, **102** (1980) 469.
- [233] R.I. Gelb and J.S. Alper, *J. Chem. Eng. Data*, **43** (1998) 383.
- [234] A.A. Zagorodni, D.N. Muiraviev and M. Muhammed, *Sep. Sci. Technol.*, **32** (1997) 413.

- [235] S.A. Abou Ali, A.M. Hindawey and G.B. Mohamed, *J. Chin. Chem. Soc.*, **31** (1984) 235.
- [236] C. Moberg and M. Weber, *React. Polym.*, **12** (1990) 31.
- [237] W. Li, M.M. Olmstead, D. Miggins and R.H. Fish, *Inorg. Chem.*, **35** (1996) 51.
- [238] G. Chessa, G. Marangoni, B. Pitteri, N. Stevanato and A. Vavasori, *React. Polym.*, **14** (1991) 143.
- [239] E. Blasius and B. Brozio, *J. Electrochem. Soc.*, **68** (1964) 52.
- [240] N.A. Penner, P.N. Nesterenko, M.M. Ilyin, M.P. Tsyurupa and V.A. Davankov, *Chromatographia*, **50** (1999) 611.
- [241] J. Oehlke, E. Schrotter, L. Piesche, S. Dove and H. Niedrich, *Pharmazie*, **38** (1983) 624.
- [242] R.T. Morrison and R.N. Boyd, *Organic Chemistry*, 6th Ed., Prentice Hall, New Jersey, 1992.
- [243] R.M. Cassidy and S. Elchuk, *Anal. Chem.*, **54** (1982) 1558.
- [244] H. Rossotti, *Diverse Atoms – Profiles of the Chemical Elements*, Oxford University Press, 1998.
- [245] J.P. Riley and R. Chester, *Introduction to Marine Chemistry*, Academic Press, London, 1971.
- [246] J. Emsley, *The Elements*, 2nd Ed., Oxford University Press, 1991.
- [247] J.J. Byerley, J.M. Scharer and G.F. Atkinson, *Analyst*, **112** (1987) 41.
- [248] H. de Beer and P.P. Coetzee, *Radiochim. Acta*, **57** (1992) 113.
- [249] A.W. Al-Shawi and R. Dahl, *J. Chromatogr. A*, **706** (1995) 175.
- [250] M.P. Harrold, A. Siriraks and J. Riviello, *J. Chromatogr.*, **602** (1992) 119.
- [251] D.J. Barkley, M. Blanchette, R.M. Cassidy and S. Elchuk, *Anal. Chem.*, **58** (1986) 2222.
- [252] R.M. Cassidy, S. Elchuk, N.L. Elliot, L.W. Green, C.H. Knight and B.M. Recoskie, *Anal. Chem.*, **58** (1986) 1181.

- [253] C.H. Knight, R.M. Cassidy, B.M. Recoskie and L.W. Green, *Anal. Chem.*, **56** (1984) 474.
- [254] D.J. Barkley, L.A. Bennett, J.R. Charbonneau and L.A. Pokrajac, *J. Chromatogr.*, **606** (1992) 195.
- [255] H. Fuping, P.R. Haddad, P.E. Jackson and J. Carnevale, *J. Chromatogr.*, **640** (1993) 187.
- [256] P.E. Jackson, J. Carnevale, H. Fuping and P.R. Haddad, *J. Chromatogr. A*, **671** (1994) 181.
- [257] H. Fuping, B. Paull and P.R. Haddad, *Chromatographia*, **42** (1996) 690.
- [258] H. Fuping, B. Paull and P.R. Haddad, *J. Chromatogr. A*, **749** (1996) 103.
- [259] H. Fuping, B. Paull and P.R. Haddad, *J. Chromatogr. A*, **739** (1996) 151.
- [260] M.Y. Khuhawar and S.N. Lanjwani, *J. Chem. Soc. Pak.*, **20** (1998) 204.
- [261] I. Croudace, P. Warwick, R. Taylor and S. Dee, *Anal. Chim. Acta*, **371** (1998) 217.
- [262] K. Grudpan, J. Jakmunee and P. Sooksamiti, *J. Radioanal. Nucl. Chem.*, **229** (1998) 179.
- [263] H.E. Carter, P. Warwick, J. Cobb and G. Longworth, *Analyst*, **124** (1999) 271.
- [264] P. Goodall and C. Lythgoe, *Analyst*, **124** (1999) 263.
- [265] T. Yokoyama, A. Makishima and E. Nakamura, *Anal. Chem.*, **71** (1999) 135.
- [266] J.B. Truscott, L. Bromley, P. Jones, E.H. Evans, J. Turner and B. Fairman, *J. Anal. At. Spectrom.*, **14** (1999) 627.
- [267] R. Stella, M.T.G. Valentini and L. Maggi, *Appl. Radiat. Isot.*, **46** (1995) 1.
- [268] C.H. Lee, M.Y. Suh, J.S. Kim, D.Y. Kim, W.H. Kim and T.Y. Eom, *Anal. Chim. Acta*, **382** (1999) 199.
- [269] M. Merdivan, M.R. Buchmeiser and G. Bonn, *Anal. Chim. Acta*, **402** (1999) 91.
- [270] B. Paull and P.R. Haddad, *Anal. Commun.*, **35** (1998) 13.
- [271] O. Abollino, E. Mentasti, C. Sarzanini, E. Modone and M. Braglia, *Fres. J. Anal. Chem.*, **343** (1992) 482.

- [272] D. Trubert, F.M. Guzman, C. Lenaour, L. Brillard, M. Hussonnois and O. Constantinescu, *Anal. Chim. Acta*, **374** (1998) 149.
- [273] L.I. Guseva and G.S. Tikhomirova, *Radiochem.*, **40** (1998) 357.
- [274] S. Ozwaldowski, R. Lipka and M. Jarosz, *Anal. Chim. Acta*, **361** (1998) 177.
- [275] X.Y. Yang and C. Pin, *Anal. Chem.*, **71** (1999) 1706.
- [276] Dept. of the Environment, Cadmium in the Environment and its Significance to Man, Pollution Paper N17, HMSO, London, 1980.
- [277] Cadmium: A Heavy Metal, WWF Special Marine Factsheet, May 1995.
- [278] A. Fitch, *Crit. Rev. Anal. Chem.*, **28** (1998) 267.
- [279] I. Novozamsky, H.J. Van der Lee and V.J.G. Houba, *Mikrochim. Acta*, **119** (1995) 183.
- [280] F.E. Smith and E.A. Arsenault, *Talanta*, **43** (1996) 1207.
- [281] C.J. Park, J.K. Suh, K.W. Lee and S.H. Lee, *Anal. Sci.*, **13** (1997) 429.
- [282] C.J. Park and J.K. Suh, *J. Anal. Atom. Spectrom.*, **12** (1997) 573.
- [283] S. Ichinoki and M. Yamazaki, *Anal. Chem.*, **57** (1985) 2219.
- [284] H.M. Kuss, *Fres. J. Anal. Chem.*, **343** (1992) 788.
- [285] K.J. Lamble and S.J. Hill, *Analyst*, **123** (1998) 103R.